Protein phosphatase 2A as a regulator and mediator of beneficial plant-microbe interactions

by

Irina O. Averkina

Thesis submitted in fulfilment of
the requirements for the degree of
PHILOSOPHIAE DOCTOR
(PhD)

Faculty of Science and Technology
Department of Chemistry, Bioscience and Environmental Engineering
2020

University of Stavanger
NO-4036 Stavanger NORWAY
www.uis.no

ISBN: 978-82-7644-998-3
ISSN: 1819-1387
PhD: Thesis UiS No. 582

Acknowledgements

I would like to express my deepest gratitude to my supervisor Professor Cathrine Lillo for her continuous help and support, theoretical guidance, insightful comments and her talent to inspire. I am also infinitely grateful to Professor Lillo for the opportunity to work as a member of her research team.

I would like to thank my co-supervisor Dr. Amr R. A. Kataya for his invaluable consultations and practical support.

My sincere thanks and appreciation to all my co-authors for their contribution to the writing of the enclosed manuscript. I wish to thank Mathilde Laplace and Damien Ferrere, the master students from the University of Clermont Auvergne in Clermont – Ferrand, France, who under supervision of Dr. Maria Terese Creighton made a comprehensive practical contribution to the enclosed manuscript by the acquisition of experimental data.

I express my sincere acknowledgement to Edward Asare and Muhammad Harris, freelance research fellows, as well as Sophie Finck and Bérénice Hourdin, the master students from the University of Clermont Auvergne in Clermont – Ferrand, France, for their great contribution to the part of my research associated with genetic engineering and biotechnology.

I would also like to acknowledge my sense of gratitude to my lab colleagues Dr. Maria Terese Creighton, Dr. Dugassa Nemie-Feyissa and Dr. Behzad Heidari Ahootapeh for sharing their practical expertise with me, their brilliant ability to cooperate, for being always approachable and helpful and, not least, for creating a beneficial working atmosphere.

I wish to express my sincere thanks to all colleagues at CORE who directly or indirectly have lent their helping hand in this venture.

Finally, I would like to take this opportunity to express many thanks to my lovely family for their patience, support and optimism.

Abstract

Protein phosphatase 2A (PP2A) is involved in the regulation of stress response, growth and hormone signalling during the plant life cycle. A variety of plant growth-promoting rhizobacteria (PGPR) and arbuscular mycorrhiza fungi (AMF) stimulate plant growth and improve plant health, but the contribution of PP2A to the beneficial plant-microbe interactions is still obscure. The treatment of Arabidopsis wild type and PP2A (related) mutants, exhibiting either low or high PP2A activity, with the PGPR *Azospirillum brasilense* (wild-type strain Sp245 and auxin-deficient strain FAJ0009) and *Pseudomonas simiae* (WCS417r) revealed the essential role of the PP2A catalytic subunits from subfamily I in a positive response to PGPR. Moreover, the role of the regulatory subunit B'θ may also be important in this regard. Furthermore, the positive effect on the fresh weight of roots and shoots was especially pronounced in Arabidopsis mutants with low PP2A activity.

The treatment of tomato plants with the above-mentioned PGPR confirmed at the molecular level that the PP2A catalytic subunit belonging to subfamily I and the regulatory subunit B'θ may be important mediators in the interaction between plants and PGPR. The role of the regulatory subunit B'φ, previously characterized as a regulator of AMF colonization, was also investigated. For this purpose, transgenic tomato plants were engineered to overexpress the B'φ subunit derived from *Solanum lycopersicum* cv. Heinz under control of the cauliflower mosaic virus 35S promoter. The resulting plants were characterized by slowed development with significantly decreased root and shoot biomass, and a threefold reduction in seed number. Semi-quantitative reverse-transcription PCR analysis of the transgenic plants showed a significant disturbance in the homeostasis of abscisic acid (ABA) and gibberellins (GAs), and a striking reduction in the content of bioactive GAs in roots.

Table of Contents

List of Figures

List of Tables

List of abbreviations

ABA	Abscisic acid
ACC	1-aminocyclopropane-1-carboxylic acid
AM	Arbuscular mycorrhiza
AMF	Arbuscular mycorrhizal fungi
ATP	Adenosine triphosphate
CaMV	Cauliflower mosaic virus
CKs	Cytokinins
Col-0	Columbia ecotype
ET	Ethylene
GAs	Gibberellins
GA20ox	GA20-oxidase
GA3ox	GA 3-oxidase
GA2ox	GA 2-oxidase
GAST1	Gibberellin-stimulated transcript 1
IAA	Indole-3-acetic acid
ipdC	Indole-3-pyruvate decarboxylase
ISR	Induced systemic resistance
JA	Jasmonic acid
LB	Luria-Bertani
LCMT-1	Leucine Carboxyl Methyl Transferase 1
MS	Murashige and Skoog
NCED-1	Nine-cis-epoxycarotenoid dioxygenase 1
NO	Nitric oxide
nos	Nopaline synthase

OA	Okadaic acid
OD	Optical density
PGPR	Plant growth-promoting rhizobacteria
PME-1	PP2A Methyl Esterase I
PP2A	Protein phosphatase type 2A
PPP	Phosphoprotein phosphatases
PPT	Phosphinothricin
PT4	Mycorrhiza inducible phosphate transporter 4
PTPA	Phosphotyrosyl phosphatase 2A phosphatase activator or protein phosphatase 2A phosphatase activator
spp.	Several species
sqRT-PCR	Semi-quantitative Reverse Transcription-Polymerase Chain Reaction
TAS14	Abscisic acid and environmental stress-inducible protein
T-DNA	Transfer DNA
VOCs	Volatile organic compounds
WT	Wild type

Appendix

List of papers

I. **Specific PP2A catalytic subunits are a prerequisite for positive growth effects in Arabidopsis co-cultivated with *Azospirillum brasilense* and *Pseudomonas simiae.*** Irina O. Averkina, Ivan A. Paponov, Jose J Sánchez-Serrano, Cathrine Lillo (2021). *Plants, vol.10, 66.*

II. **Pinpointing regulatory protein phosphatase 2A subunits involved in beneficial symbiosis between plants and microbes.** Irina O. Averkina, Muhammad Harris, Edward Ohene Asare, Berenice Hourdin, Ivan A. Paponov, Cathrine Lillo. *Submitted to BMC Plant Biology*.

Contributions to other papers with different aspects. Assay methods and results of PP2A activity are included in the thesis:

III. **Methylation of protein phosphatase 2A – influence of regulators and environmental stress factors.** Maria T. Creighton, Anna Kolton, Amr R. A. Kataya, Jodi Maple-Grødem, Irina O. Averkina, Behzad Heidari, Cathrine Lillo (2017). *Plant Cell Environment, vol. 40, issue 10, pp. 2347-2358.*

IV. **Light regulation of nitrate reductase by catalytic subunits of protein phosphatase 2A.** Maria T. Creighton, Maite Sanmartín, Amr R. A. Kataya, Irina O. Averkina, Behzad Heidari, Dugassa Nemie-Feyissa, Jose J Sánchez-Serrano, Cathrine Lillo (2017). *Planta, vol. 246, issue 4, pp. 701-710.*

1 Introduction

1.1 Principles of beneficial plant-microbe interactions in rhizosphere

The term “rhizosphere” was introduced by Lorenz Hiltner (1862-1923), a pioneer in rhizosphere microbial research, on April 9, 1904, during his lecture at a meeting of the German Agricultural Society. His great dream was to apply the recent discoveries in soil microbiology to agricultural practice. Rhizosphere means the soil area influenced by plant roots. Due to his studies, it became known that the plant growth-promoting rhizobacteria (PGPR) inhabit soil and plant roots, establishing a long-term mutually beneficial association with the host plant. In this association, the bacteria sustain plant growth via nitrogen fixation, bacterial phytohormone production, increased nutrient uptake, enhanced biotic and abiotic stress resistance, vitamin production and phosphorus solubilisation (Hartmann et al. 2008; Maheshwari 2011). The host plant in return supplies the bacteria with carbon and energy sources such as sugars, organic acids and amino acids (Glick 2014).

PGPR have been applied in agriculture in many countries since their discovery. Due to their beneficial properties, this type of bacteria has been tested as inoculants in crop production, initially with cereals, but later with other plants. Recent studies demonstrate that bacteria from the *Azospirillum* genus increase the growth of every plant species tested so far (113 species across 35 families) that makes this genus a universal PGPR (Maheshwari 2011). *Azospirillum* has the ability to utilize dinitrogen (N_2) from the air by converting it to ammonia (NH_3). The fixed nitrogen is then assimilated in plant cells into amino acids and nucleotides. The process of biological nitrogen fixation is of enormous agricultural importance because only certain bacteria can fix nitrogen and support nitrogen needs of plants (Madigan et al. 2009). *Azospirillum* was the first commercial inoculant used for improved nitrogen uptake in field applications (Maheshwari 2011). The bacteria from this genus are

medium-sized (3–5 µm), microaerophilic, nitrogen-fixing, gram-negative, very motile curved rods with spirilloid movements carried out by either a single polar flagellum (swimming) or several lateral flagella (swarming). The beneficial effect of *Azospirillum* on plants is mainly attributed to the production of plant growth stimulators such as auxins (Spaepen et al. 2007), cytokinins (CKs), abscisic acid (ABA), gibberellins (GAs) (Cohen et al. 2008; Cohen et al. 2009) and nitric oxide (NO) (Bashan and de-Bashan 2010). In plants, these stimulators or phytohormones control cell division (auxins, CKs), cell growth (auxins), cell elongation (GAs), root growth and development (NO) and response to stresses (ABA) caused by bacterial or fungal infections or environmental changes such as light, temperature, nutrient fluctuations and drought (Amenta et al. 2015; Castillo et al. 2015; Rodrigues et al. 2015). The bacterial phytohormone production is reported to cause changes in root architecture and as a consequence an improved uptake of water and nutrients (Steenhoudt and Vanderleyden 2000). The most important hormone produced by *Azospirillum* is the auxin molecule, indole-3-acetic acid (IAA) (Castillo et al.). *Azospirillum brasilense* Sp245 is a type strain for *Azospirillum* species (Castillo et al. 2015). It is one of the most studied strains with complete sequence genome available in many databases (Alexandre 2015; Wisniewski-Dye et al. 2011). Another beneficial capacity ascribed to PGPR is related to biological control or ability to suppress plant pathogens. However, this role of *Azospirillum* is reported to be moderate and the mechanism is not well defined (Rodrigues et al. 2015). The ability to suppress plant pathogens could be attributed to antimicrobial compounds such as phenyl acetic acid, some volatile metabolites (Somers et al. 2005; Abdulkareem et al. 2014) or siderophores (iron chelators) that bind iron from the environment (Tortora et al. 2011). *Azospirillum* strains were also suggested to improve mineral uptake in plants via solubilization of insoluble mineral compounds by different organic acids produced in the bacteria in response to the plant sugar exudates (Bashan and de-Bashan 2010).

Another frequently studied PGPR genus is *Pseudomonas* (Podile and Kishore 2006), also called fluorescent pseudomonads (Bultreys et al. 2003), gram-negative, aerobic, motile rod-shaped bacteria (Pathma et al. 2011). Like *Azospirillum* spp., many *Pseudomonas* spp. stimulate plant growth and change the root architecture by shortening the primary root and enhancing the development of lateral roots. The enhanced plant growth is mainly attributed to bacterial auxins (only some specific strains) or auxin-mimicking compounds, CKs, B-group vitamins and volatile organic compounds (VOCs) (Garcia de Salamone et al. 2001; Pathma et al. 2011; Wintermans et al. 2016; Zamioudis et al. 2013). Resistance to abiotic and biotic stresses in plants colonized by pseudomonads is often associated with 1-aminocyclopropane-1-carboxylate (ACC) deaminase activity. ACC, the ethylene (ET) precursor, is generally present in non-stressed plants. Upon the stress response in plants, ACC converted to ET can both alleviate and exacerbate the stress effect depending on the conditions. In the most severe cases, the increased amount of ET can cause plant senescence, chlorosis and abscission. Plants, treated with PGPR with ACC deaminase activity, produce less ET as its precursor ACC is cleaved by the enzyme and consumed by the above-mentioned PGPR (Glick 2015). *Pseudomonas simiae* WCS417r (hereafter WCS417r) is among the most well-studied strains from this genus (Berendsen et al. 2015). Despite the auxin-dependent responses in Arabidopsis colonized by WCS417r, Zamioudis et al. (2013) and Ortiz-Castro et al. (2019) failed to confirm an auxin production in this strain. However, the latter research group identified cyclopeptides with auxin-mimicking activity in the WCS417r bacterial extract. WCS417r belongs to the most promising group of PGPR with an excellent ability to mediate biocontrol of plant pathogens by the production of antimicrobial compounds, siderophores and cell wall-degrading enzymes (Berendsen et al. 2015; Pathma et al. 2011; Stringlis et al. 2018a; Stringlis et al. 2019).

However, plant associations are not limited by bacteria. Another very interesting event in plant physiology is the formation of arbuscular

mycorrhiza (AM). Mycorrhiza is a term proposed by the German botanist Albert Bernhard Frank in 1885 to refer to roots that are closely intergrown with a fungus in one organ — the fungus root (from Greek myco is "fungus", rhiza is "root") (Koide and Mosse 2004). The term "arbuscular" originates from characteristic structures, the arbuscules, observed within the cortex of the host plant. Along with storage vesicles, these structures are usually (but not limited to) considered distinctive for AM symbioses (Dickson 2004). However, the morphology of AM associations is still dependent on both plant taxa and fungal identity (Cavagnaro et al. 2001). According to estimates today, 85% of all plants interact with arbuscular mycorrhizal fungi (AMF) (Miozzi et al. 2019). The young roots of these plants are completely woven over with thin branching filaments (hyphae) of the fungus. Now, it is well known that mycorrhiza is a symbiosis (mutually beneficial cohabitation) of certain fungi and plant roots where the fungi supply the host plant with mineral nutrients (e.g. phosphorus, nitrogen etc.), facilitates water absorption from surrounding soil (Smith and Read 2008a; Augé 2001) and help to resist infections (Fritz et al. 2006; Fiorilli et al. 2018; Jung et al. 2012). The host plant in return supplies AMF with sugars produced by photosynthesis as an energy source (Dickson 2004). Therefore, AMF has been in a great focus in terms of agricultural applications during the last decades. Strictly considered, the discovery of mycorrhiza should be credited to Albert Bernard Frank who described a regular and characteristic infection of plant roots by AMF in 1885 (Rayner 1926–1927). However, the first trustworthy information about AM began to be published only 50 years ago. The phenomenon of this symbiosis had long remained beyond the grasp of investigators until more advanced equipment and more sophisticated methods for study in this area became available. The problematics of AMF research can be explained by the impossibility of cultivating these fungi in the laboratory. As it turned out later, AMF belong to phylum Glomeromycota and are obligate root symbionts, incapable of growing independently without a host plant (Schüßler and Kluge 2001). The beneficial effect of AMF was first

studied in strawberries, apple and other fruit trees. Later, the improved plant growth was reported in tobacco, maize and oats. The observations of plant growth promotion caused by AMF colonization led to the great increase in popularity of the arbuscular mycorrhiza research and many decades later application of AMF in agriculture (Koide and Mosse 2004).

1.2 Induced systemic resistance in plants

In 1991 for the first time, several research groups reported increased resistance to phytopathogens in plants colonized by PGPR (Alstr et al. 1991; Van Peer 1991; Wei et al. 1991). Nowadays, the state of an enhanced defensive ability developed in plants in response to PGPR and AMF is well recognized as induced systemic resistance (ISR). ISR is primarily controlled by the plant hormones ET and jasmonic acid (JA) (van Loon et al. 1998; Pieterse et al. 2014; Pieterse et al. 1998), varies depending on bacterial or fungal strains and appears to be plant-microbe and pathogen specific (Leeman et al. 1995; Pieterse et al. 1996; Ton et al. 1999; Van Peer 1991; Van Wees et al. 1997). The onset of ISR in plants leads to many local changes in gene expression (Verhagen et al. 2004) associated with deposition of callose, lignin and phenolics (Duijff et al. 1997), changes in enzymatic activity including PP2A activity (Charpentier et al. 2014; Chen et al. 2000; Durian et al. 2016; Karthikeyan et al. 2006; Magnin-Robert et al. 2007; Rahikainen et al. 2016) and stress-related genes (Charpentier et al. 2014; Segonzac et al. 2014; Stringlis et al. 2018a; Verbon et al. 2019; Verhagen et al. 2004). However, these transcriptome changes are mild and incomparable with those observed during a pathogen attack. Therefore, ISR by beneficial microbes appears as priming of effective resistance mechanisms and results in earlier and stronger defence reactions upon a pathogenic assault (Ahn 2007; Alfano 2007; Liu 2007; Segarra et al. 2009).

1.3 Protein phosphatase 2A as a mediator in plant-microbe signalling: strategies and approaches

Recent research is mounting evidence that the plant innate immune system governs the plant response associated with beneficial plant-microbe interactions (Hacquard et al. 2017; Pieterse et al. 2014). An important role in the immune signalling and regulation (Kataya et al. 2015; Segonzac et al. 2014) and defence response to various plant pathogens is ascribed to protein phosphatase type 2A (PP2A) (Durian et al. 2016; He et al. 2004). However, the PP2A studies are mainly conducted on Arabidopsis and since this model plant is not an AM host (Cosme et al. 2018; Veiga et al. 2013) the contribution of these studies to the AMF-plant associations, for the most part, is still beyond the research grasp. Even though, Arabidopsis-PGPR interactions have already been intensively studied with *P. simiae* and *A.brasilense* by several research groups (Spaepen et al. 2014; Verbon et al. 2019; Verhagen et al. 2004; Zamioudis et al. 2013), the role of PP2A in these interactions remained outside of the scope of their investigation. Charpentier et al. (2014) showed that the regulatory PP2A subunit B'φ functions in ABA promotion of AM symbiosis in *Medicago truncatula.* He et al. (2004) and Pais et al. (2009) found that subfamily I of the PP2A catalytic subunits in tomato facilitates the plant defence responses associated inter alia with bacterial and fungal elicitors. Therefore, to translate the knowledge from Arabidopsis to agricultural plants such as tomato and identify underlying mechanisms for adaptation of plants to the challenging conditions is of great importance. The growth-promoting bacteria and fungi are constantly reported to be important for the adaptation and survival of agricultural plants (Marschner and Dell 1994; Boyer et al. 2016; Beneduzi et al. 2012; Pathma et al. 2011; Smith and Read 2008c; Bona et al. 2017; Hart et al. 2015).

In this regard, a reverse genetic approach is a powerful tool to study PP2A as a possible regulator of plant signaling associated with

beneficial microbes. Application of various Arabidopsis mutants with gain-of-function (over-expressors) or loss-of-function (null) mutations in PP2A subunits is a primary strategy in the study of the interaction between plants and PGPR. However, a loss-of-function mutation only in one PP2A subunit may be partially or entirely masked by the activity of other redundantly acting genes. Therefore, the application of PP2A mutants with altered PP2A activity is important guidance in the selection of an appropriate mutant. Unfortunately, this strategy is more relevant for Arabidopsis but not for tomato due to a very limited number of the PP2A tomato mutants available in the mutant libraries. So, the gene expression analysis of tomato plants stimulated by beneficial microbes or/and studies of gain-of-function mutations in the PP2A gene family (e.g. mentioned above B'φ) can give important clues to the role of PP2A in the beneficial plant-microbe interactions. The information obtained from the studies of PP2A in various plant species to date made it possible to identify several genes that could hypothetically play an important role in establishing the symbiosis between tomato plants and beneficial microbes (Error! Reference source not found.). Even though most of the PP2A subunits listed in **Table 1** are frequently studied in Arabidopsis, the anticipated orthologs in the tomato genome were found by application of phylogenetic analysis (Error! Reference source not found.) assuming that gene/protein sequence similarity confer the gene function similarity in different plant species.

Table 1. Most relevant PP2A genes for the plant-microbe interaction study in tomato

PP2A subunit	Plant system	Presumable ortholog in tomato	Function	Reference
B'φ	*Medicago truncatula*	B'φ	ABA promotion of AM colonization. Atypical gene family	(Charpentier et al. 2014; Booker and DeLong 2017)
B'θ	Arabidopsis	B'θ	Regulation of innate immunity, biotic stress	(Kataya et al. 2015; Durian et al. 2016)
B'κ	Arabidopsis	B'κ	Response to bacterial antimicrobial compounds	(Durian et al. 2016)
Bβ (Clade I)	Tomato	Bβ (Clade I)	Atypical gene family	(Booker and DeLong 2017)
Bβ (Clade III)	Arabidopsis *Medicago sativa*	Bβ (Clade III)	Nitrate reductase activation, ABA signaling in roots	(Heidari et al. 2011; Toth et al. 2000)
C1, C2 Subfamily I	Arabidopsis, tomato, potato	C1, C2 Subfamily I	Response to bacterial and fungal elicitors, ABA signaling	(Durian et al. 2016; He et al. 2004; Pais et al. 2009; Pernas et al. 2007)
A1	Maize Arabidopsis	Aα or AβI	Root development and growth, auxin, ABA signalling, stress response	(Blakeslee et al. 2008; Kwak et al. 2002; Wang et al. 2017; Zhou et al. 2004)
A1, A2, A3	Arabidopsis	Aα, AβI, AβII	Auxin distribution in seedling roots, nitrate reductase activation	(Heidari et al. 2011; Lillo et al. 2014; Michniewicz et al. 2007)

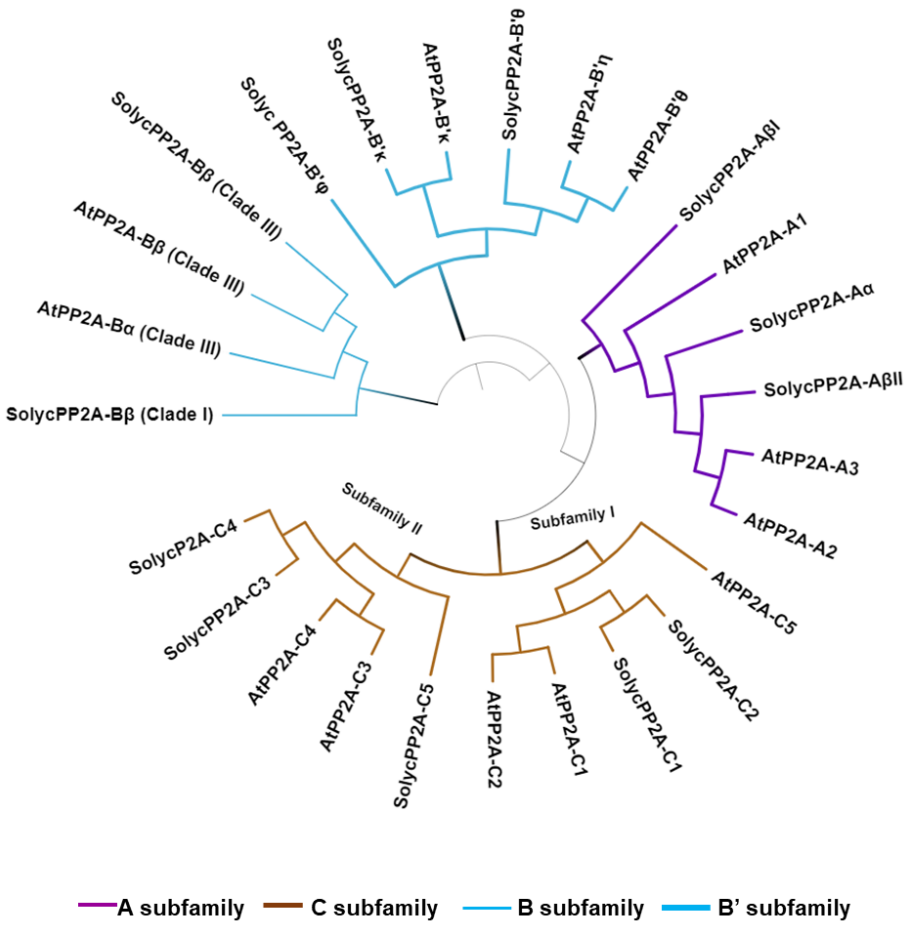

Figure 1. Phylogenetic relationship between some *Arabidopsis thaliana* (At) and *Solanum lycopersicum* (Solyc) PP2A subunits.

.

1.4 Protein phosphatase type 2A

The reversible phosphorylation of proteins is a common cellular mechanism for regulating protein activity. The phosphorylation and dephosphorylation of proteins have been found to modify protein function in multiple ways. A protein kinase transfers a phosphoryl group

from ATP to a protein. In eukaryotic cells the protein phosphorylation on serine, threonine and tyrosine residues is predominant. A protein phosphatase reverses the action of the protein kinase by cleaving phosphate from serine, threonine or tyrosine residues (Campbell 2009). This mechanism is widely utilized by all living cells, where 90% of all eukaryotic protein dephosphorylation reactions are catalysed by serine/threonine phosphoprotein phosphatases (PPPs) (Moorhead et al. 2007). Among PPPs, PP2A is one of the most abundant and extensively studied members (Virshup and Shenolikar 2009). PP2A is an essential part of the reversible phosphorylation playing a crucial role in the diversity of important biological processes such as cell growth and signalling (Janssens and Goris 2001), cell cycle regulation (Krasinska et al. 2011; Nilsson 2019), phototropism and stomatal opening (Tseng and Briggs 2010), tumour suppression (Janssens et al. 2005), cytoskeleton dynamics (Lee and Pallas 2007), regulation of multiple signal transduction pathways (Haesen et al. 2014; Lillo et al. 2014), hormone signalling and stress response (Durian et al. 2016; Creighton et al. 2017a; Chen et al. 2014), apoptosis (Reynhout and Janssens 2019), cell motility (Basu 2011) and many others. PP2A is highly conserved and found in all eukaryotic cells (Lechward et al. 2001). The ability of PP2A to manage this complex signalling network lies in its combinatorial and regulatory complexity because PP2A functions as a heterotrimeric protein complex. The PP2A core enzyme or A/C dimer consists of a catalytic C subunit and a scaffolding A subunit. The A/C dimer subsequently associates with a variable regulatory/targeting B subunit forming a heterotrimeric protein complex (Xing et al. 2006). The genome of the model plant Arabidopsis codes for three scaffolding subunits, five catalytic subunits and seventeen regulatory subunits. This diversity of subunits gives rise to over 200 biochemically distinct PP2A complexes (Lillo et al. 2014). Each complex exhibits a unique substrate recognition surface which in turn determinates enzyme activity, substrate specificity and subcellular localization (Ballesteros et al. 2013; Groves et al. 1999; Janssens and Goris 2001; Mumby 2007).

1.5 PP2A subunits in Arabidopsis and tomato

Similar to Arabidopsis, the tomato genome codes for three scaffolding A subunits and five catalytic C subunits (Booker and DeLong 2017; Lillo et al. 2014). The catalytic subunits in turn form two distinct subfamilies based on the sequence analysis (Casamayor et al. 1994; Perez-Callejon et al. 1998; He et al. 2004): subfamily I (C1, C2, C5 for Arabidopsis and C1, C2 for tomato) and subfamily II (C3 and C4 for Arabidopsis, and C3, C4 and C5 for tomato. Seventeen regulatory B subunits in Arabidopsis and nine in tomato divide into phylogenetically unrelated and structurally distinct B/B55, B' and B'' subfamilies (Booker and DeLong 2017; Lillo et al. 2014). In Arabidopsis, different isoforms of regulatory B subunits within the same subfamily are usually named by a specific Greek letter such as Bα and Bβ, B'α, β, γ, δ, ε, ζ, η, θ, and κ or B''α, β, γ, δ, ε and TON2 (Farkas et al. 2007; Lillo et al. 2014). However, it is worth noting that PP2A subunits in plants are most studied, genetically mapped and characterized in Arabidopsis, while in tomato such information is either not complete or simply unavailable. Based on the analysis of the phylogeny of PP2A subunits in flowering plants by Booker and DeLong (2017), B' gene subfamily turned out to be the most diverse and splits into five clades including the B'φ clade. The predicted B'φ gene product does not relate to any of Arabidopsis isoforms and is considered to be lost in the Arabidopsis genus (Error! Reference source not found.). Unlike Arabidopsis, the tomato genome possesses the B'φ clade (hereafter B'φ) but it is not well studied and characterized yet. Booker and DeLong (2017) pointed out that B'φ was present only in the plant species capable of forming arbuscular mycorrhizal or rhizobial associations and mentioned the recent studies of this gene in *M. truncatula,* confirming the essential role of B'φ in mycorrhizal symbiosis (Charpentier et al. 2014). Subunits from B/B55 subfamily are much less diverse and form a divergent clade (clade I) (lost in Arabidopsis but not in tomato), a small clade (clade II) (lost in tomato and Arabidopsis) and clade III (found in both above plant species). The B'' subfamily includes

the FASS/TON2 clade (or clade I) and more diverse clade II (Booker and DeLong 2017). Interestingly, 85% of the analysed plant species carry only one gene for the PP2A subunits from B/B55 (clade I), B'' (clade I) and B'φ clades and defined as atypical non-expanding PP2A gene families. The reduced expansion within these clades may indicate that these genes are involved in very specific physiological processes and their duplication might be detrimental for the plant (Li et al. 2016).

1.6 PP2A holoenzyme assembly

The A/C dimer exists as an abundant entity in cells rather than just an intermediate during the PP2A trimeric complex assembly and is regulated by numerous cellular proteins (Goldberg 1999). Here, just some of them will be described. Phosphotyrosyl phosphatase 2A phosphatase activator (PTPA) is identified as a crucial modulator of the PP2A serine/threonine phosphatase activity in *S. cerevisiae* and mammalians (Longin et al. 2004). The peptidyl-propyl cis/trans isomerase ability of PTPA (Jordens et al. 2006) was shown to cause conformational changes in the C subunit of PP2A and thus convert the A/C dimer to an active form. The active PP2A core enzyme can subsequently accept a B subunit or be methylated by leucine carboxyl methyltransferase (LCMT-1) on the carboxy-terminal leucine. The methylated form of the A/C dimer is reported to be more active (Chen et al. 2014). It is also found that in mammalian cells the methylated PP2A core enzyme is required for recruiting a B subunit from B and B' subfamily of B subunits (Hwang et al. 2016), some papers provide evidence that the recruitment of B subunits from B'' family also requires methylation of the PP2A coenzyme (Xing et al. 2006). On the other hand, the fully methylated PP2A core enzyme becomes a substrate for PP2A-specific methylesterase (PME-1), which removes the methyl group from the carboxy-terminal leucine of the C subunit. In addition to the esterase function, PME-1 stabilizes an inactive conformation of the A/C dimer that can be reactivated by PTPA (Janssens and Goris 2001) **(Figure 2**).

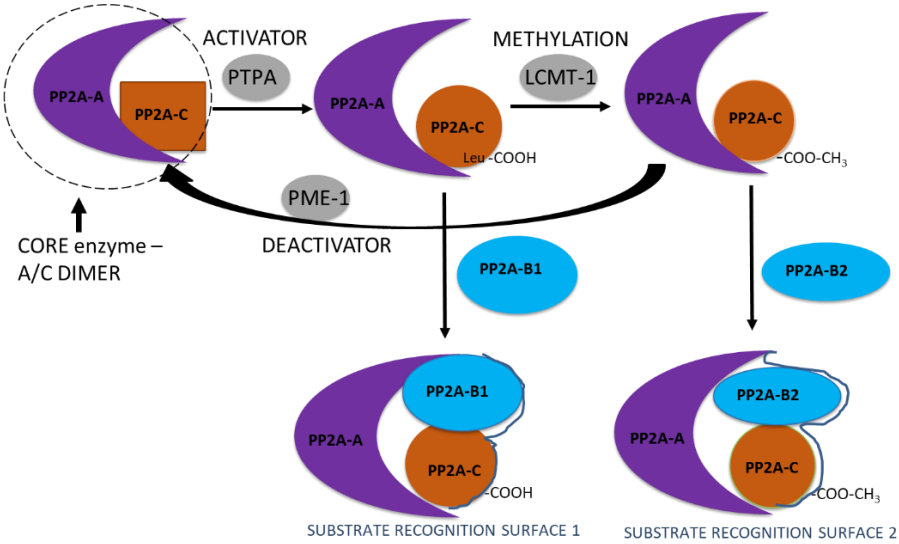

Figure 2. A simplified model of PP2A regulation in Arabidopsis.
During the PP2A trimeric complex assembly, PTPA converts the C subunit of the A/C dimer to a form that can accept a B subunit or be methylated by LCMT-1 on the carboxy-terminal leucine (Leu) before accepting a B subunit. On the other hand, the fully methylated PP2A core enzyme becomes a substrate for PME-1, which removes the methyl group from the carboxy-terminal leucine of the C subunit and stabilizes an inactive conformation of the A/C dimer that can be reactivated by PTPA.

1.7 PP2A inhibitors as a research tool

The biggest discovery in favour of the fact that PP2A mediates tumour suppression was the finding of potent tumour-inducing toxins, such as okadaic acid (OA), which primarily targets the PP2A catalytic subunits. Acting against some other PPPs as well (Honkanen and Golden 2002), OA is a selective inhibitor of PP2A at 1-2 nM concentration (Cohen et al. 1989). OA is a polyketide, polyether derivative of a C_{38}-fatty acid. It is a toxin produced by various species of dinoflagellates, although first isolated from the sponge *Halichondria okadai* (Lackie 2010). The

active-site pocket of the C subunit in the form of a hydrophobic cage accommodates the hydrophobic end of OA. Bound to the catalytic subunit, OA disrupts binding of a regulatory B subunit to the catalytic C subunit of the A/C dimer and thereby prevents the formation of the PP2A heterotrimeric protein complex (Xing et al. 2006; Walter et al. 1990). Nowadays, application of small molecule inhibitors such as OA to study the roles of sensitive protein phosphatases is still a widely used research tool in studies designed to provide insight into the biological functions of PP2A (Swingle et al. 2007).

2 Project background

Tomato is an excellent research material because it has many interesting features such as fleshy fruit, a sympodial shoot and compound leaves, which other model plants (e.g., rice and Arabidopsis) do not have. Most of these traits are agronomically important and cannot be studied using other model plant systems. Besides, the tomato belongs to the extremely large family Solanaceae and is closely related to many commercially important plants such as potato, eggplant, peppers, tobacco and petunias. Knowledge obtained from studies conducted on tomato can be easily applied to these plants from the Solanaceae family and specifically for fleshy-fruited plants (Kimura and Sinha 2008). Tomato is a leading greenhouse vegetable crop in many countries. The greenhouse production makes the cultivation of tomatoes possible in the most northern lands all year round. The Rogaland district is an extremely important area for greenhouse production in Norway. According to the statistics form "Regional plan for agriculture in Rogaland 2011", it was harvested 930700 kg tomatoes in 2009 in Rogaland which makes up 86% of all tomato production in the country and 10 656 837 kg tomatoes in 2010 which makes up 85% of all tomato production. Among cucumber, corn, potato and vegetables, tomatoes take a leading place in the list of the vegetable crop production in Norway. So, Rogaland can rightly be called a tomato province in Norway. Following the national objective to exclude all use of fossil energy in the greenhouse industry by 2030, the main challenge in Rogaland will be to reorganize the greenhouse industry so that it could function only on renewable energy sources. In addition to the transition to renewable energy sources, energy reduction can be achieved by better isolation and improved ventilation systems as well as by using more energy-efficient machinery. Numerous technologies have been recently developed that can reduce the use of fossil energy up to 100% and the total energy use up to 80%, using renewable Norwegian resources (water, sun). Application of such

technologies will require drastic reductions in greenhouse ventilation (closed/semi- closed greenhouse), which will have serious consequences for the greenhouse climate and thus for plant production and product quality. Little is known about how to take advantage of such technologies to attain high yield and quality under Norwegian conditions. The use of plant growth-promoting microorganisms could play a significant role in the adaptation of greenhouse plants to the challenging conditions in greenhouses. Already one hundred years ago, the German scientist Lorenz Hiltner hypothesized that quality of plant products, their resistance to infections and diseases may be dependent on the microbial composition of the soil (Hartmann et al. 2008). Nowadays, PGPR and AMF are sold and used as bio-fertilizers in Brazil, Argentina, Mexico, Italy, France, Australia, Pakistan, Germany, the USA, Africa, Belgium, India and Uruguay (Reis et al. 2011; Rodrigues et al. 2015). In Norway, the application of bio-fertilizers could be considered in greenhouses. This opportunity is now being studied in the laboratory of Professor Lillo in the Centre for Organelle Research (CORE) at the University of Stavanger in collaboration with NIBIO, Særheim. However, harnessing the symbiosis between such microorganisms and plants requires deep knowledge with applications of gene technologies. The PP2A protein complex important for adaption to various environmental conditions (bacterial and fungal invasions, drought and lack of nutrients) has been studied for several years in the laboratory of Professor Lillo (Lillo et al. 2014). So far, all the PP2A work has been carried out with the model plant Arabidopsis. A certain regulator of PP2A called B'φ regulatory subunit is expected to play an important role in tomato regarding interaction with microorganisms (Booker and DeLong 2017; Charpentier et al. 2014). Therefore, the main goal of the current project is to reveal if PP2A and, in particular, its regulatory subunit B'φ are involved in the interactions with the plant growth-promoting microorganisms on the example of certain PGPR and AMF.

3 Main objectives

To explore whether PP2A is involved in beneficial plant-microbe interaction, the following research objectives were established:

- Assay PP2A activity in Arabidopsis WT and mutant lines with mutations targeting the PP2A catalytic subunits and regulator proteins, and identify the genotypes exhibiting a significant alteration in the PP2A activity compared with that in WT.

- Study the phenotypic response of the identified mutants to inoculation with PGPR.

- Based on the knowledge available from PP2A studies on Arabidopsis, tomato, and some other model plants, define PP2A subunits for gene expression analysis in tomato roots subjected to inoculation with PGPR and AMF.

- Collect and evaluate data from the gene expression analysis of *B'φ* and other PP2A subunits presumably associated with plant-microbe interaction in order to outline specific PP2A subunits involved in beneficial plant-microbe interactions in tomato.

- Deduce the physiological role of the regulatory subunit B'φ in tomato by the gene expression analysis in different plant tissues under various growing conditions and in roots stimulated by PGPR and AMF.

- Supplement the B'φ research with a comprehensive study of transgenic tomato plants overexpressing B'φ covering the characterization of the phenotype and response to AMF.

4 Materials and methods

4.1 Chemicals and commercial kits

Table 2. Chemical and commercial kits

Commercial kit	Manufacturer
Serine/Threonine Phosphatase Assay Kit	Promega, USA
GenElute Plasmid Miniprep kit	Sigma, USA
Illustra GFX PCR DNA and Gel Band Purification Kit	GE Healthcare, England
pGEM®-T Easy Vector System	Promega, USA
Expand high fidelity PCR system	Roche, Mannheim, Germany
RNeasy® Plant Mini Kit	Qiagen, Hilden, Germany
T4 DNA Ligase 3U/µl with 10xCutSmart buffer	Promega, USA
Restriction enzymes: SpeI and XhoI	Biolabs, USA
Phire® Plant Direct PCR Kit	Thermo Fisher Scientific, Waltham, USA
SuperScript™ VILO™ cDNA Synthesis Kit	Invitrogen by Thermo Fisher Scientific, USA
DreamTaq DNA Polymerase Kit	Thermo Fisher Scientific, Vilnius Lithuania
HyperLadder™ 1kb	Bioline, USA
GelRed® Nucleic Acid Gel Stain	Biotium, USA

4.2 Plant material

4.2.1 Arabidopsis thaliana

In this study, plants of *Arabidopsis thaliana* Columbia ecotype (Col-0) were used as wild-type (WT) plants. The following T-DNA insertion mutant lines with *Arabidopsis thaliana* (Col-0) as background were studied: *lcmt-1* (SALK_079466 *(Alonso et al. 2003); ptpa* over-expressor (*ptpa ox*) (4.5x) (GABI_606E07), *pme1* knockout line (insertion in At4g10050 intron 10, GK_804C11) (Creighton et al.

2017b); *b'α* (SALK_077700); *b'β* (SALK_151740C); *b'γ* (SALK_039172); *b'ζ* (SALK_107944); *b'ϑ* (SAIL_300_B01) from the European Arabidopsis Stock Centre in Nottingham, UK (Kleinboelting et al. 2012). The homozygous mutant selection was performed via PCR using primers recommended at the SALK institute website SIGnAL available from http://www.signal.salk.edu/tdnaprimers.2.html. T-DNA insertions in each of the PP2A-C genes were identified in the TAIR and SIGnAL databases (http://signal.salk.edu; www.arabidopsis.org). The T-DNA insertion lines for *c1* (SALK_102599), *c4* (SALK_035009), *c5* (SALK_139822) and *c3* (SAIL_182_A02) were obtained from the Arabidopsis Biological Resource Center (ABRC) (Ballesteros et al. 2013). The *c2* line, originally identified and characterized in the Wassilewskija ecotype (Pernas et al. 2007), was introgressed into Col-0 after six sequential crosses (Ballesteros et al. 2013). The double mutants *c2c4*, *c2c5* and *c4c5* were received from Departamento de Genetica Molecular de Plantas, Centro Nacional de Biotecnologia CSIC, Madrid, Spain (Ballesteros et al. 2013). The *c2c4* and *c2c5* mutants were obtained by crossing *c2* (Col-0) with *c4* or *c5* respectively; *c4c5* was obtained by crossing *c4* with *c5* (Ballesteros et al. 2013; Creighton et al. 2017b).

4.2.2 Solanum lycopersicum

Plants of *Solanum lycopersicum* cv. Heinz (tomato) were used in the PGPR and AMF studies and in the *Agrobacterium*-mediated transformation protocol to deduce the physiological role of the *B'φ* gene.

4.3 Bacterial strains

4.3.1 Plant growth-promoting rhizobacteria

Azospirillum brasilense Sp245 wild-type strain (Spaepen et al. 2014) and its ipdC-knockout mutant FAJ0009 (Sp245 ipdC::Tn5), impaired in auxin biosynthesis capacity because of knock-out mutation in the key

gene for auxin biosynthesis Indole-3-pyruvate decarboxylase (ipdC) (Costacurta et al. 1994; Spaepen et al. 2007), were kindly provided by Laurent Legendre and Claire Prigent-Combaret at the University of Lyon1, France.

Pseudomonas simiae (formerly *Pseudomonas fluorescens*) WCS417r - a rifampicin-resistant mutant of the biocontrol strain *Pseudomonas simiae* WCS417 originally isolated from the rhizosphere of wheat grown in Brasil (Pieterse et al. 1996), was kindly provided by Corne´ M.J. Pieterse and I.A. Hans van Pelt from Plant-Microbe Interactions, Department of Biology, Faculty of Science, Utrecht University, The Netherlands.

4.3.2 Escherichia coli

JM109 strain of *E. coli* (Sigma-Aldrich, USA) has a high transformation efficiency. JM109 cells are suitable for bacterial transformations and recover high-quality plasmid DNA. JM109 strain contains mutations in *recA1* and *endA1* genes. These mutations aid in minimizing recombination and ensuring plasmid stability. This strain was used for subcloning of the coding region of *PP2A-B'φ*. JM109 was kindly provided by Dr. Amr Ramzy Abass Kataya, CORE, Norway.

4.3.3 Agrobacterium tumefaciens

Agrobacterium tumefaciens is living in soil, Gram-negative bacterium that widely used by biotechnologist for plant transformation due to its ability to transfer a foreign DNA to the plant genome (Slater et al. 2008).

ABI-1: The ABI-1 strain is a derivative of the well-known GV3101 strain (pMP90RK) (Ruan et al. 2018). ABI-1 carries a helper plasmid (Ti-plasmid) with the virulence genes required for T-DNA transfer and kanamycin resistance marker. It also possesses the RK2 replicase and the trf gene required for plasmid replication and rifampicin resistance marker on the chromosome. This strain was transformed with

the cloning vector pBA002 harbouring the coding region of *PP2A-B'φ* and used for *in-planta* transformation of tomato. Kindly provided by Dr. Amr Ramzy Abass Kataya, CORE, Norway.

4.4 Inoculum of arbuscular mycorrhizal fungi (AMF)

The inoculum of AMF was obtained from the granular formulation under a commercial name "Rootgrow" (PlantWorks Ltd, Sittingbourne, UK) containing propagules of spores, hyphal and root fragments colonized by *Funneliformis mossaeae, F. geosporus, Claroideoglomus claroideum, Glomus microagregatum, Phizophagus irregularis* (Bona et al. 2017).

4.5 Cloning vector

The cloning vector pBA002 was used for the tomato transformation in *Agrobacterium*-mediated DNA (T-DNA) transfer binary system. This binary vector contains a T-DNA region for the transgene insertion, the cauliflower mosaic virus (CaMV) 35S promotor, which drives the expression of a transgene at a high level in dicotyledons and considered to be expressed in all plant tissues (Slater et al. 2008). The nopaline synthase (nos) gene is used as a terminator to ensure a correct position of the transgene transcription. The pBA002 vector also carries spectinomycin marker for selection in bacteria and the herbicide phosphinothricin (PPT) or glufosinate-ammonium (or more common under trade name Basta) resistance for selection in plants. The genes which are responsible for resistance to spectinomycin and Basta are the enzyme aminoglycoside-3"-adenyltransferase (Svab et al. 1990) and PPT resistance gene (bar) encoding the enzyme phosphinothricin acetyltransferase (Slater et al. 2008) respectively. This vector was kindly provided by Prof. Simon G Møller, CORE, Norway.

4.6 Methods

4.6.1 Surface sterilization of seeds

4.6.1.1 **Arabidopsis seeds**

For surface sterilization of seeds, saturated solution of calcium hypochlorite ($Ca(ClO)_2$) was prepared by adding 250 mg of $Ca(ClO)_2$ to 25 ml of distilled water with one drop of Tween-20. The mixture was shaken vigorously and left to settle down to obtain a supernatant. The supernatant was mixed with 95% ethanol to obtain ≈ 0.1% (v/v) $Ca(ClO)_2$ in ethanol. 0.1 ml of seeds were placed in a 1.5 ml Eppendorf tube for treatment with 1 ml of 0.1% (v/v) $Ca(ClO)_2$ for 5 min followed by three washes with 95% ethanol. After the last removal of ethanol, the seeds were left with an open lid to dry overnight in a laminar flow cabinet. Thereafter, the tubes were tightly closed and sealed with para-film.

4.6.1.2 **Tomato seeds**

Seeds of *S. lycopersicum* cv. Heinz were surface sterilized with 75% ethanol for 1 min and 15% hydrogen peroxide for 15 min, rinsed 5 times with autoclaved distilled water. The sterilized seeds were sown in an appropriate medium right after the sterilization.

4.6.2 PP2A activity study

4.6.2.1 **Chemicals and buffers**

To perform the PP2A activity assay, Serine/Threonine Phosphatase Assay Kit (**Table 2**) was used. The buffers prepared for the assay are listed in **Table 3.** The procedure was performed in 50 µL reactions according to the protocols and recommendations provided by the

manufacturer (Promega 2009) using OA as a specific PP2A inhibitor. The details of the procedure are described in the below subchapters.

Table 3. Solutions and buffers for PP2A activity assay.

Buffer or solution name	**Buffer/solution composition**
Column storage buffer (Promega 2009)	10 mM Tris (pH 7.5) 1mM EDTA
Column calibration buffer (Promega 2009)	0.05 M Tris (pH 7) 0.1 mM EDTA (pH 8) 2 mM DTT (1,4-Dithiothreiol)
Extraction buffer (Chen et al. 2014; McAvoy and Nairn 2010)	0.05 M Tris (pH 7) 0.1 mM EDTA (pH 8) 2 mM DTT 0.01% (w/v) Brij 35
10 x reaction buffer (Promega 2009)	0.5 Tris (pH 7) 2 mM EDTA 0.2% (v/v) 2 – Mercaptoethanol 1 mg/ml BSA (Bovine serum albumin)
Phosphorylated peptide (RR(pT)VA)	0.1 mM (Promega,Madison, WI, USA)
Okadaic acid stock solution	0.1 mM Okadaic acid sodium salt (Sigma-Aldrich, U.S.)
Quick StartTM Bradford 1xDye reagent	Premixed **(**Bio-Rad, USA)

4.6.2.2 **Plant material and growing conditions for Arabidopsis**

4.6.2.2.1 Standard cultivation in soil

Seeds were sown in soil (3 parts of potting soil and 1 part of vermiculite) and stratified in the dark at 4°C for three days prior to cultivation under artificial light at 22°C and 12 h light/12 h dark regimen. On the day of harvesting the plants were exposed to artificial light for 3 h. The young and mature leaves of rosette stage plants were harvested 6 weeks after germination, quickly frozen in liquid nitrogen, pulverized and stored at -80°C until use.

4.6.2.2.2 Standard cultivation on ½ MS

Surface-sterilized seeds of Arabidopsis were sown (approximately 70 seeds per plate) in square Petri dishes (120 mm x 120 mm) with agar-solidified medium (1/2 MS, 1% sucrose, 0.7% agar, pH 5.8) (Murashige and Skoog 1962) (**Appendix, Table A1**). The plates were placed in the dark at 4°C for 3 days for stratification before cultivation under artificial light with 16 h light/8 h dark regimen and 22 °C. The seedlings were harvested 10 days after germination either in whole or in separate as roots and shoots. The harvested plant tissue was immediately ground in liquid nitrogen in a pre-cooled mortar, aliquoted in 1.5 mL Eppendorf tubes and stored at – 80 °C until use.

4.6.2.2.3 Cultivation with bacteria

Surface-sterilized seeds of Arabidopsis were sown (approximately 70 seeds per plate) in square Petri dishes with agar-solidified medium (1/2 MS, 1% sucrose, 0.7% agar, pH 5.8). The plates were placed in the dark at 4°C for 2 days for stratification prior to cultivation at a 16-h photoperiod for 5 days at 25 °C. To study the effect of the bacteria-plant interactions on PP2A activity, the seedlings were transplanted to new plates (70 seedlings per plate) with agar-solidified medium inoculated with corresponding bacterial strain as in **4.6.2.2.4** and **4.6.2.2.5**. All the plants were cultivated under artificial light with 16 h light/8 h dark regimen and 22 °C for 14 days with subsequent harvesting and storage at – 80 °C.

4.6.2.2.4 Preparation of plates inoculated with Pseudomonas simiae WCS417r

P. simiae WCS417r was cultured on King B medium (King et al. 1954) added 50 μg/ml of rifampicin at 28 C° overnight. The grown colonies were loosened in 10 ml of 10 mM $MgSO_4$ (Pieterse et al. 1996; Van Wees et al. 2013). The bacterial solution was collected into a 15 ml Falcon tube and centrifuged at 4000 g for 5 min with 2 subsequent

washes in fresh 10 ml of 10 mM $MgSO_4$ and centrifugation at 4000 g for 5 min. After the last wash, the supernatant was removed and the pellet was resuspended in fresh 10 ml of 10 mM $MgSO_4$, followed by measuring OD_{600} and diluting to $OD_{600} \approx 0.005$ or 10^5 cells/ml (Verhagen et al. 2010). 500 µL of the bacterial suspension was evenly spread on square Petri dishes (120 mm x 120 mm) with agar–solidified medium (1/2 MS, 0.5% sucrose, 0.7 % agar, pH 5.8) and left to dry for 30 min prior to seedling transplantation. Control plates were evenly coated with 500 µL of 10 mM $MgSO_4$.

4.6.2.2.5 Preparation of plates inoculated with Azospirillum brasilense Sp245 and FAJ0009

A. brasilense Sp245 and FAJ0009 were cultured on Luria-Bertani (LB) agar supplemented with 2.5 mM $CaCl_2$ and 2.5 mM $MgSO_4$ at 37 C° for 48 hours. For FAJ0009, 50 µg/ml kanamycin was added to the growth medium. The grown colonies were loosened and dissolved in 10 ml of 10 mM $MgSO_4$. The bacterial suspension was collected into a 15 ml Falcon tube and centrifuged for 5 min at 4000 g and 16 C°, the supernatant was removed, and the cells were resuspended in 10 ml of 0.85% NaCl and centrifuged under the same conditions. The supernatant was removed, and the cells were resuspended in another 10 ml of 10 mM $MgSO_4$ followed by measuring $OD_{600.}$ The suspension was diluted to obtain $OD_{600} \approx 0.05$ or 10^6 cells/ml (Spaepen et al. 2014). 500µl of the bacterial suspension was spread evenly on square Petri dishes (120 mm x 120 mm) with agar–solidified medium (1/2 MS, 1 % sucrose, 0.7 % agar, pH 5.8) and left to dry for 30 min prior to the seedling transplantation. Control plates were evenly coated with 500 µL of 10 mM $MgSO_4$.

4.6.2.3 **Sample preparation for PP2A activity assay**

The pulverized frozen plant tissue (≈ 0.1 g) was added 400 µl of the extraction buffer, the mixture was vigorously vortexed and incubated on

ice for 30 min combined with vortexing for 1 min from time to time. After the incubation, the samples were centrifuged at 17 000g (or maximum speed) for 60 min at 4 °C. 250 µl of the supernatant was loaded into a prepared spin column provided in the kit and eluted by centrifugation at 600 g for 5 min at 4 °C. The collected eluate was transferred to a new Eppendorf tube and kept on ice until use.

4.6.2.4 **Protein quantification assay**

The amount of total protein in extracts was quantified spectrophotometrically by Bradford protein assay (Bradford 1976; Bio-Rad n.d.) following a 1 ml cuvette assay format (Bio-Rad n.d.). A standard curve was created by plotting the 595 nm values (y-axis) versus the standard protein (BSA) concentrations (1250; 1000; 750; 500; 250; 125 µg/ml) (x-axis). Prior to absorbance reading at 595 nm, 10 µl of each protein extract was mixed with 1 ml of Quick StartTM Bradford 1xDye reagent (**Table 3**) and left for the colour development at room temperature for 5 min. The protein concentration was calculated by the equation of the standard curve, typically $y = x + 0.1$ and multiplied by the dilution factor of 2. Thus, the volume of each extract necessary for one reaction was calculated considering 5 µg of protein per 50 µl of the reaction mixture.

4.6.2.5 **PP2A activity assay**

To study PP2A activity, the reaction mixtures were prepared in 1.5 mL Eppendorf tubes as follows: phosphate-free water up to 50 µl, 5 µL of 10xreaction buffer, desalted extract (volume calculated considering 5 µg of total protein per one reaction) and 5 µL of 1 mM phosphopeptide (RRA(pT)VA). Reaction mixtures were incubated at 37 °C for 5 min and the reaction was terminated by adding 50 µL of the molybdate dye. The reaction mixtures terminated at time zero were used as controls. In reactions with OA, 0.1 or 0.25 µl of 1 µM OA solution was added to the reaction mixtures to reach 2 or 5 nM concentration of OA respectively

(Cohen et al. 1989). All the reaction mixtures were vortexed and pipetted into a corresponding well on a 96-well plate for incubation at room temperature for 15 min prior to the absorbance reading at 630 nm (Promega 2009). After the absorbance screening at 630 nm the absorbance values were converted into corresponding amounts of free phosphate using a trend line equation of the standard curve (Promega 2009). PP2A activity was calculated as the difference of phosphate released with and without OA.

4.6.3 Phenotype study of bacteria-plant interactions

4.6.3.1 **Growing conditions for plants**

Surface-sterilized seeds of Arabidopsis were sown on square Petri dishes (plates) (120 mm x 120 mm) agar-solidified medium (1/2 MS salts, 1% sucrose, pH 5.8, 0.8% agar). The plates were placed in the dark at 4°C for 2 days for stratification prior to cultivation under artificial light with 16 h light/8 h dark regimen and 22 °C for 5 days. To study the plant-bacteria interaction, the 5-day-old seedlings were then transferred to new plates (5 plants per plate) with bacteria-inoculated ½ MS medium composed specifically for each type of bacteria (**Table 4**).

Table 4. Medium composition for plant-bacteria co-cultivation.

Type of bacterium	Medium composition
Pseudomonas WCS417r	1/2 MS salts, 0,5 % sucrose, pH 5.8, 0.8% agar (Verhagen et al. 2010; Pieterse et al. 1996)
Azospirillum Sp245 and FAJ0009	1/2 MS salts, 1% sucrose, 0,05% MES (2-(N-Morpholino) ethanesulfonic acid), pH 6.0, 0.8% agar (Spaepen et al. 2014)

4.6.3.2 **Inoculation of agar plates with *P. simiae* WCS417r**

The mutant lines including WT, *c4, lcmt-1 and* $ptpa_{ox}$ were inoculated as described in **4.6.2.2.4**. For the *c2c5, c2c4* and *c4c5* and *b'*-mutants, the inoculation volume and inoculum concentration were changed from 500 to 300 µL or from 10^5 to $2x10^4$ cells/ml respectively due to changed light conditions. To study the phenotype response of Arabidopsis, 5-day-old seedlings grown as in **4.6.3.1** were transplanted to a fresh medium with an appropriate bacterial strain and cultivated for two weeks. Plants with a respective genotype grown on not inoculated medium were used as controls.

4.6.3.3 **Inoculation of agar plates with *Azospirillum* strains**

For WT, *lcmt-1*, $ptpa_{ox}$ and *c4*, the bacterial suspensions of *Azospirillum* Sp 245 and FAJ0009 were prepared as in **4.6.2.2.5** with the final concentration of OD_{600} =1 or $5x10^8$ cells/ml in 10 mM $MgSO_4$. One volume of this suspension was mixed with 9 volumes of warm (45 ºC) ½ MS medium (**Table 4**). 10 ml of the mixture was poured on 30 ml of already solidified ½ MS medium and allowed to solidify.

For WT, *c2c5, c2c4* and *c4c5*, the bacterial culture of *Azospirillum* Sp245 and FAJ0009 was grown as in **4.6.2.2.5**. The appeared colonies were used to produce an overnight culture in 5 ml of liquid Luria-Bertani (LB broth) supplemented with 2.5 mM $CaCl_2$, 2.5 mM $MgSO_4$ and 50 mg/L kanamycin whenever needed and incubated at 37 C° shaking at 180 rpm overnight. The overnight culture (0.1 ml) was subcultured in 50 ml of supplemented LB broth and incubated under the same conditions. On the following day, the bacterial suspension was collected in a 50 ml Falcon tube and centrifuged at 4000 x g for 5 min at 16 C°. After removing the supernatant, the pelleted bacteria was re-suspended in 10 mM MgSO4 and prepared as for WT, *lcmt-1*, $ptpa_{ox}$ and *c4*. Plants with a respective genotype grown on not inoculated medium were used as controls. The control Petri dishes were prepared in the same manner but using 10 mM MgSO4 instead of the bacterial suspension.

4.6.3.4 **Chlorophyll measurement**

Five shoots from each plate were weighted and thoroughly ground with 2 ml of 96% ethanol in a mortar. The obtained suspension was transferred to a 2 ml collection tube and centrifuged for 1 min at 21000 g. Prior to measuring absorbance at 654 nm, 300 µl of the supernatant was diluted with 1.2 ml of 95% ethanol. The chlorophyll content was calculated as A_{654} × 1000/39.8× extraction volume (ml) /weight of fresh tissue (mg) × dilution factor of 5 = µg chlorophyll per mg leave tissue (Wintermans 1965).

4.6.3.5 **Quantification of root system**

The root length, root thickness and number of lateral roots of Arabidopsis plants were measured using Image-J, a public domain Java image processing program available from https://imagej.nih.gov/ij/download.html.

4.6.4 Agrobacterium-mediated transformation of tomato

4.6.4.1 **Vector construction**

To construct a cloning vector harbouring *PP2A-B'φ* over-expressor (ox), the coding region of *PP2A-B'φ* including intron from *S. lycopersicum* cv. Heinz (NCBI Reference Sequence: LOC101256045) was amplified by Expand High Fidelity PCR System (Roche 2011) using flanking primers B'φ_XhoI (5'-TAGCACTCGAGATGACAAATTTTCTTGATTCTGAGACAG-3') and B'φ_SpeI (5'-CCACTAGTTCACATTGCTGCATTTTCAATTTTTTCCC-3') containing XhoI and SpeI restriction sites underlined in the nucleotide sequences. The resulting PCR product of 1505 bp including the side overhangs was separated on an agarose gel and purified with Illustra GFX PCR DNA and Gel Band Purification Kit (**Table 2**) according to the manufacturer's guidelines. The purified PCR

product was subjected to A/T ligation with pGEM-T vector using pGEM®-T Easy Vector System (**Table 2**) following the manufacturer's protocol. After ligation, the pGEM-T-PP2A-B'φ plasmid was used in the transformation of *E. coli* JM109, see **4.6.4.2**. The transformants were screened for the *PP2A-B'φ* insert on LB agar with ampicillin/IPTG/X-Gal and then by PCR using forward vector-specific primer (T7) and reverse PP2A-B'φ-specific primer (**Appendix**, **Table A3**). The positive colonies were minipreped using GenElute Plasmid Miniprep kit (**Table 2**) with subsequent sequencing in Microsynth Seqlab (Germany). The minipreped pGEM-T-*PP2A-B'φ* and pBA002 vectors were digested with XhoI and SpeI restriction enzymes (the protocol was generated online at https://nebcloner.neb.com/#redigest) with subsequent ligation using T4 DNA Ligase (**Table 2**) according to the manufacturer's protocol. The ligation product was verified by PCR and used in the transformation of *E. coli* JM109, see **4.6.4.2**. The transformants were selected on LB agar with 50 µg/ml spectinomycin as a selective marker and subjected to colony PCR using the forward pBA002-spesific primer and the reverse PP2A-B'φ-specific primer (**Appendix, Table A3**). The positive colonies were subcultured in 5 ml of liquid LB medium to amplify the plasmid DNA. The plasmid DNA was then isolated as minipreps (GenElute Plasmid Miniprep kit) and sent for sequencing to Microsynth Seqlab along with PP2A-B'φ- and pBA002-specific primers (**Appendix**, **Table A3)**. The sequencing reactions provided verification of the whole sequence of the DNA-insert which showed to be 99% identical because of three mismatches between the theoretical and obtained DNA-insert sequences of the *PP2A-B'φ* gene.

4.6.4.2 **Transformation of competent *E. coli* cells**

Competent *E. coli* JM109 were prepared as described by Chung et al. (1989) and stored at -80 C°. Ice-cold competent cells (75 µl) were thawed on ice and mixed with 7.5 µl of the ligation product, see **4.6.4.1,** by swirling the pipet tip in the cell mixture and carefully pipetting up and

down once. Following the incubation on ice for 30 min, the mixture was heated at 42 °C for 50 sec and cooled down on ice for 3 min. Then the cell culture was added 0.925 ml of LB broth and incubated at 37 °C for 2 h in a shaker at 250 rpm with subsequent inoculation on LB agar with X-Gal/IPTG/Amp for pGEM-T-*PP2A-B'φ* or on LB agar with 50 µg/ml of spectinomycin for pBA002-*PP2A-B'φ* plasmid prior to incubation at 37 °C overnight.

4.6.4.3 **Colony PCR**

Direct colony PCR was used to confirm the successful plasmid transfer into *E. coli* or *A. tumefaciens* colonies. In the case of *E. coli* JM109, a small amount of a colony was directly added and mixed well with the PCR reaction. In the case of *A. tumefaciens* ABI-1, small amount of colony was diluted in 10 µl distilled water and incubated for 3 min at 100 C° (Weigel and Glazebrook 2002) prior to adding to a PCR reaction. The PCR reactions were performed with the PP2A-B'φ- and pBA002-specific primers (**Appendix**, **Table A3**) and the DreamTaq DNA Polymerase (**Table 2**) according to the manufacturer's guidelines.

4.6.4.4 **Transformation of competent *A. tumefaciens***

Competent cells of *A. tumefaciens* ABI-1 were prepared using calcium chloride preparation of *Agrobacterium* competent cells (Tuominen 2008). Shortly, 2 ml of ABI-1 overnight LB-culture was subcultured in fresh 50 ml of LB broth with 50 µg/ml kanamycin, incubated at 28 C° for 4 hours until the concentration had reached $>10^8$ cells/ml. The bacterial culture was chilled on ice with subsequent centrifugation at 6000 g for 10 min at 4 C°. The pellet was resuspended in 1 ml of ice-cold 20 mM calcium chloride. The competent cells were snap-frozen in liquid nitrogen and stored at –80 C° as 0.1 ml aliquots. The cloning vector pBA002-*PP2A-B'φ* was transferred into the competent bacteria cells via the freeze-thaw procedure (Holsters et al. 1978). Shortly, the thawed-on ice competent cells of ABI-1 were added 1 µg of the

minipreped cloning vector. The mixture was snap-frozen in liquid nitrogen for 5 min and then heated by incubating at the 37 C° in a water bath for 15 min with subsequent adding 500 µL LB broth the tubes and incubating at 28 C° for 2-4 h. After incubation, the bacterial culture was plated on LB agar supplemented with 50 µg/ml kanamycin and spectinomycin and incubated at 28 C° for 48 h.

4.6.4.5 Plant material for transformation

Surface-sterilized seeds of tomato were sown on square Petri dishes (120 mm x 120 mm) with agar-solidified medium (4.3 g/l MS salts (Sigma-Aldrich, USA), 3% sucrose, 0.8 % agar, pH 5.8) and cultivated at 22 °C for 20 days or until the cotyledons completely opened. Three days before transformation the hypocotyls were cut in 7-10 mm fragments (explants) and placed on pre-culture medium (MS salts, 3 % sucrose, vitamins, 0.5mg/L IAA, 1 mg/l BAP, 0.7% agar, pH 5.8) (Chetty et al. 2013) and incubated for 72 hours in the dark at 27 °C (Pawar et al. 2013; Sun et al. 2015).

4.6.4.6 Preparation of bacterial culture for tomato transformation

Three days prior to the tomato transformation, 5-ml of LB broth supplemented with 50 µg/ml of kanamycin and 50 µg/ml spectinomycin was inoculated with *A. tumefaciens* ABI-1 carrying the pBA002-*PP2A-B'φ* plasmid (**4.6.4.4**) and incubated at 28 °C on a shaker at 200 rpm for 2 days. After 2 days, 1 ml of the above culture was subcultured in 100 ml of LB broth containing the same antibiotics and incubated for another 24 h under the same conditions until OD_{600} reached 1. Following incubation, the bacterial culture was centrifuged at 5000 rpm for 10 min, the pellet was resuspended in liquid MS medium (Sun et al. 2015) to OD_{600} = 0.2 (Pawar et al. 2013) and used for the tomato transformation.

4.6.4.7 **Tomato transformation**

On the day of transformation, all the explants (**4.6.4.5**) were immersed in *Agrobacterium* suspension (**4.6.4.6**) and shaken with circular movements for 20 min at room temperature. The blotted explants were dried with autoclaved filter paper, transferred to the co-cultivation medium (MS salts, vitamins, 3% sucrose, 0.7 % agar, 0.5 mg/L IAA and 1 mg/l BAP) and incubated for 2 days in the dark at room temperature (Sun et al. 2015; Chetty et al. 2013). Later, the explants were placed on the shoot induction medium (SIM) (MS salts, vitamins, 3% sucrose, 0.7 % agar, 250 mg/l cefotaxime, 250 mg/l carbenicillin, 10 mg/l BASTA, 0.5 mg/L IAA and BAP 2 mg/l) for further cultivation at 22 °C with 16 h photoperiod for 90 days changing SIM each 30 days. Explants developing Basta-resistant calli produced shoots. The shoots were excised from the calli and transferred to the root induction medium (RIM) (MS salts, vitamins, 3% sucrose, 0.7 % agar, 250 mg/l cefotaxime, 250 mg/l, carbenicillin, 0.5 mg/L IAA, 10 mg/l BASTA) and cultivated for 30 days. Non-differentiated cells were transplanted to a fresh SIM for further cultivation and growth with a subsequent transfer to RIM. Plants developed from the tomato explants with 3 cm high shoots and at least 1 cm long roots were then transferred either to vermiculite or soil and watered with an appropriate Hoagland solution or water weekly. The transformed plants were considered as $b'\varphi_{ox}$ (F_0 progeny) and used for the seed harvesting, phenotype study, AMF colonization and gene expression analysis.

4.6.4.8 **Growing conditions of WT and transgenic plants for the seed collection**

Plants developed from the tomato cv. Heinz explants as described in **4.6.4.7** were genotyped with the Phire® Plant Direct PCR Kit (**Table 2**) according to the kit manual. The positives were transferred first to vermiculite and after two months of cultivation to soil for seed production. All the transgenic plants were cultivated at 22 °C, under

artificial light with 12 h light/12 h dark regimen and watered with Hoagland solution weekly. The WT plants were cultivated in soil under the same conditions but at 16 h light/ 8 h dark regimen. The tomato fruits were harvested as soon as they looked ripen with abscission layer formed between the calyx and the fruit. Nine transgenic lines were obtained. The harvested seeds were sorted by line numbers and stored for various studies.

4.6.5 Plant genotyping and transgene detection

All the transgenic plants were genotyped for the 35S:PP2A-B'φ insert using Phire® Plant Direct PCR kit (**Table 2**) before any analysis. The harvesting of leave tissue was performed according to "Dilution protocol" and the PCR program was worked out following the manufacturer's recommendations. The primers, PCR program and expected PCR products are shown in **Appendix, Table A3**. The PCR products were separated on 1.2% agarose gel at 90V for 40 min and visualized using ChemiDoc imaging system (Bio-Rad).

4.6.6 Tomato growing conditions for various studies

4.6.6.1 **Standard growing conditions and plant material for gene expression analysis in different plant organs**

Tomato plants were grown in soil (75% potting soil and 25% vermiculite) in 0.5 L plastic plant pots or in double autoclaved vermiculite in 0.4 L standard Magenta boxes at 22 °C and under artificial light with 16 h light/8 h dark regimen, watered weekly with tap water and (only for vermiculite) monthly with Hoagland solution. On the day of harvesting, each plant was carefully pulled out from the box to strip the root. The root tissue was detached and snap-frozen in liquid nitrogen with subsequent storage at – 80 °C until used in the gene expression analysis. The young leaves and flower buds of 5-12 mm were harvested

and snap-frozen in liquid nitrogen at the same time. The plant tissue was kept at – 80 ºC until used in the gene expression analysis.

4.6.6.2 Growing conditions for plants inoculated with PGPR for gene expression analysis

WT tomato plants were grown in 0.4 L standard Magenta boxes with double autoclaved vermiculite at 22 °C and under artificial light with 16 h light/8 h dark regimen and watered weekly with Hoagland solution and with tap water whenever needed. On the 41st day after sowing, the plants were inoculated with 50 ml of corresponding bacteria suspended in 10 mM $MgSO_4$ as described in **4.6.2.2.4** and **4.6.2.2.5,** with the concentration of $5x10^7$ cells/ml for *Azospirillum* strains and 2.5 $x10^5$ cells/ml for *P. simiae* WCS417r. The plants added 50 ml of 10 mM $MgSO_4$ were used as controls. The root tissue for the gene expression analysis was harvested 2 h, 24 h, 1 week and 3 weeks after the inoculation. The plant tissue was snap-frozen in liquid nitrogen with subsequent storage at – 80 °C until used in the gene expression analysis. To measure the plant growth parameters at the end of the experiment, the plants were pulled out from the vermiculite, the roots were washed and dried prior to weighing.

4.6.6.3 Growing conditions for plants for AMF experiments

For cultivation with AMF, 1.5 ml of "Rootgrow" granules were added to the planting hole in each pot/Magenta box and covered with small amount of soil or vermiculite before sowing tomato seeds or planting seedlings. No granules (soil) or triple autoclaved granules (vermiculite) were added to the growing medium for control plants. The plants were grown at 22 °C and under artificial light with 16 h light/8 h dark (soil) or 12h light/12 dark regimen (vermiculite) and watered weekly with tap water (soil) or Hoagland solution (vermiculite) with ten times reduced phosphate concentration (0.1 mM PO_4^{3-}) for at least first seven weeks or until plants showed profound signs of phosphate deficiency to induce the

germination of AMF and then watered with regular Hoagland weekly (soil and vermiculite). Two weeks prior to harvesting, the plants were watered only with tap water. On the day of harvesting, each plant was pulled out from the box to strip the root. The root tissue was detached, rinsed with tap water and prepared for microscopy on the same day. For the gene expression analysis, the detached root tissue was snap-frozen in liquid nitrogen with subsequent storage at – 80 °C until use.

4.6.6.4 Growing conditions for plants used for microscopy and gene expression studies of *b'φox* (F_0)

Plants of *b'φox* lines (F_0) described in **4.6.4.7** were transferred to 0.4 l Magenta boxes with double autoclaved vermiculite or 0.5 L plastic plant pots with soil (75% potting soil and 25% vermiculite). WT plants were cultivated in Petri dishes under axenic conditions for 18 days at 22 °C and under artificial light with 16 h light/ 8 h dark regimen, transferred to a corresponding growing medium and cultivated further in the same manner as the transgenic plants. For AMF studies, the plants were planted and cultivated as in **4.6.6.3**.

4.6.6.5 Growing conditions for phenotyping, microscopy and gene expression studies of *b'φox* (F_1)

Seeds collected from *b'φox* (F_0) and WT plants were sown in double autoclaved and properly soaked with tap water vermiculite, cultivated under artificial light with 12h light/12 dark regimen, at 22 ºC and watered with Hoagland solution weekly for 9 weeks. For the gene expression analysis, the young leaves from the top of each plant were harvested and snap-frozen in liquid nitrogen with subsequent storage at – 80 °C until use. The cultivation with AMF and subsequent harvesting of roots for microscopy analysis was performed as described in **4.6.6.3** for vermiculite.

4.6.7 Sample preparation for bright-field microscopy

The harvested roots were thoroughly washed with tap water, dried with a paper tissue, boiled in 10% KOH for 1 min and left in this solution overnight at room temperature. On the following day, the roots were rinsed 3 times with tap water, dried and dipped in 3.7% solution of hydrochloric acid for 2-3 minutes. After removing the acid solution, the staining solution was added. The staining solution was prepared as follows: lactophenol with trypan blue (25% phenol, 25% lactic acid, 25% glycerol, 25 % of 4 mg/ml trypan blue stock solution, final concentration was 1 mg/ml or 0.1%) (Weigel and Glazebrook 2002) was added two volumes of 95% ethanol. The root tissue was placed in 1.5 ml Eppendorf tubes, covered with the staining solution and heated on boiling water bath for 1 minute with subsequent incubation on a shaker at room temperature for 4-16 hours. After removing the staining solution, the roots were covered with the destaining solution (2.5 g/ml chloral hydrate) (Vierheilig et al. 2005), incubated for 6 hours at room temperature before the solution was replaced with a fresh one and incubated overnight. The destaining solution was removed prior to covering the roots with 70 % glycerol.

4.6.8 Estimation or root colonization by AMF

Three slides with 20 stained root fragments by 5-8 mm from each plant were prepared. The stained roots were examined under a light microscope with 10x and 100x magnification lenses for AM structures such as spores, vesicles and arbuscules. The frequency of AMF colonization (F%) was calculated as a percentage of the root fragments with AM structures.

4.6.9 Semiquantitative RT-PCR analysis of gene expression

A semiquantitative reverse-transcriptase polymerase chain reaction (sqRT-PCR) (also called gel-based RT-PCR) is a highly sensitive and specific method useful for the detection of rare transcripts as well as to assess the expression levels of multiple transcripts from the same RNA sample. The gene expression analysis based on sqRT-PCR usually consists of several steps: RNA isolation, cDNA synthesis, PCR, separation of PCR products by gel electrophoresis, visualization and densitometric analysis of amplified PCR products (bands).

4.6.9.1 **RNA isolation**

Total RNA from 50-100 mg of frozen plant tissue was extracted using RNeasy mini kit from Qiagen **(Table 2**). Sample handling before RNA extraction was performed according to the manufacturer's guidelines (QIAGEN 2012). The isolated RNAs were quantified on NanoDrop Spectrophotometer. The RNA extracts were diluted to 100 ng/µl and stored at -80 ℃ if not used on the same day.

4.6.9.2 **Reverse transcription**

First-strand cDNA was synthesized from 1 µg of the total RNA using SuperScript IV VILO Master Mix (**Table 2**). The cDNA synthesis was performed following the manufacturer's reverse transcription protocol for SuperScript IV VILO Master Mix (with ezDNase enzyme treatment) (TFS 2014). The obtained cDNAs were diluted to 12.5 ng/µl and used as a template for amplification in PCR for analysing the expression of genes listed in **Appendix, Table A3**.

4.6.9.3 **PCR amplification**

Polymerase chain reaction (PCR) was performed in 10 µl reactions using DreamTaq DNA Polymerase kit (**Table 2**). The protocol and program

for thermal cycling conditions (**Appendix, Table A3**) were fulfilled according to the manufacturer's guidelines (TFS 2016).

4.6.9.4 **Densitometric gene expression analysis**

The PCR products were separated on 1.2% agarose gels by electrophoresis at 90 V, 1.2% and 40 min and visualized using GelRed® fluorescent nucleic acid dye gel. The picture of each gel blot was taken in the Bio-Rad ChemiDoc imaging system (Bio-Rad) and the amount of each PCR product was quantified with help of Bio-Rad Image-Lab 6.0 Software. The expression level of the reference gene *ACTIN41* was measured three times in each tomato plant and used as an endogenous mRNA standard. The averaged value of the band intensities from at least three biological replicates (three plants of the same line and treatment) was used to calculate a transcript level. Relative quantification of the transcript levels was based on the normalization of the target gene band densities with respect to an averaged *ACTIN41* band density to allow comparison of mRNA levels.

4.6.10 Statistical analysis

All experimental data were analysed with the Excel statistical package (version Microsoft 365). The results were summarized as mean ±standard error (SE). Student's t-test (unpaired samples t-test) was applied to compare the means of two data sets. A Pearson product-moment correlation was conducted to determine the strength of a linear relationship between PP2A activity and fresh weight changes in Arabidopsis WT and mutants caused by PGPR. The correlation was assumed as strong whenever the Pearson product-moment correlation coefficient (Pearson's coefficient) (r) was $|r| > 0.7$ (Akoglu 2018). Possible outliers for fresh weight changes were detected by visually inspecting the scatter plots of PP2A activity against fresh weight changes in Arabidopsis for wayward (extreme) points that bucked the trend of the data.

4.6.11 Phylogenetic analysis

To trace evolutionary relationships in terms of common ancestry and orthology between tomato and Arabidopsis, a phylogenetic analysis of PP2A subunits studied in this research was performed. The coding sequences of PP2A subunits from Arabidopsis (**Table 5**) were acquired from the TAIR database (www.arabidopsis.org/) and NCBI Genbank (https://www.ncbi.nlm.nih.gov/genbank/) using TAIR as a primary source and the nomenclature described by Lillo C. et al. (2014).
The protein-coding sequences of PP2A subunits of tomato (
Table 6) were acquired from International tomato annotation group (ITAG) (https://solgenomics.net/) and NCBI Genbank (https://www.ncbi. nlm.nih.gov/genbank/) respectively, using NCBI as a primary source. The PP2A subunits were named in accordance with the data listed in Booker and DeLong (2017) whenever a clear title was missing in Genbank. The PP2A-C3 and –C4 subunits were defined using the information provided by He et al. (2004) combined with the gene and protein multiple sequence alignment performed with online software Clustal Omega (https://www.ebi.ac.uk/Tools/msa/clustalo/).

Table 5. Protein coding sequences of *Arabidopsis thaliana* used for the phylogenetic tree in *Error! Reference source not found.***.**

PP2A subunit	AGI locus ID	NCBI reference
AtPP2A-C1	At1g59830	NP_176192.1
AtPP2A-C2	At1g10430	NP_001322206.1
AtPP2A-C3	At3g58500	NP_567066.1
AtPP2A-C4	At2g42500	NP_565974.1
AtPP2A-C5	At1g69960	NP_177154.1
AtPP2A-A1	At1g25490	NP_173920.1
AtPP2A-A2	At3g25800	NP_001326959.1
AtPP2A-A3	At1g13320	NP_001184981.1
AtPP2A-Bα	At1g51690	NP_001185199.1
AtPP2A-Bβ	At1g17720	NP_849681.1
AtPP2A-B'η	At3g26020	NP_001030770.1
AtPP2A-B'θ	At1g13460	NP_172803.1
AtPP2A-B'κ	At5g25510	NP_197933.1

Table 6. Protein coding sequences of tomato used for the phylogenetic tree in Figure 1.

PP2A subunit	ITAG 4.0 ID	NCBI reference
SolycPP2A-C1	Solyc05g006590.3.1	NP_001234516.2
SolycPP2A-C2	Solyc01g011340.2	NP_001233804.1
SolycPP2A-C3	Solyc01g005950.4.1	NP_001334782.1
SolycPP2A-C4	Solyc01g034020.3.1	XP_004228954.1
SolycPP2A-C5	Solyc01g073650.3.1	XP_004229332.1
SolycPP2A-AβI-1	Solyc04g007100.4.1	XP_004236962.1
SolycPP2A-AβI-2	Solyc04g007100.4.1	XP_010319425.1
SolycPP2A-AβII-1	Solyc05g009600.4.1	XP_004238945.1
SolycPP2A-AβII-2	Solyc05g009600.4.1	XP_019069577.1
SolycPP2A-Aα	Solyc06g069180.3.1	NP_001333821.1
SolycPP2A-Bβ (Clade I)	Solyc06g071560.2	XP_004241504.1
SolycPP2A-Bβ-1 (Clade III)	Solyc12g044800.3.1	XP_010314308.1
SolycPP2A-Bβ-2 (Clade III)	Solyc12g044800.3.1	XP_004252372.1
SolycPP2A-Bβ-3 (Clade III)	Solyc12g044800.3.1	XP_019067115.1
SolycPP2A-B'θ	Solyc05g014340.2	XP_004239176.1
SolycPP2A-B'κ	Solyc12g006920.1	XP_004251590.1
SolycPP2A-B'φ	Solyc01g111790.1	XP_010315393.2

The protein sequences listed in **Table 5** and **Table 6** were aligned in Clustal Omega in NEXUS mode and visualized as a phylogenetic tree using iTOL online software (https://itol.embl.de/) in **Figure 1**.

5 Results

The first PP2A activity assays were done in connection with research on different aspects, i.e. nitrate reductase activation and PP2A methylation in response to environmental signals (Papers III and IV). The most important findings described in detail in **5.1 - 5.3** are presented in Paper I, and the most important findings described in **5.4.-5.5** are presented in Paper II.

5.1 PP2A activity in Arabidopsis WT and mutants

At first, the extractable PP2A activity was assayed in young and mature leaves of 6-week-old Arabidopsis plants including WT and mutant lines *lcmt-1, pme1 and* $ptpa_{ox}$ with mutations in the genes associated with the PP2A regulation: *LCMT-1, PME1* and *PTPA* respectively (**Figure 3**). The obtained results showed that the $ptpa_{ox}$ line had a significantly higher PP2A activity compared with WT and supported findings published by Chen et al. (2015). Afterwards, the extractable PP2A activity was assayed in 10-day-old Arabidopsis seedlings, which included WT, single and selected double mutants of the PP2A catalytic subunits, using OA as PP2A selective inhibitor (**Figure 4B**). The total phosphatase activity was also measured and calculated as phosphate release detected during the reaction without OA (**Appendix, Figure A1**). Both datasets indicated that the PP2A activities, as well as the total phosphatase activities, were considerably lower in *c2, c4, c2c5, c2c4* and *c4c5* mutants compared with WT. It is noteworthy that the PP2A mutants exhibited also different phenotypes (**Figure 4A**). These mutants along with *lcmt-1,* which was previously studied for PP2A activity (Chen et al. 2014; Creighton et al. 2017a), were selected for more detailed analysis separately in roots and shoots. For this experiment, the procedure was updated in terms of the OA concentration which was increased from 2 nM to 5 nM to improve the inhibitory efficiency of OA in the cell extract matrix (Swingle et al. 2007). The activity values for shoots and roots showed the same trend as

in the whole seedlings displaying a significant reduction in both PP2A and total activities in roots and shoots (**Figure 5** and **Appendix, Figure A2**) except for the value found in the root of *c2*. A 30% reduction of the PP2A activity in *lcmt-1* was in line with results previously reported by Chen et al. (2014).

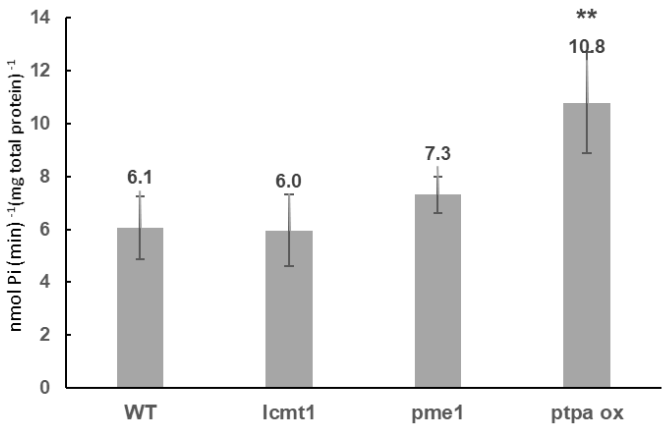

Figure 3. PP2A activity in WT, *lcmt-1, pme1 and ptpa$_{ox}$*.
PP2A activity was assayed in young and mature leaves of rosette stage plants grown in soil and harvested 6 weeks after germination. Activity is given as phosphate release inhibited by 2 nM OA. Values are means ±SE from five plants (n=5). Two asterisks denote values significantly different from WT according to student's t-test at p-value < 0.05.

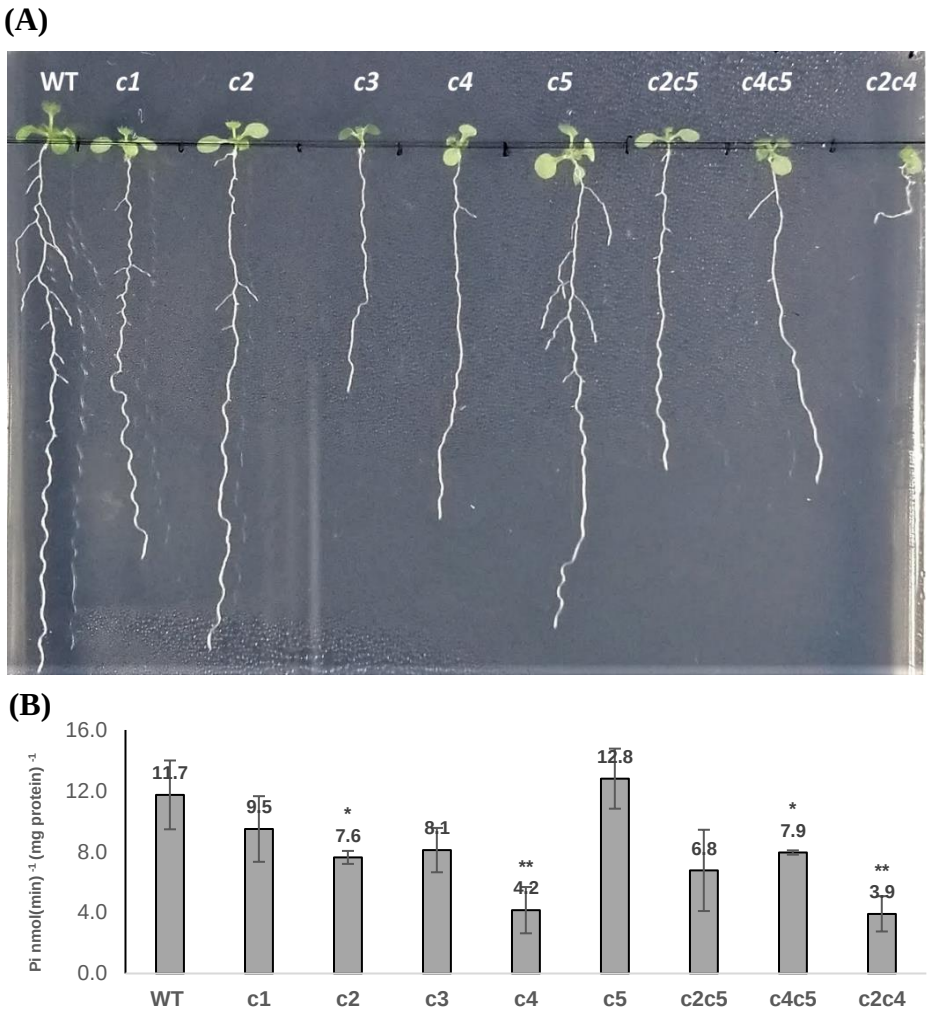

Figure 4. Visual phenotype and PP2A activity of 10-day-old seedlings of WT and various PP2A mutants.
(**A)** Arabidopsis seedlings 10 days after germination on ½ MS medium. (**B)** PP2A activity assayed in WT and selected mutant lines. Activity is given as phosphate release inhibited by 2 nM OA. Values are means ±SE from three independent experiments. One or two asterisks denote values significantly different from WT according to student's t-test at p-value <0.1 or 0.05 respectively.

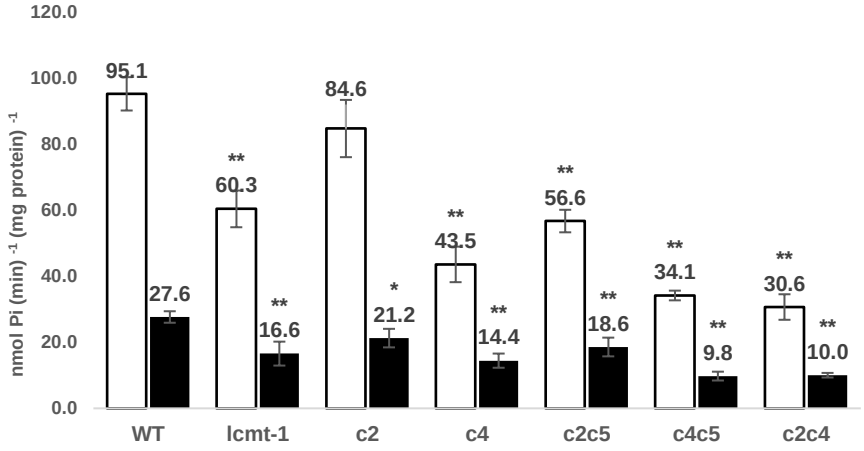

Figure 5 . PP2A activity in WT and selected mutant lines.
Activity was assayed separately in roots (white bars) and shoots (black bars) of 10-day-old seedlings grown on ½ MS medium. Activity is given as phosphate release inhibited by 5 nM OA. Numbers above each column are means ±SE collected from three independent experiments (n=3). Values marked with one or two asterisks are significantly different from WT according to student's t-test at p-value <0.1 or 0.05 respectively.

5.2 PP2A activity in Arabidopsis WT treated with PGPR

To check if PP2A activity was influenced by treatment with PGPR, its values in roots and shoots of Arabidopsis seedlings co-cultivated with Sp245 and WCS417r for two weeks was compared with those of non-treated control plants, **Figure 6**. Despite the pronounced phenotype response observed in the plants grown with bacteria, PP2A activity had no deviations from the control values, therefore, no impact of the PGPR inoculation on PP2A activity was detected.

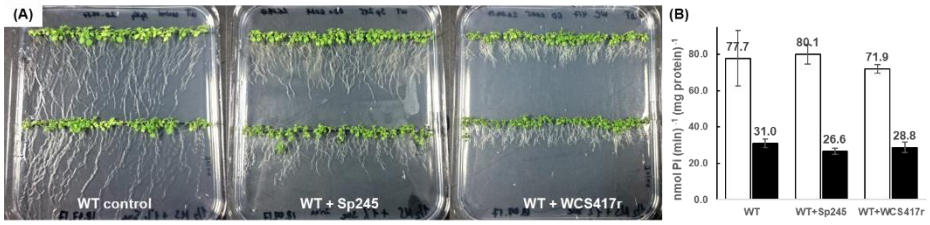

Figure 6. Visual phenotype and PP2A activity of Arabidopsis not treated and treated with PGPR.
(A) Control plants were grown without bacteria (left plate) or co-cultivated with Sp245 (middle plate), or with WCS417r (right plate) for 14 days. (B) PP2A activity assayed separately in roots (white bars) and shoots (black bars). Numbers above each column are means ± SE collected from three independent experiments (n=3). Values for plants treated with bacteria were not significantly different from non-treated plants according to student's test at $p < 0.1$.

5.3 Phenotype response of Arabidopsis to Pseudomonas and Azospirillum

To deduce the role of PP2A in the signalling between plants and PGPR, the mutant lines of Arabidopsis with significant deviations in PP2A activity, both increased as in *ptpa*$_{ox}$ ((**Figure 3**); (Chen et al. 2015)) and reduced as in *lcmt-1*, the single mutant *c4* and the double mutants *c2c5*, *c4c5* and *c2c4* (**Figure 5**), were studied. The cultivation of Arabidopsis mutant lines with PGPR and data acquisition were performed as in **4.6.3**. The lines including WT, *c4*, *lcmt-1* and *ptpa*$_{ox}$ were studied first. The second series of experiments was a follow-up of the first one where WT, *c2c5*, *c4c5* and *c2c4* were studied. Since the light growing conditions were slightly different due to different sampling times, the results of the first and second series are presented in separate diagrams with their respective WT references. To study the phenotype response of Arabidopsis, one-week-old seedlings grown in Petri dishes were transplanted to a fresh medium with an appropriate bacterial strain and cultivated for two weeks. Plants from a corresponding mutant line grown on the non-inoculated medium were used as controls.

5.3.1 Cultivation with Pseudomonas simiae WCS417r

For this study, Arabidopsis plants were cultivated as in **4.6.3.1** and **4.6.3.2.** Already by visual inspection, the root architecture of all WCS417r-treated plants looked strikingly influenced by the bacteria resulting in a shorter primary root and branched root organization (**Figures 7** and **9**). It was reflected in the lateral root density which was significantly higher in all the lines treated with WCS417r relative to the corresponding controls (**Figures 8F** and **10F**). Furthermore, the primary root length of the treated plants ranged from 26 to 36% of that of the control plants (**Figures 7, 8A, 9 and 10A**). The quantification of lateral roots revealed an increase in lateral root number in all the lines but *c2c5* and *lcmt-1*. Shoot fresh weight, root fresh weight and primary root thickness increased in all the lines upon WCS417r treatment except for *c2c5* (**Figures 8** and **10**). Chlorophyll content increased in all the treated plants with its significantly higher values in WT, *lcmt-1* and *c4* with respect to the corresponding controls (**Figures 8G** and **10G**). The treated *lcmt-1* almost reached the WT values both in the chlorophyll content and shoot fresh weight. The same changes were observed in *c4* and *c4c5* lines. The effect of WCS417r treatment on fresh weight in WT and in the mutant lines on a percentage basis was summarized and arranged in increasing order of PP2A activity in **Figure 11**. According to this summary, the fresh weight was significantly higher in plants treated with WCS417r. Considering all the results, the effect of the inoculation with WCS417r on the fresh weight decreased as PP2A activity increased, and this tendency can be traced especially for the shoot fresh weight. The maximal increase of fresh weight with almost the same per cent changes was observed in *c4* and *c4c5*. The minimal changes might have been assigned to $ptpa_{ox}$, if there were not a considerable deviation from the above tendency found in *c2c5* and *c2c4*. The growth-promoting effect of WCS417r in the latter mutants was hampered in roots or even reversed in shoots, showing inhibition of the shoot growth by 5 and 21% in *c2c5* and *c2c4*, respectively, compared with the control plants.

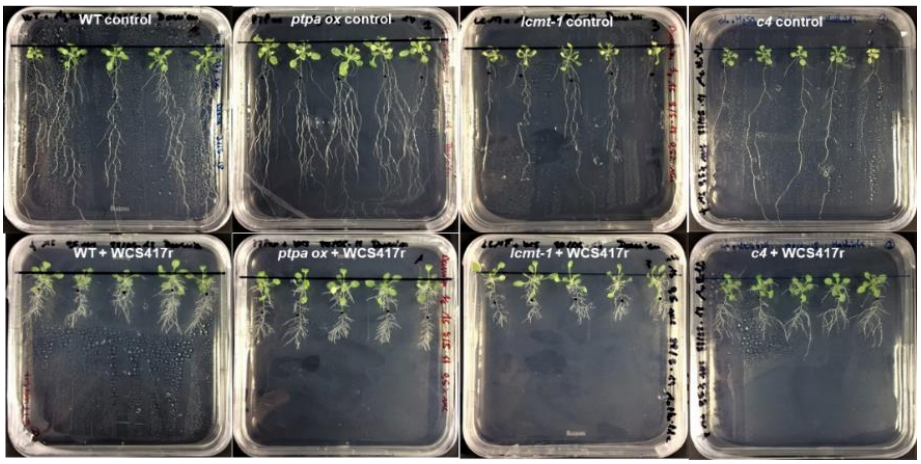

Figure 7. Visual phenotype of Arabidopsis WT and mutants treated with *P. simiae* WCS417r.
Seedlings of Arabidopsis WT and mutants (*ptpa*$_{ox}$, *lcmt-1 and c4*) cultivated without (upper row) and with *P. simiae* WCS417r for two weeks.

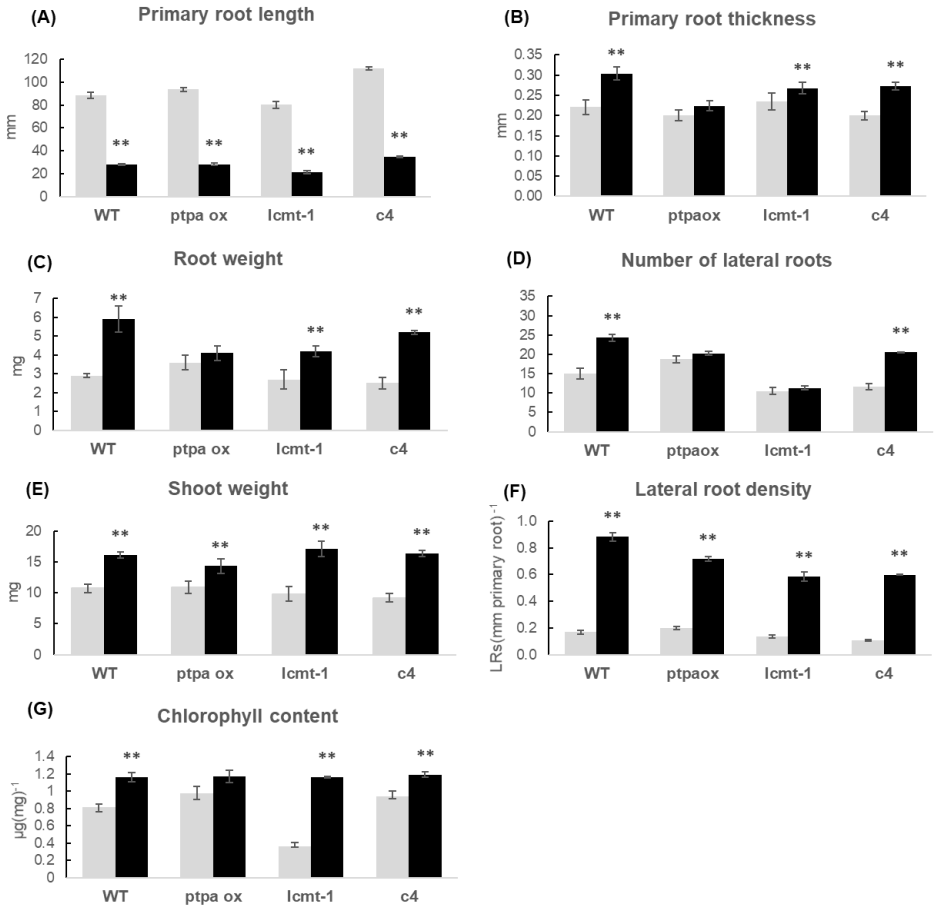

Figure 8. Growth parameters of WT and mutants treated with *P. simiae* WCS417r.
Seedlings of Arabidopsis WT, *ptpa*$_{ox}$, *lcmt-1* and *c4* were cultivated without (grey bars) and with (black bars) *P. simiae* WCS417r for two weeks. (A) primary root length; (B) primary root thickness; (C) root fresh weight; (D) number of lateral roots; (E) shoot fresh weight; (F) lateral root (LRs) density and (G) chlorophyll content. For root length, primary root thickness, lateral root density and number of lateral roots, data are means ± SE of 30 plants (n=30). For fresh weight and chlorophyll content, the plants in each plate were pooled for measurements and values are means ±SE of six independent experiments (n=6). The root and shoot weights (C) and (E) represent means ±SE per single plant. The chlorophyll values (G) represent µg chlorophyll per mg leaf tissue. Columns marked with two asterisks are significantly different from the control without bacteria according to student's t-test at p-value < 0.05.

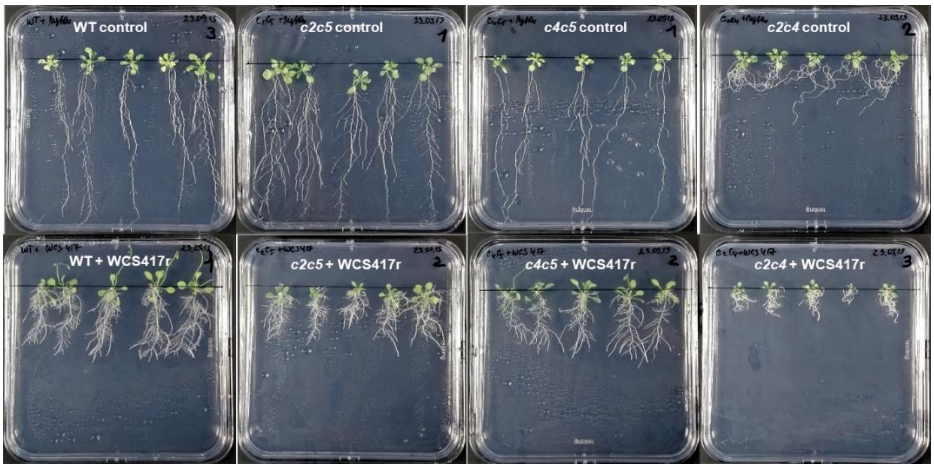

Figure 9. Visual phenotype of Arabidopsis WT and double mutants treated with *P. simiae* WCS417r.
Seedlings of Arabidopsis WT and double mutants *c2c5*, *c4c5* and *c2c4* were cultivated without (upper row) and with *P. simiae* WCS417r (lower row) for two weeks.

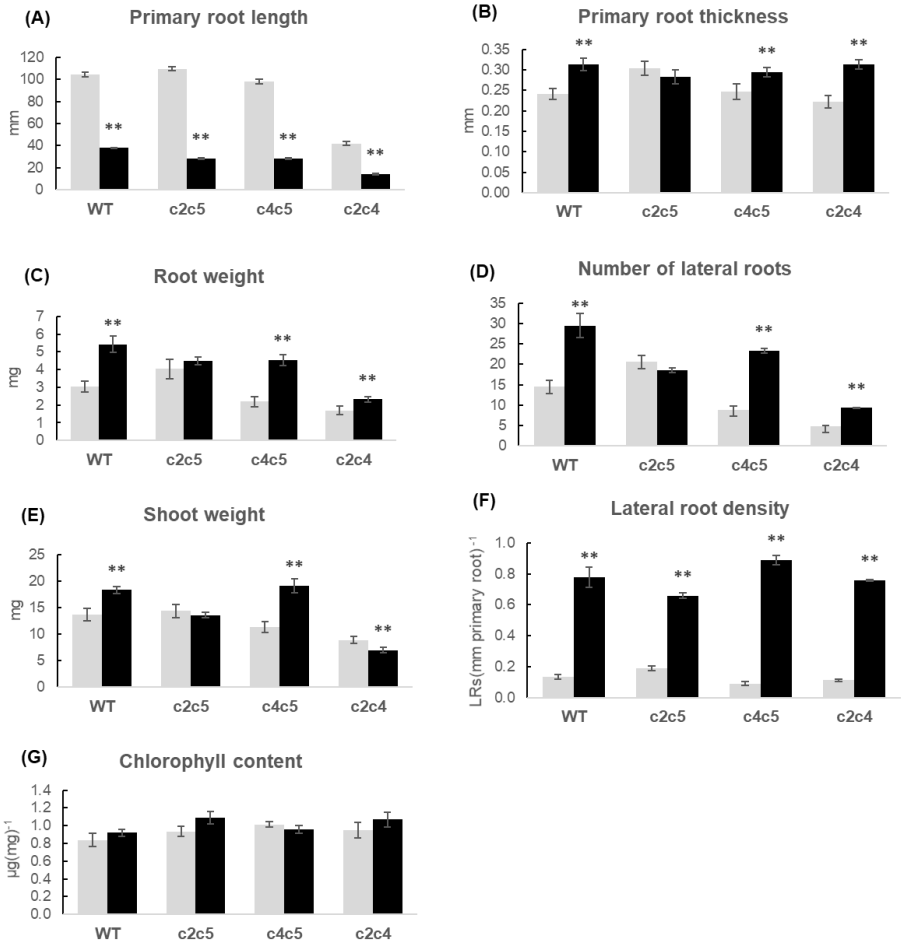

Figure 10. Growth parameters of WT and double mutants treated with *P. simiae* WCS417r. Seedlings of Arabidopsis WT and double mutants *c2c5*, *c4c5* and *c2c4* were cultivated without (grey bars) and with (black bars) *P. simiae* WCS417r for two weeks. (A) primary root length; (B) primary root thickness; (C) root fresh weight; (D) number of lateral roots; (E) shoot fresh weight; (F) lateral root (LRs) density and (G) chlorophyll content. For root length, primary root thickness, lateral root density and number of lateral roots, data are means ± SE of 45 plants (n=45). For fresh weight and chlorophyll content, the plants in each plate were pooled for measurements and values are means ±SE of nine independent experiments (n=9). The root and shoot weights (C) and (E) represent means ±SE per single plant. The chlorophyll values (G) represent µg chlorophyll per mg leaf tissue. Columns marked with two asterisks are significantly different from the control without bacteria according to student's t-test and p-value < 0.05.

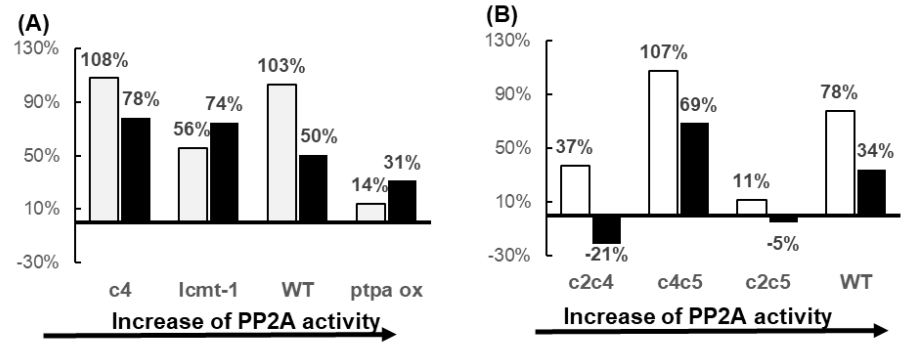

Figure 11. Per cent changes in fresh weight of Arabidopsis WT and mutants caused by *P. simiae* WCS417r.
Fresh weight changes in roots (white bars) and shoots (black bars). Data are from Figures 8 and 10. The data sets are arranged in order of increasing PP2A activity (from Figure 5).

The *c2* and *b'* mutant lines (*b'α, b'β*, *b'γ, b'θ, b'ζ)* were also subjected to inoculation with WCS417r (**Appendix, Figure 4A**). These mutants had previously been implicated in the response to bacterial pathogens (Segonzac et al. 2014; Jin et al. 2016; Durian et al. 2016). By observations, all the lines showed a similar response to the inoculation. However, the quantification of various root parameters (**Appendix, Figure A5**), revealed that *c2*, *b'α* and *b'θ* developed significantly fewer lateral roots in response to the bacteria than their respective controls. The most outstanding decrease in this value was found in *b'θ* (by 50%) along with corresponding decrease by 22% in *c2* and 13% in *b'α.*

5.3.2 Cultivation with Azospirillum brasilense Sp245 and FAJ0009

For this study, Arabidopsis plants were cultivated as in **4.6.3.1** and **4.6.3.3.** The plants showed a pronounced response to inoculation with *Azospirillum* strains resembling the response to WCS417r (**Figures 12** and **14**). For Sp245-treated plants, the primary root length ranged from 23 to 55 % of that in non-treated plants (**Figure 13A** and **15A**). An

increase in the root fresh weight was in general due to elevated lateral root density (**Figures 13F** and **15F**). Although, WT, *ptpa*$_{ox}$, *c4* and *c2c4* had also a thicker primary root compared with the non-treated controls (**Figures 13B** and **15B**). The primary root length in plants treated with FAJ0009 was not affected in the first series of experiments (**Figures 12** and **13**), while a quite significant reduction (55% on average) of this value was observed in the second series of experiments (**Figures 14** and **15**). Comparing the changes caused in WT upon the bacteria inoculation in the two series, deviations in the experimental conditions in the second series favoured a stronger response of the plants. Unlike the observed reduction of number of lateral roots in the Sp245-treated plants, most of the lines responded to FAJ0009 by increasing this number except for *c2c5* and *c4c5*, which showed a significant decrease or no changes in this value with respect to untreated plants. Otherwise, the plants responded to *Azospirillum* strains similarly although to a lesser degree in the case of FAJ0009. Chlorophyll content generally was unchanged or insignificantly reduced in most of the Sp245-treated plants, only *c2c5* showed a striking chlorophyll reduction upon the Sp245 treatment (**Figure 15G**). The same effect on chlorophyll content was observed in the FAJ0009-treated plants. After inoculation with *Azospirillum* strains, a notable improvement in growth was observed in *lcmt-1*, *c4*, *c4c5* and *c2c4*, even though to a lesser extent in the FAJ0009-treated plants **(Figures 13C, E** and **15C, E**). The effect of inoculation with Sp245 and FAJ0009 on fresh weight of Arabidopsis plants on a percentage basis was summarized and arranged in increasing order of PP2A activity in **Figure 16**. According to this summary, the fresh weight was significantly higher in most of the plants treated with *Azospirillum* strains compared with untreated plants except for *c2c5*, which showed a significant reduction in shoot fresh weight. The chart in **Figure 16** resembles the summary made for WCS417r in **Figure 11**. In general, the effect of inoculation on the fresh weight (both roots and shoots) of the *Azospirillum*-treated plants decreased with an increasing PP2A activity. The maximal increase of fresh weight was found in *c4* and *c4c5* treated

with Sp245 (**Figure 16 A,B**). However, upon cultivation with FAJ0009, *c2c4* showed the maximal growth improvement compared with the other genotypes (**Figure 16 C,D)**. The minimal response or even stunted growth was detected in *c2c5* treated with both strains, even though this response was less profound in the case of FAJ0009.

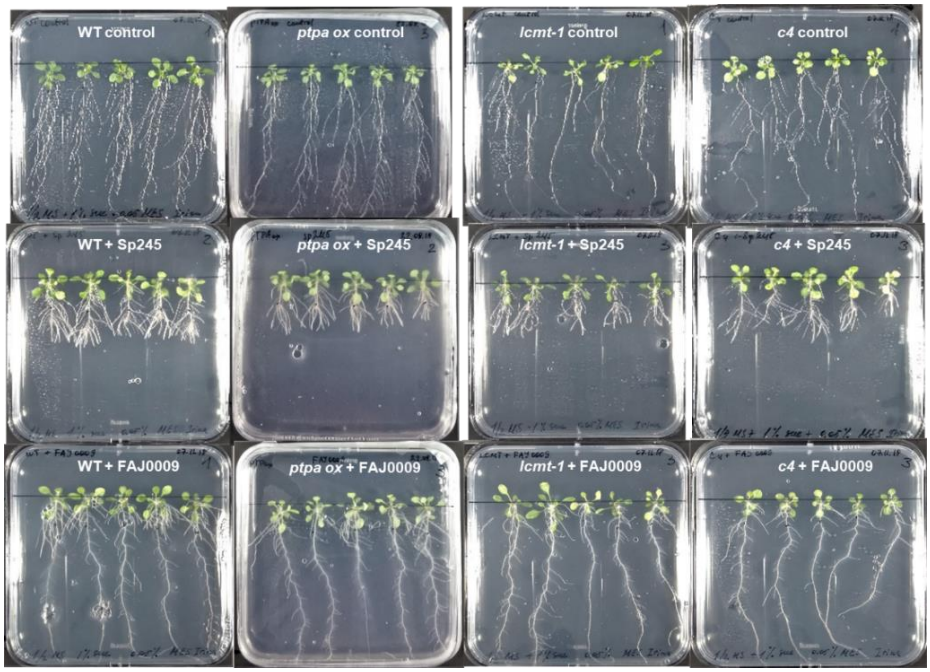

Figure 12. **Visual phenotype of Arabidopsis WT and mutants treated with *A. brasilense*.** Seedlings of Arabidopsis WT and mutants *ptpa*$_{ox}$, *lcmt1*, *c4* were cultivated without bacteria (upper row) and with *A. brasilense* Sp245 (middle row) and *A. brasilense FAJ0009* (lower row) for two weeks.

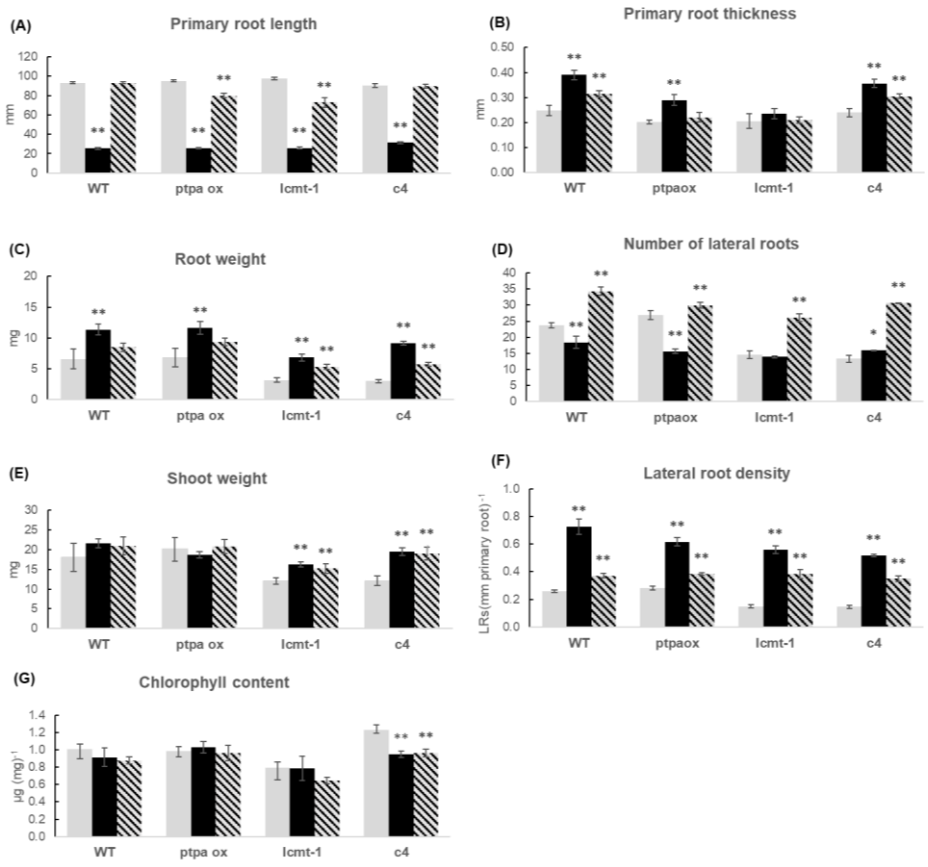

Figure 13. Growth parameters of WT and mutants treated with *A. brasilense Sp*245 and FAJ0009.

Growth parameters of WT and mutants *ptpa*$_{ox}$, *lcmt1*, *c4* cultivated without bacteria (grey bars), with *A. brasilense* Sp245 (black bars) and with *A. brasilense* FAJ0009 (hatched bars) for two weeks. (A) primary root length; (B) primary root thickness; (C) root fresh weight; (D) number of lateral roots; (E) shoot fresh weight; (F) lateral root (LRs) density and (G) chlorophyll content. For root length, primary root thickness, lateral root density and number of lateral roots, data are means ± SE of 30 plants (n=30). For fresh weight and chlorophyll content, the plants in each plate were pooled for measurements and values are means ±SE of six independent experiments (n=6). The root and shoot weights (C) and (E) represent means ±SE per single plant. The chlorophyll values (G) represent µg chlorophyll per mg leaf tissue. Columns marked with two asterisks are significantly different from the control without bacteria according to student's t-test and p-value < 0.05.

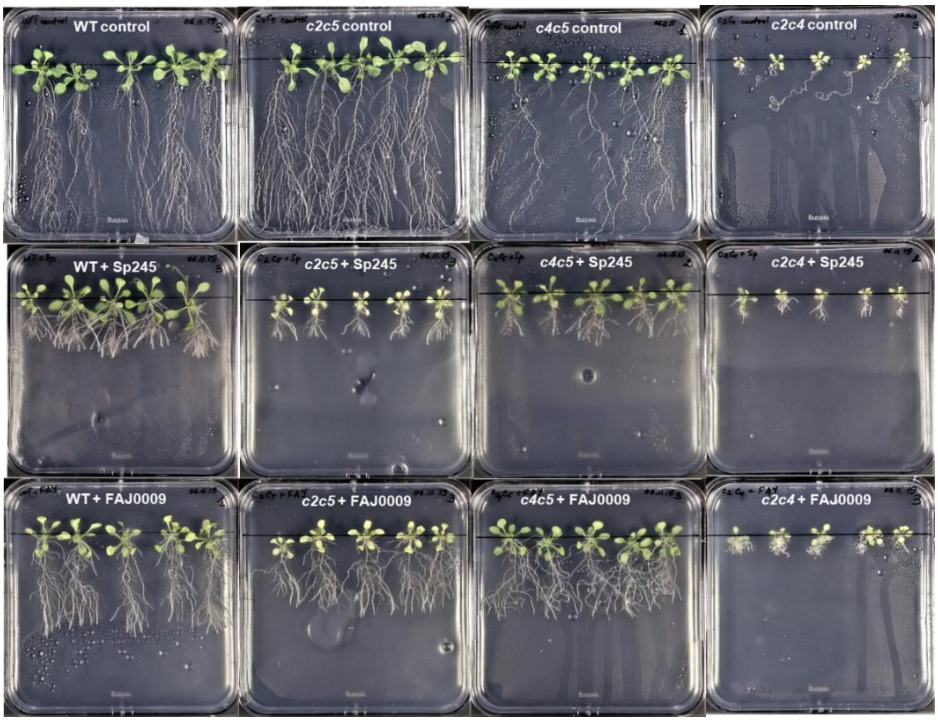

Figure 14. Visual phenotype of Arabidopsis WT and double mutants treated with *A. brasilense*.
Seedlings of Arabidopsis WT and double mutants *c2c5, c4c5, c2c4* were cultivated without bacteria (upper row) and with *A. brasilense* Sp245 (middle row), and with *A. brasilense* FAJ0009 (lower row) for two weeks.

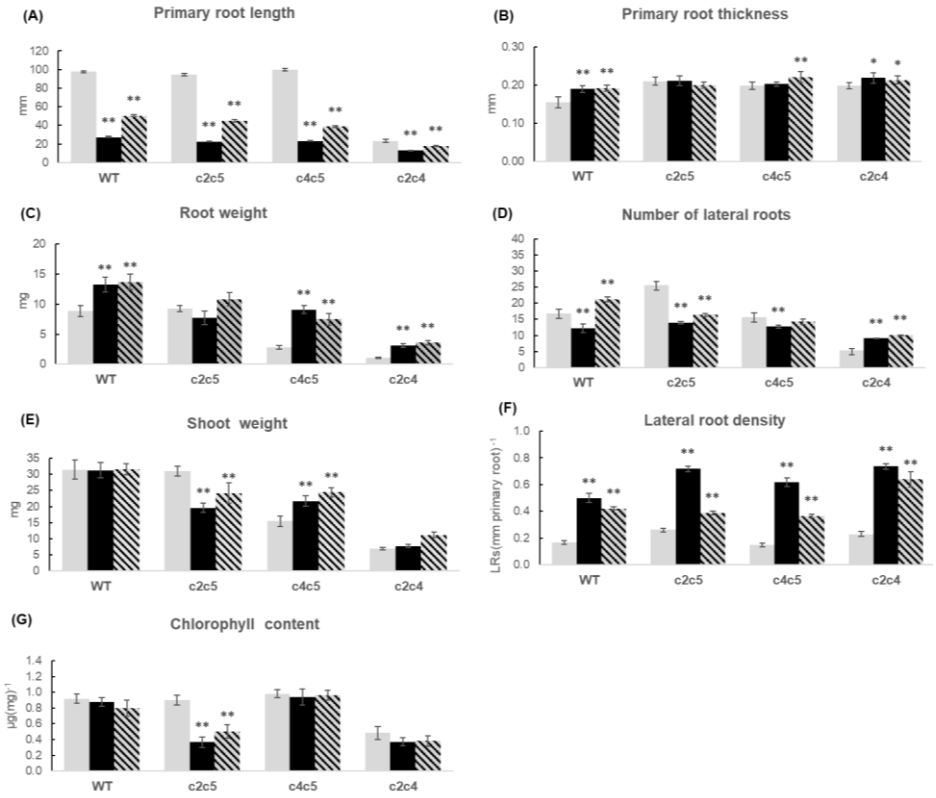

Figure 15 Growth parameters of WT and double mutants treated with *A. brasilense*.
Growth parameters of WT and double mutants *c2c5*, *c4c5* and *c2c4* cultivated without bacteria (white bars*)*, with *A. brasilense* Sp245 (black bars) and with *A. brasilense* FAJ0009 (hatched bars) for two weeks. (A) primary root length; (B) primary root thickness; (C) root fresh weight; (D) number of lateral roots; (E) shoot fresh weight; (F) lateral root (LRs) density and (G) chlorophyll content. For root length, primary root thickness, lateral root density and number of lateral roots, data are means ± SE of 45 plants (n=45). For fresh weight and chlorophyll content, the plants in each plate were pooled for measurements and values are means ±SE of nine independent experiments (n=9). The root and shoot weights (C) and (E) represent means ±SE per single plant. The chlorophyll values (G) represent µg chlorophyll per mg leaf tissue. Columns marked with one or two asterisks are significantly different from the control without bacteria according to student's t-test at p-value < 0.1 and 0.05 respectively.

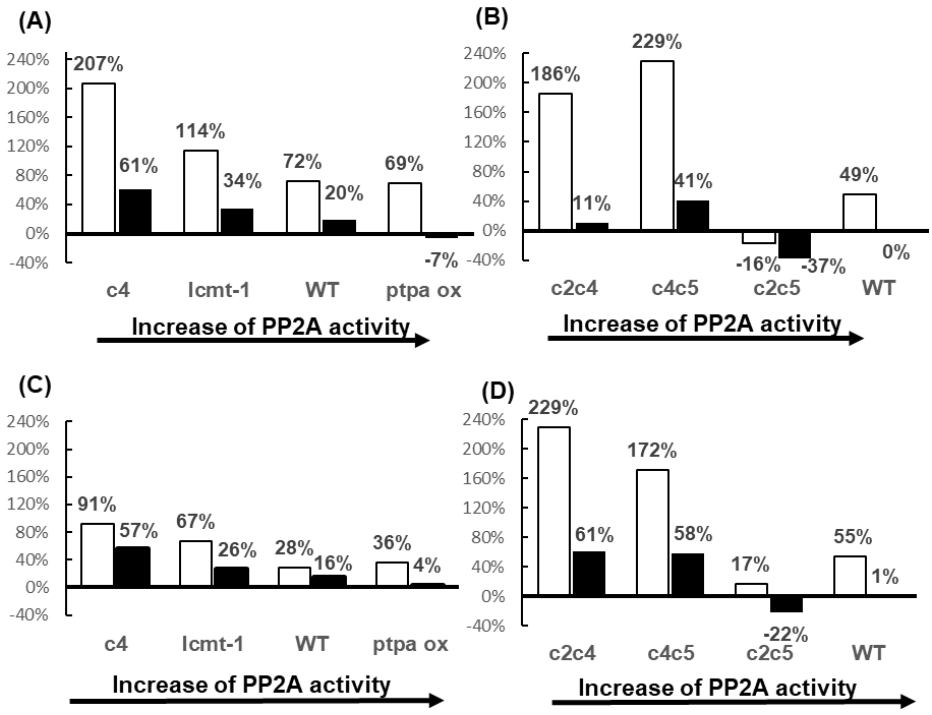

Figure 16. Per cent changes in fresh weight of Arabidopsis WT and mutants caused by *A. brasilense*.

Changes in Arabidopsis root (white bars) and shoot (black bars) fresh weight caused by (A), (B) *A. brasilense* Sp245 and (C), (D) *A. brasilense* FAJ0009. Calculations were done based on data in Figure 13 and 15. The data sets are arranged in order of increasing PP2A activity (from Figure 5).

5.4 Functional analysis of B'φ in tomato

5.4.1 Expression pattern in different tomato tissues

The transcript abundance of *B'φ* and other most relevant PP2A genes, listed in **Table 1**, were studied in diverse plant organs (**Figure 17A**) of 3.5-month-old tomato plants grown under standard conditions in different growing media (vermiculite versus soil), see **4.6.6.1**. Since *B'φ* was previously found to be regulated by ABA in *Medicago truncatula* (Charpentier et al. 2014) and the expression of *Bβ* (Clade III) was upregulated by ABA in roots of *Medicago sativa* (Toth et al. 2000), the ABA-responsive gene, *TAS14*, was included in the gene screening. *TAS14* is a tomato dehydrin gene that is induced by ABA, mannitol and NaCl but not by cold or wounding and serves as an ABA-induced marker of ABA responses in tomato (Godoy et al. 1990).

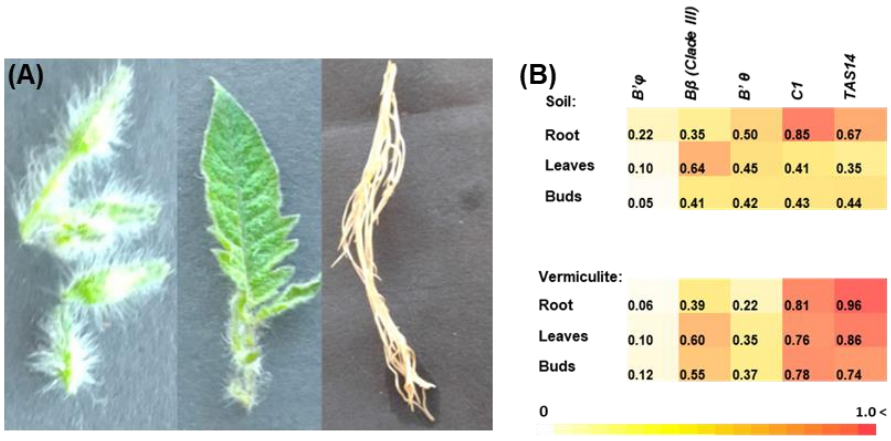

Figure 17. Analysis of transcript distribution of selected PP2A subunits in different plant tissues.
(A) Plant material from 3.5-month-old tomato plants used for RNA isolation.: flower buds (left), young leaves (middle) and roots (right). (B) Relative expression pattern of PP2A subunits in different plant tissues as determined by sqRT-PCR. The values denote the average level of expression from three biological replicates (n=3) normalized by the reference gene *ACTIN41*. Mean values ± SE are given in **Appendix**, **Table A4**. White and red colours indicate the zero and the highest expression level respectively.

The sqRT-PCR analysis (**Figure 17B**) showed that *B'φ* was weakly expressed in all the analysed plant tissues, although to a different extent depending on the growing medium, with the highest level in the roots grown in soil. Cultivation in vermiculite caused a 3.5-fold reduction in the expression of *B'φ* in roots and a 2.5-fold increase in flower buds compared with cultivation in soil while in young leaves the expression was low and not influenced by the type of growing medium used. *Bβ* (Clade III) was well expressed in all the tomato tissues and the pattern of expression was similar for both soil and vermiculite. *B'θ* was equally moderately expressed in all the types of tissue with slightly higher levels in the soil-grown plants. *C1* and *TAS14* showed the highest levels of expression in roots regardless of growing medium and very strong correlation in the expression pattern. Both genes were also moderately or highly expressed in aerial organs grown in soil and vermiculite respectively. No correlation in expression patterns between *B'φ, Bβ* (Clade III) and *TAS14* was observed.

5.4.2 Effect of PGPR treatment

To get some clues to transcriptional regulation of genes presumably associated with the response to PGPR, listed in **Table 1**, tomato plants grown in vermiculite for 40 days were subjected to inoculation with PGPR (see **4.6.6.2**). The transcript levels of the target genes were quantified 2 h, 24 h, 1 week and 3 weeks after the inoculation (**Figures 18 and 19**) followed by measurement of root and shoot fresh weight at the end of the experiment (**Figure 20**). By visual inspection, all the plant groups looked similarly developed, although WCS417r-treated plants had a slightly larger root system (**Figure 20A**). This finding was also confirmed after weighing the roots (**Figure 20B**).

The sqRT-PCR analysis revealed groups of genes involved in both early response and late response to PGPR. Already 2 h after inoculation, the expression of *B'θ* was significantly downregulated while the expression of *Bβ* (Clade III) was upregulated keeping this tendency

persistent during all three weeks. By the end of the experiment, the response of *B'θ* had weakened but the upregulation of the expression of *Bβ* (Clade III) strengthened and became significant relative to non-treated plants. By 24th h after the inoculation, another group of genes including *Bβ* (Clade I), A*βI*, A*βII* and *TAS14* responded explicitly but to a various extent. *Bβ* (Clade I) responded with a 5-to-10-fold upregulation of expression which eased up after one week and was not detected by week 3. A*βI* and A*βII* showed decreased expression, although this response was stronger and more significant in A*βI*. It is noteworthy that plants inoculated with WCS417r exhibited downregulation of the expression of both isoforms of A subunits and a significantly less transcript level of A*βI* already by 2nd h after the inoculation. Having the same level of expression as the non-treated plants after one week, by the end of the experiment, A*βI* and A*βII* showed an increased level of expression in all the PGPR-treated plants. But this response was significantly different from that of the non-treated plants only in *Azospirillum*-treated plants. *TAS14* responded to the PGPR inoculation with a weak downregulation of the expression at 24 h time point in all the PGPR-treated plants ranging from 11% to more significant 30% in Sp245-treated plants. The late response to PGPR with a significant upregulation of the *C1* expression was detected first in WCS417r-treated plants after one week. But by the end of the experiment, a similar upregulation was observed in all the PGPR-treated plants. *B'φ* had very low expression during all the time course experiment. However, the WCS417r-treated plants had persistently a significantly higher level of *B'φ* expression at week 1 and 3 compared with the non-treated plants (**Figures 18** and **19**). Interestingly, the expression of *B'φ* went down by the third week in all the plants including the controls. The response of *B'φ* also positively correlated with the root fresh weight values (**Figure 20B**) indicating a possible role of this gene in root growth and development. The remaining *B'κ* and *C2* genes showed no clear response to PGPR and were persistently moderately to highly expressed in all the plant groups.

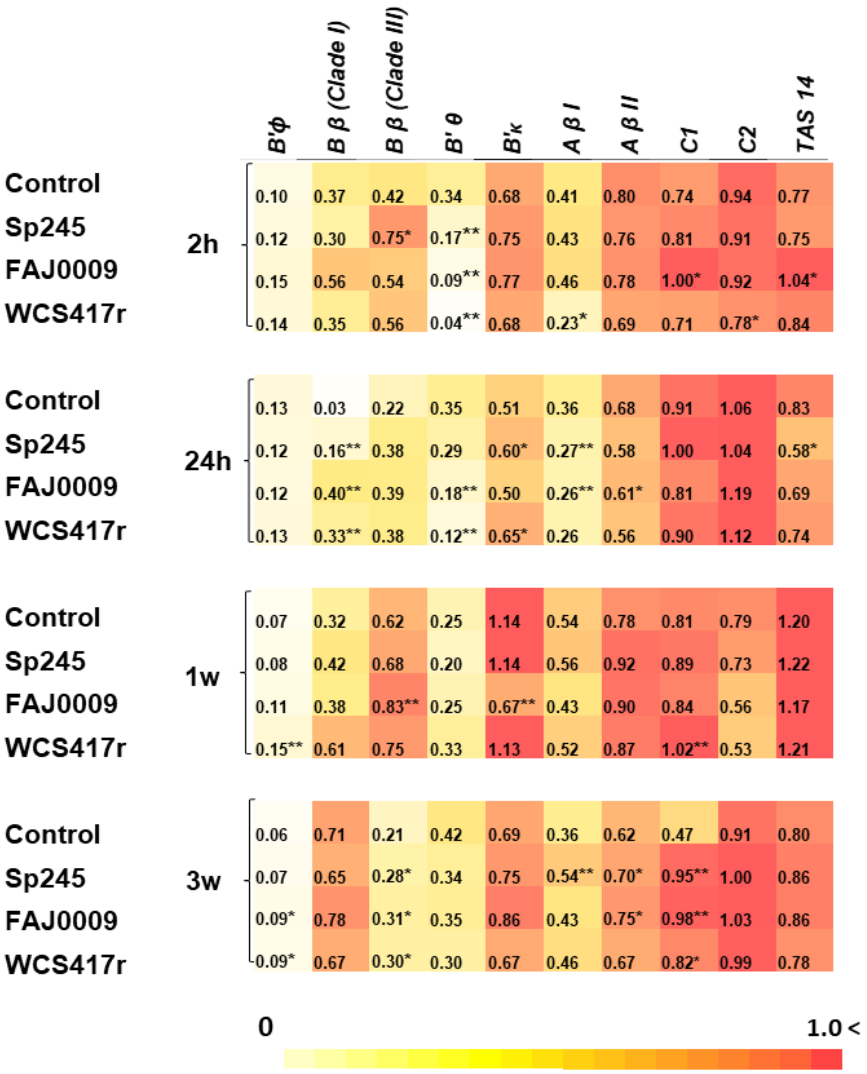

Figure 18. Time course analysis of the expression of PP2A subunits and *TAS14* in tomato roots of not treated and treated with PGPR.
Tomato plants were grown in vermiculite for 40 days before the treatment. The expression level was measured in the roots 2 h, 24 h, 1 week and 3 weeks after the treatment. The values denote the average level of expression from three biological replicates normalized by the reference gene *ACTIN41*. Mean values ± SE are given in **Appendix**, **Table A5**. Values marked with one or two asterisks are significantly different from the corresponding control according to student's t-test at p-value < 0.1 or 0.05 respectively. White and red colours indicate the zero and the highest expression level respectively.

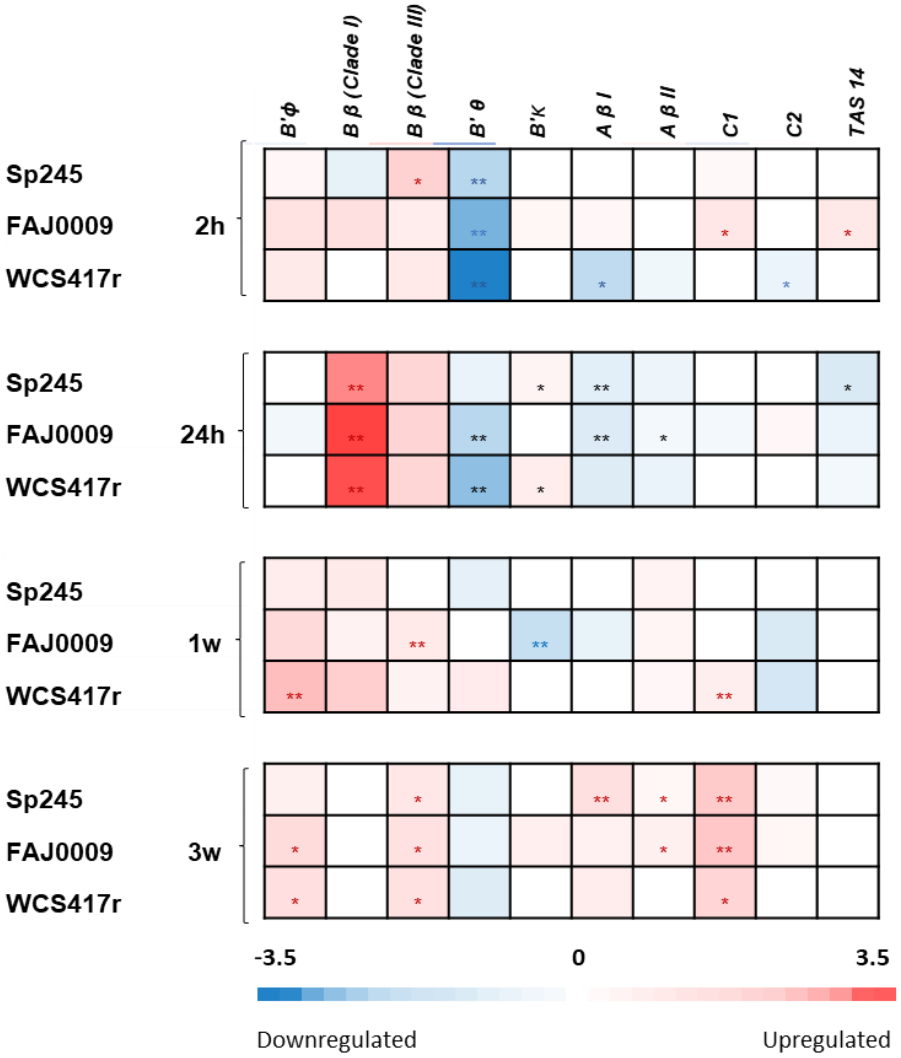

Figure 19. Time course analysis of changes in expression of PP2A subunits and *TAS14* in roots treated with PGPR.

Changes in gene expression in the roots treated with PGPR with respect to not treated roots**.** Dataset is based on the values from

Figure 18. Cells marked with one or two asterisks are significantly different from the corresponding control according to student's t-test at p-value < 0.1 or 0.05 respectively. Blue and red colours indicate decreased and increased expression respectively, relative to a corresponding control. The colours visualize Log_2(sample/control).

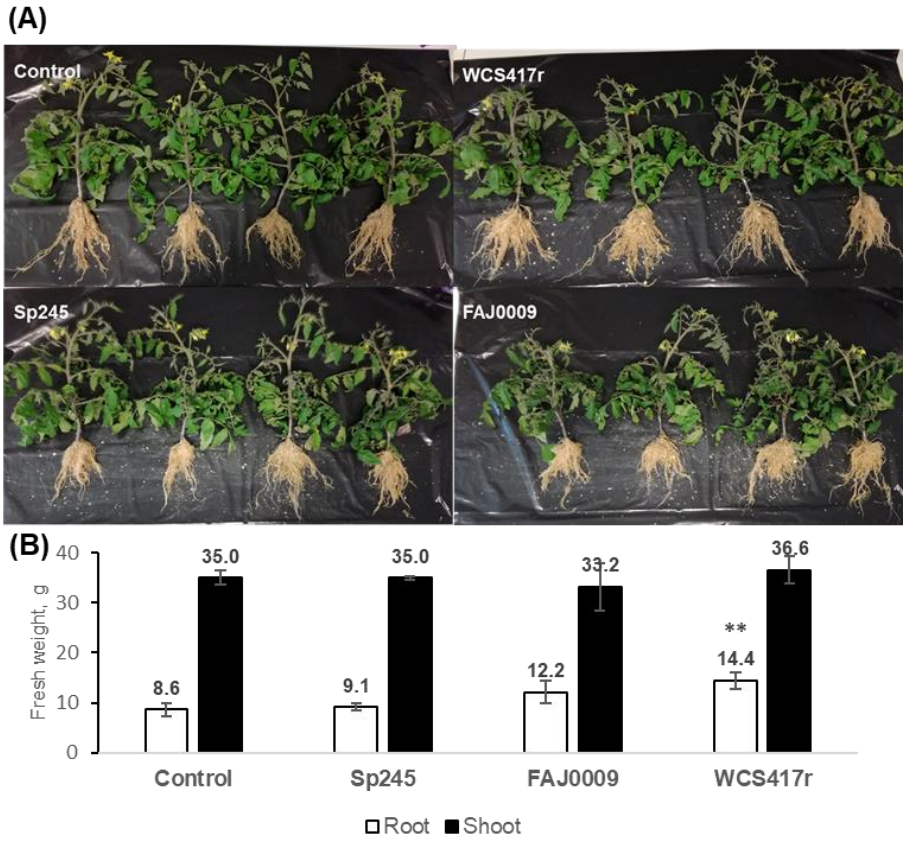

Figure 20. Visual phenotype of tomato plants three weeks after treatment with PGPR.
(A) Two-month-old tomato plants not cultivated (upper left photo) and cultivated with WCS417r (upper right photo), Sp245 (lower left photo) and FAJ0009 (lower right photo) for three weeks in vermiculite. (B) Root (white bars) and shoot (black bars) fresh weight. Data are means ± SE of 4 plants (n = 4). The bar marked with two asterisks is significantly different from the control plants according to student's t-test at p-value < 0.05.

5.4.3 Effect of colonization by AMF

The finding that *B'φ* in *M. truncatula* was induced upon AM formation (Charpentier et al. 2014) was a good reason for studying the transcript levels of the PP2A subunits in tomato roots colonized by AMF. To this end, tomato plants were inoculated with AMF as described in **4.6.6.3** and grown for 3.5 months both in soil and vermiculite with a subsequent comparative analysis of the roots for AM formation under the light microscope (as in **4.6.7**). By microscopy analysis, it was found that the type of growing medium greatly influenced AM morphology. Roots grown in soil formed a canonical AM usually observed when the root was colonized by more than one AMF species (Smith and Read 2008b), while the roots grown in vermiculite formed vesicular mycorrhiza (VM). No AM was observed in the control plants (**Figure 21**). Nevertheless, to confirm the AM/VM functionality in the tomato roots, the *PT4* gene, coding for mycorrhiza inducible inorganic phosphate transporter, was used as a marker of AM symbiosis. The PT4 protein is an absolute requirement for the phosphate transfer from the fungus via arbuscules to the plant as well as for the maintenance of a functioning AM symbiosis (Javot et al. 2007).

The sqRT-PCR analysis of the roots grown in vermiculite and in soil showed two interesting finding. Firstly, a functioning AM in the AMF roots was confirmed by elevated expression of *PT4,* by 116% in soil and by 30% in vermiculite (**Figure 22A**) which was consistent with the results from the microscopy analysis (**Figure 21**). Secondly, expression patterns of the PP2A subunits were also influenced by the type of growing medium (**Figure 22B**). Interestingly, the transcripts of most of the studied PP2A subunits were less abundant in the roots grown in vermiculite than those grown in soil. Of the catalytic subunits, *C1* responded to AM with significantly decreased expression in soil versus upregulation in vermiculite. Like *TAS14*, *C2* was highly expressed in all the plant groups and showed no response to AM (**Figure 22**). The expression of *Bβ* (Clade III) and *AβI* was significantly upregulated by

45% and 55% respectively, while the expression of *B'θ* was ten-fold downregulated only in the AMF roots grown in soil, resembling the response to PGPR in **Figure 19**. But these genes showed no response to AM (VM) in vermiculite (**Figure 22**). Unlike the mycorrhizal roots from soil, the expression of *B'κ* and *Bβ (Clade I)* increased in the mycorrhizal roots from vermiculite by 15% and 30% respectively. *B'φ* showed no specific response to AM.

The recent studies showing the importance of GAs along with ABA in the development of AM (Martin-Rodriguez et al. 2016; Martín-Rodríguez et al. 2015; Herrera-Medina et al. 2007), suggested to include the GA-regulated gene in the gene expression analysis for monitoring the level of active GAs in the AMF-colonized roots. For this purpose, *GAST1* (GA-stimulated transcript 1) is commonly used. It was previously found that treatment with gibberellic acid (GA_3) induces the *GAST1* expression while treatment with ABA inhibits it (Shi and Olszewski 1998). In this study, the expression of *GAST1* decreased (about 40%) in mycorrhizal roots grown both in soil and in vermiculite underpinning the important role of GAs in the regulation of AM formation previously found by Martin-Rodriguez et al. (2016) (**Figure 22B**).

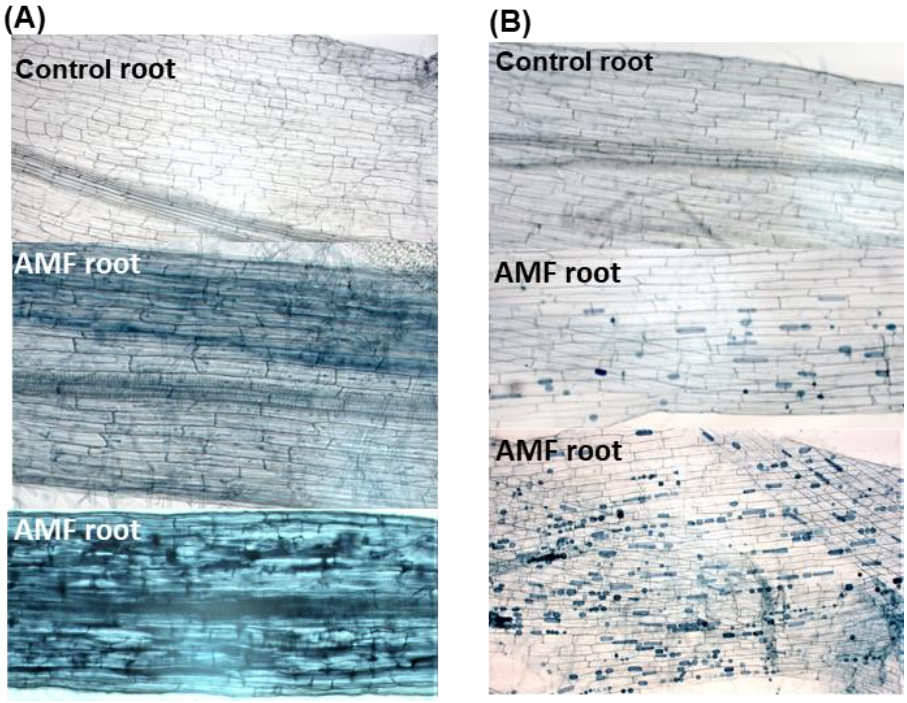

Figure 21. Morphology of AM colonization in tomato roots stained with trypan blue 3.5 months after planting and inoculation with AMF.
Bright-field images of roots grown in soil (A) and in double autoclaved vermiculite (B).

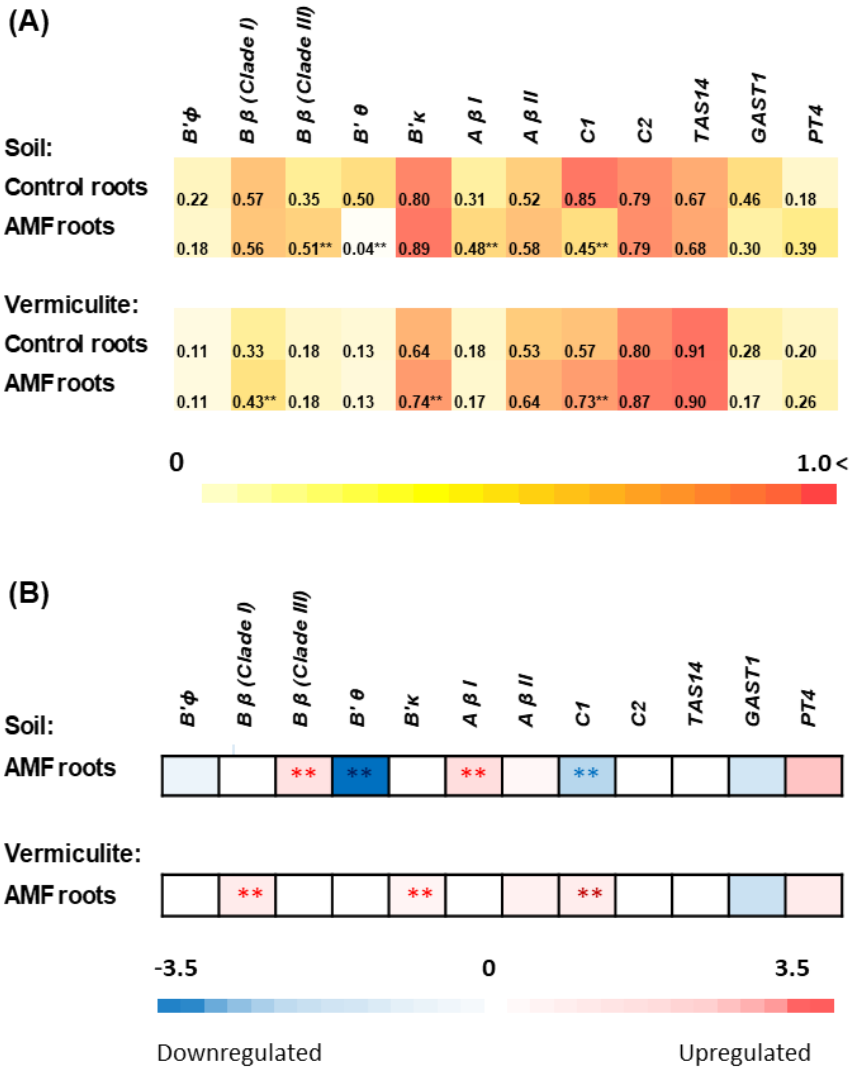

Figure 22. Transcriptional analysis of PP2A subunits and AM-associated genes in the roots of not treated and AMF-treated 3.5-month-old tomato plants grown in soil and vermiculite. (A) SqRT-RCR gene expression analysis. The values denote the average level of expression from three biological replicates (n=3) normalized by the reference gene *ACTIN41*. Mean values ± SE are given in **Appendix**, **Table A6**. White and red colours indicate the zero expression and the highest expression level respectively. (B) Changes in gene expression in AMF- roots with respect to not treated roots**.** Dataset is based on the values from (A). Blue and red colours indicate decreased and increased expression respectively, relative to control. The colours visualize Log_2(sample/control). Values marked with two asterisks are significantly different from the corresponding control according to student's t-test at p-value < 0.05. All the significantly different values were checked by PCR three times for reproducibility.

5.5 The characterization of transgenic tomato overexpressing B'φ subunit

5.5.1 Transgenic tomato lines overexpressing B'φ

Tomato hypocotyl explants infected with *A. tumefaciens* ABI-1 harbouring the 35S:PP2A-B'φ insert were subjected to several rounds of segregation in Basta-supplemented agar-solidified MS medium. Basta was used as a selective marker for the transgenic plants. All the plant developed from the explants were genotyped for the 35S:PP2A-B'φ insert using the vector-specific primers (**Appendix**, **Table A3**) and Phire® Plant Direct PCR Kit (**Table 2**). The positives were designated as *b'φ$_{ox}$* (F_0) and used in gene expression and AMF studies. The seeds collected from transgenic plants 10, 20, 23 were named as transgenic lines L10, L20 and L23 and used for planting *b'φ$_{ox}$* (F1) mutants for phenotyping, gene expression and AMF studies.

5.5.2 Phenotypic characterization of b'φ$_{ox}$ lines

Both *b'φ*$_{ox}$ (F_0) and (F_1) were characterized phenotypically, although more detailed and representatively in the case of *b'φ$_{ox}$* (F_1) (**Figures 23**, **24** and **25**). The plants shown in **Figure 23A, C** and **D** were cultivated in vermiculite as described in **4.6.6.3** and **4.6.6.4** for 3.5 months but without adding "Rootgrow". The fruits in **Figure 23B** were collected from WT and *b'φ*$_{ox}$ (F_0) grown in soil under the growing conditions described in **4.6.4.8**. All the observed transgenic plants from F_0 had similar alterations in morphology compared to WT such as a smaller plant with slender and sparse roots, smaller leaves, thinner stems (**Figures 23A, C, D**) and strikingly fewer seeds in fruits (**Figure 26**). For a more conclusive study, the seeds from *b'φ*$_{ox}$ L23 (**Figure 24**), L10 and L20 (**Figure 25)** were planted in vermiculite for monitoring germination and growth, and measuring basic growth parameters such as root fresh weight, shoot fresh weight, stem thickness, number of leaves etc. (**Figure**

26). Cultivated as described in **4.6.6.5**, the *b'φ*$_{ox}$ mutants showed no difference in germination time compared to WT. Moreover, during the first three weeks, all the plants looked like WT. The *b'φ*$_{ox}$ phenotype was observed by the fourth week after germination and had the same traits which were previously detected in *b'φ*$_{ox}$ (F_0). Eight weeks after germination, the plants were carefully taken out from the vermiculite for measuring the growth parameters. The transformants from all three lines shared similar phenotypic traits despite some negative genotyping results (**Figures 24D** and **25D**). Therefore, the values of the growth parameters from L10, 20 and 23 were pooled together and designated as *b'φ*$_{ox}$ (F_1) without specifying a mutant line number (**Figure 26**). By visual inspection, the *B'φ* overexpression caused remarkable alterations in the phenotype of *b'φ*$_{ox}$ (F_1) with the most obvious morphological changes in roots and leaves. These changes negatively affected the root and shoot fresh weights, stem thickness and root-to-shoot ratio (**Figure 26A**). The fresh weight of both root and shoot was reduced by 70%, the stem thickness and the root-to-shoot ratio by 20 % relative to WT. A reduced number of leaves in *b'φ*$_{ox}$ compared to WT at the time of counting may indicate slowed growth of *b'φ*$_{ox}$ plants. The seed count showed a 60% reduction in the number of seeds per fruit regarding WT, unlike the fruit weight, which was comparable with WT (**Figure 26B**).

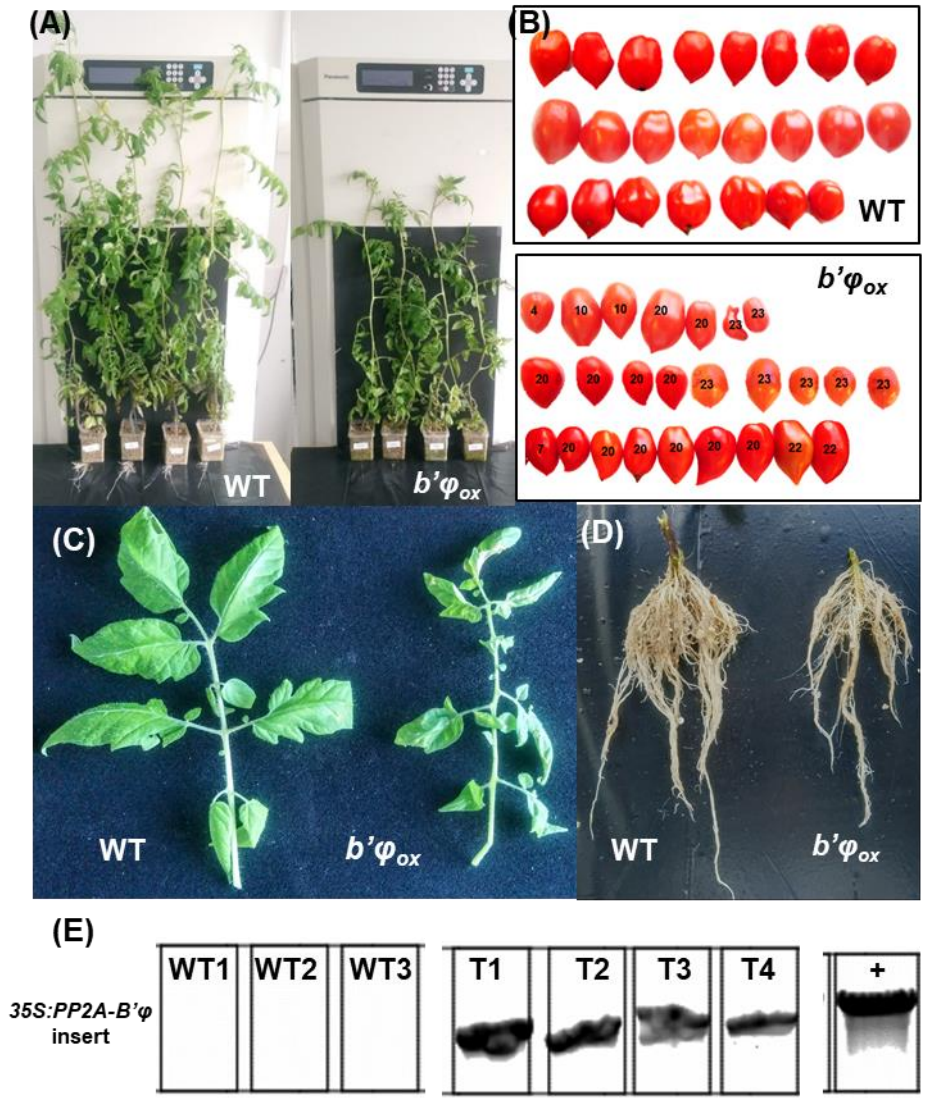

Figure 23. Phenotypic alterations in transgenic plants developed from tomato hypocotyl explants (*b'φox* (F0)).

(A) 3.5-month-old plants. (B) Fruits collected from WT (upper frame) and from *b'φox* (lower frame), numbers denote a transgenic plants number. (C) Sixth leaves of WT and *b'φox*. (D) Roots of WT and *b'φox* plants. (E) Genotyping of transformants for 35S:PP2A-B'φ insert. WTs were used as negative controls, miniprep of pBA002-B'φ plasmid was used as a positive control.

Figure 24. Phenotypic characterization of *b'φox* L23 (F_1).
(A) 25-day-old tomato plants. (B) 8-week-old tomato plants (C) 8-week-old tomato plants taken from the growing medium (D) Genotyping of transformants (L23) for *35S:PP2A-B'φ* insert. WTs and miniprep of pBA002-B'φ plasmid were used as negative and positive controls respectively.

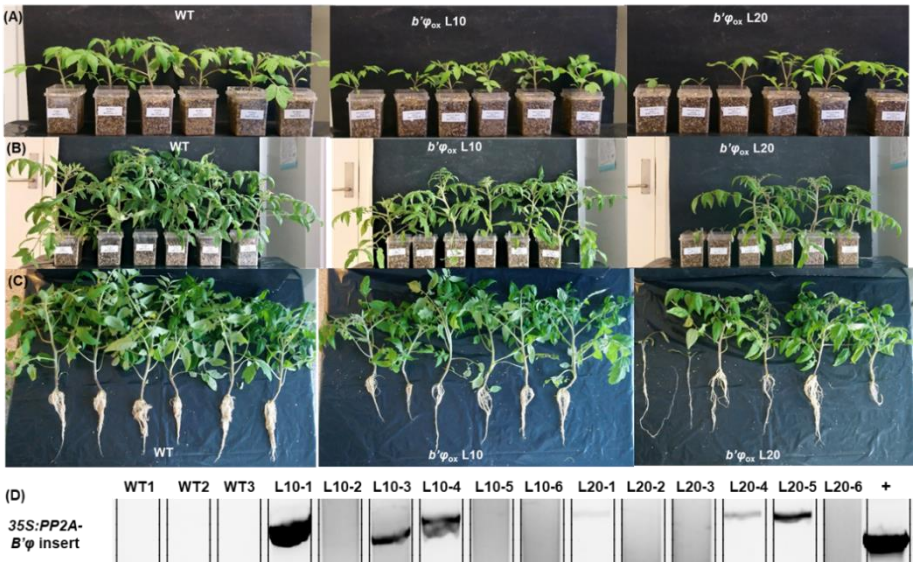

Figure 25. Phenotypic characterization of *b'φox* L10 and L20 (F_1).
(A) 25-day-old tomato plants. (B) 8-week-old tomato plants (C) 8-week-old tomato plants taken from the growth medium (D) Genotyping of transformants (L) for *35S:PP2A-B'φ* insert. WTs and miniprep of pBA002-B'φ plasmid were used as negative and positive controls respectively.

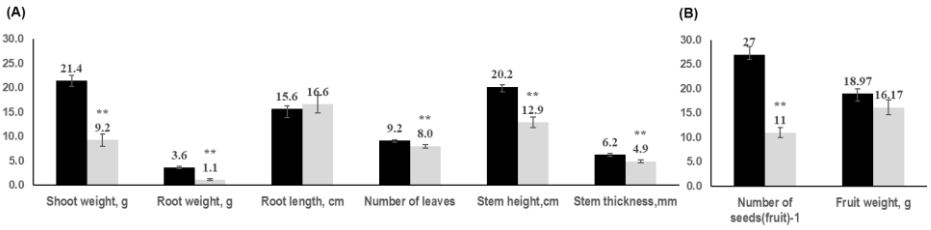

Figure 26. Growth parameters of tomato WT and *b'φox*.
(A) Tomato seedlings of WT and *b'φox* were cultivated in vermiculite for 9 weeks after sowing. The values are means ±SE of 12 plants for WT and 18 plants for *b'φox* (F_1) (measurements from two experiments and three mutant lines (**Figures 24** and **25**), n=12 and 18 respectively. (B) Fruit fresh weight and seed number are from corresponding WT and *b'φox* (F_0) tomato fruits collected after ripening (**Figure 23B**). Data are means of 35 fruits, n=35, ±SE given. According to student's t-test at p-value <0.1 or 0.05, columns marked with one or two asterisks respectively are significantly different from WT.

5.5.3 Effect of B'φ overexpression on AMF colonization

Tomato plants of WT and *b'φ$_{ox}$* (F_0 and F_1) were cultivated as described in **4.6.6.4** and **4.6.6.5** with a subsequent staining of the roots as in **4.6.7**. All the mutants were genotyped before the AMF study and examined for the phenotype (**Figure 27**, **28** and **29**). The frequency (F%) of AM in roots was assessed in soil and in vermiculite according to **4.6.8**. Due to a low level of mycorrhization in the roots grown in soil (**Figure 30A**), F% was estimated twice: 3.5 and 8.5 months after adding "Rootgrow". But no significant differences in F% were observed between WT and *b'φ$_{ox}$* grown in soil (**Figure 29A**). However, some qualitative changes of AM such as hypercolonization in 2% of the total fragments were detected only in *b'φ$_{ox}$* (F_0) (**Figure 26C** left image under *b'φ$_{ox}$*). When grown in vermiculite, *b'φ$_{ox}$* (F_0 and F_1) showed, on average, a 40% reduction in F% compared to WT (**Figure 29B**) without any specific changes in AM morphology (**Figures 27D** and **28G**). Nevertheless, AMF hypercolonization was still observed in 2% of the total root fragments in the *b'φ$_{ox}$* plants from L20 (**Figure 28G).** Such hypercolonization was never detected in the WT plants grown in soil or in vermiculite in this study.

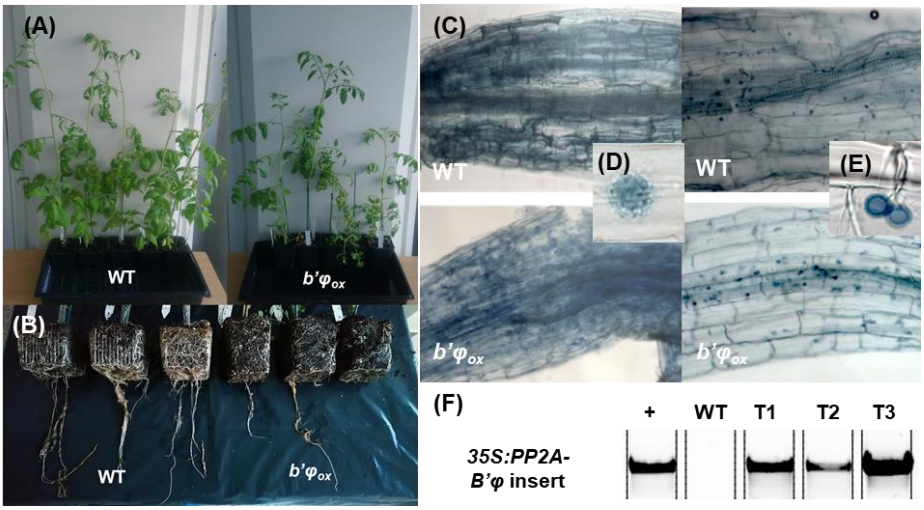

Figure 27. AMF colonization study of WT and *b'φ*$_{ox}$ (F$_0$) in soil.
(A) Tomato plants 2 months after planting in the soil inoculated with AMF. (B) Roots of the studied tomato plants 8.5 months after planting in soil inoculated with AMF. (C) Bright-field images of mycorrhiza morphology found in the roots of WT and *b'φ*$_{ox}$ (F$_0$) from (B) stained with trypan blue. (D) Bright-field image of arbuscule and (E) fungal spores found in the roots. (F) Genotyping of transformants (T) for *35S:PP2A-B'φ* insert, WT was used as a negative control, miniprep of pBA002-B'φ plasmid was used as a positive control.

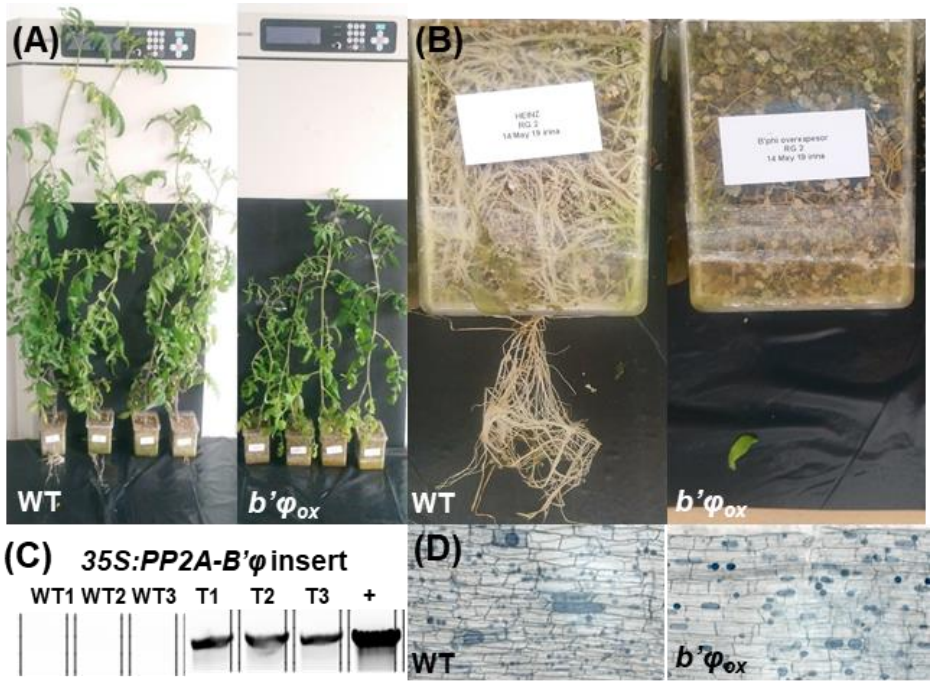

Figure 28. AMF colonization study of WT and *b'φox* (F_0) in vermiculite.
(A) Tomato plants 3.5 months after planting in vermiculite inoculated with AMF. (B) Roots of the studied plants. (C) Genotyping of transformants (T) for *35S:PP2A-B'φ* insert, WT was used as a negative control, miniprep of pBA002-B'φ plasmid was used as a positive control. (D Bright-field images of mycorrhiza morphology found in the roots of WT and *b'φox* (F_0) roots from (B) stained with trypan blue.

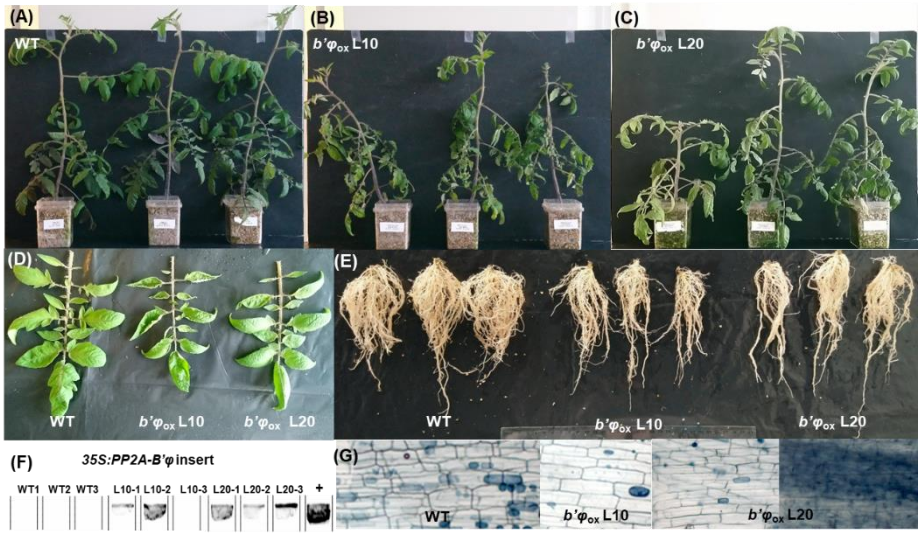

Figure 29. AMF colonization study of WT and *b'φox* (F_1) in vermiculite.
(A) WT (B), (C) *b'φox* (F_1) L10 and L20 tomato plants 3 months after sowing in vermiculite inoculated with AMF. (D) Sixth leaves of the studied plants. (E) Roots of the studied plants (F) Genotyping of transformants (L10 and L20) for *35S:PP2A-B'φ* insert, WTs and miniprep of pBA002-B'φ plasmid were used as negative and positive controls respectively. (G) Bright-field images of mycorrhiza morphology found the roots of in WT and *b'φox* (F_1) from (E), stained with trypan blue.

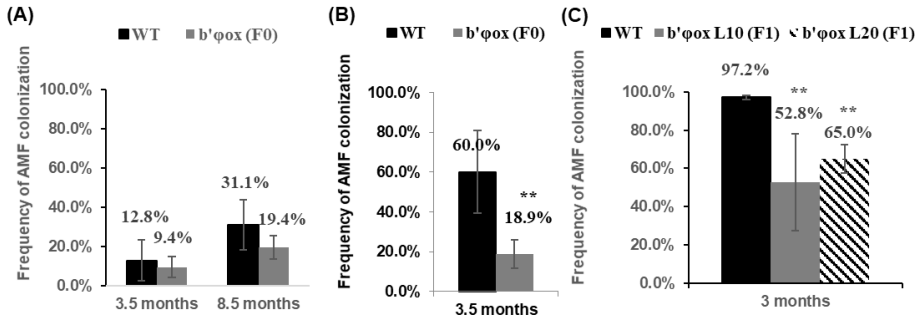

Figure 30. Frequency (F%) of root colonization in WT and b'φox after inoculation with AMF.
Colonization frequency for WT (black bars) and *b'φox* (grey bars and hatched bar) (A) in soil 3.5 and 8.5 months after inoculation; (B) in vermiculite after 3.5 months; (C) in vermiculite after 3 months with another batch of *b'φox* (F_1 plants).Values are means ±SE from three plants. According to student's t-test at p-value < 0.05, columns marked with two asterisks are significantly different from WT.

5.5.4 Gene expression analysis of b'φ$_{ox}$ lines

5.5.4.1 Comparative analysis of mycorrhizal and non-mycorrhizal roots

To study changes in the gene expression in the roots of *b'φ$_{ox}$* (F_0), tomato plants were cultivated as in **4.6.6.4** and **4.6.6.3** for 3.5 months in vermiculite. Both AMF-colonized and non-treated roots of *b'φ$_{ox}$* (F_0) with their respective WT references were used for the analysis. Along with a ten-fold increase in the expression of *B'φ* detected in the transformants, screening of the PP2A subunits, ABA (*TAS14*), GA (*GAST1*) and AM responsive (*PT4*) genes revealed significantly reduced expression of *TAS14* (ranging from a 19 to 38% reduction) and *GAST1* (a three-fold reduction) and increased expression of *Bβ* (Clade I) regardless of the presence of AMF colonization (**Figure 31A**). The change in the expression level of *TAS14* became more profound in AMF-colonized roots (38% reduction) compared with non-colonized roots (19% reduction). Even though the expression of *B'κ* and *AβII* was also significantly upregulated in the transgenic plants, this upregulation was negated upon the AMF colonization (**Figure 31B**). Contrary to the upregulated expression of *C1* in response to AMF observed in WT (**Figure 22**), this gene was not influenced by AMF in the transgenic plants (**Figure 31**).

To find out whether the downregulation of the expression of *TAS14* and *GAST1* was associated with alterations in ABA and GA synthesis, the following genes were also assayed by sqRT-PCR. The gene *NCED-1* encodes 9-cis-epoxycarotenoid-dioxygenase which is important in ABA biosynthesis (**Appendix**, **Figure A 9**) and generally considered to be rate-limiting (Taylor et al. 2005; Qin and Zeevaart 1999). The genes coding for GA20-oxidases (GA20ox (1-4)) and GA 3β-hydroxylase (GA3ox (1- 2)) have been previously characterized as important regulators of the GA biosynthesis pathway (Lange et al. 1994; Lester et al. 1997; Martin et al. 1997; Martín-Rodríguez et al. 2015)

where they are negatively regulated by active GAs (Martin et al. 1996; Phillips et al. 1995). GA 20-oxidases and GA 3β-hydroxylases catalyze the final steps in the formation of active GAs (**Appendix, Figure A8**) and are potential control points in the regulation of GA homeostasis (Ait-Ali et al. 1999). The sqRT-PCR analysis of the above genes showed 25% downregulation of the expression of *NCED*-1 in the transgenic plants that was slightly ameliorated upon AMF colonization (**Figure 32A**). The expression of the GA-biosynthesis genes in the non-mycorrhizal roots of *b'φ$_{ox}$* was up- or downregulated relative to those in WT but not considerably in terms of the transcript levels, except for *GA20ox-2* and *3* which expression was upregulated by approximately 37 and 20% respectively. Being irresponsive to AMF in *b'φ$_{ox}$*, *GA20ox-2* responded with a significantly increased (by 75%) transcript level in WT upon AMF colonization and exceeded the corresponding *b'φ$_{ox}$* values **(Figure 32A)**. The upregulation of the *GA20ox-3* expression became even more significant in the AMF-colonized roots of *b'φ$_{ox}$*.

5.5.4.2 Expression analysis of ABA and GA-associated genes in young leaves of *b'φ$_{ox}$* (F$_1$) lines

For the gene expression analysis in young leaves of *b'φ$_{ox}$* (F$_1$), the plants form WT, L10 and L20 were cultivated as in **4.6.6.5** (**Figure 25**). Unlike the changes found in roots, the sqRT-PCR analysis of the young leaves showed no difference in the transcript abundance of *Bβ (Clade I), B'κ*, *AβII* (not shown), *TAS14*, *NCED-1* and *GAST1* between the transgenic and WT plants. However, a four-fold increase in the *B'φ* expression detected by sqRT-PCR seemed to cause a significant upregulation of the expression of *GA20ox-1 and -2* in both transgenic lines (**Figure 33**). The expression level of *GA20ox-1* increased by 13 and 23% in L10 and L20 respectively. The expression level of GA*20ox-2* increased 2.4 and 3.6 times in L10 and L20 respectively compared to WT.

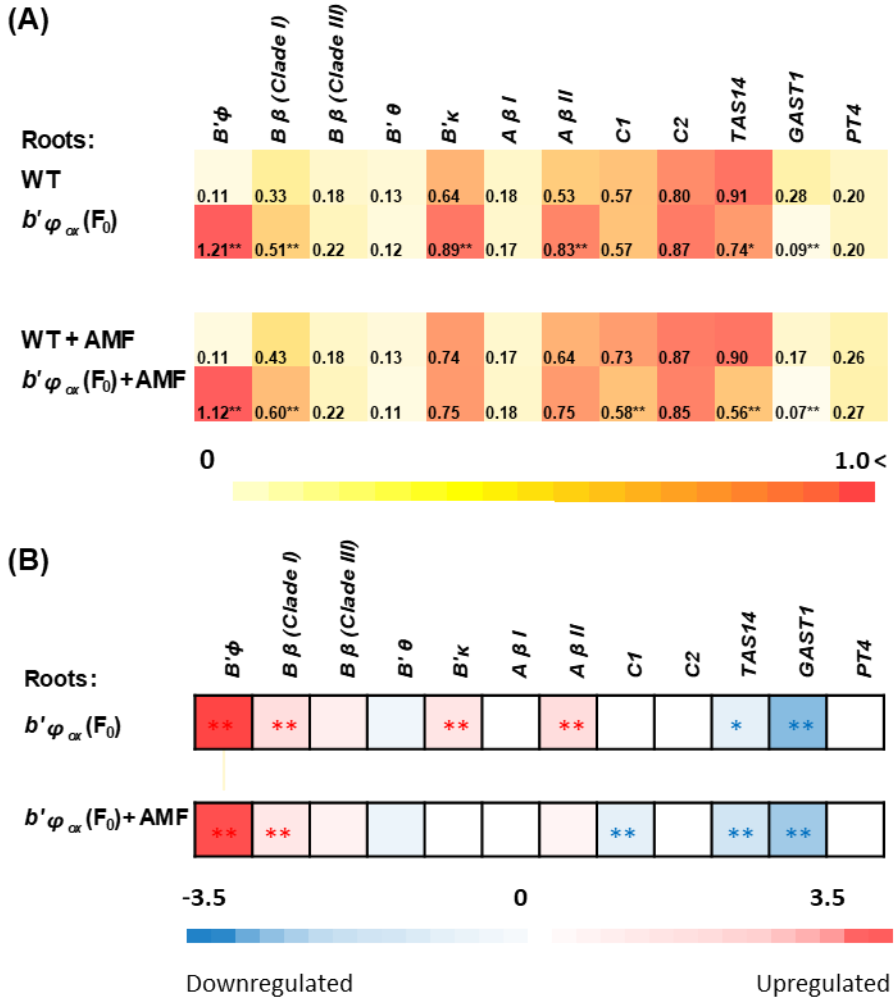

Figure 31. Comparative transcriptional analysis of PP2A subunits and AM-associated genes in WT and *b'φ*$_{ox}$ (F$_0$) roots of not treated and AMF-treated 3.5-month-old tomato plants grown in vermiculite.

(A) SqRT-RCR gene expression analysis. The values denote an average level of expression from three biological replicates (n=3) normalized by the reference gene *ACTIN41*. Mean values ± SE are given in **Appendix, Table A7.** White and red colours indicate the zero expression and the highest expression levels respectively. (B) Changes in the gene expression in *b'φ*$_{ox}$ (F$_0$) roots with respect to WT**.** Dataset is based on the values from (A). Blue and red colours indicate decreased and increased expression respectively, relative to WT values. The colours visualize Log$_2$(sample/control). Values marked with one or two asterisks are significantly different from WT according to student's t-test at p-value < 0.1 and 0.05 respectively. All the significantly different values were checked by PCR three times for reproducibility.

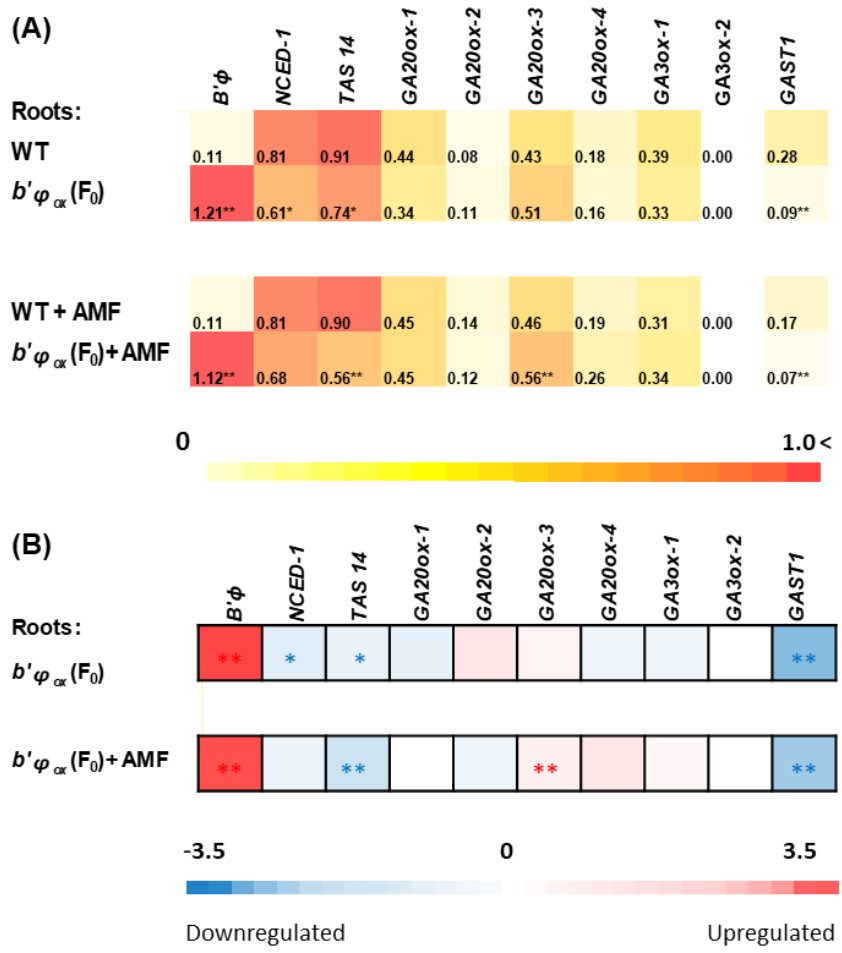

Figure 32. Comparative transcriptional analysis of *B'φ* subunit, ABA- and GA-associated genes in WT and *b'φ*$_{ox}$ (F_0) roots of not treated and AMF-treated 3.5-month-old tomato plants grown in vermiculite.

(A) SqRT-RCR gene expression analysis. The values denote an average level of expression from three biological replicates (n=3) normalized by the reference gene *ACTIN41*. Mean values ± SE are given in **Appendix, Table A8.** White and red colours indicate the zero expression and the highest expression levels respectively. (B) Changes in the gene expression in *b'φ*$_{ox}$ (F_0) roots with respect to WT**.** Dataset is based on the values from (A). Blue and red colours indicate decreased and increased expression respectively, relative to WT values. The colours visualize Log_2(sample/control). Values marked with one or two asterisks are significantly different from WT according to student's t-test at p-value < 0.1 and 0.05 respectively. All the significantly different values were checked by PCR three times for reproducibility.

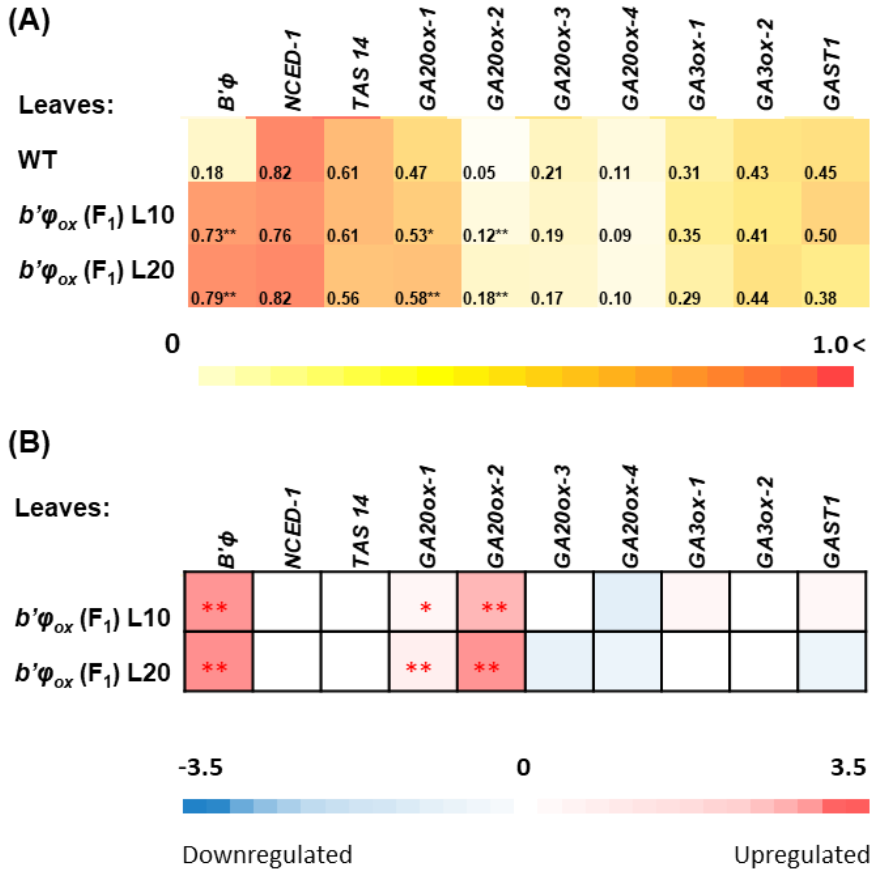

Figure 33. Comparative transcriptional analysis of *B'φ* subunit and ABA and GA-associated genes in *b'φ*$_{ox}$ (F$_1$) and WT leaves of 2-month-old tomato plants grown in vermiculite.

(A) Sq RT-RCR gene expression analysis. The values denote an average level of expression from three biological replicates (n=3) normalized by the reference gene *ACTIN41*. Mean values ± SE are given in **Appendix, Table A9.** White and red colours indicate the zero expression and the highest expression levels respectively. (B) Changes in the gene expression in *b'φ*$_{ox}$ (F$_1$) roots with respect to WT**.** Dataset is based on the values from (A). Blue and red colours indicate decreased and increased expression respectively, relative to WT values. The colours visualize Log_2(sample/control). Values marked with one or two asterisks are significantly different from WT according to student's t-test at p-value < 0.1 and 0.05 respectively. All the significantly different values were checked by PCR three times for reproducibility.

6 Discussion

6.1 Phenotypic response of Arabidopsis WT and mutants to PGPR

Prior to studying the role of PP2A in plant responses to PGPR, several mutants with mutations targeting PP2A regulation (*ptpa*$_{ox}$ and *lcmt-1*) or its catalytic capacity (null-mutation in one or two catalytic subunits) were screened for PP2A activity. The screening revealed the genotypes representing PP2As with altered activity: the maximum level was found in *ptpa*$_{ox}$ (**Figure 3**) and a considerably reduced level was found in *lcmt-1* (reduction by 30%), *c4* (reduction by 55%), *c2c5* (reduction by 41%), *c4c5* (reduction by 64 %) and *c4c5* (reduction by 68%) relative to WT (values for roots, **Figure 5**). Subsequently, these mutants were subjected to PGPR inoculation and phenotypic response analysis.

In agreement with previously reported results from different research groups, Arabidopsis WT and mutants in this study generally responded to PGPR with a shortening of the primary root and increased lateral root density. In most of the tested genotypes, shoot growth was also promoted. Comparative analysis of shoot and root fresh weights between PGPR-treated and corresponding non-treated controls from the above genotypes revealed a strong negative correlation in terms of the PP2A activity (correlation coefficients shown in **Appendix**, **Figures A5 and A6**). The more PP2A activity, the less plant growth promotion by PGPR (**Figures 11 and 16**). And the knockout of *C2* especially in combination with *C5* subunit showed to be crucial for growth response to PGPR. Indeed, an increase of C5 and to some extent of C2 transcripts in Arabidopsis in response to biotic cues such as pathogens and pathogenic elicitors and decrease under abiotic stress conditions has already been reported by Durian et al. (2016). Furthermore, Hu et al. (2017) showed that the C5 subunit is required for normal root and shoot growth under salt stress. Moreover, Pernas et al. (2007) found that the C2 subunit was a component of the signalling pathway that represses

responses to ABA associated with root development and abiotic stress. Pernas et al. (2007) also showed that the null mutation in the C2 subunit in Arabidopsis did not alter the responsiveness to auxin, cytokinins and gibberellins amid high sensitivity to ABA. *Azospirillum* and *Pseudomonas* are known to both produce ABA as well as influence the ABA levels in Arabidopsis (Cohen et al. 2008; Dodd et al. 2010; Belimov et al. 2014). The *c2c5* mutant is lacking both these stress-protecting genes, and this may explain no improved growth upon cultivation with PGPR. The *c2c5* mutant also responded with a considerable decrease in chlorophyll upon co-cultivation with *Azospirillum*. However, this growth parameter was unchanged in most of the mutants including *c2c5* or even significantly improved as in *lcmt-1* and *c4* when co-cultivated with *Pseudomonas*. Indeed, colonization by PGPR stimulates plant growth and induces systemic resistance against multiple pathogens ((Pieterse et al. 2014; Zamioudis et al. 2013; Spaepen et al. 2014). The onset of ISR has been reported to be associated with the iron deficiency marker genes MYB72 (MYB transcription factor gene) and IRT1 (iron uptake gene) activated by inoculation with PGPR including WCS417r (Stringlis et al. 2018a), Sp245 and FAJ0009 (Spaepen et al. 2014). Verbon et al. (2019) proved that the WCS417-stimulated iron uptake in Arabidopsis increases the chlorophyll content on the iron-sufficient medium but decreases it on the iron-deficient medium resulting in the chlorotic appearance of the shoots. This finding may explain the increased chlorophyll content in the presence of WCS417r observed in the Arabidopsis plants (**Figures 8** and **10**). However, no similar findings were reported about *Azospirillum* strains. Moreover, a 100-fold higher bacterial density of Sp245 and FAJ0009 compared to WCS417r applied to the root environment in this study could also matter.

Auxin, or auxin mimicking compounds, produced by PGPR clearly have an influence on plant root growth, as frequently reported for various *Pseudomonas* (Persello-Cartieaux et al. 2001; Zamioudis et al. 2013; Stringlis et al. 2018b) and *Azospirillum* (Bruto et al. 2014;

Spaepen et al. 2014) strains. Knockout of the *C4* gene alone or in combination with *C5* or *C2* resulted in low PP2A activity (**Figure 5**), and reduced root and shoot weights compared with WT Arabidopsis (**Figures 4A, 8B, C** and **10B, C**). The C4 subunit is essential for transport and distribution of auxin in roots (Ballesteros et al. 2013; Boyer et al. 2016), therefore, the striking effect of inoculation with WCS417r and Sp245 could be, at least partly, explained by a bacteria-produced substitute for auxin otherwise distributed by PP2A to various tissues. Spaepen et al. (2014) previously showed that when Arabidopsis was co-cultivated with the auxin mutant FAJ0009 for one week, there was hardly any effect on the root architecture and confirmed a general view that the effect on the root architecture was caused by auxin. But in the present study, co-cultivation of Arabidopsis with FAJ0009 for two weeks also affected the root architecture and promoted plant growth (**Figures 12 - 14**). Possibly a low auxin level in FAJ0009 would still induce effect after prolonged co-cultivation with Arabidopsis, or the induced plant root growth might be caused by nitric oxide (Creus et al. 2005; Molina-Favero et al. 2008). Using a genetic approach, Molina-Favero et al. in (Molina-Favero et al. 2008) demonstrated that the root growth promotion in tomato caused by both Sp245 and FAJ0009 was highly dependent on nitric oxide produced, in particular by nitrate reductase. In combination with a pharmacological approach, nitric oxide was recognized as a signalling molecule involved in *Azospirillum*-plant interactions (Creus et al. 2005; Molina-Favero et al. 2008; Molina-Favero et al. 2007) and playing a role in cross-talk between NO and auxin in the growth-promoting effects (Cassán et al. 2015).

Global transcript analysis of Arabidopsis treated with Sp245 or FAJ0009 revealed induction of genes involved in systemic acquired resistance after three days, a type of resistance usually induced by pathogens (Spaepen et al. 2014). The plant immune system appears to recognize all bacteria as invaders and give a defence response, although milder for PGPR than for pathogenic bacteria. Spaepen et al. (2014) further analysed gene expression in Arabidopsis roots at different time

points after inoculation with Sp245 and FAJ0009 and found a large set of genes that represented the plant response to PGPR independent of bacterially produced auxin. It is therefore not surprising that a clear phenotype was established also for seedlings inoculated with FAJ0009 (**Figures 12-15**). Altogether the global transcript studies, as well as results in the present work, indicate a complex mechanism behind the observed plant growth-promoting effects which could not be solely ascribed to auxin level and distribution. In a GWAS study to find maize genes of importance for responsiveness to *A. brasilense*, candidate genes confirmed the general impression that genes involved in defence, hormone biosynthesis, signalling pathways and root growth were of importance (Vidotti et al. 2019). Exposure of rice seedlings to *A. brasilense* and subsequent RNA-seq showed that several hormone-related genes, including auxin efflux carriers, and also defence-related genes were induced (Thomas et al. 2019). PP2A promotes (polar) auxin transport by dephosphorylating auxin efflux carriers (Ballesteros et al. 2013). Furthermore, PP2A is also involved in establishing immune responses in Arabidopsis (Segonzac et al. 2014; Jin et al. 2016). Since the most pronounced PGPR effects were found in Arabidopsis mutants with lowered PP2A activity (**Figure 16**) this would not promptly fit with the importance of PP2A in polar auxin transport. The results may be more easily interpreted according to the involvement of PP2A in immune responses; the high effect of PGPR in plants with low PP2A activity is compatible with a lowered PP2A activity suppressing the immune response and thereby favouring (mutualistic) interactions with PGPR.

Studying the phenotypic response of *c2* and *b'*-mutants to WCS417r revealed that *c2, b'*α and especially *b'θ* responded with a significant reduction in the number of lateral roots compared to WT and the other *b'*-mutants. Firstly, this finding strengthens the results obtained with the *c2c5* mutant, and secondly, outlines the regulatory subunits for further studies of beneficial plant-bacterial interactions.

6.2 PP2A as a regulatory enzyme in plant-microbe interactions

Transcriptional analysis of the PP2A subunits from the tomato genome, which were previously characterized either as hypothetical mediators in establishing a symbiosis between plants and beneficial microbes or as belonging to atypical non-expanding protein families, revealed subunits that might be associated with tomato-PGPR signalling and mediating early or late plant responses to PGPR. The genes encoding *Bβ (Clade I), B'θ* and *AβI* were highly responsive to PGPR already within 24 h, while *Bβ (Clade III)* and *C1* showed a late response observed one week after the bacterial inoculation (**Figures 18 and 19**). *Bβ (Clade III), AβI, B'θ* and *C1* were also involved in the response to AMF in the roots grown in soil **(Figure 22**). However, *Bβ (Clade III), AβI and B'θ* showed no response to AMF in the roots grown in vermiculite. A quite limited microbiome in double autoclaved vermiculite, as opposed to a diverse and plentiful microbiome stimulated by AMF in soil (Giovannini et al. 2020), could be one of the possible explanations why these genes responded differently in two different growing media. A significant increase in the expression level of *B'κ* and *Bϐ (Clade I)* only in the mycorrhizal roots grown in vermiculite could be ascribed to specific growing conditions in this medium, which subsequently also affected the AM morphology (**Figure 21**). The *C1* gene repeatedly showed high responsiveness to both PGPR and AMF regardless of the type of growing medium, underpinning the importance of the catalytic subunits from subfamily I for the plant-microbe interactions and supporting the results obtained for Arabidopsis discussed in the previous section.

6.3 Transcriptional characterization of B'φ in WT tomato plants

The analysis of the transcript abundance of *B'φ* in roots, young leaves and unopened flower buds of the WT tomato plants grown in soil or in

vermiculite pointed out that *B'φ* was expressed at a very low level in all the plant organs (**Figure 17**). The expression of *TAS14*, used as ABA-responsive marker, in plants grown in vermiculite was very high indicating elevated ABA levels which could be associated with abiotic stress, contrary to the soil-grown plants, where ABA levels were considerably lower in leaves and flower buds. The assay of the expression of *TAS14* was included throughout all the experiments in order to deduce the role of ABA in the regulation of *B'φ* suggested by Charpentier et al. (2014).

During the treatment with PGPR, an enhanced, up to 73% compared with non-treated plants, root biomass was observed in the roots with a significant upregulation of *B'φ* expression which was detected one and three weeks after inoculation. That upregulation was associated only with two out of three bacterial strains, although the values with statistical significance for both the *B'φ* expression and the root biomass were found only in the plants inoculated with WCS417r (**Figures 19 and 20B**). Therefore, it remained unclear whether the upregulation of the *B'φ* expression arose in response to PGPR or to developmental changes associated with faster growing roots. Furthermore, no correlations between the *B'φ* and *TAS14* expression levels were observed.

The colonization by AMF with AM formation did not cause any significant response in the expression of *B'φ* unlike e.g. *C1*, *GAST1* and *PT4* (**Figure 22A**). However, it would be premature to draw any conclusions about the role of B'φ in the promotion of arbuscule formation proposed by Charpentier et al. (2014) since only mycorrhizal roots with either a low level of mycorrhization (soil) or a zero level of arbusculation (vermiculite) were studied **(Figure 30A,** WT values for 3.5-month cultivation with AMF in soil or **Figure 21B** respectively).

6.4 B'φ overexpression alters tomato morphology

To gain an insight into the function of the B'φ subunit, transgenic tomato plants overexpressing B'φ were designed using genetic engineering techniques. The gain-of-function mutation in *B'φ* in tomato has not been previously studied. The overexpression of *B'φ* was maintained by the constitutive promoter CaMV 35S which is considered to be expressed in all plant tissues (Slater et al. 2008). The resulting transgenic tomato plants produced a characteristic phenotype with smaller leaves, reduced stem thickness, reduced shoot and root biomass (**Figure 26A**). Moreover, these plants also exhibited slowed growth and development, and decreased root-to-shoot ratio compared to WT. These developmental differences became clear four weeks after sowing. No substantial delay in germination time was noticed. The transgenic plants were not visually distinguishable from WT seedlings for the first three weeks after germination. Thereafter, the growth rate was slowed and by the end of the eighth week, while most of the WT plants had already developed 9 leaves and begun to flower, the transgenic plants had only 8 leaves and small or no flower buds. By visual inspection, neither the size nor form of flowers and fruits were altered, unlike the seed number per fruit which was considerably reduced compared to WT (**Figure 26B**). The similar phenotype alterations were reported in tomato, potato and tobacco subjected to the genetic manipulations with GA biosynthesis or degradation with a consequent alteration of the production of active GAs. This alteration has been shown to modify the shoot and fruit growth and development in a similar manner as it was observed in the current $b'\varphi_{ox}$ lines (Carrera et al. 2000; Xiao et al. 2006; Chen et al. 2016). Numerous experiments previously conducted with the mutants with impaired GA production have enabled the identification of genes and enzymes responsible for each step of GA biosynthesis (Hedden and Kamiya 1997; Hedden and Proebsting 1999). However, the genes responsible for the specific regulation of GA production in roots were not tested in those

studies, because most of the mutants have been screened only for stunted shoots.

On the other hand, the decreased root-to-shoot ratio in the transgenic plants could also be attributed to adverse ABA regulation in response to the *B'φ* overexpression (Saab et al. 1990). In addition, the considerable reduction of AM frequency in the *b'φ*$_{ox}$ lines relative to WT may indicate GA-ABA imbalance that has been reported to impair AM development in ABA-deficient tomato mutants (Herrera-Medina et al. 2007; Martin-Rodriguez et al. 2016). The suppression of ABA biosynthesis in that mutants also caused a reduction in arbuscule abundance. Unfortunately, the arbuscule study remained beyond the grasp of the present research because of a simultaneous application of several AMF species. Competition among these species could influence the AM morphology as well as the arbuscule development and abundance posing a major challenge in interpreting the results (Jansa et al. 2008; Smith and Read 2008b).

6.5 Transcriptional analysis of PP2A subunits in the transgenic plants

Transcriptional analysis of the PP2A subunits in the roots of the transgenic plants colonized and not colonized by AMF revealed that *Bβ* from Clade I had a significant increase in the expression most likely in response to the *B'φ* overexpression (**Figure 31B**). Like *B'φ*, this gene is also absent from the Arabidopsis genome. It remains unclear whether a significant increase in the expression level of *B'κ* and *AβII* detected only in non-mycorrhizal roots of *b'φ*$_{ox}$ could be ascribed to the transgene (**Figure 31B**). Moreover, further research is required to determine if the response of *C1* and *GA20ox-2* to AMF observed in the roots of WT was arrested by the *B'φ* overexpression in *b'φ*$_{ox}$.

6.6 B'φ overexpression specifically influenced the abundance of GA- and ABA-associated transcripts in roots

Considering the morphological alterations in the *b'φ$_{ox}$* lines, the expression analysis of GA- and ABA-associated genes was also performed. The emphasis was on the genes involved in GA and ABA biosynthesis and response. The gene expression study revealed a substantial difference in transcript profiles between WT and the transgenic plants both in roots and young leaves. This difference was tissue-specific and more profound in the roots because the expression of both ABA- and GA-associated genes were affected, whereas in the leaves, only the GA biosynthesis genes were influenced by *B'φ* overexpression (**Figures 32B and 33B**). The expression of the ABA-responsive gene *TAS14* and the GA-responsive gene *GAST1* was significantly downregulated in the roots of *b'φ$_{ox}$* though this downregulation was more profound in the *GAST1* expression. The substantial decrease of the *GAST1* expression pointed out a lowered level of bioactive GAs (GA_3 in particular). But this decrease does not seem to be associated with impaired GA biosynthesis, since the expression levels of the GA biosynthesis genes were not affected, or with increased ABA level, a negative regulator of the *GAST1* expression (Shi and Olszewski 1998). A corresponding decrease in the *NCED-1* expression indicated that the lower levels of the *TAS14* transcripts in *b'φ$_{ox}$* could be ascribed to changes in the ABA biosynthesis. This finding is consistent with the results published by Charpentier et al. (2017) where B'φ was identified as a component of ABA-controlled pathway involved in the promotion of AM colonization. And, thus, the decrease of ABA level in the roots of *b'φ$_{ox}$* could be considered as the response to the *B'φ* overexpression. However, it became evident that the *B'φ* overexpression also caused disturbances in GA homeostasis suggesting an important role of B'φ in GA-ABA balance. Indeed, an optimal GA-ABA balance was shown to be crucial for normal plant development in general (Weiss and Ori 2007)

and during AM formation in particular (Martin-Rodriguez et al. 2016) which may explain the reduced AM frequency and morphological changes in *b'φ*$_{ox}$. Moreover, ABA and GAs relationship has an antagonistic manner, thus, low ABA level should promote GA biosynthesis and vice versa (Weiss and Ori 2007; Seo et al. 2006). But this mechanism seemed to be disrupted with the *B'φ* overexpression. Even though the transcript profile obtained for young leaves showed no alterations in the expression of *GAST1* and *TAS14*, the transcript levels of the GA biosynthesis genes *GA20ox-1* and *-2* were significantly elevated upon the *B'φ* overexpression, apparently for maintaining an optimal level of bioactive GAs. The different effect of the *B'φ* overexpression on the content of bioactive GAs in roots and young leaves could imply that feedback regulation of the GA biosynthesis genes may vary with tissue and type of GA20ox or GA3ox involved, that is in turn could be conditioned by the predominance of one of the two GA-biosynthetic pathways (**Appendix, Figure A8**). It is also noteworthy that the *B'φ* overexpression in roots of the transgenic plants was 2.5 times higher than that in young leaves. However, it remained unclear whether the drop of the level of bioactive GAs in roots and the elevated expression of *GA20ox-1* and *-2* in young leaves were due to activation of genes coding for Gibberellin 2-oxidases (GA2ox) responsible for the GA catabolism, namely the conversion of bioactive GAs into a biologically inactive form by means of 2β-hydroxylation. Studying the tomato mutants specifically overexpressing GA2ox-1 in fruits, Chen et al. (2016) reported a significant reduction of the seed number per fruit and the downregulation of the *GAST1* expression. Xiao et al. (2006) reported defects in vegetative development of transgenic tomato with reduced content of bioactive GAs similar to those observed in *b'φ*$_{ox}$. But they did not provide the information about the seed number per fruit and whether the alteration in the root development of those mutants was observed.

7 Conclusion

In this study, the role of PP2A as an important mediator in beneficial plant-microbe interactions was tested. To this end, Arabidopsis WT and various PP2A mutants with hight and low PP2A activity were treated with PGPR and studied phenotypically. The response of genes encoding certain PP2A subunits in tomato to the treatment with AMF and PGPR was also investigated by sqRT-PCR. In both model plants, the microbial stimulation revealed that the catalytic subunits from subfamily I (C2 and C5 in Arabidopsis and C1 in tomato) as well as the regulatory subunit B'θ, may play a special role in beneficial plant-microbe interactions. The role of the other PP2A subunits studied in this regard remains questioned and requires more in-depth analysis. Apart from C1 and B'θ, the most interesting findings from the PP2A study in tomato could be credited to Bβ from Clade I and III, B'κ and AβI.

Even though the microbial stimulation triggered no response in the regulatory B'φ subunit, the application of the transgenic tomato plants overexpressing B'φ for the phenotypic and gene expression analyses provided valuable information about the physiological role of this subunit which before this study was obscure. In the present research, it has become clear that B'φ can influence the ABA-GA balance by modulating the concentration of active GAs and is most likely controlled by ABA. However, it is necessary to check the expression of the genes controlling GA deactivation/catabolism in the roots and leaves of the transgenic tomato plants and to obtain the corresponding expression profiles of GA- and ABA-associated genes in fruits. It would be also reasonable to test if treatment with GA restores the WT phenotype in *b'φ$_{ox}$* lines.

8 References

Abdulkareem M, Aboud HM, Saood HM, Shibly MK (2014) Antagonistic Activity of Some Plant Growth Rhizobacteria to Fusarium Graminearum. *3 (1):6*. doi:10.33687/phytopath.003.01.0660

Ahn IP (2007) Rhizobacteria-Induced Priming in Arabidopsis Is Dependent on Ethylene, Jasmonic Acid, and NPR1. *Molecular plant-microbe interactions* v. 20 (no. 7): pp. 759-768-2007 v.2020 no.2007. doi:10.1094/MPMI-20-7-0759

Ait-Ali T, Frances S, Weller JL, Reid JB, Kendrick RE, Kamiya Y (1999) Regulation of gibberellin 20-oxidase and gibberellin 3beta-hydroxylase transcript accumulation during De-etiolation of pea seedlings. *Plant physiology* 121 (3):783-791. doi:10.1104/pp.121.3.783

Akoglu H (2018) User's guide to correlation coefficients. *Turkish Journal of Emergency Medicine* 18 (3):91-93. doi:10.1016/j.tjem.2018.08.001

Alexandre G (2015) Chemotaxis in Azospirillum. In: Cassán FD, Okon Y, Creus CM (eds). *Handbook for Azospirillum*: Technical Issues and Protocols. Springer International Publishing, Cham, pp 101-114. doi: 10.1007/978-3-319-06542-7_6

Alfano G (2007) Systemic Modulation of Gene Expression in Tomato by Trichoderma hamatum 382. *Phytopathology*, v. 97 (no. 4):pp. 429-437-2007 v.2097 no.2004. doi:10.1094/PHYTO-97-4-0429

Alonso JM, Stepanova AN, Leisse TJ, Kim CJ, Chen H, Shinn P, Stevenson DK, Zimmerman J, Barajas P, Cheuk R, Gadrinab C, Heller C, Jeske A, Koesema E, Meyers CC, Parker H, Prednis L, Ansari Y, Choy N, Deen H, Geralt M, Hazari N, Hom E, Karnes M, Mulholland C, Ndubaku R, Schmidt I, Guzman P, Aguilar-Henonin L, Schmid M, Weigel D, Carter DE, Marchand T, Risseeuw E, Brogden D, Zeko A, Crosby WL, Berry CC, Ecker JR (2003) Genome-wide insertional

mutagenesis of Arabidopsis thaliana. *Science*. 301 (5633):653-657. doi: 10.1126/science.1086391

Alstr, Ouml, M S (1991) Induction of disease resistance in common bean susceptible to halo blight bacterial pathogen after seed bacterization with rhizosphere pseudomonads. *The Journal of General and Applied Microbiology*. 37 (6):495-501. doi:10.2323/jgam.37.495

Amenta M, Molina-Favero C, Creus CM, Lamattina L (2015) Nitric Oxide in Azospirillum and Related Bacteria: Production and Effects. In: Cassán FD, Okon Y, Creus CM (eds) *Handbook for Azospirillum*: Technical Issues and Protocols. Springer International Publishing, Cham, pp 155-180. doi:10.1007/978-3-319-06542-7_9

Augé RM (2001) Water relations, drought and vesicular-arbuscular mycorrhizal symbiosis. *Mycorrhiza*, 11 (1):3-42. doi:10.1007/s005720100097

Ballesteros I, Dominguez T, Sauer M, Paredes P, Duprat A, Rojo E, Sanmartin M, Sanchez-Serrano JJ (2013) Specialized functions of the PP2A subfamily II catalytic subunits PP2A-C3 and PP2A-C4 in the distribution of auxin fluxes and development in Arabidopsis. *Plant*, J 73 (5):862-872. doi:10.1111/tpj.12078

Bashan Y, de-Bashan LE (2010) Chapter Two - How the Plant Growth-Promoting Bacterium Azospirillum Promotes Plant Growth—A Critical Assessment. In: Sparks DL (ed) *Advances in Agronomy*, vol 108. Academic Press, pp 77-136. doi:https://doi.org/10.1016/S0065-2113(10)08002-8

Basu S (2011) PP2A in the regulation of cell motility and invasion. *Curr Protein Pept Sci* 12 (1):3-11. doi:10.2174/138920311795659443

Belimov AA, Dodd IC, Safronova VI, Dumova VA, Shaposhnikov AI, Ladatko AG, Davies WJ (2014) Abscisic acid metabolizing rhizobacteria decrease ABA concentrations in planta and alter plant growth. *Plant Physiol Biochem* 74:84-91. doi:10.1016/j.plaphy.2013.10.032

Beneduzi A, Ambrosini A, Passaglia LM (2012) Plant growth-promoting rhizobacteria (PGPR): Their potential as antagonists and biocontrol agents. *Genet Mol Biol* 35 (4 (suppl)):1044-1051. doi:10.1590/s1415-47572012000600020

Berendsen RL, van Verk MC, Stringlis IA, Zamioudis C, Tommassen J, Pieterse CM, Bakker PA (2015) Unearthing the genomes of plant-beneficial Pseudomonas model strains WCS358, WCS374 and WCS417. *BMC Genomics* 16:539. doi:10.1186/s12864-015-1632-z

Bio-Rad (n.d.) Quick Start™ Bradford Protein Assay. Instruction Manual. Bio-Rad Laboratories, Inc. Available from < http://kirschner.med.harvard.edu/files/protocols/BioRad_proteinassay.pdf >[Accessed 12 of October 2016],

Blakeslee JJ, Zhou HW, Heath JT, Skottke KR, Barrios JA, Liu SY, DeLong A (2008) Specificity of RCN1-mediated protein phosphatase 2A regulation in meristem organization and stress response in roots. *Plant Physiol* 146 (2):539-553. doi:10.1104/pp.107.112995

Bona E, Cantamessa S, Massa N, Manassero P, Marsano F, Copetta A, Lingua G, D'Agostino G, Gamalero E, Berta G (2017) Arbuscular mycorrhizal fungi and plant growth-promoting pseudomonads improve yield, quality and nutritional value of tomato: a field study. *Mycorrhiza* 27 (1):1-11. doi:10.1007/s00572-016-0727-y

Booker MA, DeLong A (2017) Atypical Protein Phosphatase 2A Gene Families Do Not Expand via Paleopolyploidization. *Plant Physiol* 173 (2):1283-1300. doi:10.1104/pp.16.01768

Boyer LR, Feng W, Gulbis N, Hajdu K, Harrison RJ, Jeffries P, Xu XM (2016) The Use of Arbuscular Mycorrhizal Fungi to Improve Strawberry Production in Coir Substrate. *Frontiers in Plant Science* 7. doi:ARTN 123710.3389/fpls.2016.01237

Bradford MM (1976) A rapid and sensitive method for the quantitation of microgram quantities of protein utilizing the principle of protein-dye binding. *Anal Biochem* 72:248-254. doi:10.1006/abio.1976.9999

Bruto M, Prigent-Combaret C, Muller D, Moenne-Loccoz Y (2014) Analysis of genes contributing to plant-beneficial functions in plant growth-promoting rhizobacteria and related Proteobacteria. *Sci Rep* 4. doi:ARTN 626110.1038/srep06261

Bultreys A, Gheysen I, Wathelet B, Maraite H, de Hoffmann E (2003) High-performance liquid chromatography analyses of pyoverdin siderophores differentiate among phytopathogenic fluorescent Pseudomonas Species. *Appl Environ Microbiol* 69 (2):1143-1153. doi: 10.1128/aem.69.2.1143-1153.2003

Carrera E, Bou J, Garcia-Martinez JL, Prat S (2000) Changes in GA 20-oxidase gene expression strongly affect stem length, tuber induction and tuber yield of potato plants. *Plant Journal* 22 (3):247-256. doi: 10.1046/ j.1365-313x.2000.00736.x

Casamayor A, Perez-Callejon E, Pujol G, Arino J, Ferrer A (1994) Molecular characterization of a fourth isoform of the catalytic subunit of protein phosphatase 2A from Arabidopsis thaliana. *Plant Mol Biol* 26 (1):523-528. doi:10.1007/bf00039564

Cassán FD, Okon Y, Creus CM (2015) Handbook for Azospirillum.Technical Issues and Protocols. Springer International Publishing. doi:10.1007/978-3-319-06542-7

Castillo P, Molina R, Andrade A, Vigliocco A, Alemano S, Cassán FD (2015) Phytohormones and Other Plant Growth Regulators Produced by PGPR: The Genus Azospirillum. In: Cassán FD, Okon Y, Creus CM (eds) Handbook for Azospirillum: Technical Issues and Protocols. Springer International Publishing, Cham, pp 115-138. doi:10.1007/978-3-319-06542-7_7

Cavagnaro TR, Gao L-L, Smith FA, Smith SE (2001) Morphology of arbuscular mycorrhizas is influenced by fungal identity. *New Phytologist* 151 (2):469-475. doi:10.1046/j.0028-646x.2001.00191.x

Charpentier M, Sun J, Wen J, Mysore KS, Oldroyd GE (2014) Abscisic acid promotion of arbuscular mycorrhizal colonization requires a

component of the PROTEIN PHOSPHATASE 2A complex. *Plant Physiol* 166 (4):2077-2090. doi:10.1104/pp.114.246371

Chen CQ, Belanger RR, Benhamou N, Paulitz TC (2000) Defense enzymes induced in cucumber roots by treatment with plant growth-promoting rhizobacteria (PGPR) and Pythium aphanidermatum. *Physiol Mol Plant* Pathol 56 (1):13-23. doi:10.1006/pmpp.1999.0243

Chen J, Hu R, Zhu Y, Shen G, Zhang H (2014) Arabidopsis PHOSPHOTYROSYL PHOSPHATASE ACTIVATOR is essential for PROTEIN PHOSPHATASE 2A holoenzyme assembly and plays important roles in hormone signaling, salt stress response, and plant development. *Plant Physiol* 166 (3):1519-1534. doi:10.1104/pp.114.250563

Chen J, Zhu X, Shen G, Zhang H (2015) Overexpression of AtPTPA in Arabidopsis increases protein phosphatase 2A activity by promoting holoenzyme formation and ABA negatively affects holoenzyme formation. *Plant Signal Behav* 10 (11):e1052926. doi:10.1080/15592324.2015.1052926

Chen S, Wang X, Zhang L, Lin S, Liu D, Wang Q, Cai S, El-Tanbouly R, Gan L, Wu H, Li Y (2016) Identification and characterization of tomato gibberellin 2-oxidases (GA2oxs) and effects of fruit-specific SlGA2ox1 overexpression on fruit and seed growth and development. *Hortic Res* 3:16059. doi:10.1038/hortres.2016.59

Chetty VJ, Ceballos N, Garcia D, Narvaez-Vasquez J, Lopez W, Orozco-Cardenas ML (2013) Evaluation of four Agrobacterium tumefaciens strains for the genetic transformation of tomato (Solanum lycopersicum L.) cultivar Micro-Tom. *Plant Cell Rep* 32 (2):239-247. doi:10.1007/s00299-012-1358-1

Cohen AC, Bottini R, Piccoli PN (2008) Azospirillum brasilense Sp 245 produces ABA in chemically defined culture medium and increases ABA content in arabidopsis plants. *Plant Growth Regulation* 54 (2):97-103. doi:10.1007/s10725-007-9232-9

Cohen AC, Travaglia CN, Bottini R, Piccoli PN (2009) Participation of abscisic acid and gibberellins produced by endophytic Azospirillum in the alleviation of drought effects in maize. *Botany* 87 (5):455-462. doi:10.1139/B09-023

Cohen P, Klumpp S, Schelling DL (1989) An Improved Procedure for Identifying and Quantitating Protein Phosphatases in Mammalian-Tissues. *Febs Letters* 250 (2):596-600

Cosme M, Fernandez I, Van der Heijden MGA, Pieterse CMJ (2018) Non-Mycorrhizal Plants: The Exceptions that Prove the Rule. *Trends Plant Sci* 23 (7):577-587. doi:10.1016/j.tplants.2018.04.004

Costacurta A, Keijers V, Vanderleyden J (1994) Molecular-Cloning and Sequence-Analysis of an Azospirillum-Brasilense Indole-3-Pyruvate Decarboxylase Gene. *Molecular & General Genetics* 243 (4):463-472

Creighton MT, Kolton A, Kataya ARA, Maple-Grodem J, Averkina IO, Heidari B, Lillo C (2017a) Methylation of protein phosphatase 2A-Influence of regulators and environmental stress factors. *Plant Cell Environ* 40 (10):2347-2358. doi:10.1111/pce.13038

Creighton MT, Sanmartin M, Kataya ARA, Averkina IO, Heidari B, Nemie-Feyissa D, Sanchez-Serrano JJ, Lillo C (2017b) Light regulation of nitrate reductase by catalytic subunits of protein phosphatase 2A. *Planta*. doi:10.1007/s00425-017-2726-4

Creus CM, Graziano M, Casanovas EM, Pereyra MA, Simontacchi M, Puntarulo S, Barassi CA, Lamattina L (2005) Nitric oxide is involved in the Azospirillum brasilense-induced lateral root formation in tomato. *Planta* 221 (2):297-303. doi:10.1007/s00425-005-1523-7

Dickson S (2004) The Arum–Paris continuum of mycorrhizal symbioses. *New Phytologist* 163 (1):187-200. doi:10.1111/j.1469-8137.2004.01095.x

Dodd IC, Zinovkina NY, Safronova VI, Belimov AA (2010) Rhizobacterial mediation of plant hormone status. *Annals of Applied Biology* 157 (3):361-379.

Duijff BJ, Gianinazzi-Pearson V, Lemanceau P (1997) Involvement of the outer membrane lipopolysaccharides in the endophytic colonization of tomato roots by biocontrol Pseudomonas fluorescens strain WCS417r. *New Phytologist* 135 (2):325-334. doi:10.1046/j.1469-8137.1997.00646.x

Durian G, Rahikainen M, Alegre S, Brosche M, Kangasjarvi S (2016) Protein Phosphatase 2A in the Regulatory Network Underlying Biotic Stress Resistance in Plants. *Front Plant Sci* 7:812. doi:10.3389/fpls.2016.00812

Farkas I, Dombradi V, Miskei M, Szabados L, Koncz C (2007) Arabidopsis PPP family of serine/threonine phosphatases. *Trends Plant Sci* 12 (4):169-176. doi:10.1016/j.tplants.2007.03.003

Fiorilli V, Vannini C, Ortolani F, Garcia-Seco D, Chiapello M, Novero M, Domingo G, Terzi V, Morcia C, Bagnaresi P, Moulin L, Bracale M, Bonfante P (2018) Omics approaches revealed how arbuscular mycorrhizal symbiosis enhances yield and resistance to leaf pathogen in wheat. *Sci Rep* 8 (1):9625-9625. doi:10.1038/s41598-018-27622-8

Fritz M, Jakobsen I, Lyngkjaer MF, Thordal-Christensen H, Pons-Kuhnemann J (2006) Arbuscular mycorrhiza reduces susceptibility of tomato to Alternaria solani. Mycorrhiza 16 (6):413-419. doi:10.1007/s00572-006-0051-z

Garcia de Salamone IE, Hynes RK, Nelson LM (2001) Cytokinin production by plant growth promoting rhizobacteria and selected mutants. *Can J Microbiol* 47 (5):404-411. doi:10.1139/w01-029

Giovannini L, Palla M, Agnolucci M, Avio L, Sbrana C, Turrini AG, M. (2020) Arbuscular Mycorrhizal Fungi and Associated Microbiota as Plant Biostimulants: Research Strategies for the Selection of the Best

Performing Inocula. . *Agronomy* 10 (1):106. doi:10.3390/agronomy10010106

Glick BR (2014) Bacteria with ACC deaminase can promote plant growth and help to feed the world. *Microbiol Res* 169 (1):30-39. doi:10.1016/j.micres.2013.09.009

Glick BR (2015) Stress Control and ACC Deaminase. In: Lugtenberg B (ed) Principles of Plant-Microbe Interactions: Microbes for Sustainable Agriculture. Springer International Publishing, Cham, pp 257-264. doi:10.1007/978-3-319-08575-3_27

Godoy JA, Pardo JM, Pintor-Toro JA (1990) A tomato cDNA inducible by salt stress and abscisic acid: nucleotide sequence and expression pattern. *Plant Mol Biol* 15 (5):695-705. doi:10.1007/bf00016120

Goldberg Y (1999) Protein phosphatase 2A: who shall regulate the regulator? *Biochem Pharmacol* 57 (4):321-328. doi:10.1016/s0006-2952(98)00245-7

Groves MR, Hanlon N, Turowski P, Hemmings BA, Barford D (1999) The structure of the protein phosphatase 2A PR65/A subunit reveals the conformation of its 15 tandemly repeated HEAT motifs. *Cell* 96 (1):99-110

Hacquard S, Spaepen S, Garrido-Oter R, Schulze-Lefert P (2017) Interplay Between Innate Immunity and the Plant Microbiota. *Annual Review of Phytopathology*, Vol 55 55:565-589. doi:10.1146/annurev-phyto-080516-035623

Haesen D, Sents W, Lemaire K, Hoorne Y, Janssens V (2014) The Basic Biology of PP2A in Hematologic Cells and Malignancies. *Front Oncol* 4:347. doi:10.3389/fonc.2014.00347

Hart M, Ehret DL, Krumbein A, Leung C, Murch S, Turi C, Franken P (2015) Inoculation with arbuscular mycorrhizal fungi improves the nutritional value of tomatoes. *Mycorrhiza* 25 (5):359-376. doi:10.1007/s00572-014-0617-0

Hartmann A, Rothballer M, Schmid M (2008) Lorenz Hiltner, a pioneer in rhizosphere microbial ecology and soil bacteriology research. *Plant and Soil* (312):7-14. doi:10.1007/s11104-007-9514-z

He XH, Anderson JC, del Pozo O, Gu YQ, Tang XY, Martin GB (2004) Silencing of subfamily I of protein phosphatase 2A catalytic subunits results in activation of plant defense responses and localized cell death. *Plant Journal* 38 (4):563-577. doi:10.1111/j.1365-313X.2004.02073.x

Hedden P, Kamiya Y (1997) GIBBERELLIN BIOSYNTHESIS: Enzymes, Genes and Their Regulation. *Annu Rev Plant Physiol Plant Mol Biol* 48:431-460. doi:10.1146/annurev.arplant.48.1.431

Hedden P, Proebsting WM (1999) Genetic analysis of gibberellin biosynthesis. *Plant Physiol* 119 (2):365-370. doi:10.1104/pp.119.2.365

Hedden P, Thomas SG (2012) Gibberellin biosynthesis and its regulation. *Biochem* J 444 (1):11-25. doi:10.1042/bj20120245

Heidari B, Matre P, Nemie-Feyissa D, Meyer C, Rognli OA, Moller SG, Lillo C (2011) Protein phosphatase 2A B55 and A regulatory subunits interact with nitrate reductase and are essential for nitrate reductase activation. *Plant Physiol* 156 (1):165-172. doi:10.1104/pp.111.172734

Herrera-Medina MJ, Steinkellner S, Vierheilig H, Ocampo Bote JA, Garcia Garrido JM (2007) Abscisic acid determines arbuscule development and functionality in the tomato arbuscular mycorrhiza. *New Phytol* 175 (3):554-564. doi:10.1111/j.1469-8137.2007.02107.x

Hoagland DR, Arnon DI (1950) The water-culture method for growing plants without soil. The College of Agriculture, Berkely,

Holsters M, de Waele D, Depicker A, Messens E, van Montagu M, Schell J (1978) Transfection and transformation of Agrobacterium tumefaciens. *Mol Gen Genet* 163 (2):181-187. doi:10.1007/bf00267408

Honkanen RE, Golden T (2002) Regulators of serine/threonine protein phosphatases at the dawn of a clinical era? *Curr Med Chem* 9 (22):2055-2075. doi:10.2174/0929867023368836

Hwang J, Lee JA, Pallas DC (2016) Leucine Carboxyl Methyltransferase 1 (LCMT-1) Methylates Protein Phosphatase 4 (PP4) and Protein Phosphatase 6 (PP6) and Differentially Regulates the Stable Formation of Different PP4 Holoenzymes. J *Biol Chem* 291 (40):21008-21019. doi: 10.1074/jbc.M116.739920

Jansa J, Smith FA, Smith SE (2008) Are there benefits of simultaneous root colonization by different arbuscular mycorrhizal fungi? *New Phytol* 177 (3):779-789. doi:10.1111/j.1469-8137.2007.02294.x

Janssens V, Goris J (2001) Protein phosphatase 2A: a highly regulated family of serine/threonine phosphatases implicated in cell growth and signalling. *Biochem* J 353 (Pt 3):417-439

Janssens V, Goris J, Van Hoof C (2005) PP2A: the expected tumor suppressor. *Curr Opin Genet Dev* 15 (1):34-41. doi:10.1016/j.gde.2004.12.004

Javot H, Penmetsa RV, Terzaghi N, Cook DR, Harrison MJ (2007) A Medicago truncatula phosphate transporter indispensable for the arbuscular mycorrhizal symbiosis. *Proc Natl Acad Sci U S A* 104 (5): 1720 -1725. doi:10.1073/pnas.0608136104

Jin L, Ham JH, Hage R, Zhao WY, Soto-Hernandez J, Lee SY, Paek SM, Kim MG, Boone C, Coplin DL, Mackey D (2016) Direct and Indirect Targeting of PP2A by Conserved Bacterial Type-III Effector Proteins. *Plos Pathogens* 12 (5). doi:ARTN e100560910.1371/journal.ppat.1005609

Jordens J, Janssens V, Longin S, Stevens I, Martens E, Bultynck G, Engelborghs Y, Lescrinier E, Waelkens E, Goris J, Van Hoof C (2006) The protein phosphatase 2A phosphatase activator is a novel peptidyl-prolyl cis/trans-isomerase. *J Biol Chem* 281 (10):6349-6357. doi: 10.1074/jbc.M507760200

Jung SC, Martinez-Medina A, Lopez-Raez JA, Pozo MJ (2012) Mycorrhiza-induced resistance and priming of plant defenses. *J Chem Ecol* 38 (6):651-664. doi:10.1007/s10886-012-0134-6

Karthikeyan M, Radhika K, Mathiyazhagan S, Bhaskaran R, Samiyappan R, Velazhahan R (2006) Induction of phenolics and defense-related enzymes in coconut (Cocos nucifera L.) roots treated with biocontrol agents. *Brazilian Journal of Plant Physiology* 18:367-377

Kataya AR, Heidari B, Lillo C (2015) Protein phosphatase 2A regulatory subunits affecting plant innate immunity, energy metabolism, and flowering time--joint functions among B'eta subfamily members. *Plant Signal Behav* 10 (5):e1026024. doi:10.1080/15592324.2015.1026024

Kimura S, Sinha N (2008) Tomato (Solanum lycopersicum): A Model Fruit-Bearing Crop. CSH Protoc 2008:pdb emo105. doi:10.1101/pdb.emo105

King EO, Ward MK, Raney DE (1954) Two simple media for the demonstration of pyocyanin and fluorescin. J Lab Clin Med 44 (2):301-307

Kleinboelting N, Huep G, Kloetgen A, Viehoever P, Weisshaar B (2012) GABI-Kat SimpleSearch: new features of the Arabidopsis thaliana T-DNA mutant database. Nucleic Acids Res 40 (Database issue):D1211-1215. doi:10.1093/nar/gkr1047

Koide RT, Mosse B (2004) A history of research on arbuscular mycorrhiza. *Mycorrhiza* 14 (3):145-163. doi:10.1007/s00572-004-0307-4

Krasinska L, Domingo-Sananes MR, Kapuy O, Parisis N, Harker B, Moorhead G, Rossignol M, Novak B, Fisher D (2011) Protein phosphatase 2A controls the order and dynamics of cell-cycle transitions. *Mol Cell* 44 (3):437-450. doi:10.1016/j.molcel.2011.10.007

Kwak JM, Moon JH, Murata Y, Kuchitsu K, Leonhardt N, DeLong A, Schroeder JI (2002) Disruption of a guard cell-expressed protein phosphatase 2A regulatory subunit, RCN1, confers abscisic acid insensitivity in Arabidopsis. *Plant Cell* 14 (11):2849-2861. doi:10.1105 /tpc.003335

Lackie JM (2010) A dictionary of biomedicine. Oxford paperback reference, 1st edn. Oxford University Press, Oxford

Lange T, Hedden P, Graebe JE (1994) Expression cloning of a gibberellin 20-oxidase, a multifunctional enzyme involved in gibberellin biosynthesis. *Proceedings of the National Academy of Sciences of the United States of America* 91 (18):8552-8556. doi:10.1073/pnas. 91.18. 8552

Lechward K, Awotunde OS, Swiatek W, Muszynska G (2001) Protein phosphatase 2A: variety of forms and diversity of functions. *Acta Biochim* Pol 48 (4):921-933

Lee JA, Pallas DC (2007) Leucine carboxyl methyltransferase-1 is necessary for normal progression through mitosis in mammalian cells. *J Biol Chem* 282 (42):30974-30984. doi:10.1074/jbc.M704861200

Leeman M, Pelt J, Ouden F, Heinsbroek M, Bakker P, Schippers B (1995) Induction of systemic resistance against fusarium wilt of radish by lipopolysaccharides of Pseudomonas fluorescens. *Phytopathology* 85 (9):1021-1027. doi:10.1094/phyto-85-1021

Lester DR, Ross JJ, Davies PJ, Reid JB (1997) Mendel's stem length gene (Le) encodes a gibberellin 3 beta-hydroxylase. *The Plant cell* 9 (8):1435-1443. doi:10.1105/tpc.9.8.1435

Li Z, Defoort J, Tasdighian S, Maere S, Van de Peer Y, De Smet R (2016) Gene Duplicability of Core Genes Is Highly Consistent across All Angiosperms. *Plant Cell* 28 (2):326-344. doi:10.1105/tpc.15.00877

Lillo C, Kataya AR, Heidari B, Creighton MT, Nemie-Feyissa D, Ginbot Z, Jonassen EM (2014) Protein phosphatases PP2A, PP4 and PP6:

mediators and regulators in development and responses to environmental cues. *Plant Cell Environ* 37 (12):2631-2648. doi:10.1111/pce.12364

Liu J (2007) Arbuscular mycorrhizal symbiosis is accompanied by local and systemic alterations in gene expression and an increase in disease resistance in the shoots. *The plant journal* v. 50 (no. 3): pp. 529-544-2007 v.2050 no.2003. doi:10.1111/j.1365-313X.2007.03069.x

Longin S, Jordens J, Martens E, Stevens I, Janssens V, Rondelez E, De Baere I, Derua R, Waelkens E, Goris J, Van Hoof C (2004) An inactive protein phosphatase 2A population is associated with methylesterase and can be re-activated by the phosphotyrosyl phosphatase activator. *Biochemical Journal* 380:111-119. doi:10.1042/Bj20031643

Madigan MT, Madigan MT, Brock TD (2009) Brock biology of microorganisms. 12th edn. Pearson/Benjamin Cummings, San Francisco, CA

Magnin-Robert M, Trotel-Aziz P, Quantinet D, Biagianti S, Aziz A (2007) Biological control of Botrytis cinerea by selected grapevine-associated bacteria and stimulation of chitinase and β-1,3 glucanase activities under field conditions. *European Journal of Plant Pathology* 118 (1):43-57. doi:10.1007/s10658-007-9111-2

Maheshwari DK (2011) Bacteria in Agrobiology: Plant Growth Responses. Springer-Verlag Berlin Heidelberg. doi:10.1007/978-3-642-20332-9_6

Marschner H, Dell B (1994) Nutrient uptake in mycorrhizal symbiosis. *Plant and Soil* 159 (1):89-102. doi:10.1007/BF00000098

Martin-Rodriguez JA, Huertas R, Ho-Plagaro T, Ocampo JA, Tureckova V, Tarkowska D, Ludwig-Muller J, Garcia-Garrido JM (2016) Gibberellin-Abscisic Acid Balances during Arbuscular Mycorrhiza Formation in Tomato. *Front Plant Sci* 7:1273. doi:10.3389/fpls.2016.01273

Martín-Rodríguez JÁ, Ocampo JA, Molinero-Rosales N, Tarkowská D, Ruíz-Rivero O, García-Garrido JM (2015) Role of gibberellins during arbuscular mycorrhizal formation in tomato: new insights revealed by endogenous quantification and genetic analysis of their metabolism in mycorrhizal roots. *Physiologia Plantarum* 154 (1):66-81. doi:10.1111/ppl.12274

Martin DN, Proebsting WM, Hedden P (1997) Mendel's dwarfing gene: cDNAs from the Le alleles and function of the expressed proteins. *Proceedings of the National Academy of Sciences of the United States of America* 94 (16):8907-8911. doi:10.1073/pnas.94.16.8907

Martin DN, Proebsting WM, Parks TD, Dougherty WG, Lange T, Lewis MJ, Gaskin P, Hedden P (1996) Feed-back regulation of gibberellin biosynthesis and gene expression in Pisum sativum L. *Planta* 200 (2):159-166. doi:10.1007/bf00208304

McAvoy T, Nairn AC (2010) Serine/threonine protein phosphatase assays. *Curr Protoc Mol Biol* Chapter 18:Unit18 18. doi:10.1002/0471142727.mb1818s92

Michniewicz M, Zago MK, Abas L, Weijers D, Schweighofer A, Meskiene I, Heisler MG, Ohno C, Zhang J, Huang F, Schwab R, Weigel D, Meyerowitz EM, Luschnig C, Offringa R, Friml J (2007) Antagonistic regulation of PIN phosphorylation by PP2A and PINOID directs auxin flux. *Cell* 130 (6):1044-1056. doi:10.1016/j.cell.2007.07.033

Miozzi L, Vaira AM, Catoni M, Fiorilli V, Accotto GP, Lanfranco L (2019) Arbuscular Mycorrhizal Symbiosis: Plant Friend or Foe in the Fight Against Viruses? *Front Microbiol* 10:1238-1238. doi:10.3389/fmicb.2019.01238

Molina-Favero C, Creus CM, Lanteri M, Crrea-Aragunde N, Lombardo MC, Barassi CA, Lamattina L (2007) Nitric Oxide and Plant Growth Promoting Rhizobacteria: Common Features Influencing Root Growth and Development. *Advances in Botanical Reseach* 46:1-33. doi:10.1016/S0065-2296(07)46001-3

Molina-Favero C, Creus CM, Simontacchi M, Puntarulo S, Lamattina L (2008) Aerobic nitric oxide production by Azospirillum brasilense Sp245 and its influence on root architecture in tomato. *Molecular Plant-Microbe Interactions* 21 (7):1001-1009. doi:10.1094/Mpmi-21-7-1001

Moorhead GBG, Trinkle-Mulcahy L, Ulke-Lemée A (2007) Emerging roles of nuclear protein phosphatases. *Nature Reviews Molecular Cell Biology* 8 (3):234-244. doi:10.1038/nrm2126

Mumby M (2007) The 3D structure of protein phosphatase 2A: new insights into a ubiquitous regulator of cell signaling. *ACS Chem Biol* 2 (2):99-103. doi:10.1021/cb700021z

Murashige T, Skoog F (1962) A Revised Medium for Rapid Growth and Bio Assays with Tobacco Tissue Cultures. *Physiologia Plantarum* 15 (3):473–497

Nilsson J (2019) Protein phosphatases in the regulation of mitosis. *J Cell Biol* 218 (2):395-409. doi:10.1083/jcb.201809138

Pais SM, Gonzalez MA, Tellez-Inon MT, Capiati DA (2009) Characterization of potato (Solanum tuberosum) and tomato (Solanum lycopersicum) protein phosphatases type 2A catalytic subunits and their involvement in stress responses. *Planta* 230 (1):13-25. doi:10.1007/s00425-009-0923-5

Pathma J, Kennedy RK, Sakthivel N (2011) Mechanisms of Fluorescent Pseudomonads That Mediate Biological Control of Phytopathogens and Plant Growth Promotion of Crop Plants. In: Maheshwari DK (ed) Bacteria in Agrobiology: Plant Growth Responses. Springer Berlin Heidelberg, Berlin, Heidelberg, pp 77-105. doi:10.1007/978-3-642-20332-9_4

Pawar, Bhausaheb & S. jadhav, A & Chimote, Vivek & Kale, Aa & Pawar SV (2013) Effect of explants, bacterial cell density and overgrowth-control antibiotics on transformation efficiency in tomato (Solanum lycopersicum L.). *Journal of Applied Horticulture* 15:95-99

Perez-Callejon E, Casamayor A, Pujol G, Camps M, Ferrer A, Arino J (1998) Molecular cloning and characterization of two phosphatase 2A catalytic subunit genes from Arabidopsis thaliana. *Gene* 209 (1-2):105-112. doi:10.1016/s0378-1119(98)00013-4

Pernas M, Garcia-Casado G, Rojo E, Solano R, Sanchez-Serrano JJ (2007) A protein phosphatase 2A catalytic subunit is a negative regulator of abscisic acid signalling. *Plant J* 51 (5):763-778. doi:10.1111/j.1365-313X.2007.03179.x

Persello-Cartieaux F, David P, Sarrobert C, Thibaud MC, Achouak W, Robaglia C, Nussaume L (2001) Utilization of mutants to analyze the interaction between Arabidopsis thaliana and its naturally root-associated Pseudomonas. *Planta* 212 (2):190-198. doi:DOI 10.1007/s00 4250000384

Phillips AL, Ward DA, Uknes S, Appleford N, Lange T, Huttly AK, Gaskin P, Graebe JE, Hedden P (1995) Isolation and Expression of Three Gibberellin 20-Oxidase cDNA Clones from Arabidopsis. *Plant Physiology* 108 (3):1049-1057. doi:10.1104/pp.108.3.1049

Pieterse CM, van Wees SC, van Pelt JA, Knoester M, Laan R, Gerrits H, Weisbeek PJ, van Loon LC (1998) A novel signaling pathway controlling induced systemic resistance in Arabidopsis. *The Plant cell* 10 (9):1571-1580. doi:10.1105/tpc.10.9.1571

Pieterse CM, Zamioudis C, Berendsen RL, Weller DM, Van Wees SC, Bakker PA (2014) Induced systemic resistance by beneficial microbes. *Annu Rev Phytopathol* 52:347-375. doi:10.1146/annurev-phyto-082712 -102340

Pieterse CMJ, vanWees SCM, Hoffland E, vanPelt JA, vanLoon LC (1996) Systemic resistance in Arabidopsis induced by biocontrol bacteria is independent of salicylic acid accumulation and pathogenesis-related gene expression. *Plant Cell* 8 (8):1225-1237

Podile AR, Kishore GK (2006) Plant growth-promoting rhizobacteria. In: Gnanamanickam SS (ed) Plant-Associated Bacteria. Springer Netherlands, Dordrecht, pp 195-230. doi:10.1007/978-1-4020-4538-7_6

Promega (2009) Technical Bulletin. Serine/Threonine Phosphatase Assay System. Instructions for use of product V2460. Accessed on: Oct. 1, 2016. [Online]. Available from < https://www.promega.com/-/media/files/resources/protocols/technical-bulletins/0/serine-threonine-phosphatase-assay-system-protocol.pdf >

Qin X, Zeevaart JAD (1999) The 9-cis-epoxycarotenoid cleavage reaction is the key regulatory step of abscisic acid biosynthesis in water-stressed bean. *Proceedings of the National Academy of Sciences* 96 (26):15354-15361. doi:10.1073/pnas.96.26.15354

Rahikainen M, Pascual J, Alegre S, Durian G, Kangasjärvi S (2016) PP2A Phosphatase as a Regulator of ROS Signaling in Plants. *Antioxidants (Basel)* 5 (1). doi:10.3390/antiox5010008

Rayner MC (1926–1927) Mycorrhiza. *New Phytologist* 25:1-50

Reis VM, Teixeira KRdS, Pedraza RO (2011) What Is Expected from the Genus Azospirillum as a Plant Growth-Promoting Bacteria? In: Maheshwari DK (ed) Bacteria in Agrobiology: Plant Growth Responses. Springer Berlin Heidelberg, Berlin, Heidelberg, pp 123-138. doi:10.1007/978-3-642-20332-9_6

Reynhout S, Janssens V (2019) Physiologic functions of PP2A: Lessons from genetically modified mice. *Biochim Biophys Acta Mol Cell Res* 1866 (1):31-50. doi:10.1016/j.bbamcr.2018.07.010

Roche (2011) Expand High Fidelity PCR System. Accessed on: Oct. 1, 2016. [Online]. Available from <https://www.sigmaaldrich.com/content/dam/sigma- aldrich/docs/Roche/Bulletin/1/ehifirobul.pdf >

Rodrigues AC, Bonifacio A, de Araujo FF, Junior MAL, do Vale Barreto Figueiredo M (2015) Azospirillum sp. as a Challenge for Agriculture. In: Maheshwari DK (ed) Bacterial Metabolites in Sustainable Agroecosystem. *Springer International Publishing*, Cham, pp 29-51. doi:10.1007/978-3-319-24654-3_2

Ruan Y, Halat LS, Khan D, Jancowski S, Ambrose C, Belmonte MF, Wasteneys GO (2018) The Microtubule-Associated Protein CLASP Sustains Cell Proliferation through a Brassinosteroid Signaling Negative Feedback Loop. *Current Biology* 28 (17):2718-+. doi:10.1016/j.cub.2018.06.048

Saab IN, Sharp RE, Pritchard J, Voetberg GS (1990) Increased endogenous abscisic Acid maintains primary root growth and inhibits shoot growth of maize seedlings at low water potentials. *Plant Physiol* 93 (4):1329-1336. doi:10.1104/pp.93.4.1329

Schüßler A, Kluge M (2001) Geosiphon pyriforme, an Endocytosymbiosis Between Fungus and Cyanobacteria, and its Meaning as a Model System for Arbuscular Mycorrhizal Research. In: Hock B (ed) Fungal Associations. Springer Berlin Heidelberg, Berlin, Heidelberg, pp 151-161. doi:10.1007/978-3-662-07334-6_9

Segarra G, Van der Ent S, Trillas I, Pieterse CMJ (2009) MYB72, a node of convergence in induced systemic resistance triggered by a fungal and a bacterial beneficial microbe. *Plant Biol (Stuttg)* 11 (1):90-96. doi: 10.1111/j.1438-8677.2008.00162.x

Segonzac C, Macho AP, Sanmartin M, Ntoukakis V, Sanchez-Serrano JJ, Zipfel C (2014) Negative control of BAK1 by protein phosphatase 2A during plant innate immunity. *Embo Journal* 33 (18):2069-2079. doi:10.15252/embj.201488698

Seo M, Hanada A, Kuwahara A, Endo A, Okamoto M, Yamauchi Y, North H, Marion-Poll A, Sun TP, Koshiba T, Kamiya Y, Yamaguchi S, Nambara E (2006) Regulation of hormone metabolism in Arabidopsis seeds: phytochrome regulation of abscisic acid metabolism and abscisic

acid regulation of gibberellin metabolism. *Plant J* 48 (3):354-366. doi: 10.1111/j.1365-313X.2006.02881.x

Shi L, Olszewski NE (1998) Gibberellin and abscisic acid regulate GAST1 expression at the level of transcription. *Plant Mol Biol* 38 (6):1053-1060. doi:10.1023/a:1006007315718

Slater A, Scott NW, Fowler MR (2008) Plant biotechnology: the genetic manipulation of plants. 2nd edn. Oxford University Press, Oxford ; New York

Smith SE, Read D (2008a) 1 - The symbionts forming arbuscular mycorrhizas. In: Smith SE, Read D (eds) Mycorrhizal Symbiosis (Third Edition). Academic Press, London, pp 13-41. doi:https://doi.org/ 10.1016/B978-012370526-6.50003-9

Smith SE, Read D (2008b) 2 - Colonization of roots and anatomy of arbuscular mycorrhizas. In: Smith SE, Read D (eds) Mycorrhizal Symbiosis (Third Edition). Academic Press, London, pp 42-90. doi: 10.1016/B978-012370526-6.50004-0

Smith SE, Read D (2008c) 5 - Mineral nutrition, toxic element accumulation and water relations of arbuscular mycorrhizal plants. In: Smith SE, Read D (eds) Mycorrhizal Symbiosis (Third Edition). Academic Press, London, pp 145-VI. doi:10.1016/B978-012370526-6.50007-6

Somers E, Ptacek D, Gysegom P, Srinivasan M, Vanderleyden J (2005) Azospirillum brasilense produces the auxin-like phenylacetic acid by using the key enzyme for indole-3-acetic acid biosynthesis. *Appl Environ Microbiol* 71 (4):1803-1810. doi:10.1128/AEM.71.4.1803-1810.2005

Spaepen S, Bossuyt S, Engelen K, Marchal K, Vanderleyden J (2014) Phenotypical and molecular responses of Arabidopsis thaliana roots as a result of inoculation with the auxin-producing bacterium Azospirillum brasilense. *New Phytologist* 201 (3):850-861. doi:10.1111/nph.12590

Spaepen S, Versees W, Gocke D, Pohl M, Steyaert J, Vanderleyden J (2007) Characterization of phenylpyruvate decarboxylase, involved in auxin production of Azospirillum brasilense. *Journal of Bacteriology* 189 (21):7626-7633. doi:10.1128/Jb.00830-07

Steenhoudt O, Vanderleyden J (2000) Azospirillum, a free-living nitrogen-fixing bacterium closely associated with grasses: genetic, biochemical and ecological aspects. *Fems Microbiol Rev* 24 (4):487-506. doi:DOI 10.1111/j.1574-6976.2000.tb00552.x

Stringlis IA, Proietti S, Hickman R, Van Verk MC, Zamioudis C, Pieterse CMJ (2018a) Root transcriptional dynamics induced by beneficial rhizobacteria and microbial immune elicitors reveal signatures of adaptation to mutualists. *Plant J* 93 (1):166-180. doi:10.1111/tpj.13741

Stringlis IA, Proietti S, Hickman R, Van Verk MC, Zamioudis C, Pieterse CMJ (2018b) Root transcriptional dynamics induced by beneficial rhizobacteria and microbial immune elicitors reveal signatures of adaptation to mutualists. *Plant J* 93 (1):166-180. doi:10.1111/tpj.13741

Stringlis IA, Zamioudis C, Berendsen RL, Bakker PAHM, Pieterse CMJ (2019) Type III Secretion System of Beneficial Rhizobacteria Pseudomonas simiae WCS417 and Pseudomonas defensor WCS374. *Front Microbiol* 10. doi:ARTN 163110.3389/fmicb.2019.01631

Sun S, Kang XP, Xing XJ, Xu XY, Cheng J, Zheng SW, Xing GM (2015) Agrobacterium-mediated transformation of tomato (Lycopersicon esculentum L. cv. Hezuo 908) with improved efficiency. *Biotechnology & Biotechnological Equipment* 29 (5):861-868. doi:10.1080/13102818.2015.1056753

Svab Z, Harper EC, Jones JD, Maliga P (1990) Aminoglycoside-3''-adenyltransferase confers resistance to spectinomycin and streptomycin in Nicotiana tabacum. *Plant Mol Biol* 14 (2):197-205. doi:10.1007/bf00018560

Swingle M, Ni L, Honkanen RE (2007) Small-molecule inhibitors of ser/thr protein phosphatases: specificity, use and common forms of abuse. *Methods Mol Biol* 365:23-38. doi:10.1385/1-59745-267-X:23

Taiz L, Zeiger E, Møller IM, Murphy AS (2015) Plant physiology and development. Sixth edition. edn. Sinauer Associates, Inc., Publishers, Sunderland, Massachusetts.

Taylor IB, Sonneveld T, Bugg TDH, Thompson AJ (2005) Regulation and Manipulation of the Biosynthesis of Abscisic Acid, Including the Supply of Xanthophyll Precursors. *Journal of Plant Growth Regulation* 24 (4):253-273. doi:10.1007/s00344-005-0070-6

TFS (2014) Phire® Plant Direct PCR Kit. Laboratory manual. . Thermo Fisher Scientific Inc, Accessed on: Oct. 1, 2016. [Online]. Available from <https://assets.thermofisher.com/TFS-Assets/LSG/manuals/ MAN 0013358_ Phire_Plant_Direct_PCR_UG.pdf>

TFS (2016) Thermo Scientific DreamTaq DNA Polymerase. Thermo Fisher Scientific Inc, Accessed on: Jan 1, 2017. [Online]. Available from <https://assets.thermofisher.com/TFS-Assets/LSG/manuals/MAN0012 036_DreamTaqDNAPolymerase_500U_UG.pdf>

Thomas J, Kim HR, Rahmatallah Y, Wiggins G, Yang QQ, Singh R, Glazko G, Mukherjee A (2019) RNA-seq reveals differentially expressed genes in rice (Oryza sativa) roots during interactions with plant-growth promoting bacteria, Azospirillum brasilense. *Plos One* 14 (5). doi:ARTN e021730910.1371/journal.pone.0217309

Ton J, Pieterse CMJ, Van Loon LC (1999) Identification of a Locus in Arabidopsis Controlling Both the Expression of Rhizobacteria-Mediated Induced Systemic Resistance (ISR) and Basal Resistance Against Pseudomonas syringae pv. tomato. *Molecular Plant-Microbe Interactions*® 12 (10):911-918. doi:10.1094/mpmi.1999.12.10.911

Tortora ML, Diaz-Ricci JC, Pedraza RO (2011) Azospirillum brasilense siderophores with antifungal activity against Colletotrichum acutatum. *Arch Microbiol* 193 (4):275-286. doi:10.1007/s00203-010-0672-7

Toth EC, Vissi E, Kovacs I, Szoke A, Arino J, Gergely P, Dudits D, Dombradi V (2000) Protein phosphatase 2A holoenzyme and its subunits from Medicago sativa. *Plant Mol Biol* 43 (4):527-536. doi:10.1023/a:1006436925253

Tseng TS, Briggs WR (2010) The Arabidopsis rcn1-1 mutation impairs dephosphorylation of Phot2, resulting in enhanced blue light responses. *Plant Cell* 22 (2):392-402. doi:10.1105/tpc.109.066423

Tuominen L (2008) Calcium Chloride Preparation of Agrobacterium Competent Cells. Department of Genetics of The University of Georgia. Available from < http://aspendb.uga.edu/downloads/Agro_CaCl2_SOP_0909.pdf> [Accessed 1st of February 2020]

van Loon LC, Bakker PA, Pieterse CM (1998) Systemic resistance induced by rhizosphere bacteria. *Annual review of phytopathology* 36:453-483. doi:10.1146/annurev.phyto.36.1.453

Van Peer R (1991) Induced resistance and phytoalexin accumulation in biological control of Fusarium wilt of carnation by Pseudomonas sp. strain WCS417r. *Phytopathology* 81:728-734

Van Wees SC, Van Pelt JA, Bakker PA, Pieterse CM (2013) Bioassays for assessing jasmonate-dependent defenses triggered by pathogens, herbivorous insects, or beneficial rhizobacteria. *Methods Mol Biol* 1011:35-49. doi:10.1007/978-1-62703-414-2_4

Van Wees SCM, Pieterse CMJ, Trijssenaar A, Van 't Westende YAM, Hartog F, Van Loon LC (1997) Differential Induction of Systemic Resistance in Arabidopsis by Biocontrol Bacteria. *Molecular Plant-Microbe Interactions*® 10 (6):716-724. doi:10.1094/mpmi.1997.10.6.716

Veiga RS, Faccio A, Genre A, Pieterse CM, Bonfante P, van der Heijden MG (2013) Arbuscular mycorrhizal fungi reduce growth and infect roots of the non-host plant Arabidopsis thaliana. *Plant Cell Environ* 36 (11):1926-1937. doi:10.1111/pce.12102

Verbon EH, Trapet PL, Kruijs S, Temple-Boyer-Dury C, Rouwenhorst TG, Pieterse CMJ (2019) Rhizobacteria-Mediated Activation of the Fe Deficiency Response in Arabidopsis Roots: Impact on Fe Status and Signaling. *Front Plant Sci* 10:909. doi:10.3389/fpls.2019.00909

Verhagen BW, Glazebrook J, Zhu T, Chang HS, van Loon LC, Pieterse CM (2004) The transcriptome of rhizobacteria-induced systemic resistance in arabidopsis. *Mol Plant Microbe Interact* 17 (8):895-908. doi:10.1094/MPMI.2004.17.8.895

Verhagen BWM, Trotel-Aziz P, Couderchet M, Hofte M, Aziz A (2010) Pseudomonas spp.-induced systemic resistance to Botrytis cinerea is associated with induction and priming of defence responses in grapevine. *Journal of Experimental Botany* 61 (1):249-260. doi:10.1093/jxb/erp295

Vidotti MS, Lyra DH, Morosini JS, Granato ISC, Quecine MC, Azevedo JL, Fritsche-Neto R (2019) Additive and heterozygous (dis)advantage GWAS models reveal candidate genes involved in the genotypic variation of maize hybrids to Azospirillum brasilense. *PLoS One* 14 (9):e0222788. doi:10.1371/journal.pone.0222788

Vierheilig H, Schweiger P, Brundtrett M (2005) An overview of methods for the detection and observation of arbuscular mycorrhizal fungi in roots. Physiol Plant 125 (4):393-404. doi:10.1111/j.1399-3054.2005.00564.x

Virshup DM, Shenolikar S (2009) From promiscuity to precision: protein phosphatases get a makeover. *Mol Cell* 33 (5):537-545. doi:10.1016/j.molcel.2009.02.015

Walter G, Ruediger R, Slaughter C, Mumby M (1990) Association of protein phosphatase 2A with polyoma virus medium tumor antigen. *Proc Natl Acad Sci USA* 87 (7):2521-2525

Wang J, Pei L, Jin Z, Zhang K, Zhang J (2017) Overexpression of the protein phosphatase 2A regulatory subunit a gene ZmPP2AA1 improves low phosphate tolerance by remodeling the root system architecture of maize. *PLoS One* 12 (4):e0176538. doi:10.1371/journal.pone.0176538

Wei G, Kloepper JW, Tuzun S (1991) Induction of systemic resistance of cucumber to Colletotrichum orbiculare by select strains of plant growth-promoting rhizobacteria. *Phytopathology* 81 (12):1508-1512. doi:10.1094/phyto-81-1508

Weigel D, Glazebrook J (2002) Arabidopsis: A Laboratory Manual. Cold Spring Harbor Laboratory Press,

Weiss D, Ori N (2007) Mechanisms of cross talk between gibberellin and other hormones. *Plant Physiol* 144 (3):1240-1246. doi:10.1104/pp.107.100370

Wintermans JFGM, & De Mots, A. (1965) Spectrophotometric characteristics of chlorophylls a and b and their phenophytins in ethanol. *Biophysics Including Photosynthesis* 109 (2):448-453. doi:10.1016/0926-6585(65)90170-6

Wintermans PCA, Bakker PAHM, Pieterse CMJ (2016) Natural genetic variation in Arabidopsis for responsiveness to plant growth-promoting rhizobacteria. *Plant Molecular Biology* 90 (6):623-634. doi:10.1007/s11103-016-0442-2

Wisniewski-Dye F, Borziak K, Khalsa-Moyers G, Alexandre G, Sukharnikov LO, Wuichet K, Hurst GB, McDonald WH, Robertson JS, Barbe V, Calteau A, Rouy Z, Mangenot S, Prigent-Combaret C, Normand P, Boyer M, Siguier P, Dessaux Y, Elmerich C, Condemine G, Krishnen G, Kennedy I, Paterson AH, Gonzalez V, Mavingui P, Zhulin IB (2011) Azospirillum genomes reveal transition of bacteria from aquatic to terrestrial environments. *PLoS Genet* 7 (12):e1002430. doi:10.1371/journal.pgen.1002430

Xiao JH, Li HX, Zhang JH, Chen RG, Zhang YY, Ouyang B, Wang TT, Ye ZB (2006) Dissection of GA 20-oxidase members affecting tomato morphology by RNAi-mediated silencing. *Plant Growth Regulation* 50 (2-3):179-189. doi:10.1007/s10725-006-9117-3

Xing Y, Xu YH, Chen Y, Jeffrey PD, Chao Y, Lin Z, Li Z, Strack S, Stock JB, Shi YG (2006) Structure of protein phosphatase 2A core

enzyme bound to tumor-inducing toxins. *Cell* 127 (2):341-353. doi:10.1016/j.cell.2006.09.025

Zamioudis C, Mastranesti P, Dhonukshe P, Blilou I, Pieterse CMJ (2013) Unraveling Root Developmental Programs Initiated by Beneficial Pseudomonas spp. Bacteria. *Plant Physiology* 162 (1):304-318. doi:10.1104/pp.112.212597

Zhou HW, Nussbaumer C, Chao Y, DeLong A (2004) Disparate roles for the regulatory A subunit isoforms in Arabidopsis protein phosphatase 2A. *Plant Cell* 16 (3):709-722. doi:10.1105/tpc.018994

Appendix

Table A1. Chemical composition of ½ MS plant nutrition medium (Murashige and Skoog 1962).

Chemical formula	**Concentration of stock solution, g/L**	**Volume used to prepare 1L of ½ MS medium**
KNO_3	95	10 ml
NH_4NO_3	120	6.5 ml
$MgSO_4 \cdot 7H_2O$	37	5 ml
KH_2PO_4	17	10 ml
$CaCl_2 \cdot 2\ H_2O$	44	5 ml
Fe/EDTA:		
Na_2EDTA	0.373	25 ml
$FeSO4 \cdot 7\ H_2O$	0.278	
Minor elements I:		5 ml
$ZnSO4 \cdot 7\ H_2O$	0.920	
H_3BO_3	0.620	
$MnSO_4 \cdot 4\ H_2O$	2.230	
Minor elements II:		5 ml
$Na_2MoO_4 \cdot 2H_2O$	0.025	
$CuSO_4 \cdot 5\ H_2O$	0.003	
$CoCl_2 \cdot 6\ H_2O$	0.003	
KI	0.083	
Agar	7	
d H_2O		Up to 1L

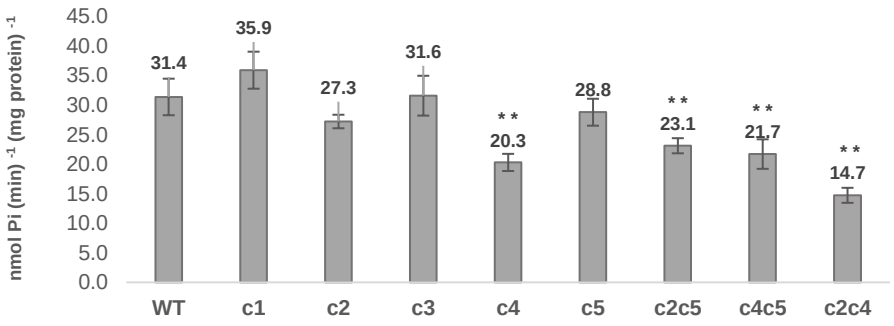

Figure A1. The total phosphatase activity in Arabidopsis WT and various mutants.
Activity was assayed in whole 10-day-old seedlings grown on ½ MS medium and is given as phosphate release detected during the reaction without OA. Numbers above each column are mean values ±SE collected from three independent experiments (n=3). Values marked with two asterisks are significantly different from WT according to student's t-test at p-value < 0.05.

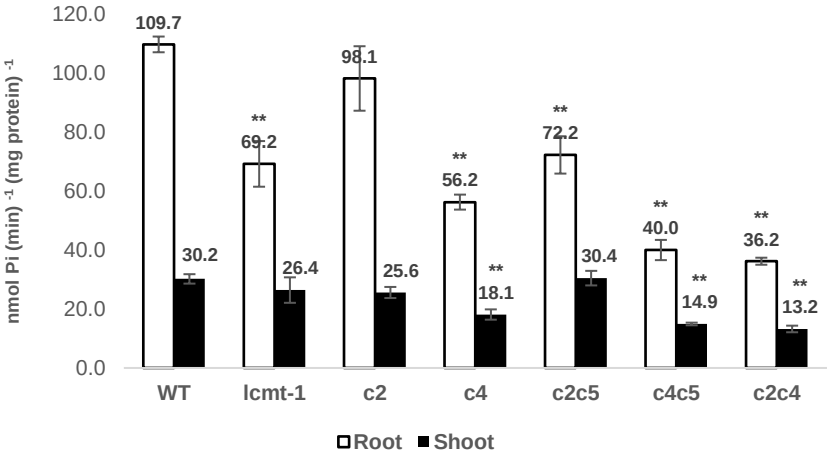

Figure A2. The total phosphatase activity in Arabidopsis WT and selected mutants.
Activity was assayed separately in roots (white bars) and shoots (black bars) from 10-day old seedlings grown on ½ MS medium and is given as phosphate release detected during the reaction without OA. Numbers above each column are mean values ±SE collected from three independent experiments(n=3). Values marked with two asterisks are significantly different from WT according to student's t-test at p-value < 0.05.

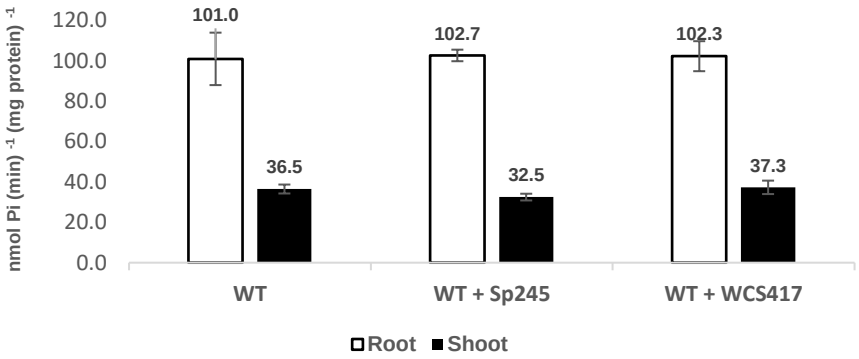

Figure A3. The total phosphatase activity of Arabidopsis WT in roots and shoots treated and not treated with PGPR.

Activity was assayed separately in roots (white bars) and shoots (black bars) and is given as phosphate release detected during the reactions without OA. Numbers above each column are mean values ±SE collected from three independent experiments (n=3). Values for plants treated with bacteria were not significantly different from non-treated plants according to student's t-test at p-value < 0.1.

Figure A4. Visual phenotype of Arabidopsis WT, *c2* and various *b'*-mutants treated with *P. simiae* WCS417r.
Seedlings of Arabidopsis WT and mutants (*c2, b'* alpha, beta, gamma, zeta and theta) grown on ½ MS and cultivated without (upper row) and with *P. simiae WCS417r* (lower row).

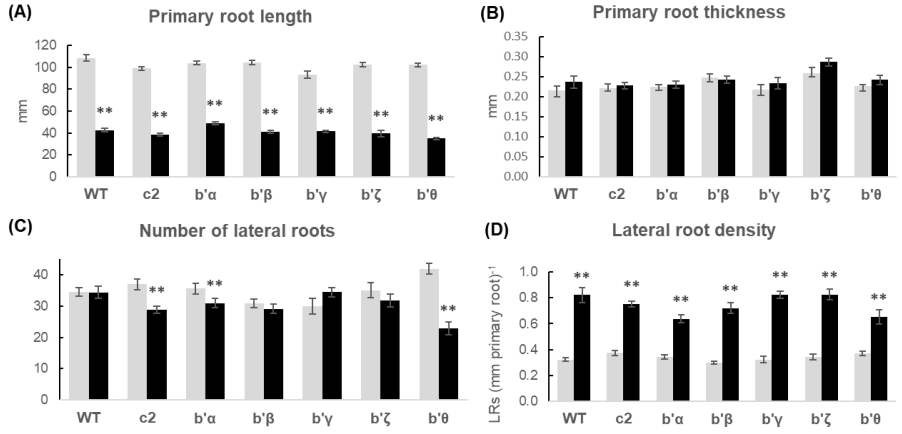

Figure A5. Growth parameters of WT, *c2* and various *b'*-mutants treated with *P. simiae* WCS417r.
Seedlings of Arabidopsis WT, *c2* and *b'*- mutants were cultivated without (grey bars) and with (black bars) *P. simiae* WCS417r for two weeks. (A) primary root length; (B) primary root thickness; (C) number of lateral roots; and (D) lateral root density. Data are means ± SE of 15 plants (n=15). Columns marked with two asterisks are significantly different from the control without bacteria according to student's t-test at p-value < 0.05.

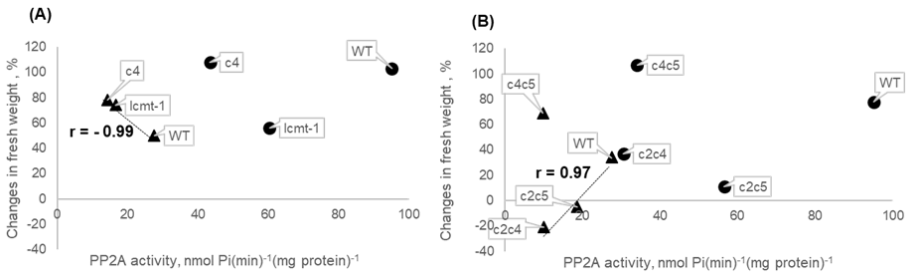

Figure A6. **Scatter plot of PP2A activity and fresh weight changes in Arabidopsis WT and mutants caused by *P. simiae* WCS417r.**
Fresh weight changes in roots (circles) and shoots (triangles). Data are from Fig. 4, 7 and 9. (A) and (B) Pearson's correlation coefficient $|r| > 0.7$ was considered as strong, (B) *c4c5* was assumed as an outlier and not used in the calculations.

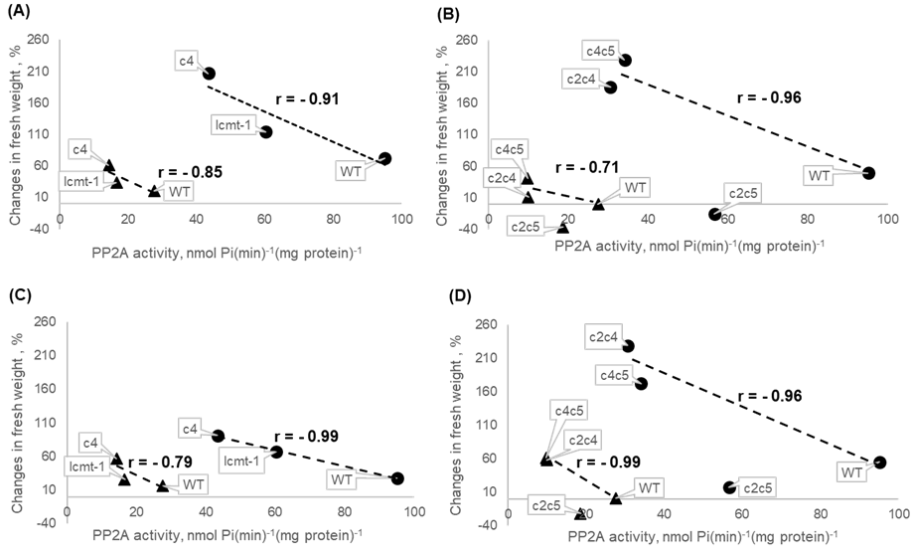

Figure A7. Scatter plot of PP2A activity and fresh weight changes in Arabidopsis WT and mutants caused by *A. brasilense*.
Fresh weight changes in roots (circles) and shoots (triangles). Only Pearson's correlation coefficient $|r| > 0.7$ was considered as strong. Data are from Fig. 4, 12 and 14. (A) and (B) *A. brasilense* Sp245, in (B) *c2c5* was assumed as an outlier and not used in the calculations. (C) and (D) *A. brasilense* FAJ0009, in (D) *c2c5* was assumed as an outlier and not used in the calculations.

Table A2. Composition of Hoagland solution (Hoagland and Arnon 1950).

Stock solutions	**Volume added/L**	**Final concentration**
1 M KH_2PO_4	1 ml	1 mM PO_4^{3-}
1M KNO_3	5 ml	5 mM NO_3^-
1M $Ca(NO_3)_2$ x4H_2O	5 ml	10 mM NO_3^-, 5mM Ca^{2+}
1M $MgSO_4$x7H_2O	2 ml	2mM Mg^{2+}, 2mM SO_4^{2-}
1% Fe-EDTA	1 ml	
Micronutrients: H_3BO_3 2.6 g/L $MnCl_2$ x 4H_2O 1.81 g/L $CuSO_4$ x 5H2O 0.089 g/L $ZnSO_4$ x 7H_2O 0.22 g/L H_2MoO_4 x H2O 0.029 g/L	1 ml	

Table A3. Primer specification.

Target gene information	PCR Program	Primers	PCR Product Size (nt)
pBA002 cloning vector [a] pBA002-B'φ ox insert [a]	Initial denaturation 98°C 5 min 1 cycle Denaturation 98°C 5s Annealing 54 °C 5s — 40 cycles Extension 72°C 40s Final extension 72°C 1 min 1 cycle	Forward: CGTCTTCAAAGCAAGTGGATTGATG Reverse: TGCTTAACGTAATTCAACAACAGAAATTAT	276 1762
B'φ PP2A-B'φ regulatory subunit (Booker and DeLong 2017) [a] NCBI Reference Sequence: XM_010317091.2	Initial denaturation 98°C 5 min 1 cycle Denaturation 98°C 5s Annealing 54 °C 5s — 40 cycles Extension 72°C 40s Final extension 72°C 1 min 1 cycle	Forward: ATGACAAATTTTCTTGATTCTGAGACAG ATCG Reverse: TCACATTGCTGCATTTTCAATTTTTTCCC	1486
B'φ PP2A-B'φ regulatory subunit [b] NCBI Reference Sequence: XM_010317091.2	Initial denaturation 95°C 3 min 1 cycle Denaturation 95°C 30s Annealing 61 °C 30s — 38 cycles Extension 72°C 40s Final extension 72°C 10 min 1 cycle	Forward: GAGACTGATCAAAGGCACCCTGGAATCG Reverse: ACAATGCGCGTTCAGCAACCTGCGAG	406
B'θ PP2A B56 (Clade 6/9/10) [b] NCBI Reference Sequence: XM_004239128.4	Initial denaturation 95°C 3 min 1 cycle Denaturation 95°C 30s Annealing 55 °C 30s — 38 cycles Extension 72°C 40s Final extension 72°C 10 min 1 cycle	Forward: AGGTGTATGGTGCCGTTGTT Reverse: GATGGCACAAGCACAGCTTCCA	389
B55β (Clade I) PP2A B55 (CLADE I, Booker 2017) [b] NCBI Reference Sequence: XM_004241456.4	Initial denaturation 95°C 3 min 1 cycle Denaturation 95°C 30s Annealing 55 °C 30s — 38 cycles Extension 72°C 40s Final extension 72°C 10 min 1 cycle	Forward: CTCACATGGAGTCTTCCCCG Reverse: AAGCCACATGCAGCAACTT	373
B55β (Clade III) PP2A B55 (CLADE III) (Booker and DeLong 2017) [b] NCBI Reference Sequence: XM_004252324.4, XM_019211570.2, XM_010316006.3 (transcript variant X1, X2, X3)	Initial denaturation 95°C 3 min 1 cycle Denaturation 95°C 30s Annealing 56 °C 30s — 38cycles Extension 72°C 40s Final extension 72°C 10 min 1 cycle	Forward: GTGGTGATGGTTCGCGAGTA Reverse: CATTTGCATCAACACCGGCA	213
B' κ PP2A-B56 (Clade B11) [b] NCBI Reference Sequence: XM_004251542.4 (transcript variant X1), XM_010315410.3 (transcript variant X2), XM_010315411.3 (transcript variant X3), XM_026028819.1 (transcript variant X4), XM_026028820.1 (transcript variant X5)	Initial denaturation 95°C 3 min 1 cycle Denaturation 95°C 30s Annealing 56 °C 30s — 38 cycles Extension 72°C 40 Final extension 72°C 10 min 1 cycle	Forward: ACCTCTGCACAAGCCAAAGT Reverse: TCCAGTGGTTCTGGCTGTTC	392

Table 3A. Primer specification (continued).

Target gene information	PCR Program	Primers	PCR Product Size (nt)
A βI B65 or PP2A-A [b] NCBI Reference Sequence: XM_004236914.4 (transcript variant X1), XM_010321123.3 (transcript variant X2)	Initial denaturation 95°C 3 min 1 cycle Denaturation 95°C 30s Annealing 56 °C 30s 38 cycles Extension 72°C 40 Final extension 72°C 10 min 1 cycle	Forward: TAGCAAAGGACAGAGTGCCC Reverse: ACTGTTTCCTGGTGTGACGG	291
A βII B65 or PP2A-A [b] NCBI Reference Sequence: XM_004238897.4 (transcript variant X1), XM_019214032.2 (transcript variant X2)	Initial denaturation 95°C 3 min 1 cycle Denaturation 95°C 30s Annealing 56 °C 30s 38 cycles Extension 72°C 40 s Final extension 72°C 10 min 1 cycle	Forward: TGCACCAGTAATGGGCTCTG Reverse: ACTGGGCCGAATGGTTTCT	166
C1 PP2A catalytic subunit (PP2Ac1) [b] NCBI Reference Sequence: NM_001247587.2	Initial denaturation 95°C 3 min 1 cycle Denaturation 95°C 30s Annealing 56 °C 30s 38 cycles Extension 72°C 40 s Final extension 72°C 10 min 1 cycle	Forward: GCGGCAACGTCCTGATTACTA Reverse: AGGCTCAATCTGTCGTGGAG	667
C2 PP2A catalytic subunit (PP2Ac2) [b] NCBI Reference Sequence: NM_001246875.2	Initial denaturation 95°C 3 min 1 cycle Denaturation 95°C 30s Annealing 54 °C 30s 38 cycles Extension 72°C 40s Final extension 72°C 10 min 1 cycle	Forward: ATGCCGTCTCATGCAGATCTA Reverse: CTTCCTTGTGGTGTCGGGCTCTA	900
TAS 14 Abscisic acid and environmental stress-inducible protein [b] NCBI Reference Sequence: NM_001247109.1	Initial denaturation 95°C 3 min 1 cycle Denaturation 95°C 30s Annealing 56 °C 30s 38 cycles Extension 72°C 40s Final extension 72°C 10 min 1 cycle	Forward: CATCACCATGAGGGGCAACA Reverse: GCGTCAGCACACTTTACACG	363
NCED-1 Nine-cis-epoxycarotenoid dioxygenase 1 [b] NCBI Reference Sequence: NM_001247526.2	Initial denaturation 95°C 3 min 1 cycle Denaturation 95°C 30s Annealing 55 °C 30s 38 cycles Extension 72°C 60s Final extension 72°C 10 min 1 cycle	Forward: GTGCAGAAAGCAGCAGCAAT Reverse: CGTAAACCACCGGTGAACCT	871
GA3ox-1 Gibberellin-3β-hydroxylase-1 [b] NCBI Reference Sequence: AB010991.1	Initial denaturation 95°C 3 min 1 cycle Denaturation 95°C 30s Annealing 56 °C 30s 38 cycles Extension 72°C 40s Final extension 72°C 10 min 1 cycle	Forward: AGGCCCAAAAGGTGAAACCA Reverse: CCGTACGGATGAAAGTGCCT	463

Table 3A. Primer specification (continued).

Target gene information	PCR Program	Primers	PCR Product Size (nt)
GA3ox-2 Gibberellin-3β-hydroxylase-2 [b] NCBI Reference Sequence: NM_001246926.3	Initial denaturation 95°C 3 min 1 cycle Denaturation 95°C 30s Annealing 51 °C 30s Extension 72°C 40s 38 cycles Final extension 72°C 10 min 1 cycle	Forward: AGGCCCAAAAGGTGAAACCA Reverse: CCGTACGGATGAAAGTGCCT	276
GA20ox-1 Gibberellin 20-oxidase-1 [b] NCBI Reference Sequence: NM_001247141.1	Initial denaturation 95°C 3 min 1 cycle Denaturation 95°C 30s Annealing 51 °C 30s Extension 72°C 40s 38 cycles Final extension 72°C 10 min 1 cycle	Forward: AGGCCCAAAAGGTGAAACCA Reverse: CCGTACGGATGAAAGTGCCT	451
GA20ox-2 Gibberellin 20-oxidase-2 [b] NCBI Reference Sequence: NM_001247699.2	Initial denaturation 95°C 3 min 1 cycle Denaturation 95°C 30s Annealing 51 °C 30s Extension 72°C 40s 38 cycles Final extension 72°C 10 min 1 cycle	Forward: CTACAAGGCTCGTCCCACAT Reverse: TGAAAGCGCCATAAATGTGTC	402
GA20ox-3 Gibberellin 20-oxidase-3 [b] NCBI Reference Sequence: NM_001247650.2	Initial denaturation 95°C 3 min 1 cycle Denaturation 95°C 30s Annealing 55 °C 30s Extension 72°C 60s 38 cycles Final extension 72°C 10 min 1 cycle	Forward: CCGGACCATGAGAAGCCAAA Reverse: GATAGTGCCATAAACGTGTCGC	752
GA20ox-4 Gibberellin 20-oxidase-4 [b] NCBI Reference Sequence: NM_001247434.2	Initial denaturation 95°C 3 min 1 cycle Denaturation 95°C 30s Annealing 53 °C 30s Extension 72°C 40s 38 cycles Final extension 72°C 10 min 1 cycle	Forward: CTACAAGGCTCGTCCCACAT Reverse: TGAAAGCGCCATAAATGTGTC	375
GAST1 Gibberellin responsive gene [b] NCBI Reference Sequence: NM_001309377.1	Initial denaturation 95°C 3 min 1 cycle Denaturation 95°C 30s Annealing 56 °C 30s Extension 72°C 40s 38 cycles Final extension 72°C 10 min 1 cycle	Forward: TCAGGTTTCAAGGGCCAACA Reverse: CACTTTGGGCCACCTCTTTTG	275
Actin41 Reference gene [b] NCBI Reference Sequence: NM_001330119.1	Initial denaturation 95°C 3 min 1 cycle Denaturation 95°C 30s Annealing 58 °C 30s 38cycles Extension 72°C 60s Final extension 72°C 10 min 1 cycle	Forward: CACTGTATGCCAGTGGTCGT Reverse: GCATCTCTGGTCCAGTAGGAAA	773

[a] Primers used with **Phire® Hot Start II DNA Polymerase**
[b] Primers used in sqRT-PCR analysis

Table A4. Supplementary to Figure 16.

Growth medium	Plant organ	Gene ID				
		B'ϕ	***B55 β (Clade III)***	***B' θ***	***C1***	***TAS14***
Soil	**Roots**	0.22 ± 0.02	0.35 ± 0.04	0.50 ± 0.04	0.85 ± 0.06	0.67 ± 0.03
	Young Leaves	0.10 ± 0.02	0.64 ± 0.02	0.45 ± 0.07	0.41 ± 0.07	0.35 ± 0.07
	Flower buds	0.05 ± 0.01	0.41 ± 0.13	0.42 ± 0.13	0.43 ± 0.03	0.44 ± 0.13
Vermiculite	**Roots**	0.06 ± 0.06	0.39 ± 0.07	0.22 ± 0.01	0.81 ± 0.07	0.96 ± 0.06
	Young leaves	0.10 ± 0.03	0.60 ± 0.07	0.35 ± 0.04	0.76 ± 0.10	0.86 ± 0.05
	Flower buds	0.12 ± 0.03	0.55 ± 0.12	0.37 ± 0.03	0.78 ± 0.08	0.74 ± 0.12

Table A5. Supplementary to Figure 17.

Treatment	Time after treatment	Gene ID									
		B'ϕ	***Bβ (Clade I)***	***Bβ (Clade II***	***B' θ***	***B'κ***	***Aβl***	***Aβll***	***C1***	***C2***	***TAS14***
Control	**2 hours**	0.10 ± 0.02	0.37 ± 0.12	0.42 ± 0.13	0.34 ± 0.01	0.68 ± 0.06	0.41 ± 0.08	0.80 ± 0.06	0.74 ± 0.05	0.94 ± 0.05	0.77 ± 0.09
Sp245		0.12 ± 0.01	0.30 ± 0.05	0.75 ± 0.03	0.17 ± 0.02	0.75 ± 0.04	0.43 ± 0.02	0.76 ± 0.03	0.81 ± 0.06	0.91 ± 0.06	0.75 ± 0.16
FAJ0009		0.15 ± 0.01	0.56 ± 0.12	0.54 ± 0.17	0.09 ± 0.05	0.77 ± 0.08	0.46 ± 0.04	0.78 ± 0.14	1.00 ± 0.01	0.92 ±0.07	1.04 ± 0.14
WCS417r		0.14 ± 0.03	0.35 ± 0.10	0.56 ± 0.10	0.04 ± 0.00	0.68 ± 0.01	0.23 ± 0.05	0.69 ± 0.03	0.71 ± 0.07	0.78 ± 0.05	0.84 ± 0.08
Control	**24 hours**	0.13 ± 0.01	0.03 ± 0.01	0.22 ± 0.01	0.35 ± 0.02	0.51 ± 0.02	0.36 ± 0.01	0.68 ± 0.03	0.91 ± 0.10	1.06 ± 0.02	0.83 ± 0.06
Sp245		0.12 ± 0.01	0.16 ± 0.04	0.38 ± 0.04	0.29 ± 0.02	0.60 ± 0.02	0.27 ± 0.03	0.58 ± 0.06	1.00 ± 0.15	1.04 ± 0.10	0.58 ± 0.05
FAJ0009		0.12 ± 0.01	0.40 ± 0.04	0.39 ± 0.04	0.18 ± 0.03	0.50 ± 0.02	0.26 ± 0.03	0.61 ± 0.01	0.81 ± 0.02	1.19 ± 0.05	0.69 ± 0.05
WCS417r		0.13 ± 0.03	0.33 ± 0.06	0.38 ± 0.01	0.12 ± 0.02	0.65 ± 0.07	0.26 ± 0.06	0.56 ±0.06	0.90 ± 0.10	1.12 ± 0.10	0.74 ± 0.09
Control	**1 week**	0.07 ± 0.01	0.32 ± 0.07	0.62 ± 0.05	0.25 ± 0.05	1.14 ± 0.01	0.54 ± 0.1	0.78 ± 0.10	0.81 ± 0.08	0.79 ± 0.15	1.20 ± 0.03
Sp245		0.08 ± 0.00	0.42 ± 0.03	0.68 ± 0.03	0.20 ± 0.03	1.14 ± 0.01	0.56 ± 0.10	0.92 ± 0.05	0.89 ± 0.04	0.73 ± 0.17	1.22 ± 0.19
FAJ0009		0.11 ± 0.06	0.38 ± 0.07	0.83 ± 0.01	0.25 ± 0.06	0.67 ± 0.06	0.43 ± 0.01	0.90 ± 0.03	0.84 ± 0.14	0.56 ± 0.02	1.17 ± 0.09
WCS417r		0.15 ± 0.08	0.61 ± 0.18	0.75 ± 0.10	0.33 ± 0.17	1.13 ± 0.14	0.52 ± 0.05	0.87 ± 0.03	1.02 ± 0.07	0.53 ±0.13	1.21 ± 0.15
Control	**3 weeks**	0.06 ± 0.01	0.71 ± 0.07	0.21 ± 0.01	0.42 ± 0.05	0.69 ± 0.06	0.36 ± 0.03	0.62 ± 0.02	0.47 ± 0.08	0.91 ± 0.06	0.80 ± 0.03
Sp245		0.07 ± 0.01	0.65 ± 0.02	0.28 ± 0.02	0.34 ± 0.08	0.75 ± 0.10	0.54 ± 0.05	0.70 ± 0.03	0.95 ± 0.15	1.00 ± 0.08	0.86 ± 0.07
FAJ0009		0.09 ± 0.01	0.78 ± 0.10	0.31 ± 0.04	0.35 ± 0.02	0.86 ± 0.12	0.43 ± 0.03	0.75 ± 0.06	0.98 ± 0.06	1.03 ± 0.05	0.86 ± 0.07
WCS417r		0.09 ± 0.01	0.67 ± 0.07	0.30 ± 0.05	0.30 ± 0.06	0.67 ± 0.22	0.46 ± 0.11	0.67 ± 0.12	0.82 ± 0.21	0.99 ± 0.13	0.78 ± 0.11

Table A6. Supplementary to Figure 21.

Growth medium	Treatment	Gene ID					
		B'ϕ	***Bβ (Clade I)***	***Bβ (Clade III)***	***B' θ***	***B'κ***	***Aβl***
Soil	Control	0.22 ± 0.02	0.55 ± 0.03	0.35 ± 0.04	0.50 ± 0.04	0.80 ± 0.01	0.31 ± 0.05
	AMF	0.18 ± 0.01	0.56 ± 0.10	0.51 ± 0.05	0.04 ± 0.02	0.89 ± 0.07	0.48 ± 0.02
		Gene ID					
		Aβll	***C1***	***C2***	***TAS14***	***GAST1***	***PT4***
	Control	0.52 ± 0.00	0.85 ± 0.06	0.79 ± 0.07	0.67 ± 0.03	0.46 ± 0.07	0.18 ± 0.07
	AMF	0.58 ± 0.07	0.45 ± 0.16	0.79 ± 0.07	0.68 ± 0.02	0.30 ± 0.08	0.39 ± 0.08
Vermiculite		Gene ID					
		B'ϕ	***Bβ (Clade I)***	***Bβ (Clade III)***	***B' θ***	***B'κ***	***Aβl***
	Control	0.11 ± 0.02	0.33 ± 0.02	0.18 ± 0.01	0.14 ± 0.01	0.64 ± 0.03	0.18 ± 0.03
	AMF	0.11 ± 0.02	0.43 ± 0.02	0.18 ± 0.01	0.13 ± 0.02	0.74 ± 0.04	0.17 ± 0.02
		Gene ID					
		Aβll	***C1***	***C2***	***TAS14***	***GAST1***	***PT4***
	Control	0.53 ± 0.06	0.57 ± 0.02	0.80 ± 0.07	0.91 ±0.09	0.28 ± 0.07	0.20 ± 0.03
	AMF	0.64 ± 0.04	0.73 ± 0.04	0.87 ± 0.02	0.90 ± 0.11	0.17 ± 0.06	0.26 ± 0.06

Table A7. Supplementary to Figure 30.

Treatment	Sample ID	Gene ID					
		B'ϕ	***Bβ (Clade I)***	***Bβ (Clade III)***	***B' θ***	***B'κ***	***Aβl***
Control	WT	0.11 ± 0.02	0.33 ± 0.02	0.18 ± 0.01	0.13 ± 0.01	0.64 ± 0.02	0.18 ± 0.03
	$b'\varphi_{ox}(F_0)$	1.21 ± 0.09	0.51 ± 0.00	0.22 ± 0.01	0.12 ± 0.01	0.89 ± 0.05	0.17 ± 0.03
		Gene ID					
		Aβll	***C1***	***C2***	***TAS14***	***GAST1***	***PT4***
	WT	0.53 ± 0.06	0.57 ± 0.02	0.80 ± 0.07	0.91 ± 0.05	0.28 ± 0.03	0.20 ± 0.02
	$b'\varphi_{ox}(F_0)$	0.83 ± 0.04	0.57 ± 0.11	0.87 ± 0.02	0.74 ± 0.05	0.09 ± 0.02	0.20 ± 0.02
AMF		Gene ID					
		B'ϕ	***Bβ (Clade I)***	***Bβ (Clade III)***	***B' θ***	***B'κ***	***Aβl***
	WT	0.11 ± 0.02	0.43 ± 0.02	0.18 ± 0.01	0.13 ± 0.02	0.74 ± 0.04	0.17 ± 0.02
	$b'\varphi_{ox}(F_0)$	1.12 ± 0.06	0.60 ± 0.00	0.22 ± 0.02	0.11 ± 0.01	0.75 ± 0.07	0.18 ± 0.03
		Gene ID					
		Aβll	***C1***	***C2***	***TAS14***	***GAST1***	***PT4***
	WT	0.64 ± 0.04	0.73 ± 0.04	0.87 ± 0.02	0.90 ± 0.06	0.17 ± 0.06	0.26 ± 0.04
	$b'\varphi_{ox}(F_0)$	0.75 ± 0.04	0.58 ± 0.03	0.85 ± 0.08	0.56 ± 0.06	0.07 ± 0.01	0.27 ± 0.02

Table A8. Supplementary to Figure 31.

Treatment	Sample ID	Gene ID									
		B'ϕ	*NCED-1*	*TAS14*	*GA20ox-1*	*GA20ox-2*	*GA20ox-3*	*GA20ox-4*	*GA3ox-1*	*GA3ox-2*	*GAST1*
Control	WT	0.11 ± 0.02	0.81 ± 0.07	0.91 ± 0.05	0.44 ± 0.04	0.08 ± 0.02	0.43 ± 0.05	0.18 ± 0.04	0.39 ± 0.05	0.00	0.28 ± 0.03
	$b'\varphi_{ox}(F_0)$	1.21 ± 0.09	0.61 ± 0.02	0.74 ± 0.05	0.34 ± 0.06	0.11 ± 0.03	0.51 ± 0.03	0.16 ± 0.04	0.33 ± 0.02	0.00	0.09 ± 0.02
AMF	WT	0.11 ± 0.02	0.81 ± 0.08	0.90 ± 0.06	0.45 ± 0.07	0.14 ± 0.04	0.46 ± 0.02	0.19 ± 0.10	0.31 ± 0.03	0.00	0.17 ± 0.06
	$b'\varphi_{ox}(F_0)$	1.12 ± 0.06	0.68 ± 0.03	0.56 ± 0.06	0.45 ± 0.01	0.12 ± 0.03	0.56 ± 0.02	0.26 ± 0.05	0.34 ± 0.01	0.00	0.07 ± 0.01

Table A9. Supplementary to Figure 32.

Sample ID	Gene ID									
	B'ϕ	*NCED-1*	*TAS14*	*GA20ox-1*	*GA20ox-2*	*GA20ox-3*	*GA20ox-4*	*GA3ox-1*	*GA3ox-2*	*GAST1*
WT	0.18 ± 0.01	0.82 ± 0.15	0.61 ± 0.03	0.47 ± 0.02	0.05 ± 0.01	0.21 ± 0.01	0.11 ± 0.01	0.31 ± 0.02	0.43 ± 0.02	0.45 ± 0.05
$b'\varphi_{ox}(F_1)$ L10	0.73 ± 0.03	0.76 ± 0.03	0.61 ± 0.01	0.53 ± 0.02	0.12 ± 0.01	0.19 ± 0.04	0.09 ± 0.01	0.35 ± 0.04	0.41 ± 0.02	0.50 ± 0.06
$b'\varphi_{ox}(F_1)$ L20	0.79 ± 0.03	0.82 ± 0.03	0.56 ± 0.04	0.58 ± 0.03	0.18 ± 0.00	0.17 ± 0.01	0.10 ± 0.01	0.29 ± 0.02	0.44 ± 0.02	0.38 ± 0.01

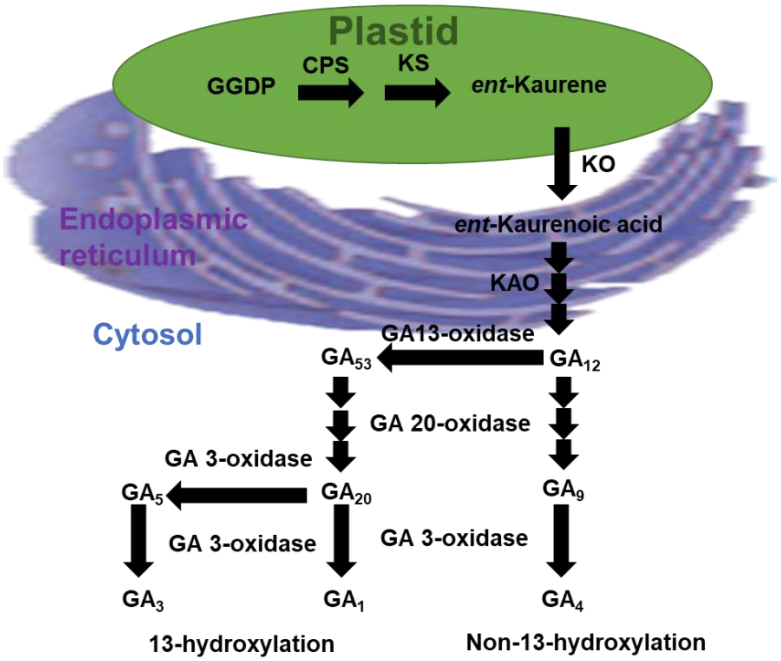

Figure A8. The GA-biosynthetic pathway from trans-geranylgeranyl diphosphate to GA_1, GA_3 and GA_4.
GGDP, *trans*-geranylgeranyl diphosphate; CPS, *ent*-copalyl diphosphate synthase; KS, *ent*-kaurene synthase; KO, *ent*-kaurene oxidase; KAO, *ent*-kaurenoic acid oxide (Hedden and Thomas 2012).

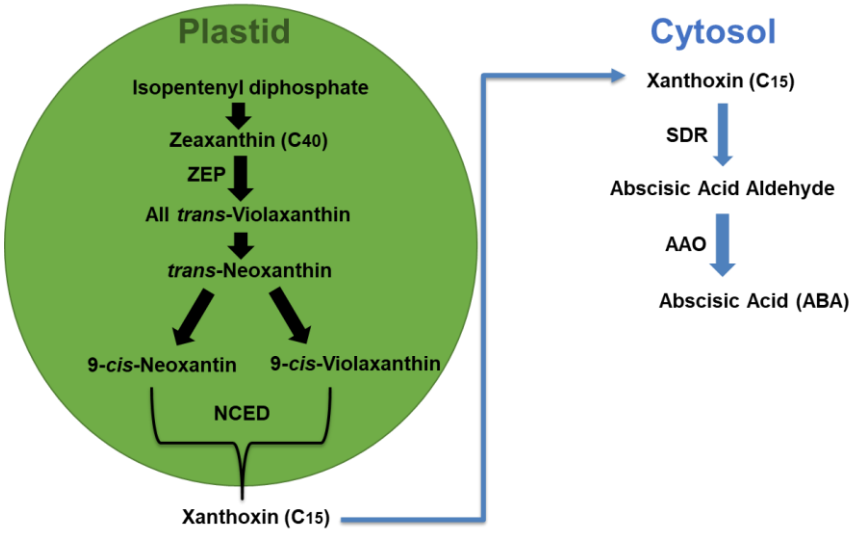

Figure A 9. Schematic representation of biosynthesis of ABA via the terpenoid pathway. The biosynthesis is initiated in plastids, where isopentenyl diphosphate is converted to C_{40} xanthophyll zeaxanthin. Zeaxanthin is further catalysed by zeaxanthin epoxidase (ZEP) to all-*trans*-Violaxanthin. All-*trans*-Violaxanthin is converted to 9-*cis*-violaxanthin or 9-cis-neoxanthin and cleaved by the 9-*cis*-epoxy carotenoid dioxygenase (NCED) to form a C_{15} intermediate product called xanthoxin. Xanthoxin is then exported to cytosol. In cytosol, xanthoxin is converted to an ABA aldehyde by the enzyme, short-chain alcohol dehydrogenase/reductase (SDR), and then oxidation of the abscisic aldehyde to ABA is catalysed by the abscisic aldehyde oxidase (AAO). (Modified from Taiz et al. 2015 and Taylor et al. 2005).

Paper I:

Specific PP2A catalytic subunits are a prerequisite for positive growth effects in Arabidopsis co-cultivated with *Azospirillum brasilense* and *Pseudomonas simiae*

plants

MDPI

Article

Specific PP2A Catalytic Subunits Are a Prerequisite for Positive Growth Effects in Arabidopsis Co-Cultivated with *Azospirillum brasilense* and *Pseudomonas simiae*

Irina O. Averkina [1], Ivan A. Paponov [2,†], Jose J. Sánchez-Serrano [3] and Cathrine Lillo [1,*]

[1] Department of Chemistry, Bioscience and Environmental Engineering University of Stavanger, 4036 Stavanger, Norway; irina.o.averkina@uis.no
[2] Division of Food Production and Society, Norwegian Institute of Bioeconomy Research, P.O. Box, 115 NO-1431 Ås, Norway; ivpa@food.au.dk
[3] Departamento de Genética Molecular de Plantas, Centro Nacional de Biotecnología, 28049 Madrid, Spain; jjss@cnb.csic.es
* Correspondence: cathrine.lillo@uis.no
† Current address: Department of Food Science, Aarhus University, 8200 Aarhus, Denmark.

Abstract: Plant growth-promoting rhizobacteria (PGPR) stimulate plant growth, but the underlying mechanism is poorly understood. In this study, we asked whether PROTEIN PHOSPHATASE 2A (PP2A), a regulatory molecular component of stress, growth, and developmental signaling networks in plants, contributes to the plant growth responses induced by the PGPR *Azospirillum brasilense* (wild type strain Sp245 and auxin deficient strain FAJ0009) and *Pseudomonas simiae* (WCS417r). The PGPR were co-cultivated with Arabidopsis wild type (WT) and PP2A (related) mutants. These plants had mutations in the PP2A catalytic subunits (C), and the PP2A activity-modulating genes *LEUCINE CARBOXYL METHYL TRANSFERASE 1* (*LCMT1*) and *PHOSPHOTYROSYL PHOSPHATASE ACTIVATOR* (*PTPA*). When exposed to the three PGPR, WT and all mutant Arabidopsis revealed the typical phenotype of PGPR-treated plants with shortened primary root and increased lateral root density. Fresh weight of plants generally increased when the seedlings were exposed to the bacteria strains, with the exception of catalytic subunit double mutant *c2c5*. The positive effect on root and shoot fresh weight was especially pronounced in Arabidopsis mutants with low PP2A activity. Comparison of different mutants indicated a significant role of the PP2A catalytic subunits C2 and C5 for a positive response to PGPR.

Keywords: Arabidopsis; *Azospirillum brasilense*; plant growth-promoting bacteria; PGPR; PP2A; *Pseudomonas simiae*; protein phosphatase 2A

Citation: Averkina, I.O.; Paponov, I.A.; Sánchez-Serrano, J.J.; Lillo, C. Specific PP2A Catalytic Subunits Are a Prerequisite for Positive Growth Effects in Arabidopsis Co-Cultivated with *Azospirillum brasilense* and *Pseudomonas simiae*. *Plants* **2021**, *10*, 66. https://doi.org/10.3390/plants10010066

Received: 9 November 2020
Accepted: 25 December 2020
Published: 30 December 2020

1. Introduction

Plant growth-promoting rhizobacteria (PGPR) positively influence plants by affecting hormone signaling, protecting plants against pathogens, and promoting the uptake of nutrients [1]. Such bacteria are expected to be important in developing better and more sustainable agricultural practices, but the underlying mechanisms and genes involved in the plant-bacteria communication are still debated. *Pseudomonas* species, which are among the most abundant bacteria in the microbiome of Arabidopsis and other plants [2,3] are candidates for improving agricultural practises. *Pseudomonas simiae* (formerly *Pseudomonas fluorescens*) has been characterized in detail, especially *P. simiae* WCS417r, and was found to stimulate biomass production, promote lateral root formation, promote auxin signaling, and trigger induced systemic resistance [3,4]. Genome wide association studies (GWAS) performed with Arabidopsis to identify plant genes important for the increased fresh weight and root growth related to *P. simiae* treatment, pointed to several interesting

genes [5]. Among these genes was *PTPA* (*PHOSPHOTYROSYL PHOSPHATASE ACTIVATOR*), a PP2A (PROTEIN PHOSPHATASE 2A) activator that was putatively related to changes in lateral root formation (Supplementary Table S2 in [5]). Inspired by this study and our long-term interest in PP2A, a *PTPA* mutant and other mutants related to the PP2A complex were included in the study presented here.

Azospirillum brasilense is also well known for its ability to influence root architecture and increase growth in plants. This bacterium is already commercially applied to various crops [6]. Generally when plants are exposed to *A. brasilense*, lateral roots increase in number, length, and thickness while the main root is shortened (reviewed in Fibach-Paldi et al. 2011) [6]. These effects have been attributed to the auxin production in *A. brasilense*, and also the production of bacterial NO appeared crucial [6]. Other signaling compounds from *A. brasilense*, which are anticipated to influence plant growth, are cytokinins and gibberellins. These bacteria also ameliorate the response of Arabidopsis to drought by enhancement of ABA (abscisic acid) levels [7]. Furthermore, *A. brasilense* can improve nutrient uptake, including nitrogen uptake, in non-nodulating as well as nodulating plants [8], and has been suggested as a remedy to increase nitrogen use efficiency in important crops such as wheat [9]. Since bacterial plant-growth promoting effects are often, at least partly, caused by auxin produced by the PGPR, a well-characterized auxin synthesis mutant *A. brasilense* (FAJ0009) was included in our study. Use of both wild type *A. brasilense* (Sp245) and FAJ0009 for testing effects on Arabidopsis, should help in uncovering how PP2A could be involved in plant growth stimulated by bacteria. Global gene expression and growth parameters had already been investigated in Arabidopsis by Spaepen and collaborators and revealed valuable data indicating a more rapid and much stronger response for the auxin-producing *A. brasilense* strain than for FAJ0009 [10].

PP2A is responsible for a considerable part of the protein phosphatase activity in all eukaryotic cells. The complete PP2A complex consists of three subunits: a catalytic (C), a scaffolding (A), and a regulatory (B) subunit [11,12]. The carboxyl terminal end of the catalytic subunit becomes methylated by LCMT1 (LEUCINE CARBOXYL METHYL TRANSFERASE 1). Formation and optimal activity of the PP2A complex is promoted by PTPA and LCMT1 [13]. The activation process and physiological consequences exerted by these regulatory proteins are still poorly understood, but PP2A methylation is essential for coping with a wide range of stress conditions, including oxidative and salt stress [13,14]. Knockout of *LCMT1* gives predominantly, or exclusively, a non-methylated PP2A enzyme [14,15]. Absence of methylation leads to decreased PP2A activity and preferences for certain subunits to be included in the full PP2A complex [16]. Interestingly, Jin et al. (2016) [17] found that mutation of the yeast *PTPA* homolog (*RRD2*), *LCMT1* homolog (*PPM1*), or *PP2A* catalytic subunit (*PPH21*) permitted yeast to better tolerate expression of a bacterial type-III effector protein from a maize pathogen, indicating that PP2A and its regulators interfere with the bacterial effector protein. In the present work we included an Arabidopsis mutant that overexpressed the *PTPA* gene and thereby possessed higher PP2A activity than WT Arabidopsis. Furthermore, a *lcmt1* knockout mutant with lack of PP2A methylation and decreased PP2A activity was included.

The PP2A catalytic subunits fall into two subfamilies in all land plants tested [18]. Subgroup 1 has been found to be involved in stress and defence responses [19–22]. Subgroup 2 has been found to be involved in regulation of auxin fluxes through dephosphorylation of PIN proteins [23], in cell division [24], and involved in regulation at the receptor level for signaling from flagellin and elongation factor Tu [25]. Plants do not have an adaptive immune system like animals, but they respond to pathogen invasion by help of an innate immune system. Many reactions occur within minutes of the pathogen attack, indicating post-translational events. Recent research points to an overlap between innate immunity and the plant mechanisms for responding to symbiotic and growth-promoting microorganisms [26]. Silencing of subfamily 1 in *Nicotiana benthamiana* resulted in constitutively expressed pathogen-related (PR) genes, and the plants developed localized cell death in stems and leaves [19]. The work with *N. benthamiana* indicated that PP2A catalytic

subfamily 1 members acted as negative regulators of plant defence responses, possibly by de-sensitizing protein phosphorylation cascades. For tomato, He and collaborators [19] showed that a PP2A catalytic subunit, also belonging to subfamily 1, was rapidly induced when exposed to a *Pseudomonas syringae* strain. For Arabidopsis, the TAIR database indicates that treatment with *Pseudomonas syringae* or *Phytophthora infestans* led to higher expression of *C1* and *C5*, respectively (both subgroup 1) [27]. Also, a PP2A catalytic subunit of the subgroup 2 was reported to be involved in the response to *P. syringae*. Indeed, Arabidopsis plants with knocked out *PP2A-C4* were more resistant towards *P. syringae* than WT Arabidopsis [25]. Complete knockout of all three subunits belonging to subgroup 1 cripples the Arabidopsis seedlings [23], but double mutants grow relatively well, and we decided to test how plant growth-promoting bacteria influence various double mutants and the *c4* single mutant.

To explore the involvement of PP2A in PGPR-plant interactions we chose three frequently studied and well-characterized bacterial strains as model organisms. These strains were *A. brasilense* Sp245 and FAJ0009, and *P. simiae* WCS417r. Our results revealed differences between Arabidopsis WT and *pp2a* mutants in their response to the PGPR, and that PGPR ameliorated growth in mutants with low PP2A activity with the exception of the *c2c5* double mutant.

2. Results

2.1. PP2A Activity in Arabidopsis WT and Selected Mutants

PP2A activity was tested in both roots and shoots of WT, *lcmt1*, two single (*c2* and *c4*) and three double (*c2c5*, *c4c5* and *c2c4*) mutants of the PP2A catalytic subunits (Figure 1). PP2A activity in roots was always much higher than in shoots (on a per mg protein basis). The low activity of these mutants had been found also in extracts from whole seedlings (S1). Mutants of *ptpa* had previously been studied in detail [13,14] and the *ptpa*$_{m}$ was revealed to be a high activity mutant with 180% PP2A activity compared with WT [14]. The *lcmt1*, *ptpa*$_{m}$, *c4* single mutant, and the three double mutants *c2c5*, *c4c5*, and *c2c4* were included in further experiments to characterize interactions between PGPR and PP2A.

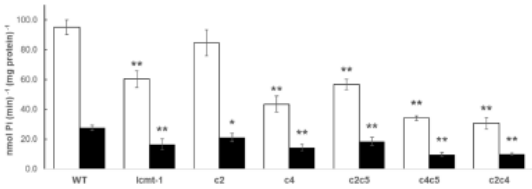

Figure 1. PP2A activity in selected Arabidopsis mutants. Activity was assayed separately in roots (white bars) and shoots (black bars) from 10-d-old seedlings grown on one-half MS medium. SE is given (n = 3, three biologically independent experiments), two asterisks indicate that values are significantly different from WT according to Student's t-test with $p < 0.05$, and for one asterisk with $p < 0.1$.

2.2. PP2A Activity in Arabidopsis WT Treated with PGPR

To check if PP2A activity was influenced by treatment with PGPR, PP2A activity in roots and shoots of Arabidopsis seedlings exposed to *P. simiae* or *A. brasilense* for two weeks was compared with non-treated control plants. Despite the pronounced phenotypic response observed for plants grown with bacteria, total in vitro PP2A activity did not deviate significantly from the control seedlings grown in the absence of bacteria (Figure 2).

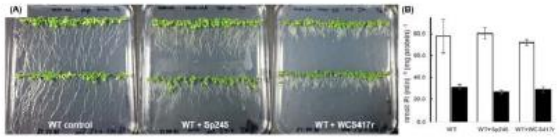

Figure 2. Visual phenotype and PP2A activity of Arabidopsis WT not treated or treated with PGPR. (**A**) Control plants were grown without bacteria (left plate) or co-cultivated with *A. brasilense* Sp245 (middle plate), or with *P. simiae* WCS417r (right plate) for 14 days. (**B**) Activity was assayed separately in roots (white bars) and shoots (black bars). Experiments were repeated three times. Values for plants treated with bacteria were not significantly different from non-treated plants at $p < 0.1$, SE is given.

2.3. Phenotypic Response of Arabidopsis WT and Mutants to *P. simiae* WCS417r

The cultivation of Arabidopsis seedlings with *P. simiae* WC417r was performed in two series. These two series are presented in separate diagrams with their respective WT reference. Arabidopsis lines including WT, *ptpa*$_{kn}$, *lcmt1*, and *c4* were first studied (Figures 3 and 4), and the second series included WT and the three double mutants *c2c5*, *c4c5*, and *c2c4* (Figures 5 and 6). Irrespective of the genotype, the root architecture of all seedlings was strikingly influenced by *P. simiae*, with a shorter primary root (Figures 3, 4A, 5, and 6A). Averaged across all genotypes, primary root length was 31 ± 1% (spreading from 26–36%) of non-treated seedlings. Primary root thickness and root weight significantly increased for all genotypes, except for *ptpa*$_{kn}$ and *c2c5* which were not significantly influenced by *P. simiae* (Figures 4B,C, and 6B,C). Number of lateral roots clearly increased in WT, *c4*, *c4c5*, and *c2c4*, but did not change significantly in *ptpa*$_{kn}$, *lcmt1*, and *c2c5* in response to *P. simiae* (Figures 4D and 6D). However, all genotypes clearly showed increased lateral root density (number of lateral roots per mm primary root) (Figures 4F and 6F). Shoot weight generally increased in response to *P. simiae*, but not for double mutants with knocked out *c2*—i.e., *c2c5* and *c2c4* (Figures 4E and 6E). Chlorophyll content was unchanged or increased in plants treated with *P. simiae*, strikingly so for the *lcmt1* mutant (Figures 4G and 6G). *Lcmt1* originally had low chlorophyll content compared with WT, but after inoculation with *P. simiae* reached WT values (Figure 4G).

Figure 3. Visual phenotype of Arabidopsis WT and mutants treated with *P. simiae* WCS417r. Seedlings of Arabidopsis WT and mutants (*ptpa*$_{kn}$, *lcmt1*, *c4*) cultivated without (upper row) and with *P. simiae* WCS417r (lower row) for two weeks.

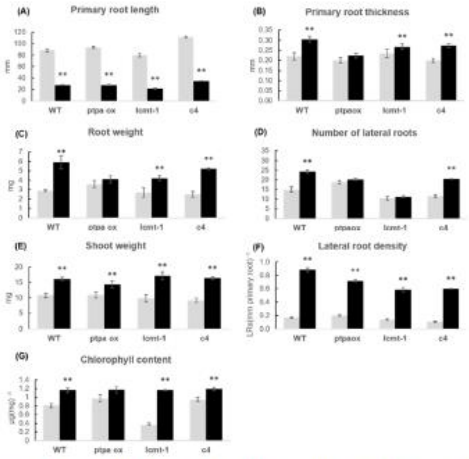

Figure 4. Growth parameters of WT and mutants treated with *P. simiae* WCS417r. Seedlings of Arabidopsis WT, *ptpaox*, *lcmt1*, and *o4* were cultivated without (grey bars) and with (black bars) *P. simiae* WCS417r for two weeks. (**A**) primary root length; (**B**) primary root thickness; (**C**) root fresh weight; (**D**) number of lateral roots; (**E**) shoot fresh weight; (**F**) lateral root density; and (**G**) chlorophyll content. For root length, primary root thickness, number of lateral roots, and root density, data are means ± SE of 30 plants (n = 30). For fresh weight and chlorophyll content, the plants in each plate were pooled for measurements, and data given is the average of six independent experiments, n = 6, ±SE is given. The root and shoot weights (**C**,**E**) represent single plant averages. The chlorophyll values (**G**) represent µg chlorophyll per mg leaf tissue. According to Student's t-test and p-value < 0.05, columns marked with two asterisks are significantly different from the control without bacteria.

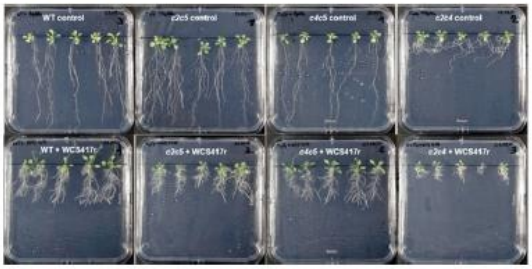

Figure 5. Visual phenotype of Arabidopsis WT and double mutants treated with *P. simiae* WCS417r. Seedlings of Arabidopsis WT and double mutants *c2c5*, *o4c5*, and *c2c4* were cultivated without (upper row) and with *P. simiae* WCS417r (lower row) for two weeks.

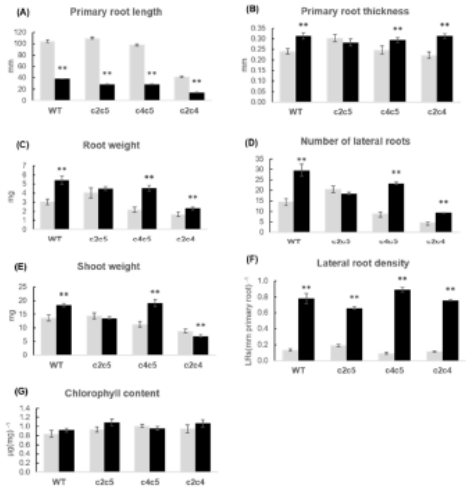

Figure 6. Growth parameters of WT and double mutants treated with *P. simiae* WCS417r. Seedlings of Arabidopsis WT and double mutants *c2c5*, *c4c5*, *c2c4* were cultivated without (grey bars) and with (black bars) *P. simiae* WCS417r for two weeks. (**A**) primary root length; (**B**) primary root thickness; (**C**) root fresh weight; (**D**) number of lateral roots; (**E**) shoot fresh weight; (**F**) lateral root density; and (**G**) chlorophyll content. For root length, primary root thickness, number of lateral roots, and root density, data are means ± SE of 30 plants (n = 30). For fresh weight and chlorophyll content, the plants in each plate were pooled for measurements, and data given is the average of six independent experiments, n = 6, ±SE is given. The root and shoot weights (**C**) and (**E**) represent single plant averages. The chlorophyll values (**G**) represent µg chlorophyll per mg leaf tissue. According to Student's t-test and p-value < 0.05, columns marked with two asterisks are significantly different from the control without bacteria.

Effects of PGPR (*P. simiae*) were tested also with some *pp2a-b´* mutants (*b'alpha, b'beta, b'gamma, b'zeta, b'theta*). These B' subunits had previously been implicated in the response to bacterial pathogens [17,25,28]. The mutants were not studied in detail, but the experiments showed that they all responded to bacteria treatment with shortened primary root and increased lateral root density. The response of *b'alpha* and *b'theta* were different from WT, with significant fewer lateral roots and lower lateral root density (Figures S2 and S3). Interestingly, *b'theta* had previously been shown to interact with C2 and C5 in vivo, and the current results are in agreement with the earlier suggestion [29] that C2 and C5 are part of PP2A complexes containing B'theta.

2.4. Phenotypic Response of Different Arabidopsis WT and Mutants Treated with Azospirillum Brasilense Sp245 and FAJ0009

Two different strains of *A. brasilense* were used for inoculation: the auxin producing wild type strain Sp245 and an auxin synthesis mutant, FAJ0009. The FAJ0009 strain is mutated in the IpdC gene resulting in an auxin production reduced by more than 90% [30]. As for *P. simiae* the experiments were divided into two series: WT, $ptpa_m$, *lcmt1* and *o4* (Figures 7 and 8), and WT, *c2c5*, *o4c5*, and *c2c4* (Figures 9 and 10). WT and all mutants

were influenced by *A. brasilense*, both Sp245 and FAJ0009 (Figures 7–10). Irrespective of the genotype, the root architecture of all seedlings was strikingly influenced by the Sp245 strain (Figures 7, 8A, 9, and 10A). Across all the experiments, the average primary root length for Sp245 treated plants was 31 ± 4% of non-treated (spread from 23 to 53%), that is a similar effect as observed for *P. simiae*. A less pronounced effect was seen for plants treated with FAJ0009 giving an average root length of 71 ± 8.0% compared with non-treated plants (spread from 34–100%). In the first series there was no significant root shortening on WT and *o4* mutant, but in the second series root shortening by FAJ0009 was significant for all genotypes, including WT. Apparently, small variations in experimental conditions may have had a large influence, that however, did not change the overall trends. An increase in primary root thickness or root weight was observed for all genotypes, at least for one of the two bacteria Sp245 or FAJ0009, with the striking exception of the *c2c5* mutant which showed no effects (Figures 8B,C and 10B,C).

Such a lack of response with *c2c5* had also been observed for *P. simiae* (Figure 6B,C). Number of lateral roots decreased for *c2o4*, but other genotypes showed variable responses with Sp245 and FAJ0009 (Figures 8D and 10D). Lateral root density increased in all genotypes in response to Sp245 as well as FAJ0009 treatment. The response to Sp245 was, however, always stronger than to FAJ009, which induced a response in-between non-treated and Sp245-treated (Figures 8F and 10F). Shoot fresh weight was usually higher or unchanged in seedlings treated with Sp245 or FAJ0009 compared with non-treated plants. However, for the *c2c5* mutant a clear decrease in shoot fresh weight was observed for treatment with both Sp245 and FAJ0009 (Figure 10E). Chlorophyll content was not positively influenced by Sp245 or FAJ0009. Notably, chlorophyll content in the *c2c5* mutant responded with a significant and strong decrease after co-cultivation with both strains of *Azospirillum* (Figure 10G).

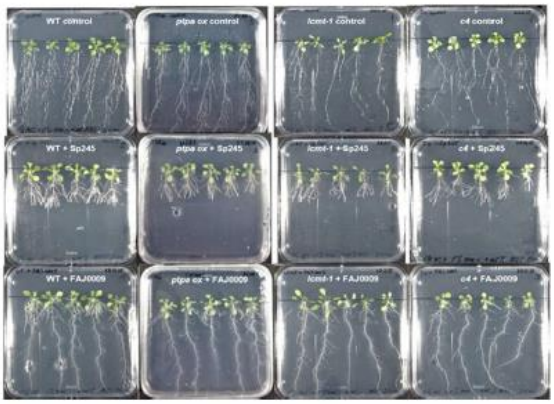

Figure 7. Visual phenotype of Arabidopsis WT and mutants treated with *A. brasilense*. Seedlings of Arabidopsis WT and mutants *ptpa*$_{ox}$, *lcnt1*, *o4* were cultivated without bacteria (upper row) and with *A. brasilense* Sp245 (middle row) and *A. brasilense* FAJ0009 (lower row) for two weeks.

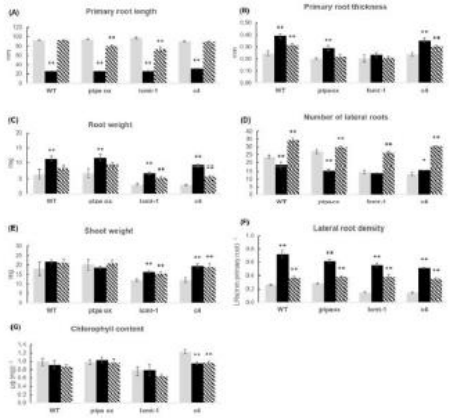

Figure 8. Growth parameters of WT and mutants influenced by *A. brasilense*. Growth parameters of WT and mutants *ptpaox*, *lonl1*, *o4* cultivated without bacteria (grey bars), with *A. brasilense* Sp245 (black bars) and with *A. brasilense* FAJ0009 (hatched bars) for two weeks. (**A**) primary root length; (**B**) primary root thickness; (**C**) root fresh weight; (**D**) number of lateral roots; (**E**) shoot fresh weight; (**F**) lateral root density; and (**G**) chlorophyll content. For root length, primary root thickness, number of lateral roots, and root density, data are means ± SE of 30 plants (n = 30). For fresh weight and chlorophyll content, the plants in each plate were pooled for measurements, and data given is the average of six independent experiments, n = 6, ±SE is given. The root and shoot weights (**C**,**E**) represent single plant averages. The chlorophyll values (**G**) represent µg chlorophyll per mg leaf tissue. According to Student's t-test and p-value < 0.05, columns marked with two asterisks are significantly different from the control without bacteria, and for one asterisk with p< 0.1.

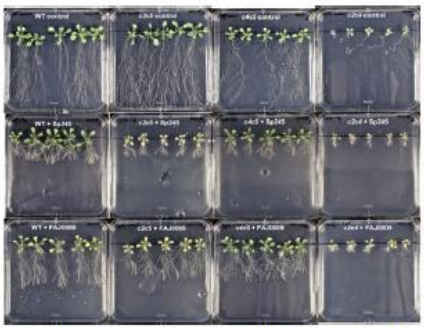

Figure 9. Visual phenotype of Arabidopsis WT and double mutants treated with *A. brasilense*. Seedlings of Arabidopsis WT and double mutants *c2c5*, *o45*, *c2c4* were cultivated without bacteria (upper row) and with *A. brasilense* Sp245 (middle row) and with *A. brasilense* FAJ0009 (lower row) for two weeks.

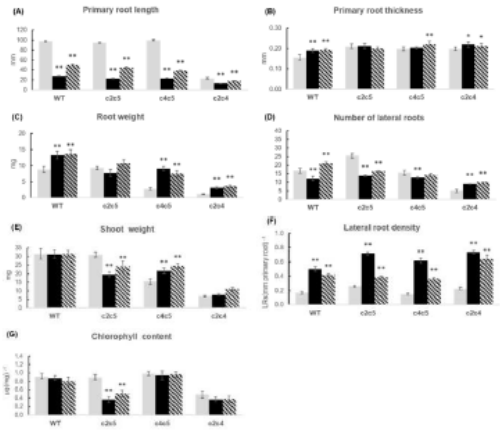

Figure 10. Growth parameters of WT and double mutants treated with *A. brasilense*. Growth parameters of WT and double mutants *c2c5*, *c4c5*, *c2c4* cultivated without bacteria (white bars), with *A. brasilense* Sp245 (black bars) and with *A. brasilense* FAJ0009 (hatched bars) for two weeks. (**A**) primary root length; (**B**) primary root thickness; (**C**) root fresh weight; (**D**) number of lateral roots; (**E**) shoot fresh weight; (**F**) lateral root density; and (**G**) chlorophyll content. For root length, primary root thickness, number of lateral roots, and root density, data are means ± SE of 30 plants (n = 30). For fresh weight and chlorophyll content, the plants in each plate were pooled for measurements, and data given is the average of six independent experiments, n = 6, ±SE is given. The root and shoot weights (**C**) and (**E**) represent single plant averages. The chlorophyll values (**G**) represent µg chlorophyll per mg leaf tissue. According to Student's t-test and p-value < 0.05, columns marked with two asterisks are significantly different from the control without bacteria, and for one asterisk with p< 0.1.

3. Discussion

When Arabidopsis or other plants are exposed to PGPR bacteria, general effects on root architecture repeatedly observed in different laboratories are shortened primary root and increased lateral root density. Such a change in root architecture was observed for WT, *lcmt1*, *ptpa*$_{kn}$, and all *pp2a* mutants tested, showing that these basic responses occurred in plants with both high and low PP2A activity and irrespective of the methylation state of the PP2A catalytic subunits (A and F in Figures 4, 6, 8, and 10). All three bacteria strains, *P. simiae*, and *A. brasilense* Sp245 and FAJ0009, induced short primary roots and increased lateral root density, but the response to FAJ0009 was much weaker. Although a response was observed in all Arabidopsis lines tested, a closer look revealed different growth responses among genotypes. Changes in root parameters for the *ptpa*$_{kn}$ mutant were very similar to WT when exposed to *A. brasilense* Sp245 or FAJ0009, but different from WT when exposed to *P. simiae* WCS417r. When treated with *P. simiae*, primary root thickness, root weight, and number of lateral roots, all increased for WT Arabidopsis, but none of these root parameters changed significantly for the *ptpa*$_{kn}$ mutant (Figures 4 and 8). According to the GWAS (genome-wide association studies) by Wintermans et al. (2016) [5], the PTPA locus was a candidate to induce deviations regarding number of lateral roots when treated with *P. simiae*, however not a candidate to induce deviations regarding shoot fresh weight or primary root length. Indeed, our experiments with the *ptpa*$_{kn}$ mutant

showed that only the response of number of lateral roots was different from WT. Since we worked with an overexpressor and observed a negative response on the number of lateral roots, the PTPA locus with a positive response in the GWAS could be a locus linked with decreased PTPA expression. This hypothesis would need further investigation and requires a suitable *ptpa* mutant with decreased/knocked-down PTPA expression that may allow to establish the importance of the locus for positive responsiveness to PGPR.

In the *lcmt1* mutant, the catalytic subunits are mainly in the non-methylated form, and this leads to decreased PP2A activity (Figure 2 and [13]). The physiological function of PP2A methylation is still enigmatic in plants, but apparently lack of methylation did not hinder positive effects from bacteria. Both root and shoot weight of *lcmt1* were positively influenced by the bacteria strains tested, and *P simiae* WCS417 also ameliorated the low chlorophyll content in *lcmt1* (Figure 4G).

Auxin, or compounds stimulating auxin signaling in plants, clearly can promote plant root growth, as has frequently been reported for various *Pseudomonas* [3,31,32] and *Azospirillum* strains [10,30]. It has previously been shown that incubation with *P. simiae* WCS417r induced genes in Arabidopsis with a strong auxin signature, and these genes stimulated the changes in root architecture and promoted plant growth [3,32]. When Arabidopsis was co-cultivated with *A. brasilense Sp245* or the auxin synthesis mutant FAJ0009 for two weeks, we observed a clear, but much weaker, effect on root architecture for FAJ0009. This confirmed that auxin produced by *A. brasilense* strongly influenced root architecture but was most likely not the only bacterial factor influencing plant growth (Figures 8 and 10).

Striking phenotypic results were obtained for the *c2c5* mutant. In contrast with the other genotypes, the *c2c5* mutant was not significant positively influenced by any of the three bacteria strains regarding primary root thickness, root weight, number of lateral roots, shoot weight, or chlorophyll content. The C2 and C5 subunits, together with C1, make up the subgroup 1 of PP2A catalytic subunits in Arabidopsis. Apparently, when both C2 and C5 were knocked out, their functions could not be fully replaced by the C1 subunit, although the three subunits may have some overlapping functions. Catalytic subgroup 1 members are suppressors of defence responses in higher plants, and C2 and C5 are therefore candidates to be involved in defence signaling processes in Arabidopsis induced by bacteria [19,28]. Lack of these catalytic subunits could possibly hamper the silencing of defence genes necessary for obtaining a balanced trade-off between growth and defence that could promote growth by PGPR. Another possibility would be that lack of C2 and C5 would impair auxin signaling; however, only group 2 catalytic subunits (C3, C4) have been shown to be important for auxin signaling. PIN (PIN FORMED) proteins are auxin transporters which are often localised in the membrane at the polar ends of cells in the direction of polar auxin transport [33]. The PP2A dephosphorylation activity is important for counteracting PID (PINOID)-mediated phosphorylation of PIN proteins. This dephosphorylation determines proper PIN localisation and facilitates polar auxin efflux from cells. PP2A catalytic subunits C3 and C4 were previously shown to be important for dephosphorylation of PINs, but single mutants of these subunits showed wild type phenotype. Only a double mutant *c3c4* showed mislocalization of PIN proteins, indicating the contribution of these subunits and their redundant roles in controlling of PIN polarity [23]. Since PP2A affects auxin signaling probably through the polar auxin transport and subgroup 2 catalytic subunits, effects of silencing subgroup 1 catalytic subunits are more likely to be related to other processes, like regulation of defence or ABA signaling. PP2A catalytic subunits C2 and C5 are necessary for optimal root growth under stress conditions such as high salt concentrations and exposure to ABA [20,22]. Expression analysis using the C2 promoter linked with GUS had shown that C2 expression correlated with root development and suggested a role for C2 in lateral root growth. Under standard growth conditions, roots of the *c2* mutant were not distinguishable from WT roots, but when exposed to ABA the *c2* mutant showed a more severe inhibition of root growth than did WT. Furthermore, a C2 overexpressor was less influenced by ABA than WT [20]. A *c5* mutant

studied by Hu et al. (2017) was hypersensitive to various salts and developed shorter roots and produced smaller leaves under stress than WT [22]. The work also showed that C5 was involved in salt tolerance most likely through interactions with chloride channel proteins in the vacuole membrane. Amelioration of growth by *A. brasilense* Sp245 during drought was shown to involve ABA production [7,34]. The effects observed in the *c2c5* mutant in the present study could be explained by lack of these subunits, which otherwise would mediate ABA and stress signaling. This would fit with previous investigations that *A. brasilense* Sp245 did produce ABA and that co-cultivation with plants induced a two-fold higher level of endogenous ABA in Arabidopsis. ABA is associated with abiotic stress like high salt concentrations and drought and is also involved in biotic stress. ABA thus functions at the crossroad of abiotic and biotic stress responses [35]. The pathogenic *Pseudomonas syringae* also induced a response in Arabidopsis which clearly involved ABA [36]. If ABA signaling could explain the effects observed when *c2c5* was co-cultivated with *P. simiae* WCS417r remains to be investigated because the response triggered by *P. simiae* was clearly different from *P. syringae* [32]. Both C2 and C5 overexpressors improved root growth under various abiotic stress treatments [20,22], and it would be interesting to explore if overexpression of these genes could enhance the positive effects from PGPR beyond that observed in WT plants.

4. Materials and Methods

4.1. Plant Material

Arabidopsis thaliana Columbia ecotype, *lcmt1* knockout line (insertion in At1g02100 exon four, SALK_079466 [37], *ptpa* overexpressor GABI_606E07 (insertion in promoter) [38] were provided by the European Arabidopsis Stock Centre in Nottingham UK, and previously characterized [14]. PP2A catalytic subunit single and double mutants derived from SALK and SAIL lines were also described previously [14,23,25,39].

4.2. Bacterial Strains

Azospirillum brasilense Sp245 wild-type strain [10] and its ipdC-knockout mutant FAJ000 (Sp245 *ipdC*::Tn5) impaired in auxin biosynthesis capacity because of knockout mutation in the key gene for auxin biosynthesis Indole-3-pyruvate decarboxylase (ipdC) [30,40], were kindly provided by Laurent Legendre (Saint-Étienne, France) and Claire Prigent-Combaret (CNRS, Lyon, France). *Pseudomonas simiae* (formerly *Pseudomonas fluorescens*) WCS417r is the rifampicin-resistant mutant of the biocontrol strain *Pseudomonas simiae* WCS417 originally isolated from the rhizosphere of wheat grown in Brazil [41], was kindly provided by Corné M.J. Pieterse and I.A. Hans van Pelt, Department of Biology, Utrecht University, Utrecht, the Netherlands.

4.3. Plant Growth Conditions for Bacteria Treatment

Surface sterilized seeds of Arabidopsis were sown in square Petri dishes (120 × 120 mm) containing half-strength Murashige and Skoog (MS) medium [42] with 1% (*w*/*v*) sucrose, pH 5.8, and 0.8% (*w*/*v*) agar (VWR International, Milano, Italy). The plates were placed in the dark at 4 °C for 2 days for stratification prior to cultivation vertically at a 16 h photoperiod for 5 days prior to transfer to new plates (five plants per plate) with bacteria-inoculated one-half MS medium.

4.4. Plant Growth Medium for Pseudomonas Treatment

Half-strength Murashige and Skoog and pH adjusted to 5.8. Sucrose (0.5%) and agar (0.8%) were added. After autoclaving the medium was poured into 12 × 12 cm Petri dishes.

4.5. Inoculating with Pseudomonas WCS 417r

Pseudomonas from glycerol stocks was streaked onto a Petri dish with King agar B supplemented with 50 mg L^{-1} rifampicin and incubated overnight at 28 °C. The grown bacterial culture was loosened in 10 mL of 10 mM $MgSO_4$ [41]. The bacterial suspension was pipetted into a 15 mL Falcon tube and centrifuged at 3900× *g* for 5 min, pelleted bacteria were washed once in 10 mM $MgSO_4$, then resuspended in 10 mM $MgSO_4$ to obtain OD_{600} = 0.005 or 10^5 cells/mL [43]. Bacterial suspension, 500 µL, was spread evenly onto each Petri dish before transferring the plants.

4.6. Plant Growth Medium for Azospirillum Treatment

Half-strength Murashige and Skoog was prepared with 2.56 mM Mes buffer and pH adjusted to 6.0. Sucrose (1%) and agar (0.8%) were added. After autoclaving the medium was poured into 12 × 12 cm Petri dishes.

4.7. Inoculating with Azospirillum spp. (Sp245 and FAJ0009)

Azospirillum Sp245 and FAJ0009 from glycerol stocks were streaked and grown on Luria–Bertani (LB) solid medium supplemented with 2.5 mM $CaCl_2$, 2.5 mM $MgSO_4$, and 50 mg L^{-1} kanamycin (only for FAJ0009) for 48 h at 37 °C. The colonies were used to produce an overnight culture in 5 mL of supplemented LB broth and incubated at 37 °C with shaking at 180 rpm overnight. The overnight culture (0.1 mL) was subcultured in 50 mL of supplemented LB broth and incubated at 37 °C under shaking at 180 rpm overnight. On the following day, the bacterial suspension was pipetted into 50 mL Falcon tubes and centrifuged at 3900× *g* for 5 min at 16 °C, the supernatant was removed, and the cells were re-suspended in 10 mL of 10 mM $MgSO_4$, washed once with 0.85% NaCl and re-suspended in fresh 10 mM $MgSO_4$ to obtain OD_{600} = 1 or 5 × 10^8 cells/mL [10]. One volume of this suspension was mixed with 9 volumes of the warm (45 °C) plant growth medium (giving OD_{600} = 0.1). Ten mL of the mixture was poured onto 30 mL of already solidified plant growth medium and allowed to solidify.

4.8. Chlorophyll Assay

Five shoots from each plate were weighted and thoroughly ground with 2 mL of 95% ethanol in a mortar. The obtained suspension was transferred to a 2 mL collection tube and centrifuged for 1 min at 21,000× *g*. Prior to measuring absorbance at 654 nm, 300 µL of the supernatant was diluted with 1.2 mL of 95% ethanol. The chlorophyll content was calculated as A_{654} × 1000/39.8 × extraction volume (mL)/weight of fresh tissue (mg) × dilution factor of 5 = µg chlorophyll per mg leave tissue [44].

4.9. PP2A Assay

The Ser/Thr Phosphatase assay system from Promega (Promega 2009, Madison, WI, USA) was used as previously described in [39]. Frozen tissue, 100 mg, was homogenized and prepared for assay with 0.1 mM phosphorylated peptide (RR(pT)VA) as substrate. Phosphate released was measured, and assays with and without 5 nM okadaic acid were compared to calculate the PP2A activity [39]. For total phosphatase activity okadaic acid was omitted. After 15 min incubation, absorbance was read at 630 nm and converted into corresponding amounts of phosphate using a trend line equation of the standard curve (Promega. Technical Bulletin. Serine/Threonine Phosphatase Assay System. Instructions for use of product V2460, Madison, WI, USA). PP2A activity was calculated as the difference of phosphate released with and without okadaic acid [39,45].

5. Conclusions

Arabidopsis mutants with high or low PP2A activity due to mutations in PP2A catalytic and regulatory proteins all responded to *Pseudomonas simiae* WCS417r and *Azospirillum brasilense* Sp245 and FAJ0009 with a change in root architecture giving a shortened primary root and higher density of lateral roots. Additionally, most mutants responded to the PGPR by an

increase in fresh weight, but a *pp2a* subgroup 1 double mutant with knocked out catalytic subunits C2 and C5 did not show increased fresh weight, indicating that these catalytic subunits play important roles for the ability to enhance growth induced by PGPR.

Supplementary Materials: The following are available online at www.mdpi.com/2223-7747/10/1/66/s1, Figure S1: PP2A activity in Arabidopsis WT single (*c1. c2. c3. c4. c5*) and double (*c2c5. c4c5. c2c4*) mutants of PP2A catalytic subunits; Figure S2: Visual phenotype of Arabidopsis WT, *c2* and various *b'*-mutants treated with *P. simiae* WCS417r; Figure S3: Growth parameters of WT, *c2* and various *b'*-mutants treated with *P. simiae* WCS417r.

Author Contributions: Conceptualization, C.L., I.O.A., and I.A.P.; Formal analysis, I.O.A.; Investigation; I.O.A.; Resources, I.O.A., J.J.S.-S., and C.L.; Writing—original draft preparation, C.L. and I.O.A.; Writing—review and editing; I.O.A., C.L., J.J.S.-S., and I.A.P.; Supervision, C.L.; Project administration, C.L. and I.A.P.; Funding acquisition, C.L. and I.A.P. All authors have read and agreed to the published version of the manuscript.

Funding: The present study was supported by the Bionær program of the Research Council of Norway ('Biofresh' project no. 255613/E50).

Institutional Review Board Statement: Not applicable.

Informed Consent Statement: Not applicable.

Data Availability Statement: Data used is within the article or supplementary material.

Conflicts of Interest: The authors declare no conflict of interest.

References

1. Jacoby, R.; Peukert, M.; Succurro, A.; Koprivova, A.; Kopriva, S. The Role of Soil Microorganisms in Plant Mineral Nutrition—Current Knowledge and Future Directions. *Front. Plant Sci.* **2017**, *8*, 1617, doi:10.3389/fpls.2017.01617.
2. Bulgarelli, D.; Schlaeppi, K.; Spaepen, S.; Van Themaat, E.V.L.; Schulze-Lefert, P. Structure and Functions of the Bacterial Microbiota of Plants. *Annu. Rev. Plant Biol.* **2013**, *64*, 807–838, doi:10.1146/annurev-arplant-050312-120106.
3. Zamioudis, C.; Mastranesti, P.; Dhonukshe, P.; Blilou, I.; Pieterse, C.M.J. Unraveling Root Developmental Programs Initiated by Beneficial Pseudomonas spp. Bacteria. *Plant Physiol.* **2013**, *162*, 304–318, doi:10.1104/pp.112.212597.
4. Yu, K.; Pieterse, C.M.J.; Bakker, P.A.; Berendsen, R.L. Beneficial microbes going underground of root immunity. *Plant Cell Environ.* **2019**, *42*, 2860–2870, doi:10.1111/pce.13632.
5. Wintermans, P.C.A.; Bakker, P.A.H.M.; Pieterse, C.M.J. Natural genetic variation in Arabidopsis for responsiveness to plant growth-promoting rhizobacteria. *Plant Mol. Biol.* **2016**, *90*, 623–634, doi:10.1007/s11103-016-0442-2.
6. Fibach-Paldi, S.; Burdman, S.; Okon, Y. Key physiological properties contributing to rhizosphere adaptation and plant growth promotion abilities of Azospirillum brasilense. *FEMS Microbiol. Lett.* **2011**, *326*, 99–108, doi:10.1111/j.1574-6968.2011.02407.x.
7. Cohen, A.C.; Bottini, R.; Pontin, M.; Berli, F.J.; Moreno, D.; Boccanlandro, H.; Travaglia, C.N.; Piccoli, P.N. Azospirillum brasilenseameliorates the response ofArabidopsis thalianato drought mainly via enhancement of ABA levels. *Physiol. Plant.* **2014**, *153*, 79–90, doi:10.1111/ppl.12221.
8. Pereg, L.; De-Bashan, L.E.; Bashan, Y. Assessment of affinity and specificity of Azospirillum for plants. *Plant Soil* **2016**, *399*, 389–414, doi:10.1007/s11104-015-2778-9.
9. Camilios-Neto, D.; Bonato, P.; Wassem, R.; Tadra-Sfeir, M.Z.; Brusamarello-Santos, L.C.C.; Valdameri, G.; Donatti, L.; Faoro, H.; Weiss, V.A.; Chubatsu, L.S.; et al. Dual RNA-seq tran-scriptional analysis of wheat roots colonized by Azospirillum brasilense reveals up-regulation of nutrient acquisition and cell cycle genes. *BMC Genom.* **2014**, *15*, 378, doi:10.1186/ 1471-2164-15-378.
10. Spaepen, S.; Bossuyt, S.; Engelen, K.; Marchal, K.; Vanderleyden, J. Phenotypical and molecular responses ofArabidopsis thaliana roots as a result of inoculation with the auxin-producing bacteriumAzospirillum brasilense. *New Phytol.* **2014**, *201*, 850–861, doi:10.1111/nph.12590.
11. Lillo, C.; Kataya, A.R.A.; Heidari, B.; Creighton, M.T.; Nemie-Feyissa, D.; Ginbot, Z.; Jonassen, E.M. Protein phosphatases PP 2A, PP 4 and PP 6: mediators and regulators in development and responses to environmental cues. *Plant Cell Environ.* **2014**, *37*, 2631–2648, doi:10.1111/pce.12364.
12. Bheri, M.; Pandey, G.K. PP2A Phosphatases Take a Giant Leap in the Post-Genomics Era. *Curr. Genom.* **2019**, *20*, 154–171, doi:10.2174/1389202920666190517110605.
13. Chen, J.; Hu, R.; Zhu, Y.; Shen, G.; Zhang, H. Arabidopsis PHOSPHOTYROSYL PHOSPHATASE ACTIVATOR Is Essential for PROTEIN PHOSPHATASE 2A Holoenzyme Assembly and Plays Important Roles in Hormone Signaling, Salt Stress Response, and Plant Development. *Plant Physiol.* **2014**, *166*, 1519–1534, doi:10.1104/pp.114.250563.

14. Creighton, M.T.; Kolton, A.; Kataya, A.R.; Maple-Grødem, J.; Averkina, I.O.; Heidari, B.; Lillo, C. Methylation of protein phosphatase 2A-Influence of regulators and environmental stress factors. *Plant Cell Environ.* **2017**, *40*, 2347–2358, doi:10.1111/pce.13038.
15. Wu, G.; Wang, X.; Li, X.; Kamiya, Y.; Otegui, M.S.; Chory, J. Methylation of a Phosphatase Specifies Dephosphorylation and Degradation of Activated Brassinosteroid Receptors. *Sci. Signal.* **2011**, *4*, ra29, doi:10.1126/scisignal.2001258.
16. Janssens, V.; Longin, S.; Goris, J. PP2A holoenzyme assembly: in cauda venenum (the sting is in the tail). *Trends Biochem. Sci.* **2008**, *33*, 113–121, doi:10.1016/j.tibs.2007.12.004.
17. Jin, L.; Ham, J.H.; Hage, R.; Zhao, W.; Soto-Hernández, J.; Lee, S.Y.; Paek, S.-M.; Kim, M.G.; Boone, C.; Coplin, D.L.; et al. Direct and Indirect Targeting of PP2A by Conserved Bacterial Type-III Effector Proteins. *PLOS Pathog.* **2016**, *12*, e1005609, doi:10.1371/journal.ppat.1005609.
18. Booker, M.A.; Delong, A. Atypical Protein Phosphatase 2A Gene Families Do Not Expand via Paleopolyploidization. *Plant Physiol.* **2017**, *173*, 1283–1300, doi:10.1104/pp.16.01768.
19. He, X.; Anderson, J.C.; Del Pozo, O.; Gu, Y.-Q.; Tang, X.; Martin, G.B. Silencing of subfamily I of protein phosphatase 2A catalytic subunits results in activation of plant defense responses and localized cell death. *Plant J.* **2004**, *38*, 563–577, doi:10.1111/j.1365-313x.2004.02073.x.
20. Pernas, M.; García-Casado, G.; Rojo, E.; Solano, R.; Sánchez-Serrano, J.J. A protein phosphatase 2A catalytic subunit is a negative regulator of abscisic acid signaling. *Plant J.* **2007**, *51*, 763–778, doi:10.1111/j.1365-313x.2007.03179.x.
21. País, S.M.; González, M.A.; Téllez-Iñón, M.T.; Capiati, D.A. Characterization of potato (Solanum tuberosum) and tomato (Solanum lycopersicum) protein phosphatases type 2A catalytic subunits and their involvement in stress responses. *Planta* **2009**, *230*, 13–25, doi:10.1007/s00425-009-0923-5.
22. Hu, R.; Zhu, Y.; Wei, J.; Chen, J.; Shi, H.; Shen, G.; Zhang, H. Overexpression of PP2A-C5 that encodes the catalytic subunit 5 of protein phosphatase 2A in Arabidopsis confers better root and shoot development under salt conditions. *Plant Cell Environ.* **2016**, *40*, 150–164, doi:10.1111/pce.12837.
23. Ballesteros, I.; Domínguez, T.; Sauer, M.; Paredes, P.; Duprat, A.; Rojo, E.; Sanmartín, M.; Sánchez-Serrano, J.J. Specialized functions of the PP2A subfamily II catalytic subunits PP2A-C3 and PP2A-C4 in the distribution of auxin fluxes and development in Arabidopsis. *Plant J.* **2013**, *73*, 862–872, doi:10.1111/tpj.12078.
24. Yue, K.; Sandal, P.; Lin, Z.; Van De Cotte, B.; Iqbal, M.; Van Bel, M.; Van De Slijke, E.; Meyer, M.R.; Gadeyne, A.; Zipfel, C.; et al. PP2A-3 interacts with ACR4 and regulates formative cell division in the Arabidopsis root. *Proc. Natl. Acad. Sci. USA* **2016**, *113*, 1447–1452, doi:10.1073/pnas.1525122113.
25. Segonzac, C.; Macho, A.P.; Sanmartín, M.; Ntoukakis, V.; Sánchez-Serrano, J.J.; Zipfel, C. Negative control of BAK 1 by protein phosphatase 2A during plant innate immunity. *EMBO J.* **2014**, *33*, 2069–2079, doi:10.15252/embj.201488698.
26. Hacquard, S.; Spaepen, S.; Garrido-Oter, R.; Schulze-Lefert, P. Interplay Between Innate Immunity and the Plant Microbiota. *Annu. Rev. Phytopathol.* **2017**, *55*, 565–589, doi:10.1146/annurev-phyto-080516-035623.
27. Winter, D.; Vinegar, B.; Nahal, H.; Ammar, R.; Wilson, G.V.; Provart, N.J. An "Electronic Fluorescent Pictograph" Browser for Exploring and Analyzing Large-Scale Biological Data Sets. *PLoS ONE* **2007**, *2*, e718, doi:10.1371/journal.pone.0000718.
28. Durian, G.; Rahikainen, M.; Alegre, S.; Brosché, M.; Kangasjärvi, S. Protein Phosphatase 2A in the Regulatory Network Underlying Biotic Stress Resistance in Plants. *Front. Plant Sci.* **2016**, *7*, 812, doi:10.3389/fpls.2016.00812.
29. Kataya, A.R.A.; Heidari, B.; Lillo, C. Protein phosphatase 2A regulatory subunits affecting plant innate immunity, energy metabolism, and flowering time – joint functions among B'η subfamily members. *Plant Signal. Behav.* **2015**, *10*, e1026024, doi:10.1080/15592324.2015.1026024.
30. Spaepen, S.; Versées, W.; Gocke, D.; Pohl, M.; Steyaert, J.; Vanderleyden, J. Characterization of Phenylpyruvate Decarboxylase, Involved in Auxin Production of Azospirillum brasilense. *J. Bacteriol.* **2007**, *189*, 7626–7633, doi:10.1128/jb.00830-07.
31. Cartieaux, F.; David, P.; Sarrobert, C.; Thibaud, M.-C.; Achouak, W.; Robaglia, C.; Nussaume, L. Utilization of mutants to analyze the interaction between Arabidopsis thaliana and its naturally root-associated Pseudomonas. *Planta* **2001**, *212*, 190–198, doi:10.1007/s004250000384.
32. Stringlis, I.A.; Proietti, S.; Hickman, R.; Van Verk, M.C.; Zamioudis, C.; Pieterse, C.M.J. Root transcriptional dynamics induced by beneficial rhizobacteria and microbial immune elicitors reveal signatures of adaptation to mutualists. *Plant J.* **2017**, *93*, 166–180, doi:10.1111/tpj.13741.
33. Blilou, I.; Xu, J.; Wildwater, M.; Willemsen, V.; Paponov, I.; Friml, J.; Heidstra, R.; Aida, M.; Palme, K.; Scheres, B. The PIN auxin efflux facilitator network controls growth and patterning in Arabidopsis roots. *Nat. Cell Biol.* **2005**, *433*, 39–44, doi:10.1038/nature03184.
34. Cohen, A.C.; Bottini, R.; Piccoli, P.N. Azospirillum brasilense Sp 245 produces ABA in chemically-defined culture medium and increases ABA content in arabidopsis plants. *Plant Growth Regul.* **2008**, *54*, 97–103, doi:10.1007/s10725-007-9232-9.
35. Pieterse, C.M.J.; Leon-Reyes, A.; Van Der Ent, S.; Van Wees, S.C.M. Networking by small-molecule hormones in plant immunity. *Nat. Chem. Biol.* **2009**, *5*, 308–316, doi:10.1038/nchembio.164.
36. De Torres-Zabala, M.; Truman, W.; Bennett, M.H.; Lafforgue, G.; Mansfield, J.W.; Egea, P.R.; Bögre, L.; Grant, M.R. Pseudomonas syringae pv. tomato hijacks the Arabidopsis abscisic acid signalling pathway to cause disease. *EMBO J.* **2007**, *26*, 1434–1443, doi:10.1038/sj.emboj.7601575.
37. Alonso, J.M.; Stepanova, A.N.; Gadrinab, C.; Heller, C.; Jeske, A.; Koesema, E.; Meyers, C.C.; Parker, H.; Prednis, L.; Ansari, Y.; et al. Genome-Wide Insertional Mutagenesis of Arabidopsis thaliana. *Science* **2003**, *301*, 653–657, doi:10.1126/science.1086391.

38. Kleinboelting, N.; Huep, G.; Kloetgen, A.; Viehoever, P.; Weisshaar, B. GABI-Kat SimpleSearch: new features of the Arabidopsis thaliana T-DNA mutant database. *Nucleic Acids Res.* **2011**, *40*, D1211–D1215, doi:10.1093/nar/gkr1047.
39. Creighton, M.T.; Sanmartin, M.; Kataya, A.R.; Averkina, I.O.; Heidari, B.; Nemie-Feyissa, D.; Sánchez-Serrano, J.J.; Lillo, C. Light regulation of nitrate reductase by catalytic subunits of protein phosphatase 2A. *Planta* **2017**, *246*, 701–710, doi:10.1007/s00425-017-2726-4.
40. Costacurta, A.; Keijers, V.; Vanderleyden, J. Molecular-Cloning and Sequence-Analysis of an Azospirillum-Brasilense In-dole-3-Pyruvate Decarboxylase Gene. *Mol. Gen. Genet.* **1994**, *243*, 463–472.
41. Pieterse, C.M.J.; Van Wees, S.C.M.; Hoffland, E.; Van Pelt, J.A.; Van Loon, L.C. Systemic Resistance in Arabidopsis Induced by Biocontrol Bacteria Is Independent of Salicylic Acid Accumulation and Pathogenesis-Related Gene Expression. *Plant Cell* **1996**, *8*, 1225, doi:10.2307/3870297.
42. Murashige, T.; Skoog, F. A Revised Medium for Rapid Growth and Bio Assays with Tobacco Tissue Cultures. *Physiol. Plant.* **1962**, *15*, 473–497, doi:10.1111/j.1399-3054.1962.tb08052.x.
43. Verhagen, B.W.M.; Trotel-Aziz, P.; Couderchet, M.; Höfte, M.; Tarpin, M. Pseudomonas spp.-induced systemic resistance to Botrytis cinerea is associated with induction and priming of defence responses in grapevine. *J. Exp. Bot.* **2009**, *61*, 249–260, doi:10.1093/jxb/erp295.
44. Wintermans, J.; De Mots, A. Spectrophotometric characteristics of chlorophylls a and b and their phenophytins in ethanol. *Biochim. et Biophys. Acta (BBA) Biophys. Incl. Photosynth.* **2003**, *109*, 448–453, doi:10.1016/0926-6585(65)90170-6.
45. Cohen, P.; Alemany, S.; Hemmings, B.A.; Resink, T.J.; Strålfors, P.; Tung, H.Y. Protein phosphatase-1 and protein phosphatase-2A from rabbit skeletal muscle. *Methods Enzym.* 1988, *159*, 390–480, doi:10.1016/ 0076-6879(88)59039-0.

Supporting information

Figure S1. PP2A activity in Arabidopsis WT single (*c1, c2, c3, c4, c5*) and double (*c2c5, c4c5, c2c4*) mutants of PP2A catalytic subunits.

Figure S2. Scatter plot of changes in Arabidopsis fresh weight caused by *P. simiae* WCS417r and related to PP2A activity ascribed to the different Arabidopsis mutants.

Figure S3. Scatter plot of changes in Arabidopsis fresh weight caused by *A. brasilense* and related to PP2A activity ascribed to the different Arabidopsis mutants.

Figure S4. Visual phenotype of Arabidopsis WT, *c2* and various *b'*-mutants treated with *P. simiae* WCS417r.

Figure S5. Growth parameters of WT, *c2* and various *b'*-mutants treated with *P. simiae* WCS417r

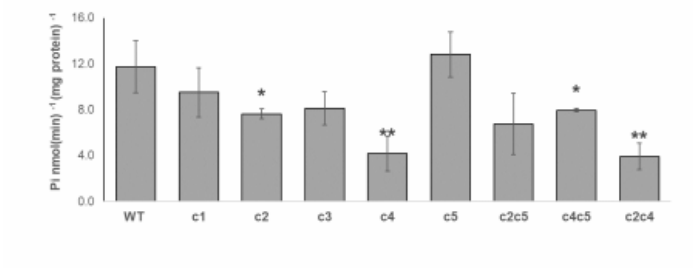

Figure S1. PP2A activity in Arabidopsis WT, single (*c1, c2, c3, c4, c5*) and double (*c2c5, c4c5, c2c4*) mutants of PP2A catalytic subunits.
Activity was assayed in the whole 10-d-old seedlings grown on ½ MS medium. SE is given (n=3, from three independent experiments), two asterisks indicate that values are significantly different from WT according to student's t-test at $p< 0.05$, and for one asterisk at $p< 0.1$.

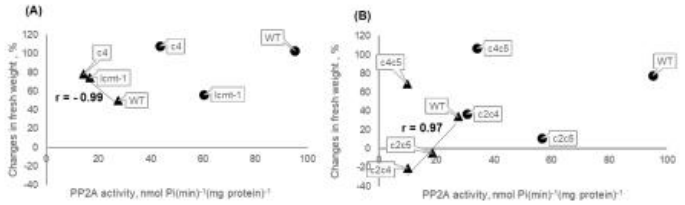

Figure S2. Scatter plot of changes in Arabidopsis fresh weight caused by *P. simiae* WCS417r and related to PP2A activity ascribed to the different Arabidopsis mutants.
Fresh weight changes in roots (circles) and shoots (triangles). Data are from Fig. 1, 4 and 6. (A) and (B) Only Pearson's correlation coefficient $|r| > 0.7$ was considered as strong, (B) *c4c5* was an outlier and not used in the calculation.

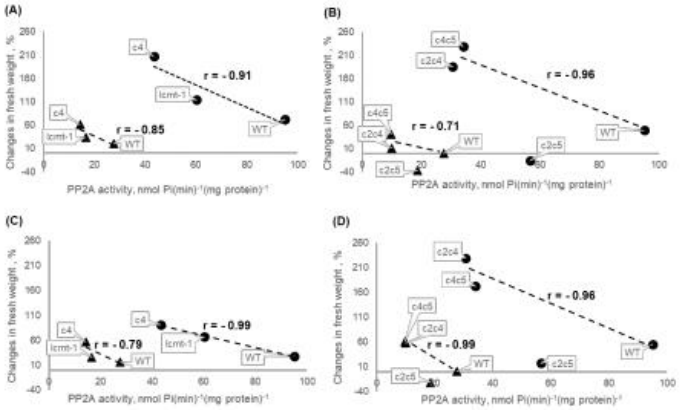

Figure S3. Scatter plot of changes in Arabidopsis fresh weight caused by *A. brasilense* and related to PP2A activity ascribed to the different Arabidopsis mutants.
Fresh weight changes in roots (circles) and shoots (triangles). Data are from Fig. 1, 9 and 11. (A) and (B) *A. brasilense* Sp245. (C) and (D) *A. brasilense* FAJ0009. Only Pearson's correlation coefficient $|r| > 0.7$ was considered as strong, (B) c2c5 and (D) *c2c5* were outliers and not used in the calculations.

Figure S4. Visual phenotype of Arabidopsis WT, *c2* and various *b'*-mutants treated with *P. simiae* WCS417r. Seedlings of Arabidopsis WT and mutants (*c2*, *b'* alpha, beta, gamma, zeta, theta) cultivated without (upper row) and with *P. simiae* WCS417r for two weeks.

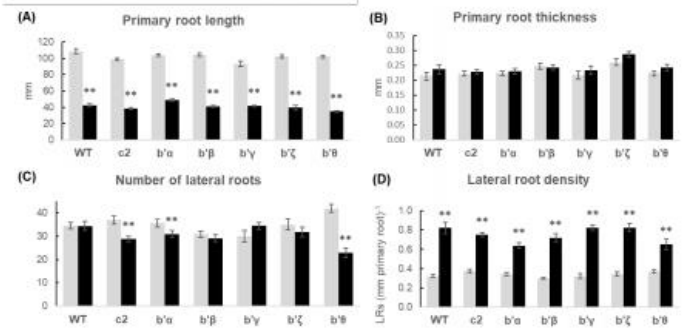

Figure S5. Growth parameters of WT, *c2* and various *b'*-mutants treated with *P. simiae* WCS417r. Seedlings of Arabidopsis WT and mutants (*c2*, *b'* alpha, beta, gamma, zeta, theta) were cultivated without (grey bars) and with (black bars) *P. simiae* WCS417r for two weeks. (A) primary root length; (B) primary root thickness; (C) number of lateral roots; and (D) lateral root density. Data are means ± SE of 15 plants (n=15). According to student's t-test and p-value < 0.05, columns marked with two asterisks are significantly different from the control without bacteria.

Paper II:

Pinpointing regulatory protein phosphatase 2A subunits involved in beneficial symbiosis between plants and microbes

Pinpointing regulatory protein phosphatase 2A subunits involved in beneficial symbiosis between plants and microbes

Irina O. Averkina[1], Muhammad Harris[1,2], Edward Ohene Asare[1], Berenice Hourdin[1], Ivan A. Paponov[3], Cathrine Lillo[1*]

1 IKBM, Department of Chemistry, Bioscience and Environmental Engineering
University of Stavanger, 4036 Stavanger, Norway
2 Faculty of Veterinary Medicine, Norwegian University of Life Sciences, 0454 Oslo, Norway
3 NIBIO, Norwegian Institute of Bioeconomy Research, Division of Food Production and Society, P.O. Box 115, NO-1431 Ås, Norway
Current address: Department of Food Science, 8200 Aarhus University, Aarhus, Denmark

Funding: The present study was supported by the Bionær program of the Research Council of Norway ('Biofresh' project no 255613/E50).

Abstract

PROTEIN PHOSPHATASE 2A (PP2A) expression is crucial for the symbiotic association between plants and various microbes, and knowledge on these symbiotic processes is important for sustainable agriculture. Treatment of tomato plants (*Solanum lycopersicum)* with the plant growth-promoting rhizobacteria (PGPR) *Azospirillum brasilense* and *Pseudomonas simiae* indicated a role for the PP2A B'θ subunit in responses to PGPR. Arbuscular mycorrhizal fungi also influenced *B'θ* transcript levels, but only in soil-grown plants with canonical arbuscular mycorrhizae, not in vermiculite-grown plants which had only vesicular mycorrhizae. Expression of the PP2A subunit *B'φ* in tomato roots was surprisingly low compared with its orthologue *B'1* in *Medicago truncatula,* which had previously been found to stimulate mycorrhization. Expression of *B'φ* was not influenced by mycorrhization. In transformed tomato plants with 10-fold enhanced *B'φ* expression, mycorrhization frequency was lowered in vermiculite-grown plants, and the high *B'φ* expression influenced the abscisic acid and gibberellic acid responses involved in plant growth and mycorrhization. Plants over-expressing *B'φ* showed less vigorous growth, and although fruits were normal size, the number of seeds was reduced by 60% compared to the original cultivar. Expression data and phenotype observations support a function of *B'φ* in growth and development in addition to a role in mycorrhization.

KEYWORDS

abscisic acid, *Azospirillum brasilense*, gibberellin, mycorrhiza, PP2A, PGPR, *Pseudomonas simiae,* tomato

1. INTRODUCTION

Plants are colonized by a wide range of microorganisms, beneficial as well as harmful (Hacquard, Spaepen, Garrido-Oter, & Schulze-Lefert, 2017; Lee et al., 2019; Müller, Vogel, Bai, & Vorholt, 2016). The beneficial microorganisms such as plant growth-promoting rhizobacteria (PGPR) and arbuscular mycorrhizal fungi (AMF) can improve nutrient acquisition and water uptake and protect the host against pathogens and abiotic stress. The effects of PGPR have been studied for many years and frequently used bacteria model species are *Azospirillum brasilense* and *Pseudomonas simiae* (Bulgarelli, Schlaeppi, Spaepen, Van Themaat, & Schulze-Lefert, 2013; Fibach-Paldi, Burdman, & Okon, 2012; Wintermans, Bakker, & Pieterse, 2016). *A. brasilense* already has practical applications in agriculture (Fibach-Paldi et al., 2012), and field studies have shown that certain pseudomonads strains and arbuscular mycorrhizal fungi can increase yield and quality of tomato plants grown under sub-optimal fertilization conditions (Bona et al., 2017). Mycorrhizae are a symbiosis between plants and fungi that evolved early, about 460 million years ago, and is likely to have been important for plants to colonize land. Mycorrhizae are important for uptake of nutrients, tolerance to drought, and may also be important for improving defence against pathogens. Arbuscular mycorrhizae (AM) are the most common type of mycorrhizae and more than 85% of land plant species can form arbuscular mycorrhizae. The mechanisms of signalling between plants and microbes, establishment and upholding of symbiosis are still far from understood.

Protein phosphatase 2A is a major protein phosphatase in plants and is involved in regulation of metabolism, development, stress responses and interactions with microbes (Durian, Rahikainen, Alegre, Brosché, & Kangasjärvi, 2016; Lillo et al., 2014; Uhrig, Labandera, & Moorhead, 2013). The PP2A complex is made up of three canonical subunits, a catalytic (C), a scaffolding (A) and a regulatory (B) subunit. In tomato there are at least five putative C, three A, and 15 B subunits (Booker & DeLong, 2017). The large number of B subunits is important for the various PP2A complexes to be specific for different substrates and cellular localizations (Farkas, Dombradi, Miskei, Szabados, & Koncz, 2007; Matre, Meyer, & Lillo, 2009). PP2A involvement in microbe and plant symbiosis is evident from work with the maize pathogenic bacterium *Pantoea stewartii* and the broad host (including tomato) pathogen *Phytophtora capsi* since both pathogens produce effectors that weaken the defence of plants by interacting with PP2A subunits (X.-R. Chen et al., 2019; Jin et al., 2016). In yeast-two-hybrid screening, the effector from *P. stewartii* interacted with a maize regulatory B' subunits, and the effector from *P. capsi* interacted with scaffolding A subunits from pepper, *Nicotiana* ssp. and Arabidopsis. The PP2A catalytic subunits divide into two clades in higher plants, and the two genes C1 and C2 form one clade in tomato (Subfamily I). The Subfamily 1 was previously found to be involved in responses to bacterial treatments in both tomato and potato plants. In tomato, *Pseudomonas syringae* enhanced expression of the catalytic subunit *C1*, and in *Nicotina benthamiana* silencing of the closely related catalytic

subunits of Subfamily I showed that they were involved in defence responses (He et al., 2004). In the present study, both Subfamily I genes of tomato were included in expression analysis.

When evaluating a range of plant species, the ability to make mycorrhizae was found to correlate with possession of a regulatory PP2A subunit called B'φ (Matthew A. Booker & Alison DeLong, 2017). The B'φ clade is evolutionary very old and has not expanded, indicating that it is involved in some basic function. The *B'φ* clade has not been much studied except for a couple of investigations using *Medicago sativa* and *M. truncatula* (Charpentier, Sun, Wen, Mysore, & Oldroyd, 2014; Tóth et al., 2000), and to our knowledge no studies have been performed with tomato on *B'φ.* Based on the work referred above, we selected the *B'φ* gene as a candidate for being involved in the formation of mycorrhizae in tomato, and included in the present study. Hormones, including abscisic acid (ABA) and gibberellins (GA), are important for development of AM in tomato roots (Herrera-Medina, Steinkellner, Vierheilig, Ocampo Bote, & Garcia Garrido, 2007). ABA also participates in the induction of AM associated with PP2A expression in *Medicago truncatula* (Charpentier et al., 2014). Since ABA is important in AM formation the tomato *Bβ (clade III)* gene was included as an ortholog of the ABA-induced gene subunit in *Medicago* ssp. (Tóth et al., 2000). Expression of reporter genes for ABA and GA responses were also assayed in the study. In Arabidopsis, *B'θ* had previously been detected to be involved in the response to microbial treatment (Kataya, Heidari, & Lillo, 2015), and its closest ortholog in tomato was therefore

included in all expression experiments here. To shed light on physiological function of PP2A in plant-microbe symbiosis, tomato plants were grown in vermiculite or soil and treated with PGPR or AMF (AM fungi). Transcripts of the selected PP2A subunits were tested in tomato (cv. Heinz) and also in the Heinz cultivar transformed, *b'φ*$_{ox}$, to study mycorrhizal colonization.

2. MATERIAL AND METHODS

2.1 Plant material

Plants of *Solanum lycopersicum* cv. Heinz were used, and transgenic plants over-expressing *B'φ* were generated from hypocotyls of the Heinz cultivar using *Agrobacterium*-mediated transformation.

2.2 Standard growing conditions for gene expression analysis in different plant organs

Tomato plants were grown in soil (75% potting soil and 25% vermiculite) in 0.5 L pots or in double autoclaved vermiculite in 0.4 L Magenta boxes (punctured at the bottom) at 22 °C in a 16 h light/8 h dark regimen. All plants were given Hoagland solution at sowing (Hoagland & Arnon, 1950). Light was provided by fluorescent lamps (Osram L58W/77). Plants were watered weekly with tap water and (only for vermiculite) monthly with Hoagland solution. Root tissue, young leaves and flower buds of 5-12 mm were snap-frozen in liquid nitrogen with subsequently stored at – 80 °C until used for gene expression analysis.

2.3 Plant growing conditions for PGPR experiment

Tomato plants were grown in 0.4 L Magenta boxes with (double) autoclaved vermiculite at 22 °C under artificial light in the 16 h light/8 h dark regimen and watered weekly with Hoagland solution. On day 41 after sowing the plants were inoculated with 50 mL of bacteria suspended in 10 mM $MgSO_4$, $5x10^7$ cells/mL for *Azospirillum* strains

and 2.5 x10^5 cells/mL for *P. simiae* WCS417r. Control plants were given 10 mM $MgSO_4$ only. Root tissue was harvested 2 h, 24 h, 1 week and 3 weeks after inoculation.

2.4 Plant growth-promoting bacterial strains (PGPR), growth and inoculation

Three bacterial strains were used: *Azospirillum brasilense* Sp245 wild-type strain (Spaepen, Bossuyt, Engelen, Marchal, & Vanderleyden, 2014), its ipdC-knockout mutant FAJ0009 (Sp245 *ipdC*::Tn5) impaired in auxin biosynthesis (Costacurta, Keijers, & Vanderleyden, 1994; Spaepen et al., 2007), and *Pseudomonas simiae* (formerly *Pseudomonas fluorescens*) WCS417r, a rifampicin-resistant strain derived from *Pseudomonas simiae* WCS417 originally isolated from the rhizosphere of wheat grown in Brasil (Pieterse, vanWees, Hoffland, vanPelt, & vanLoon, 1996). For tomato inoculation, *P. simiae* WCS417r was cultured on King B medium (King, Ward, & Raney, 1954) with 50 μg/mL rifampicin at 28°C overnight. Colonies were loosened in 10 mL of 10 mM $MgSO_4$ (Pieterse et al., 1996; Van Wees, Van Pelt, Bakker, & Pieterse, 2013), collected into a 15 mL Falcon tube and centrifuged at 4000 g for 5 min followed by 2 subsequent washes, the pellet was resuspended in fresh 10 mM $MgSO_4$ to the appropriate concentration (Verhagen, Trotel-Aziz, Couderchet, Hofte, & Aziz, 2010). *Azospirillum* strains were cultured at 37°C for 48 h on LB agar supplemented with 2.5 mM $CaCl_2$ and 2.5 mM $MgSO_4$. For FAJ0009, 50 μg/mL kanamycin was added. Colonies were used to produce an overnight culture in 5 mL of

LB broth supplemented with 2.5 mM $CaCl_2$, 2.5 mM $MgSO_4$ at 37°C shaking at 180 rpm overnight. The overnight culture (0.1 mL) was subcultured in 50 mL of appropriately supplemented LB broth and incubated under the same conditions. On the following day, the bacteria were pelleted and re-suspended in 10 mM $MgSO_4$ to the appropriate concentration and used for inoculation.

2.5 Plant growing conditions for AMF experiments

The inoculum of AMF was obtained from the granular formulation under the commercial name "Rootgrow" (PlantWorks Ltd, Sittingbourne, UK) containing propagules of spores, hypha and root fragments colonized by *Funneliformis mossaeae, F. geosporus, Claroideoglomus claroideum, Glomus microagregatum, Phizophagus irregularis* (Bona et al., 2017). Rootgrow, 1.5 mL granules, were added to the planting hole in each pot/Magenta box and covered with a small amount of soil or vermiculite before sowing tomato seeds or planting seedlings. No granules (soil) or triple autoclaved granules (vermiculite) were added to the growing medium for control plants. The plants were grown at 22 °C in a 16 h light/8 h dark (soil) or 12h light/12 dark (vermiculite) regimen and watered weekly with tap water (soil) or Hoagland solution (vermiculite) with ten times reduced phosphate concentration (0.1 mM PO_4^{3-}) for at least seven weeks or until plants showed profound signs of phosphate deficiency. Thereafter, the plants were watered with regular Hoagland weekly (soil and vermiculite). Two weeks prior to harvesting, the plants were watered only with tap water.

2.6 Sample preparation for bright-field microscopy

The harvested roots were washed with tap water, boiled in 10% KOH for 1 min and left in this solution overnight at room temperature. Roots were then rinsed with tap water and dipped in 3.7% solution of hydrochloric acid for 2-3 minutes. After removing the acid solution, staining solution was added. Staining solution was made from one volume of: 25% phenol, 25% lactic acid, 25% glycerol, 25 % of 4 mg/mL trypan blue stock solution, plus two volumes of 95% ethanol (Weigel & Glazebrook, 2002). Root tissue was placed in Eppendorf tubes, covered with the staining solution, and heated in a boiling water bath for 1 min with subsequent incubation on a shaker at room temperature for 4-16 h. After removing the staining solution, the roots were covered with a destaining solution (2.5 g/mL chloral hydrate) (Vierheilig, Schweiger, & Brundtrett, 2005) and incubated for 6 h at room temperature before the solution was replaced with a fresh one and incubated overnight. The destaining solution was removed prior to covering the roots with 70 % glycerol. Three slides with 20 stained root fragments, 5-8 mm, from each plant were examined under a light microscope with 10x and 100x magnification for AM structures such as spores, vesicles and arbuscules. The frequency of AMF colonization (F%) was calculated as a percentage of the root fragments with AM structures.

2.7 Plasmid construct and agrobacterium preparation

To generate transgenic plants over-expressing *B'φ*, the full-length DNA sequence (1494 bp) of the *B'φ* gene (NCBI Reference Sequence: LOC101256045) was cloned into the pBA002 binary vector at the Xhol/SpeI sites (Kost, Spielhofer, & Chua, 1998) using flanking primers *B'φ*: forward primer (5'-TAGCACTCGAGATGACAAATTTTCTTG ATTCTGAGACAG-3') and B'φ: reverse primer (5'-CCACTAGT TCACATTGCTGCATTTTCAATTTTTTCCC-3'). The pBA002 plasmid contains the cauliflower mosaic virus 35S promotor, which constitutively drives the expression of the transgene in all plant tissues at a high level (Slater, Scott, & Fowler, 2008).

The pBA002 plasmid also harbours spectinomycin resistance for selection in bacteria and the herbicide phosphinothricin (BASTA) resistance for selection in plants. To generate transgenic $b'\varphi_{ox}$ plants, the pBA002-B'φ plasmid was transferred into the ABI-1 strain of *Agrobacterium tumefaciens* by the freeze-thaw procedure (Holsters et al., 1978). *Agrobacterium tumefaciens* ABI-1 strain, a derivative of the well-known GV3101 strain (pMP90RK) (Ruan et al., 2018), was kindly provided by Dr. Amr Ramzy Abass Kataya, UiS, Norway. Prior to the tomato transformation, 5 mL of LB broth with 50 μg/mL kanamycin and 50 μg/mL spectinomycin was inoculated with *A. tumefaciens* and incubated at 28 °C on a shaker at 200 rpm for two days, then1 mL of the culture was subcultured in 100 mL of LB broth containing the same antibiotics and incubated for about 24 h under the same conditions until OD_{600} reached 1. The bacteria were pelleted and resuspended in liquid

MS medium (Sun et al., 2015) to OD_{600} = 0.2 (Pawar, Bhausaheb & S. jadhav, A & Chimote, Vivek & Kale, & Aa & Pawar, 2013) and used for the tomato transformation.

2.8 Plant tissue and transformation by *Agrobacterium*

Tomato seeds were surface sterilized with 75% ethanol for 1 min and 15% hydrogen peroxide for 15 min, rinsed with water, germinated on MS medium (4.3 g/L MS salts (Sigma-Aldrich, USA), 3% sucrose, 0.8 % agar, pH 5.8) and cultivated at 22 °C in a 16 h light/8 h dark regimen for 20 days or until the cotyledons had opened completely. Three days before transformation the hypocotyls were cut into 7-10 mm fragments (explants) and placed on pre-culture medium (MS salts, 3 % sucrose, vitamins, 0.5mg/L indole-3-acetic acid (IAA), 1 mg/L benzylaminopurine (BAP), 0.7% agar, pH 5.8) (Chetty et al., 2013) and incubated for 72 h in the dark at 27 °C (Pawar et al., 2013; Sun et al., 2015). For transformation, all the explants were immersed in the *Agrobacterium* suspension and shaken for 20 min at room temperature, blotted dry and transferred to the co-cultivation medium (MS salts, vitamins, 3% sucrose, 0.7 % agar, 0.5 mg/L IAA and 1 mg/L BAP) and incubated for two days in the dark at room temperature (Chetty et al., 2013; Sun et al., 2015). Explants were then placed on shoot induction medium (MS salts, vitamins, 3% sucrose, 0.7 % agar, 250 mg/L cefotaxime, 250 mg/L carbenicillin, 10 mg/L BASTA, 0.5 mg/L IAA and BAP 2 mg/L) for further cultivation at 22 °C with 16 h photoperiod for 90 days, subcultured to fresh medium every 30 days. Explants

developing Basta-resistant calli produced shoots. The shoots were excised from the calli and transferred to root induction medium (MS salts, vitamins, 3% sucrose, 0.7 % agar, 250 mg/L cefotaxime, 250 mg/L carbenicillin, 0.5 mg/L IAA, 10 mg/L BASTA) and cultivated for 30 days. Plants developed from the tomato explants were genotyped using Phire® Plant Direct PCR Kit (Thermo Fisher Scientific, Waltham, USA) and transferred either to vermiculite or soil for further growth. The transformed plants obtained from the explants were considered as F_0 progeny of *b'φ*$_{ox}$. Transgenic lines from F_0 and F_1 progenies were used for further analyses.

2.9 Semi-quantitative RT-PCR analysis

Total RNA was isolated from roots, leaves or flower buds using RNeasy® Plant Mini Kit (Qiagen, Hilden, Germany), and cDNA was synthesized using SuperScript™ VILO™ cDNA Synthesis Kit (Invitrogen by Thermo Fisher Scientific, USA). Polymerase chain reaction (PCR) was performed in 10 µL reactions using DreamTaq DNA Polymerase kit (Thermo Fisher Scientific, Vilnius, Lithuania). The PCR products were separated on agarose gel and quantified using Bio-Rad Image-Lab 6.0 Software. The averaged value of the band intensities from three plants was used to calculate a transcript level. Relative quantification of the transcript levels was based on normalization of the target gene band densities with respect to *ACTIN41*. The primer sequences for semi-quantitative RT-PCR are listed in Supplementary table 1.

2.10 Statistical analysis

Data were analysed by student's t-test using the Excel statistical package (version Microsoft 385) or one-way ANOVA with Turky's multiple range test using the IBM SPSS Statistics 26.

3. RESULTS

3.1 Expression of *PP2A* subunit genes in different tissues

Expression levels of selected *PP2A* subunit genes and *TAS14* as an ABA responsive gene (Godoy, Pardo, & Pintor-Toro, 1990) are presented in Figure 1. Strikingly, *B'φ* was expressed at very low levels in all tissues tested, in some tissues barely detectable. Expression of *B'θ* was not much influenced by type of tissue but was always lower in vermiculite-grown plants compared with soil-grown plants, the lowest value was in roots of vermiculite-grown plants. The *Bβ (clade III)* gene showed its lowest expression in roots, highest in leaves and medium values in flower buds, but showed no correlation with the *TAS14* reporter gene. The *C1* gene was highly expressed in roots in both soil and vermiculite, but more moderately in leaves and buds of soil-grown compared with vermiculite-grown plants. *TAS14* was always more highly expressed in vermiculite compared with soil, indicating more ABA or higher ABA sensitivity in vermiculite-grown plants. Publicly available expression analysis from the Sol genetics database (Fernandez-Pozo et al., 2015) revealed similar expression patterns for these genes in roots and leaves in *S. lycopersicum* seedlings confirming very low levels of *B'φ* in all tissues (Supplemental S1Figure a, b).

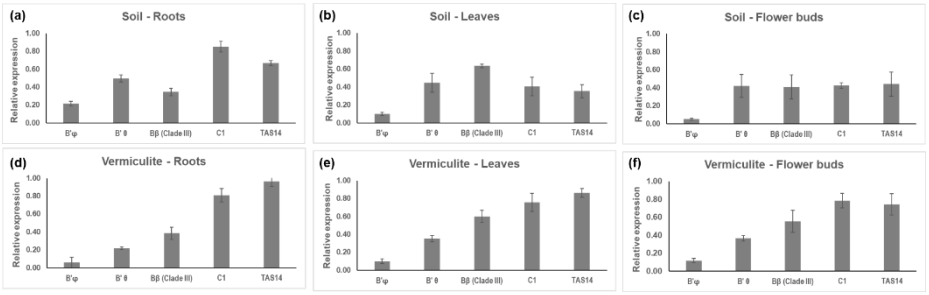

FIGURE 1. Gene expression of selected PP2A subunits in different plant tissue from 3.5-month-old-tomato plants determined by sqRT-PCR. (a-c) Plants grown in soil and (d-e) Plants in vermiculite. Transcript levels of *B'φ, B'θ, Bβ (clade III), C1* and *TAS14* were measured in (a, d) Roots; (b, e) Leaves; and (c, f) Flower buds. Values denote the average level of expression from three biological replicates normalized by the reference gene *ACTIN41*. Mean values ±SE are shown.

3.2 Effects of PGPR treatment

Gene expression was studied in roots from plants grown in vermiculite and treated with three strains of PGPR, *A. brasilense* Sp245, *A. brasilense* FAJ0009 (auxin producing deficient mutant) and *P. simiae* WCS417r. Samples were harvested from 2 h to 3 weeks after inoculation (Figure 2). *B'φ* expression was slightly increased one week after treatment with *P. simiae* WCS417r but was still the gene expressed at the lowest level compared with all other genes tested (Figure 2a-g). The similar effects of *A. brasilense* and its auxin-deficient FAJ0009 strain on *B'φ* expression indicate that the expression of this gene is independent of auxin. A most striking result was the transiently decreased expression

of *B'θ* after 2 h and 24 h in bacteria-treated roots, especially in response to *P. simiae* WCS417r (Figure 2b). This response was also auxin independent because *A. brasilense* FAJ0009 strain induced a similar or stronger effect than wild type *A. brasilense*. *B'θ* expression then regained control levels after 1 and 3 weeks. For the *Bβ (Clade I)* gene, expression was decreased in the control after 24 h, but this decrease was largely prevented by bacterial treatments. The control then regained activity, and after 3 weeks there was no difference between control and inoculated plants (Figure 2c). For *Bβ (Clade III)* there was also a tendency that bacterial treated plants showed higher activity than the control (Figure 2d). Expression of *C1* decreased after 3 weeks in control plants, but this was prevented in the bacterial treated plants (Figure 2e). Expression of the *C2* gene and the TAS reporter gene were not much influenced by any of the bacterial strains (Figures 2f, g).

Fresh weight of roots and shoots was measured three weeks after inoculation and showed that roots of PGPR-treated plants had higher fresh weight than control plants, but this was significant only for WCS417r (Figure 3). This effect was independent of auxin, as inoculation with the auxin-deficient FAJ0009 strain showed rather stronger but not significant increase in root growth compared with the Sp245 strain.

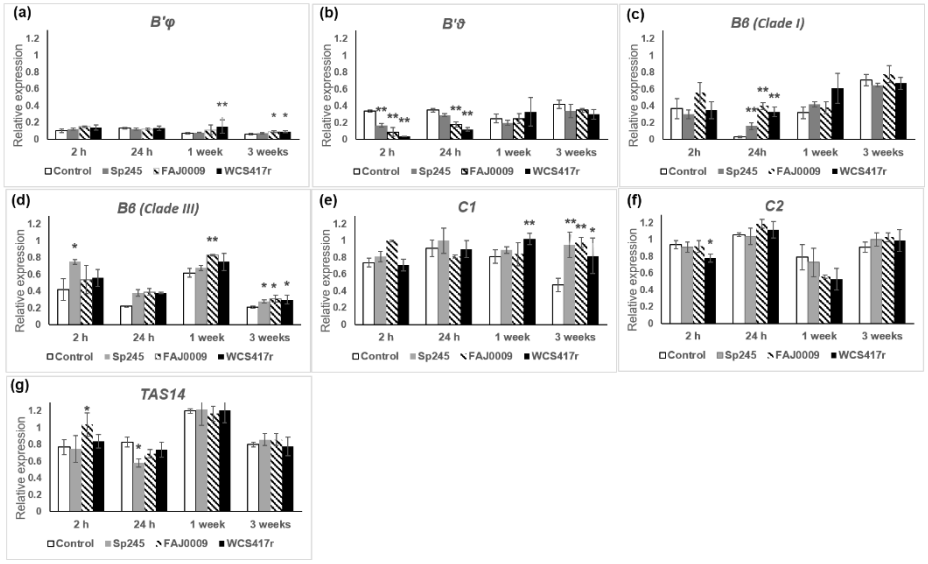

FIGURE 2. Time course for expression of selected *PP2A* subunits and *TAS14* in tomato roots inoculated with PGPR. Tomato plants were grown in vermiculite for 40 days. Thereafter, treated with 10 mM $MgSO_4$ (control) (white bars), Sp245 (grey bars), FAJ0009 (hatched bars) and WCS417r (black bars) and harvested after 2h, 24 h, 1 week and 3 weeks. Genes analysed were (a) *B'φ*; (b) *B'θ*; (c) *Bβ (clade I)*; (d) *Bβ (clade III)*; (e) *C1*; (f) *C2;* (g) *TAS14*. Columns marked with one or two asterisks are significantly different from the corresponding control according to student's t-test at p-value < 0.1 or 0.05 respectively.

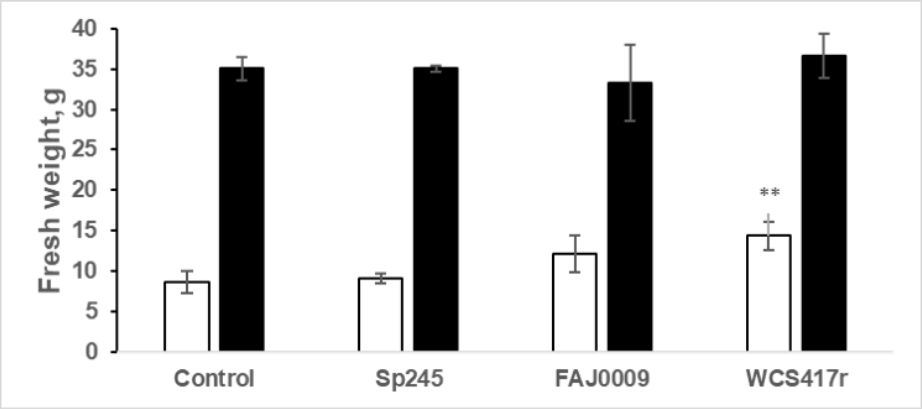

FIGURE 3. Fresh weight of plants after inoculation with PGPR and grown in vermiculite for three weeks. Tomato roots are represented by white bars and shoots by black bars. Data are means ± SE of 4 plants (n = 4). The bar marked with two asterisks is significantly different from the control plants according to student's t-test at p-value < 0.05. Pictures of plants are in Figure S2.

3.3 Effects of colonization by AMF

Tomato plants were inoculated with AMF in both soil and vermiculite. Since establishment of mycorrhizae is a time-requiring process, samples for gene expression were harvested 3.5 months after planting and inoculation with AMF. Microscopy analysis showed that the type of growing medium strongly influenced AM morphology. Roots grown in soil formed canonical AM usually observed when roots are colonized by more than one AMF species (S. E. Smith & D. Read, 2008). Roots in vermiculite formed vesicular mycorrhizae (VM). No AM was observed in the control plants (Figure 4).

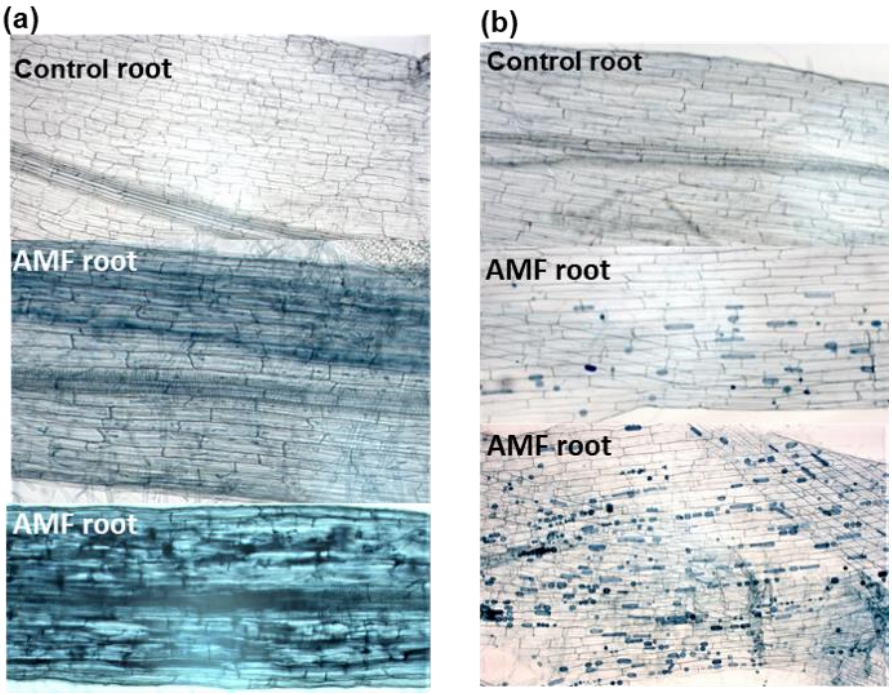

FIGURE 4. Morphology of AM colonization in tomato roots stained with trypan blue 3.5 months after inoculation with AMF. Bright-field images of roots grown in (a) soil and in (b) double autoclaved vermiculite

The selected PP2A subunit genes were tested in plants grown in soil and vermiculite after treatment with AMF. A reporter gene for GA levels, *GAST1* (*GA-STIMULATED TRANSCRIPT 1*) was included in the analysis (Herrera-Medina et al., 2007; Martín-Rodríguez et al., 2016). *PT4* (*PHOSPHATE TRANSPORTER 4*) was included as a reporter gene for mycorrhizae-inducible inorganic phosphate transporter and is a marker for AM symbiosis (Javot, Penmetsa, Terzaghi, Cook, & Harrison, 2007). The *PT4* reporter gene was up-regulated after addition

of AMF by 116 % for soil-grown plants, in agreement with AM formation (Figure 5a). The up-regulation in vermiculite-grown plants was only 30% and this may be explained by the formation of VM instead of AM. *TAS14* expression was higher in plants grown in vermiculite than in soil, as previously observed (Figures 1, 5). After AMF inoculation, *TAS14* remained constant, while the data indicated that *GAST1* was down-regulated, suggesting that the ABA to GA ratio was changed in favour of mycorrhizae formation (Martín-Rodríguez et al., 2016). These experiments confirmed that *B'φ* was the *PP2A* gene expressed at the lowest level with especially low values in vermiculite-grown plants (Figures 1, 5). The expression of *B'φ* was not influenced by AMF. The expression of *B'θ* in roots was significantly lower in control plants grown in vermiculite compared with soil (Figure 5), in agreement with previous experiments (Figure 1a, d). Strikingly, as for PGPR treatment, *B'θ* was down-regulated by AMF treatment, though only in soil-grown plants (Figure 5a). The *Bβ (CladeIII)* was up-regulated in soil, whereas *Bα (Clade I)* was up-regulated in vermiculite in AMF treated plants. *C1* also showed different effects of AMF in soil and vermiculite. *C2* was not influenced by AMF treatment.

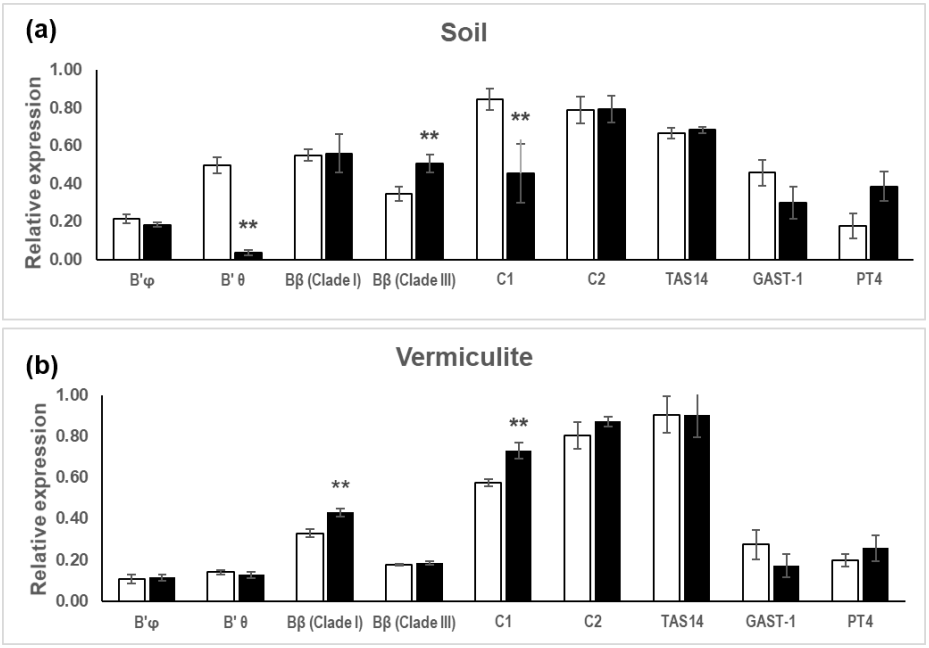

FIGURE 5. Expression of *PP2A* subunit genes and AM-associated genes in roots not treated or treated with AMF. Tomato plants had been grown for 3.5 months after the mock treatment (white bars) and AMF treatment (black bars) and were grown in (a) soil or (b) vermiculite. The values are averages from three biological replicates normalized by the reference gene *ACTIN41*. Values marked with two asterisks are significantly different from the corresponding control according to student's t-test at p-value < 0.05, n=3.

3.4 *B'φ* over-expressor plants

Transformed plants over-expressing *B'φ*, *b'φ*$_{ox}$, showed no difference from original genotype (WT) regarding growth during the first weeks (Figure 6a). Thereafter, differences became visible (Figure 6b, c). The *b'φ*$_{ox}$ plants showed less vigorous growth compared with non-

transformed plants. In 8-week-old *b'φ*$_{ox}$ fresh weight of shoots and roots was reduced by 66 and 70 %, respectively (Figure 6d). Root length was similar in original genotype and *b'φ*$_{ox}$, but number of leaves, stem height and stem thickness were reduced in *b'φ*$_{ox}$. Although fruits had similar weight, the number of seeds was reduced by 60% per fruit (Figure 6e).

To study mycorrhizal colonization, WT and *b'φ*$_{ox}$ (F0, F1) were inoculated with AMF in soil and vermiculite. The frequency of AM in roots was assessed 3.5 months after adding AMF, and due to the low colonization, the assessment was repeated after 8.5 months for soil-grown plants (Figure 7a). No significant differences in colonization frequency were found between WT and *b'φ*$_{ox}$ in soil (Figure 7a). The colonization frequency was higher in plants grown in vermiculite compared with those grown in soil, and a clear difference was seen between WT and *b'φ*$_{ox}$ in three different experiments involving both *b'φ*$_{ox}$ progenies F0 and F1. On average the colonization frequency was lowered by approximately 50% in *b'φ*$_{ox}$.

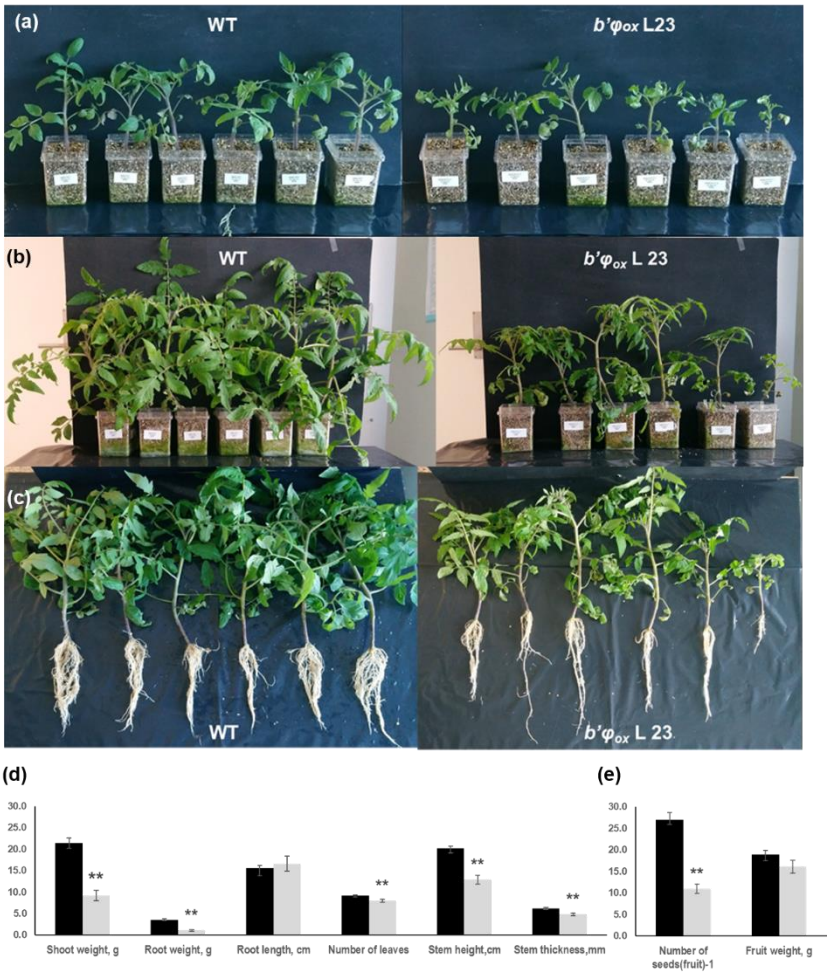

FIGURE 6. Phenotypic characterization of *b'φox* **(**over-expressor). Original genotype **(**WT) and *b'φox* plants (a) 25 days old; (b, c) 8 weeks old; (d) Mean values of shoot weight, root weight, root length, number of leaves and stem height for 12 WT plants (black columns) and 18 *b'φox* plants (grey columns) (F_1 of three mutant lines); (e) Fruit fresh weight and seed number are from tomato fruits collected after ripening. Data are means of 35 fruits, n=35. SE is given. Columns marked with one or two asterisks are significantly different from WT according to student's t-test at p-value <0.1 or 0.05, respectively.

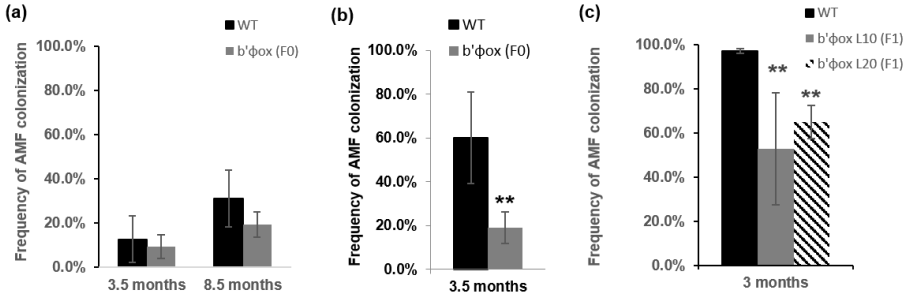

FIGURE 7. Frequency of root colonization in original genotype (WT) and *b'φ*$_{ox}$ after inoculation with AMF. Colonization frequency for WT (black bars) and *b'φ*$_{ox}$ (grey bars and hatched bar) (a) in soil 3.5 and 8.5 months after inoculation; (b) in vermiculite after 3.5 months; (c) in vermiculite after 3 months with another batch of *b'φ*$_{ox}$ (F1 plants). Values are means ±SE from three plants. According to student's t-test at p-value < 0.05, columns marked with two asterisks are significantly different from WT.

3.5 Gene expression in WT and *b'φ*$_{ox}$

Expression levels of *B'φ* were, as expected, much higher in *b'φ*$_{ox}$ than in WT, about 10-fold higher (Figure 8). Over-expression of *B'φ* stimulated expression of the *Bβ* (clade I) gene in roots both treated (expression level up by 40%) and not treated with AMF (expression level up by 55%) (Figure 8). For other PP2A subunit genes there were only small differences between WT and *b'φ*$_{ox}$. Over-expression of *B'φ* led to decreased expression of both ABA reporter genes *TAS14* and *NCED-1*,

and the GA reporter gene *GAST1*. This strongly indicates that *B'φ* is important for regulation of the ABA/GA hormone balance in tomato roots. A lower ABA response in these plants is in agreement with less colonization by AMF.

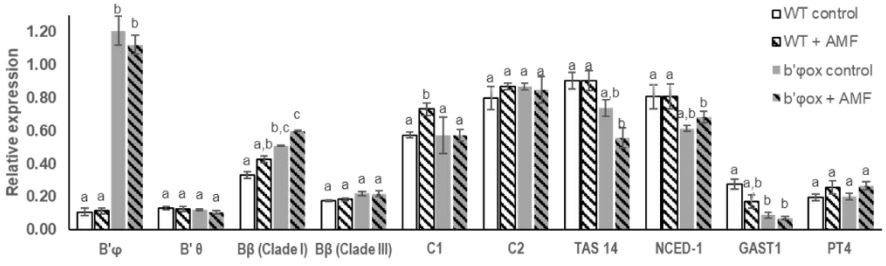

FIGURE 8. Expression analysis of PP2A subunits, hormone and AM-associated genes in roots of original genotype (WT) and *b'φ*$_{ox}$ of non-treated and AMF-treated plants. WT (white, white-hatched columns) and *b'φ*$_{ox}$ plants (grey, grey-hatched columns) had been grown for 3.5 months in vermiculite without (white or grey columns) or with AMF (hatched columns). The values are averages from three biological replicates normalized by the reference gene *ACTIN41*. For each gene, different letters represent significant different values according to one-way ANOVA and Tukey's multiple range test, n= 3, ($p < 0.05$).

4. DISCUSSION

When tomato plants were treated with PGPR, the most striking effect was the transient down-regulation of *B'θ* expression observed after 2 h and 24 h (Figure 2). All three bacteria types, *A. brasilense* Sp245, *A.*

brasilense FAJ0009 and *P. simiae* (WCS417r) caused such a transient decrease in *B'θ* expression. The strongest effect was induced by *P. simiae*. Interestingly, plants that had been grown in soil with AMF also showed low expression level of *B'θ* (Figure 5a), and only small changes in expression of other PP2A genes, indicating that down-regulation of *B'θ* is involved in plant-AMF interactions. However, it cannot be excluded that adding AMF may also have stimulated growth of PGPR in the soil, and in the next round, this would influence *B'θ* expression. The work indicated that *B'θ* was involved in the changes in morphology and in the frequency of root colonization associated with a complex crosstalk occurring between plants, AMF, and native soil bacteria. AMF inoculation inhibited *B'θ* expression only in the soil (where native bacteria were present), and only soil-grown roots showed the canonical arbuscular form usually observed when roots are colonized by more than one AMF species (S. Smith & D. Read, 2008). The important role of *B'θ* downregulation is also supported by the observation that this downregulation was related to the upregulation of the widely used AM colonization marker *PT4* (Figure 6). However, the lower basal expression level of *B'θ* in vermiculite than in soil may have contributed to the higher frequency of colonization (vesicular mycorrhizae) observed in vermiculite-grown compared with soil-grown roots. Previous work had pointed to the Arabidopsis *B'θ* and its two most closely related genes as being involved in biotic responses (Durian et al., 2016; Kataya et al., 2015). The current results confirm that *B'θ* plays an important role in plant-microbe interactions, and here specifically point to an effect

from plant growth-promoting microbes. In Arabidopsis plants with knocked out *B'θ*, proliferation of the pathogenic *Pseudomonas syringae* after infiltration was decreased relative to WT plants (Kataya et al., 2015). A defence reaction against proliferation of pathogens by lowering expression of *B'θ* could possibly be a helpful rection induced by symbiosis with PGPR and AMF. Such a putative positive effect of PGPR and AMF against pathogens would be interesting to test in tomato.

The most striking results from expression analysis of the PP2A subunit *B'φ* gene in the original tomato genotype, was the very low level in all tissues under all growth conditions investigated (Figures 1, 2, 5, 8). Initially we attempted to make knock-out tomato plants using artificial microRNA for targeting *B'φ* mRNA to achieve gene silencing. However, in contrast to what had been found for the orthologue in *Medicago spp.* (Charpentier et al., 2014; Tóth et al., 2000), the *B'φ* mRNA was already at a very low level in tomato. Therefore, selecting knock-out/down plants seemed unreasonable and technically difficult to verify further. We decided to make transformed plants over-expressing the *B'φ* gene to obtain further information concerning functions of this gene. The over-expressor plants had a characteristic phenotype with smaller leaves, reduced stem thickness, reduced root and shoot fresh weight, and poor seed set per fruit (Figure 6). Such changes are likely reflecting altered hormone levels, and both the ABA reporter gene *TAS14* and the GA reporter gene *GAST1* were down-regulated in *B'φ* over-expressor plants (Figure 8). The observed phenotype could, at least partly, be explained by a low GA level (S. Chen et al., 2016; Koornneef, Bosma, Hanhart,

Van der Veen, & Zeevaart, 1990). Formation of mycorrhizae had previously been linked to enhanced ABA levels (Charpentier 2014). Over-expression of *B'φ* appeared to inhibit AM formation (Figure 7) at least for vermiculite-grown plants, and this could be caused by a lowered ABA responsiveness in roots and disturbance of the hormone balance as indicated by the *TAS14* reporter gene (Figure 8). The results obtained in the present work strengthen the suggestion that *B'φ* has a role in regulation of AM formation. However, other functions of *B'φ* is likely to still be discovered and may not be related to formation of AM. The Sol database (Fernandez-Pozo et al., 2015) confirmed the very low expression levels for *B'φ in S. lycopersicum*. Roots from 3-week-old plants had non-detectable or very low expression levels for *B'φ*, about 500-fold lower than *C1* expression levels (Figure S1a). In the Sol database, low levels of *B'φ* transcripts are also reported for *S. pimpinellifolium.* The interesting exceptions were tissues dissected with laser capture microdissection of ovary and fruit tissues combined with high-throughput RNA sequencing during early fruit development (0-4 days post anthesis) (Pattison et al., 2015) In ovules (day 0), *B'φ* expression was one third of *C1* and higher than for other B subunits (*B'θ, B'κ, B'α, Bβ* -clade I) (Figure S1c). This suggests that *B'φ* may have a function in the early fruit development, and hence also formation of seeds. Considering that *B'φ* has a function in early fruit development, the very high levels of ectopically expressed *B'φ* in the transformed plants (Figure 8), may distort seed formation (Figure 6). Taken together, the phenotype observations, our expression data and publicly available

expression data support a function of *B'φ* in seed formation in addition to a role in mycorrhizae formation.

Acknowledgements

Funding: The present study was supported by the Bionær program of the Research Council of Norway ('Biofresh' project no 255613/E50).

Author contribution

I.O.A., I.A.P. and C.L. and conceived and designed the experiments.
I.O.A., M.H., E.O.A., B. H. performed the experiments
I.O.A. and C.L. drafted the manuscript.
I.O.A., I.A.P. and C.L. edited the manuscript

ORCID Cathrine Lillo orcid.org/0000-0002-8470-8983
ORCID Ivan Paponov orcid.org/0000-0002-2138-0722
ORCID Irina Averkina orcid.org/0000-0003-1002-6215

Supporting information

S1 Table. List of primers
S1 Figure. Expression of PP2A subunit genes in *S. lycopersicum* roots and leaves, and *S. pimpinellifolium* ovules and leaves.
S2 Figure. Visual phenotype of tomato plants three weeks after treatment with PGPR.

References

Bona, E., Cantamessa, S., Massa, N., Manassero, P., Marsano, F., Copetta, A., . . . Berta, G. (2017). Arbuscular mycorrhizal fungi and plant growth-promoting pseudomonads improve yield, quality and nutritional value of tomato: a field study. *Mycorrhiza, 27*(1), 1-11. doi:10.1007/s00572-016-0727-y

Booker, M. A., & DeLong, A. (2017). Atypical protein phosphatase 2A gene families do not expand via Paleopolyploidization. *Plant physiology, 173*(2), 1283-1300.

Bulgarelli, D., Schlaeppi, K., Spaepen, S., Van Themaat, E. V. L., & Schulze-Lefert, P. (2013). Structure and functions of the bacterial microbiota of plants. *Annual review of plant biology, 64*, 807-838.

Charpentier, M., Sun, J., Wen, J., Mysore, K. S., & Oldroyd, G. E. D. (2014). Abscisic acid promotion of arbuscular mycorrhizal colonization requires a component of the PROTEIN PHOSPHATASE 2A complex. *Plant physiology, 166*(4), 2077-2090.

Chen, S., Wang, X., Zhang, L., Lin, S., Liu, D., Wang, Q., . . . Wu, H. (2016). Identification and characterization of tomato gibberellin 2-oxidases (GA2oxs) and effects of fruit-specific SlGA2ox1 overexpression on fruit and seed growth and development. *Horticulture research, 3*(1), 1-9.

Chen, X.-R., Zhang, Y., Li, H.-Y., Zhang, Z.-H., Sheng, G.-L., Li, Y.-P., . . . Kuan, T. (2019). The RXLR effector PcAvh1 is required for full virulence of Phytophthora capsici. *Molecular Plant-Microbe Interactions, 32*(8), 986-1000.

Chetty, V. J., Ceballos, N., Garcia, D., Narvaez-Vasquez, J., Lopez, W., & Orozco-Cardenas, M. L. (2013). Evaluation of four Agrobacterium tumefaciens strains for the genetic transformation of tomato (Solanum lycopersicum L.) cultivar Micro-Tom. *Plant Cell Rep, 32*(2), 239-247. doi:10.1007/s00299-012-1358-1

Costacurta, A., Keijers, V., & Vanderleyden, J. (1994). Molecular-Cloning and Sequence-Analysis of an Azospirillum-Brasilense Indole-3-Pyruvate Decarboxylase Gene. *Molecular & General Genetics, 243*(4), 463-472. Retrieved from <Go to ISI>://WOS:A1994NP13800013

Durian, G., Rahikainen, M., Alegre, S., Brosché, M., & Kangasjärvi, S. (2016). Protein phosphatase 2A in the regulatory network underlying biotic stress resistance in plants. *Frontiers in plant science, 7*, 812.

Farkas, I., Dombradi, V., Miskei, M., Szabados, L., & Koncz, C. (2007). Arabidopsis PPP family of serine/threonine phosphatases. *Trends in plant science, 12*(4), 169-176.

Fernandez-Pozo, N., Menda, N., Edwards, J. D., Saha, S., Tecle, I. Y., Strickler, S. R., . . . Foerster, H. (2015). The Sol Genomics Network (SGN)—from genotype to phenotype to breeding. *Nucleic acids research, 43*(D1), D1036-D1041.

Fibach-Paldi, S., Burdman, S., & Okon, Y. (2012). Key physiological properties contributing to rhizosphere adaptation and plant growth promotion abilities of Azospirillum brasilense. *FEMS Microbiology Letters, 326*(2), 99-108.

Godoy, J. A., Pardo, J. M., & Pintor-Toro, J. A. (1990). A tomato cDNA inducible by salt stress and abscisic acid: nucleotide sequence and expression pattern. *Plant molecular biology, 15*(5), 695-705.

Hacquard, S., Spaepen, S., Garrido-Oter, R., & Schulze-Lefert, P. (2017). Interplay between innate immunity and the plant microbiota. *Annual review of Phytopathology, 55*, 565-589.

He, X., Anderson, J. C., Pozo, O. d., Gu, Y. Q., Tang, X., & Martin, G. B. (2004). Silencing of subfamily I of protein phosphatase 2A catalytic subunits results in activation of plant defense responses and localized cell death. *The Plant Journal, 38*(4), 563-577.

Herrera-Medina, M. J., Steinkellner, S., Vierheilig, H., Ocampo Bote, J. A., & Garcia Garrido, J. (2007). Abscisic acid determines arbuscule development and functionality in the tomato arbuscular mycorrhiza. *New Phytologist, 175*(3), 554-564.

Hoagland, D. R., & Arnon, D. I. (1950). The water-culture method for growing plants without soil. *Circular. California agricultural experiment station, 347*(2nd edit).

Holsters, M., de Waele, D., Depicker, A., Messens, E., van Montagu, M., & Schell, J. (1978). Transfection and transformation of Agrobacterium tumefaciens. *Mol Gen Genet, 163*(2), 181-187. doi:10.1007/bf00267408

Javot, H., Penmetsa, R. V., Terzaghi, N., Cook, D. R., & Harrison, M. J. (2007). A Medicago truncatula phosphate transporter indispensable for the arbuscular mycorrhizal symbiosis. *Proceedings of the National Academy of Sciences, 104*(5), 1720-1725.

Jin, L., Ham, J. H., Hage, R., Zhao, W., Soto-Hernández, J., Lee, S. Y., . . . Coplin, D. L. (2016). Direct and indirect targeting of PP2A by conserved bacterial type-III effector proteins. *PLoS pathogens, 12*(5), e1005609.

Kataya, A. R. A., Heidari, B., & Lillo, C. (2015). Protein phosphatase 2A regulatory subunits affecting plant innate immunity, energy metabolism, and flowering time–joint functions among B'η subfamily members. *Plant signaling & behavior, 10*(5), e1026024.

King, E. O., Ward, M. K., & Raney, D. E. (1954). Two simple media for the demonstration of pyocyanin and fluorescin. *J Lab Clin Med, 44*(2), 301-307. Retrieved from https://www.ncbi.nlm.nih.gov/pubmed/13184240

Koornneef, M., Bosma, T. D. G., Hanhart, C. J., Van der Veen, J. H., & Zeevaart, J. A. D. (1990). The isolation and characterization of gibberellin-deficient mutants in tomato. *Theoretical and Applied Genetics, 80*(6), 852-857.

Kost, B., Spielhofer, P., & Chua, N. H. (1998). A GFP-mouse talin fusion protein labels plant actin filaments in vivo and visualizes the actin

cytoskeleton in growing pollen tubes. *Plant J, 16*(3), 393-401. doi:10.1046/j.1365-313x.1998.00304.x

Lee, S. A., Kim, Y., Kim, J. M., Chu, B., Joa, J.-H., Sang, M. K., . . . Weon, H.-Y. (2019). A preliminary examination of bacterial, archaeal, and fungal communities inhabiting different rhizocompartments of tomato plants under real-world environments. *Scientific reports, 9*(1), 1-15.

Lillo, C., Kataya, A. R. A., Heidari, B., Creighton, M. T., Nemie-Feyissa, D., Ginbot, Z., & Jonassen, E. M. (2014). Protein phosphatases PP 2A, PP 4 and PP 6: mediators and regulators in development and responses to environmental cues. *Plant, cell & environment, 37*(12), 2631-2648.

Martín-Rodríguez, J. A., Huertas, R., Ho-Plágaro, T., Ocampo, J. A., Turečková, V., Tarkowská, D., . . . García-Garrido, J. M. (2016). Gibberellin–abscisic acid balances during arbuscular mycorrhiza formation in tomato. *Frontiers in plant science, 7*, 1273.

Matre, P., Meyer, C., & Lillo, C. (2009). Diversity in subcellular targeting of the PP2A B′ η subfamily members. *Planta, 230*(5), 935-945.

Müller, D. B., Vogel, C., Bai, Y., & Vorholt, J. A. (2016). The plant microbiota: systems-level insights and perspectives. *Annual review of genetics, 50*, 211-234.

Pattison, R. J., Csukasi, F., Zheng, Y., Fei, Z., van der Knaap, E., & Catalá, C. (2015). Comprehensive tissue-specific transcriptome

analysis reveals distinct regulatory programs during early tomato fruit development. *Plant physiology, 168*(4), 1684-1701.

Pawar, Bhausaheb & S. jadhav, A & Chimote, Vivek & Kale, & Aa & Pawar, S. V. (2013). Effect of explants, bacterial cell density and overgrowth-control antibiotics on transformation efficiency in tomato (Solanum lycopersicum L.). *Journal of Applied Horticulture, 15*, 95-99.

Pieterse, C. M. J., vanWees, S. C. M., Hoffland, E., vanPelt, J. A., & vanLoon, L. C. (1996). Systemic resistance in Arabidopsis induced by biocontrol bacteria is independent of salicylic acid accumulation and pathogenesis-related gene expression. *Plant Cell, 8*(8), 1225-1237. Retrieved from <Go to ISI>://WOS:A1996VE73200002

Ruan, Y., Halat, L. S., Khan, D., Jancowski, S., Ambrose, C., Belmonte, M. F., & Wasteneys, G. O. (2018). The Microtubule-Associated Protein CLASP Sustains Cell Proliferation through a Brassinosteroid Signaling Negative Feedback Loop. *Current Biology, 28*(17), 2718-+. doi:10.1016/j.cub.2018.06.048

Slater, A., Scott, N. W., & Fowler, M. R. (2008). *Plant biotechnology : the genetic manipulation of plants* (2nd ed.). Oxford ; New York: Oxford University Press.

Smith, S., & Read, D. (2008). Colonization of roots and anatomy of arbuscular mycorrhiza. *Mycorrhizal Symbiosis. Academic Press: London*, 42-90.

Smith, S. E., & Read, D. (2008). 2 - Colonization of roots and anatomy of arbuscular mycorrhizas. In S. E. Smith & D. Read (Eds.), *Mycorrhizal Symbiosis (Third Edition)* (pp. 42-90). London: Academic Press.

Spaepen, S., Bossuyt, S., Engelen, K., Marchal, K., & Vanderleyden, J. (2014). Phenotypical and molecular responses of Arabidopsis thaliana roots as a result of inoculation with the auxin-producing bacterium Azospirillum brasilense. *New Phytologist, 201*(3), 850-861. doi:10.1111/nph.12590

Spaepen, S., Versees, W., Gocke, D., Pohl, M., Steyaert, J., & Vanderleyden, J. (2007). Characterization of phenylpyruvate decarboxylase, involved in auxin production of Azospirillum brasilense. *Journal of Bacteriology, 189*(21), 7626-7633. doi:10.1128/Jb.00830-07

Sun, S., Kang, X. P., Xing, X. J., Xu, X. Y., Cheng, J., Zheng, S. W., & Xing, G. M. (2015). Agrobacterium-mediated transformation of tomato (Lycopersicon esculentum L. cv. Hezuo 908) with improved efficiency. *Biotechnology & Biotechnological Equipment, 29*(5), 861-868. doi:10.1080/13102818.2015.1056753

Tóth, É. C., Vissi, E., Kovács, I., Szöke, A., Ariño, J., Gergely, P., . . . Dombrádi, V. (2000). Protein phosphatase 2A holoenzyme and its subunits from Medicago sativa. *Plant molecular biology, 43*(4), 527-536.

Uhrig, R. G., Labandera, A.-M., & Moorhead, G. B. (2013). Arabidopsis PPP family of serine/threonine protein phosphatases: many targets but few engines. *Trends in plant science, 18*(9), 505-513.

Van Wees, S. C., Van Pelt, J. A., Bakker, P. A., & Pieterse, C. M. (2013). Bioassays for assessing jasmonate-dependent defenses triggered by pathogens, herbivorous insects, or beneficial rhizobacteria. *Methods Mol Biol, 1011*, 35-49. doi:10.1007/978-1-62703-414-2_4

Verhagen, B. W. M., Trotel-Aziz, P., Couderchet, M., Hofte, M., & Aziz, A. (2010). Pseudomonas spp.-induced systemic resistance to Botrytis cinerea is associated with induction and priming of defence responses in grapevine. *Journal of Experimental Botany, 61*(1), 249-260. doi:10.1093/jxb/erp295

Vierheilig, H., Schweiger, P., & Brundtrett, M. (2005). An overview of methods for the detection and observation of arbuscular mycorrhizal fungi in roots. *Physiol Plant, 125*(4), 393-404. doi:10.1111/j.1399-3054.2005.00564.x

Weigel, D., & Glazebrook, J. (2002). *Arabidopsis: A Laboratory Manual*: Cold Spring Harbor Laboratory Press.

Wintermans, P. C. A., Bakker, P. A. H. M., & Pieterse, C. M. J. (2016). Natural genetic variation in Arabidopsis for responsiveness to plant growth-promoting rhizobacteria. *Plant molecular biology, 90*(6), 623-634.

Supporting information

S1 Table. List of primers.

Target gene	Sequence (5'- 3')	Annealing (°C)	PCR Product Size (bp)
pBA002 cloning vector [a,b] pBA002-B'φ ox insert [a,b]	Forward: CGTCTTCAAAGCAAGTGGATTGATG Reverse: TGCTTAACGTAATTCAACAACAGAAATTAT	54	276 1762
B'φ PP2A-B'φ regulatory subunit (Booker and DeLong 2017) [a] NCBI Reference Sequence: XM_010317091.2	Forward: ATGACAAATTTTCTTGATTCTGAGACAG ATCG Reverse: TCACATTGCTGCATTTTCAATTTTTTCCC	54	1486
B'φ PP2A-B'φ regulatory subunit [b] NCBI Reference Sequence: XM_010317091.2	Forward: GAGACTGATCAAAGGCACCCTGGAATCG Reverse: ACAATGCGCGTTCAGCAACCTGCGAG	61	406
B'9 PP2A B56 (Clade 6/9/10) [b] NCBI Reference Sequence: XM_004239128.4	Forward: AGGTGTATGGTGCCGTTGTT Reverse: GATGGCACAAGCACAGCTTCCA	55	389
Bβ (Clade I) PP2A B55 (CLADE I, Booker 2017) [b] NCBI Reference Sequence: XM_004241456.4	Forward: CTCACATGGAGTCTTCCCCG Reverse: AAGCCACATGCAGCAACTT	55	373
Bβ (Clade III) PP2A B55 (CLADE III) (Booker and DeLong 2017) [b] NCBI Reference Sequence: XM_004252324.4, XM_019211570.2, XM_010316006.3 (transcript variant X1, X2, X3)	Forward: GTGGTGATGGTTCGCGAGTA Reverse: CATTTGCATCAACACCGGCA	56	213
B' κ PP2A-B56 (Clade B11) [b] NCBI Reference Sequence: XM_004251542.4 (transcript variant X1), XM_010315410.3 (transcript variant X2), XM_010315411.3 (transcript variant X3), XM_026028819.1 (transcript variant X4), XM_026028820.1 (transcript variant X5)	Forward: ACCTCTGCACAAGCCAAAGT Reverse: TCCAGTGGTTCTGGCTGTTC	56	392
A βI B55 or PP2A-A [b] NCBI Reference Sequence: XM_004236914.4 (transcript variant X1), XM_010321123.3 (transcript variant X2)	Forward: TAGCAAAGGACAGAGTGCCC Reverse: ACTGTTTCCTGGTGTGACGG	56	291
A βII B55 or PP2A-A [b] NCBI Reference Sequence: XM_004238897.4 (transcript variant X1), XM_019214032.2 (transcript variant X2)	Forward: TGCACCAGTAATGGGCTCTG Reverse: ACTGGGCCGAATGGTTTCT	56	166

S1 Table. List of primers (continued).

Target gene	Sequence (5'- 3')	Annealing (°C)	PCR Product Size (bp)
C1 PP2A catalytic subunit (PP2Ac1) [b] NCBI Reference Sequence: NM_001247587.2	Forward: GCGGCAACGTCCTGATTACTA Reverse: AGGCTCAATCTGTCGTGGAG	56	667
C2 PP2A catalytic subunit (PP2Ac2) [b] NCBI Reference Sequence: NM_001246875.2	Forward: ATGCCGTCTCATGCAGATCTA Reverse: CTTCCTTGTGGTGTCGGGCTCTA	54	900
TAS 14 Abscisic acid and environmental stress-inducible protein [b] NCBI Reference Sequence: NM_001247109.1	Forward: CATCACCATGAGGGGCAACA Reverse: GCGTCAGCACACTTTACACG	56	363
NCED-1 Nine-cis-epoxycarotenoid dioxygenase 1 [b] NCBI Reference Sequence: NM_001247526.2	Forward: GTGCAGAAAGCAGCAGCAAT Reverse: CGTAAACCACCGGTGAACCT	55	871
GA3ox-1 Gibberellin-3β-hydroxylase-1 [b] NCBI Reference Sequence: AB010991.1	Forward: AGGCCCAAAAGGTGAAACCA Reverse: CCGTACGGATGAAAGTGCCT	56	463
GA3ox-2 Gibberellin-3β-hydroxylase-2 [b] NCBI Reference Sequence: NM_001246926.3	Forward: AGGCCCAAAAGGTGAAACCA Reverse: CCGTACGGATGAAAGTGCCT	51	276
GA20ox-1 Gibberellin 20-oxidase-1 [b] NCBI Reference Sequence: NM_001247141.1	Forward: AGGCCCAAAAGGTGAAACCA Reverse: CCGTACGGATGAAAGTGCCT	51	451
GA20ox-2 Gibberellin 20-oxidase-2 [b] NCBI Reference Sequence: NM_001247699.2	Forward: CTACAAGGCTCGTCCCACAT Reverse: TGAAAGCGCCATAAATGTGTC	51	402
GA20ox-3 Gibberellin 20-oxidase-3 [b] NCBI Reference Sequence: NM_001247650.2	Forward: CCGGACCATGAGAAGCCAAA Reverse: GATAGTGCCATAAACGTGTCGC	55	752
GA20ox-4 Gibberellin 20-oxidase-4 [b] NCBI Reference Sequence: NM_001247434.2	Forward: CTACAAGGCTCGTCCCACAT Reverse: TGAAAGCGCCATAAATGTGTC	53	375
GAST1 Gibberellin responsive gene NCBI Reference Sequence: NM_001309377.1	Forward: TCAGGTTTCAAGGGCCAACA Reverse: CACTTTGGGCCACCTCTTTTG	56	275
Actin 41 Reference gene [b] NCBI Reference Sequence: NM_001330119.1	Forward: CACTGTATGCCAGTGGTCGT Reverse: GCATCTCTGGTCCAGTAGGAAA	58	773

[a]Primers used with **Phire® Hot Start II DNA Polymerase**
[b] Primers used in sqRT-PCR analysis

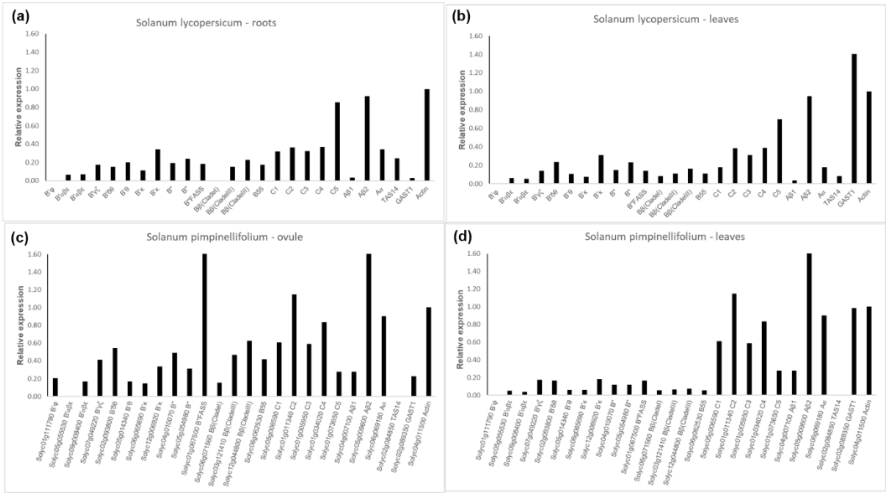

S1 Figure. Expression of PP2A subunit genes in *S. lycopersicum* roots and leaves, and *S. pimpinellifolium* ovules and leaves.
Publicly available data from the Sol genetics database. Genes presented are named according to International Tomato Annotation Group, and orthologues in Arabidopsis. The genes presented are PP2A subunits: eight different B', three B'', four B/B55, five C and three A (Ab2 is 2.23, exceeding the scale), additionally TAS14, GAST1 and Actin. All are normalized to Actin 41 (set to 1).

S2 Figure. Visual phenotype of tomato plants three weeks after treatment with PGPR.
Two-month-old tomato plants not cultivated (upper left photo) and cultivated with WCS417r (upper right photo);Sp245 (lower left photo) and FAJ0009 (lower right photo).

Paper III:

Methylation of protein phosphatase 2A – influence of regulators and environmental stress factors

Received: 28 February 2017 | Revised: 8 July 2017 | Accepted: 11 July 2017
DOI: 10.1111/pce.13038

WILEY Plant, Cell & Environment

ORIGINAL ARTICLE

Methylation of protein phosphatase 2A—Influence of regulators and environmental stress factors

Maria T. Creighton[1] | Anna Kolton[1,2] | Amr R.A. Kataya[1] | Jodi Maple-Grødem[1] | Irina O. Averkina[1] | Behzad Heidari[1] | Cathrine Lillo[1]

[1]Centre for Organelle Research, Faculty of Science and Technology, University of Stavanger, Stavanger N-4036, Norway

[2]Faculty of Biotechnology and Horticulture, University of Agriculture in Krakow, Kraków 31-425 Kraków, Poland

Correspondence
Cathrine Lillo, Centre for Organelle Research, Faculty of Science and Technology, University of Stavanger, Stavanger N-4036, Norway.
Email: cathrine.lillo@uis.no

Funding information
University of Krakow to AK; Norges Forskningsråd, Grant/Award Number: grant no 213853/F20 to CL; University of Stavanger; Norwegian Research Council

Abstract

Protein phosphatase 2A catalytic subunit (PP2A-C) has a terminal leucine subjected to methylation, a regulatory mechanism conserved from yeast to mammals and plants. Two enzymes, LCMT1 and PME1, methylate and demethylate PP2A-C, respectively. The physiological importance of these posttranslational modifications is still enigmatic. We investigated these processes in *Arabidopsis thaliana* by mutant phenotyping, by global expression analysis, and by monitoring methylation status of PP2A-C under different environmental conditions. The *lcmt1* mutant, possessing essentially only unmethylated PP2A-C, had less dense rosettes, and earlier flowering than wild type (WT). The *pme1* mutant, with 30% reduction in unmethylated PP2A-C, was phenotypically comparable with WT. Approximately 200 overlapping genes were twofold upregulated, and 200 overlapping genes were twofold downregulated in both *lcmt1* and *pme1* relative to WT. Differences between the 2 mutants were also striking; 97 genes were twofold upregulated in *pme1* compared with *lcmt1*, indicating that *PME1* acts as a negative regulator for these genes. Analysis of enriched GO terms revealed categories of both abiotic and biotic stress genes. Furthermore, methylation status of PP2A-C was influenced by environmental stress, especially by hypoxia and salt stress, which led to increased levels of unmethylated PP2A-C, and highlights the importance of PP2A-C methylation/demethylation in environmental responses.

KEYWORDS

flowering time, hypoxia, LCMT, methylation, PME, PP2A, PTPA, salt stress, RNA-seq

1 | INTRODUCTION

The protein phosphatase 2A (PP2A) complex is made up of three types of subunits, a catalytic (C), scaffolding (A), and regulatory (B) subunit. These three classes of building blocks are conserved among eukaryotes, but isoforms within each group have arisen, almost exclusively, after the evolutionary splitting of plants and animals (Booker & DeLong, 2016; Moorhead, De Wever, Templeton, & Kerk, 2009). In Arabidopsis, there are 5 C, 3 A, and 17 B subunits, theoretically enabling up to 255 combinations in the PP2A complex. The B subunits are further divided into three groups in plants: B/B55 (two members in Arabidopsis), B′ (nine members in Arabidopsis), and B″ (six members in Arabidopsis; Farkas, Dombradi, Miskei, Szabados, & Koncz, 2007).

Protein phosphatase 2A is known to be involved in the responses to a wide range of external as well as internal signals in Arabidopsis (Uhrig, Labandera, & Moorhead, 2013). One of the first processes identified to strongly implicate PP2A in plants was hormone signalling, and polar transport of auxin was found to require PP2A for dephosphorylation and correct orientation of auxin efflux proteins (PINs; Garbers, DeLong, Deruere, Bernasconi, & Soll, 1996; Michniewicz et al., 2007). Other hormone signalling, for example, brassinosteroid signalling, also involves PP2A. PP2A complexes containing B′α and B′β activate brassinosteroid signalling by dephosphorylating the transcription factor (TF) BZR1 in the nucleus (Tang et al., 2011), and, conversely, PP2A complexes containing B′η (or close B′η homologs) act as negative regulators by dephosphorylating the brassinosteroid receptor BRI1 outside the nucleus (Wang et al., 2016; Wu et al., 2011). PP2A is also implicated in abscisic acid (Kwak et al., 2002; Pernas, Garcia-Casado, Rojo, Solano, & Sanchez-Serrano, 2007; Waadt et al., 2015) and ethylene signalling (Muday et al., 2006; Skottke, Yoon, Kieber, & DeLong, 2011). Furthermore, PP2A dephosphorylates enzymes in primary metabolism, that is, key enzymes in nitrogen assimilation, sugar, and lipid metabolism (Douglas, Pigaglio, Ferrer,

Halfords, & MacKintosh, 1997; Huber, MacKintosh, & Kaiser, 2002; Kataya, Heidari, & Lillo, 2015). Iron nutrition also involves PP2A, where expression of key players of iron homeostasis (FIT1, FRO2, and FER1) is promoted by PP2A (Arnaud et al., 2006; Chen et al., 2010). PP2A also plays a key role in stress and defence responses. *Pp2a-c2* and *pp2a-c5* knockout lines were impaired in root growth in the presence of NaCl. Conversely, overexpression of *PP2A-C5* led to salt resistance (Hu et al., 2016; Pernas et al., 2007). Knockdown of the PP2A activator PTPA (phosphotyrosyl phosphatase activator/PP2A activator) resulted in hypersensitivity to NaCl and impaired root growth (Chen, Hu, Zhu, Shen, & Zhang, 2014). Furthermore, one of the B' subunit ($B'\zeta$) was induced fourfold, and $B''\alpha$ was induced twofold under salt stress (Lillo et al., 2014). In wheat, also a B'' (*TaPP2A-B'α*) was found to respond to NaCl, and overexpression of this gene in Arabidopsis promoted root growth in the presence of NaCl (Liu, Li, Mao, & Jing, 2014). Knockdown of certain B' subunits has been shown to reduce the growth of *Pseudomonas syringae* pv. tomato DC3000 after Arabidopsis infection (Kataya et al., 2015; Trotta et al., 2011). Recent work by Segonzac et al. (2014) showed that PP2A negatively controlled the flg22-triggered immune response in Arabidopsis by interacting with the leucine-rich repeat receptor kinase BAK1. The investigation by Jin et al. (2016) showed that conserved bacterial effector proteins (T3Es) targeted PP2A to promote infection. In all these investigations with *P. syringae* or bacterial elicitors, B' subunits appeared to be involved.

Posttranslational modifications play an important role in conveying environmental and developmental signals, and can modify enzyme activity and influence protein–protein interactions and protein interactions with membranes or other cellular components. Phosphorylation is the most common posttranslational modification of proteins, but other types of protein modification are gaining attention. The importance of methylation and acetylation for the function of histones and epigenetics in environmental and developmental responses is well known (Braun & Gingras, 2012; Brautigan, 2013; Hill, 2015). PP2A catalytic and scaffolding subunits are generally constitutively expressed in Arabidopsis, although the *PP2A-C5* catalytic subunit gene shows more variable expression. *PP2A-C1* and *PP2A-A3* are especially stably expressed and are often used as reference genes in transcription analysis (Lillo et al., 2014). PP2A catalytic subunit (PP2A-C) is subjected to carboxymethylation of the very terminal amino acid (leucine), which influences assembly and properties of PP2A (Janssens, Longin, & Goris, 2008). The enzymes mediating methylation/demethylation of PP2A, LCMT1 (leucine carboxyl methyl transferase 1), and PME1 (PP2A methylesterase 1) have been studied mainly in animals and yeast but are conserved also in plants (Lillo et al., 2014). In the Arabidopsis brassinosteroid receptor mutant (*bri1*), a suppressor mutation was identified as a mutation in the *SBI1*/*LCMT1* gene (Wu et al., 2011). In *Saccharomyces cerevisiae*, methylation of the catalytic subunit promotes assembly of both B/B55 (Cdc55) and B' (Rts1) with the core AC dimer, methylation being slightly more important for Cdc55 incorporation into the PP2A complex (Gentry et al., 2005; Janssens et al., 2008; Wu et al., 2000). In mammals, assembly of the B/B55 (PR55) subunits into the PP2A complex was strongly promoted by PP2A-C methylation whereas assembly of B', B'', and B''' into the complex was only slightly or not at all influenced by methylation (Janssens et al., 2008; Longin et al., 2007). In plants, the effects of methylation on PP2A complex formation have not been studied.

Methylation of PP2A-C can lead to more frequent localization to certain membranes or membrane rafts. Longman, Ranieri, Avkiran, and Snabaitis (2014) reported that stimulation of A1 receptors (a type of G-coupled receptors in mammals) increased the association of LCMT1 with PP2A-C and thereby augmented the carboxymethylation of the C subunits and facilitated association of PP2A-C with membrane-rich particulate compartments. Sontag, Nunbhakdi-Craig, and Sontag (2013) reported coenrichment of LCMT1, methylated PP2A-C, and Bα in cholesterol-rich membrane rafts of mammalian N2a cells. In Arabidopsis, it was found that unmethylated PP2A-C was present almost entirely in the cytosol fraction and not in the microsomal fraction that had only methylated PP2A-C. However, Arabidopsis plants with knocked out *LCMT1* (*sbi1* mutant) were void of methylated PP2A-C and had unmethylated PP2A-C both in the microsomal and cytosolic fractions. This indicates that, when present, active LCMT1 will methylate all PP2A-C in microsomes (Wu et al., 2011).

In addition to catalysing demethylation of PP2A-C, PME1 has a function in stabilizing the PP2A complex, keeping part of the PP2A-C pool in an inactive state (Longin et al., 2004; Wepf, Glatter, Schmidt, Aebersold, & Gstaiger, 2009). Studies of the crystal structure of mammalian PME1 and PP2A revealed that PME1 directly binds to the active site of PP2A-C and inactivates PP2A by displacing the metal ions at the active site (Xing et al., 2008). Another PP2A regulator, PTPA, was needed to reactivate PP2A (Longin et al., 2004). Mammalian PTPA fused with a truncated scaffolding A was crystallized and was shown to make broad contacts around the PP2A-C active site. PTPA facilitated binding of LCMT1 and methylation of mammalian PP2A-C (Guo et al., 2014). Plant PTPA has not been much studied, but knockdown of *PTPA* in Arabidopsis to 10% of normal transcript levels resulted in very low levels of methylated PP2A-C and reduced PP2A activity by 40–50% (Chen et al., 2014). The investigations by Chen et al. (2014) are in support of a model where PTPA transiently binds to the PP2A-AC dimer, activates PP2A, and facilitates binding of B subunits and/or binding of LCMT1 that methylates the catalytic subunit before further binding of B subunits.

In yeast, addition of glucose triggered rapid (minutes) posttranslational activation of PP2A, and this was associated with carboxymethylation of the C-terminal leucine of PP2A-C (Castermans et al., 2012). Deletion of the yeast *PME1* homolog (Ppe1) increased activation, whereas deletion of the *LCMT1* homolog (Ppm1) decreased, but did not abolish, activation (Castermans et al., 2012). Hence, in yeast, environmental signals (glucose) led to rapid changes in methylation levels of PP2A-C.

To date, the physiological implications of PP2A-C methylation are poorly understood in all organisms. In this work, we investigated how various environmental conditions influenced the methylation status of Arabidopsis PP2A, and we compared plants with low methylation level (*lcmt1*) with plants with high methylation level (*pme1*, $ptpa_{ox}$, and WT) to reveal the importance of methylation status for physiology and gene expression.

2 | MATERIAL AND METHODS

2.1 | Plant material and standard growth conditions

T-DNA insertion lines of *Arabidopsis thaliana* (Columbia background) were obtained from the European Arabidopsis Stock Centre in Nottingham UK: *icmt-1* knockout line (insertion in At1g02100 exon four, SALK_079466; Alonso et al., 2003); *ptpa* overexpressor (4.5×) line (insertion in the At4g08960 promoter, GABI_606E07), and *pme1* knockout line (insertion in At4g10050 intron 10, GK_804C11) (Kleinboelting, Huep, Kloetgen, Viehoever, & Weisshaar, 2012; Figure S1). Homozygous mutants were selected using primers recommended at the SALK institute website SIGnAL (http://www.signal.salk.edu/tdnaprimers.2.html). Inspection of the RNA-seq data alignment to the TAIR 10 gene model showed that *icmt1* transcript of exon 4 was completely missing and reads spanning other exons were very few, indicating complete knockout of the gene (Figure S2). For the *pme1* mutant, a complete knockout was confirmed (Figure S2). It should be noted that the three last exons of *PME1*, downstream of the T-DNA insert site in *PME1*, were overexpressed, giving an artificially high FPKM (fragment per kilobase per million mapped reads) value.

Seeds were surface sterilized by calcium-hypochlorite/ethanol and sown on 12 × 12 cm plates containing ½ MS salts (Murashige & Skoog, 1962), 0.4% phytagel (Sigma-Aldrich) and 1% sucrose. The plates were placed in darkness at 4 °C for 3 days for stratification and then placed vertically under artificial light at a 16-hr day length (100 $\mu mol\text{-}m^{-2}\ s^{-1}$) and 22 °C, unless otherwise stated.

2.2 | Plant growth for immunoblot analysis

For salt stress, seedlings were transferred after six (batch 1) or four (batch 2) days of growth to new ½ MS plates with or without 100-mM NaCl. Samples were then harvested after 1 hr, 24 hr, or 4 days. For iron deficiency, seedlings were sown on ½ MS without iron (−Fe) and harvested after 6 days of growth. For low nitrogen conditions, seeds were sown on medium with nitrogen supplied only as 0.1-mM KNO_3 (−N), and harvested after 7 days of growth. The effect of low oxygen availability was tested on rosette stage plants grown in soil and watered regularly with Hoagland solution with 15-mM KNO_3 (Hoagland & Arnon, 1950). After 6 weeks, half of the pots were kept in control conditions, the other pots were submerged in nutrient solution to create a hypoxic environment for the roots. The rosettes were harvested after 7 days. All samples were frozen immediately in liquid nitrogen and kept at −80 °C until further analysis.

2.3 | Immunoblotting

Samples were homogenized in extraction buffer (50-mM Na-phosphate, pH 7, 1-mM EDTA, and 0.1% Triton-x) and centrifuged at 15,000 *g* at 4 °C for 25 min (Chen et al., 2014). The supernatant was used for protein quantification (Bradford, 1976) and for immediate boiling with Laemmli buffer (Bio-Rad Laboratories, GmbH, München, Germany) for gel electrophoreses. Total protein, 10 µg for roots and 20 µg for shoots and rosette stage leaf samples, was separated by SDS-PAGE using a 12% Mini-PROTEAN® TGX™GEL (Bio-Rad Laboratories). Proteins were electro-blotted onto a 0.2-µm PVDF membrane using a Trans-Blot®Turbo™ Transfer system (Bio-Rad Laboratories). Protein transfer was confirmed by Ponceau red staining (Sigma-Aldrich, St. Louis, USA). Membranes were blocked overnight at 4 °C in PBST/MLK (PBS 0.1% Tween-20/5% milk), before incubating with primary antibody specific for unmethylated-PP2A-C (demethylated-PP2A-C (4i57): sc-80990, Santa Cruz Biotechnology Inc., CA, USA; 1:1000 dilution in PBST) at room temperature for 2 hr. Following washing 6 × 5 min with PBST, membranes were incubated with secondary antibody goat anti mouse IgG-HRP (Santa Cruz Biotechnology Inc.; 1:5000 dilution in PBST/MLK) for 1.5 hr, washed in PBST 6 × 5 min, and exposed to ECL detection kit (Amersham™ECL™Prime Western Blotting Detection Reagent RPN2232, GE Healthcare, Buckingshire, UK). Band intensity was quantified using Image J software (https://imagej.nih.gov/ij/index.html). For total PP2A-C detection, alkali-induced demethylation of proteins was carried out according to the Merck-Millipore certificate for analysis (Anti-methyl-PP2A, C subunit, clone 2A10, 04-1479, Merck KGaA, Darmstadt, Germany) with slight modifications: Proteins were transferred to PVDF membrane and exposed to NaOH (0.2 N) for 30 min at 37 °C with gentle shaking. The membrane was washed 6 × 10 min with PBST, followed by blocking and incubation with antibody against unmethylated PP2A-C as described.

2.4 | Total RNA extraction and RNA-seq analysis

Total RNA was extracted from 10-day-old seedlings using RNeasy®Plant Mini Kit (Qiagen, Chatsworth, CA, USA; Qiagen, Hilden, Germany) and RNase-Free DNase Set on-column DNase treatment (Qiagen). GATC Biotech (Konstanz, Germany) carried out the RNA-seq for three biological samples of WT and three of each mutant. Sets of genes from mutants and WT, at least twofold differentially expressed, were analysed using PANTHER's overexpression test and TAIR's GO defined annotations (Berardini et al., 2004; Mi, Muruganujan, Casagrande, & Thomas, 2013).

2.5 | PP2A activity assay

The Ser/Thr Phosphatase Assay System from Promega (Promega 2009, Madison, WI, USA) was used. Frozen tissue, 100 mg, was homogenized in 400-µl buffer (50-mM Tris-HCl, pH 7, 0.1-mM EDTA, 2-mM DTT, and 0.01% w/v Brij 35; Cohen et al., 1988; McAvoy & Nairn, 2010) with subsequent centrifugation at 17,000 *g* at 4 °C for 1 hr. Extracts were desalted on spin columns and protein quantified by Bradford assay (Bradford 1xDye Reagent Quick Start™ from Bio-Rad). Assay mixtures with 10-µg protein and 0.1-mM phosphorylated peptide (RRA(pT)VA) were incubated at 37 °C for 5 min and terminated by adding 100 µl of the molybdate dye. Reaction mixtures terminated at time zero were used as controls. To inhibit the activity of PP2A (Cohen, Klumpp, & Schelling, 1989), 2-nM okadaic acid sodium salt (Sigma-Aldrich) was used in the assay buffer (50-mM Tris–HCl, pH 7, 0.2-mM EDTA, 0.02% (v/v) 2-mercaptoethanol, and 0.1-mg/ml bovine serum albumin). PP2A activity was calculated as the difference of phosphate released with and without 2-nM okadaic acid. It should be noted that PP4 (Brewis, Street, Prescott, & Cohen, 1993) and PP6 (Prickett & Brautigan, 2006) are also inhibited by low concentrations of okadaic acid and may contribute to the activity.

3 | RESULTS

3.1 | PP2A-C methylation status in WT, *pme1*, $ptpa_{ox}$, and *lcmt1* seedlings under control conditions

The knockout mutant lines *pme1* (GK_804C11) and *lcmt1* (SALK_079466), and an overexpressor line $ptpa_{ox}$ (GK_606E07) with 4.5 times higher *PTPA* transcript levels than WT, were included in the experiments (Figures S1 and S2). The level of unmethylated PP2A-C protein in *pme1* seedlings was significantly lower than in WT, on average lowered by 28% in shoots and 37% in roots (Figure 1a). The level of total PP2A-C (methylated and unmethylated) was not significantly different in *pme1* and WT seedlings (Figure 1b). This shows that more PP2A-C is in the methylated form in the absence of *PME1*. Higher levels of methylated PP2A-C in *pme1* is expected, because knockout of *PME1* should lead to less methylesterase activity, which otherwise would cleave off the methyl group. The $ptpa_{ox}$ line was similar to *pme1* (Figure 1). The difference between WT and *lcmt1* was striking; unmethylated PP2A-C reached approximately fivefold higher levels in *lcmt1* compared to WT (Figure 1a). These data support the view that all PP2A-C in the *lcmt1* mutant is present in an unmethylated state (Wu et al., 2011). Assuming that the *lcmt1* mutant has only unmethylated PP2A-C, the columns in Figure 1a,b represent the same amount of protein for *lcmt1*. On the basis of the results for *lcmt1*, data in Figure 1a can be divided by a factor (5.3) to have the same scale and compare the figures. It can then be concluded that, in WT, the methylated form of PP2A-C is dominating and accounts for about 81% of the PP2A-C in WT seedlings, and, for *pme1* and $ptpa_{ox}$, the level of methylated PP2A-C was even higher, 87% and 86% of the total PP2A-C.

3.2 | Salt stress and methylation status

After 6 days under control growth conditions, seedlings were transferred to fresh medium with or without 100-mM NaCl and harvested after 1 and 24 hr. The level of unmethylated PP2A-C increased in roots of WT, *pme1*, and $ptpa_{ox}$ in response to NaCl treatment (Figure 2a and 2c), whereas total PP2A-C was constant or decreased (Figure 2b and 2d). After 1 hr (or 24 hr), the increase of unmethylated PP2A-C was 51% (118%), 79% (143%), and 89% (192%) for WT, *pme1*, and $ptpa_{ox}$, respectively. After 4 days, there were no longer increased unmethylated PP2A-C levels for NaCl treated plants (Figure S3). Shoots were also tested, but no effects on unmethylatd PP2A-C were found (Figure S4).

3.3 | Nutrient limitation and methylation status

Seedlings were grown for 7 days with normal N (29 mM) or with low N (0.1 mM). In shoots, the level of unmethylated PP2A-C was lowered under N limitation relative to control conditions by 46%, 79%, and 64% for WT, *pme1*, and $ptpa_{ox}$, respectively (Figure 3a). Roots did not show reproducible changes in PP2A-C levels (Figure S5). Experiments with plants grown on iron-deficient medium also showed that iron deficiency could lead to less unmethylated PP2A-C but, surprisingly, only for the *pme1* mutant (Figure S6).

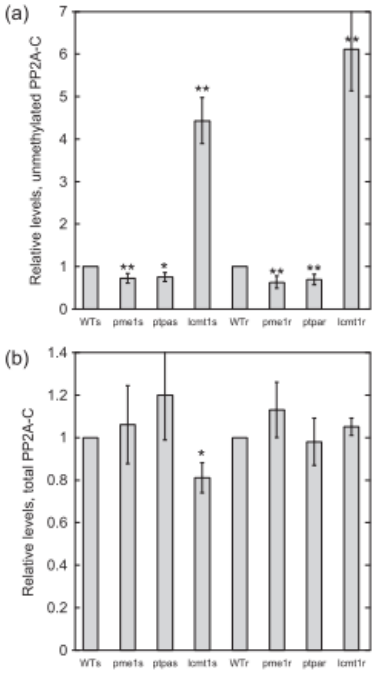

FIGURE 1 Relative levels of unmethylated and total PP2A catalytic subunits (PP2A-C) in shoots and roots of Arabidopsis WT, *pme1* (knockout), *ptpa* (overexpressor), and *lcmt1* (knockout) mutants under control conditions. Seedlings were grown in continuous light on ½ MS salts with 1% sucrose for 7 days before harvesting. Samples were analysed by immunoblots using antibodies towards the unmethylated form of PP2A-C. (a) Unmethylated PP2A-C in shoots "s" and roots "r," WT levels are set to 1. (b) Total PP2A-C in shoots and roots, WT levels are set to 1. For total PP2A-C, the blots were treated with NaOH to demethylate all PP2A-C before detection with the antibody. The mean values of 11 independent experiments are shown; SE is given. Columns marked are significantly different from WT according to student's *t* test, $p < .05$ two stars; $p < .1$ one star

3.4 | Hypoxia and methylation status

Arabidopsis rosette stage plants grown on soil for 6 weeks were used for hypoxia exposure. Pots were submerged in excess nutrient (Hoagland) solution for 7 days, whereas the soil of control plants was kept moist with nutrient solution, as usual. The level of unmethylated PP2A-C was increased in rosette leaves when plants were exposed to hypoxic conditions for 1 week. The experiment was repeated three times, and the increase of unmethylated PP2A-C was strikingly high in

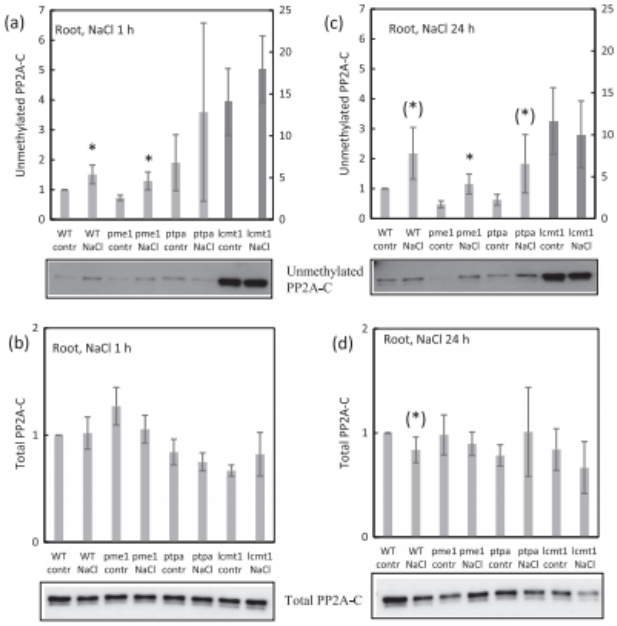

FIGURE 2 Levels of unmethylated and total PP2A-C in seedling roots of WT, *pme1*, $ptpa_{ox}$, and *lcmt1* treated with 100-mM NaCl. Seedlings were grown in control conditions for 6 days and then transferred to fresh media without (control) or with 100-mM NaCl. (a) Unmethylated PP2A-C after 1-hr exposure to NaCl and (b) total PP2A-C after 1-hr exposure to NaCl. (c) Unmethylated PP2A-C after 24-hr exposure to NaCl and (d) total PP2A-C after 24-hr exposure to NaCl. Representative blots are shown. Note that, due to high levels of unmethylated PP2A-C, *lcmt1* samples (dark grey columns) correspond to the scale bar to the right. The mean values of four independent experiments are shown; SE is given. Columns marked are significantly different from WT according to student's *t* test, $p < .05$ two stars; $p < .1$ one star; ($p < .12$ one star in brackets)

all three experiments. On average, unmethylated PP2A-C increased by a factor of 9.5, 21, 4.3, and 1.6 for WT, *pme1*, $ptpa1_{ox}$, and *lcmt1*, respectively, relative to control plants (Figure 3c). Also, the level of total PP2A-C increased in all plant types, on average by 55% (Figure 3d). When considering *lcmt1* as an internal standard (all PP2A-C unmethylated), it can be estimated that, after hypoxia treatment, unmethylated PP2A-C constitutes 39%, 33%, and 18% of total PP2A-C for WT, *pme1*, and $ptpa_{ox}$, respectively. The experiments clearly showed that hypoxia of roots led to increased levels of unmethylated PP2A-C in the leaves.

3.5 | Global expression analysis—RNA-seq

RNA sequencing of seedlings grown in control conditions revealed that the expression of 638 genes in the *pme1* mutant was changed twofold or more (increased or decreased) in comparison with the WT control. For the *lcmt1* mutant relative to WT, this number was similar (660 genes). In *pme1* and *lcmt1*, 381 and 272 genes, respectively, were twofold upregulated, relative to WT. For both mutants, 201 same genes were upregulated, that is, 74% of the genes (twofold) upregulated in *lcmt1* were also (twofold) upregulated in *pme1*. The number of downregulated genes was 257 for *pme1* and 388 for *lcmt1*, and 202 of these genes were identified as downregulated in both mutants (Figure 4a). When transcripts in *lcmt1* and *pme1* were directly compared (not related to WT), 124 genes were more than twofold differentially expressed. Intriguingly, 97 of these genes were more highly expressed in *pme1* than in *lcmt1*, pointing to a difference between PME1 and LCMT1 regarding an effect of inhibiting versus stimulating expression of a large number of genes. Different sets of genes (Figure 4a and Table S1a–c) were examined using the PANTHER overexpression test and TAIR's GO (gene ontology) defined annotations (Berardini et al., 2004; Mi et al., 2013). When the genes at least twofold upregulated or downregulated in *pme1* relative to WT were tested for enriched groups, mainly gene sets related to stress

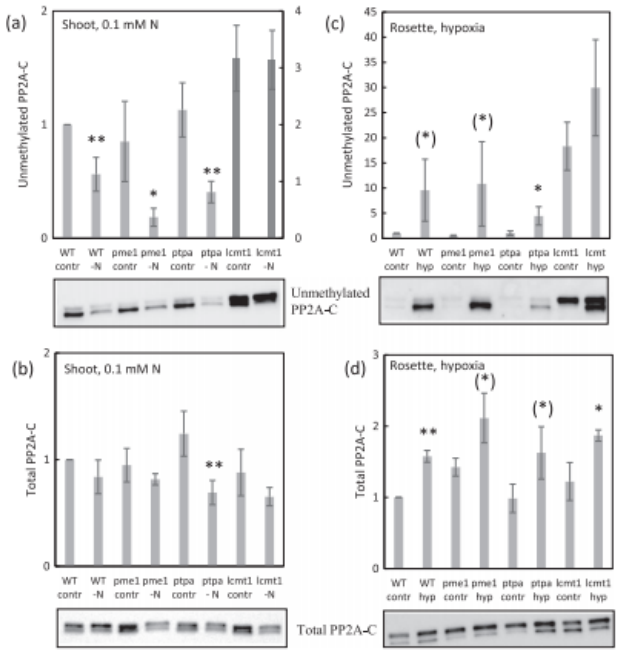

FIGURE 3 Levels of unmethylated and total PP2A-C in Arabidopsis seedling shoots of WT, *pme1*, $ptpa_{ptx}$, and *lcmt1* grown on low levels of nitrogen (N), and leaves of rosette stage plants under hypoxia treatment. ((a) and (b)) seedlings were grown in continuous light for 7 days on MS medium (29-mM N; contr) or MS medium with 0.1-mM N (−N). (a) unmethylated PP2A-C in shoots and (b) total PP2A-C in shoots. Representative blots are shown. The experiments were repeated four times. Note that, due to high levels of unmethylated PP2A-C, *lcmt1* samples in (a) (dark grey columns) correspond to the scale bar to the right. ((c) and (d)) Arabidopsis was grown in soil and watered with Hoagland solution. After 6 weeks, pots were submerged in nutrient solution for 7 days to create hypoxia conditions (hyp), and control plants were kept moist with the nutrient solution (contr). (c) unmethylated PP2A-C in rosette leaves and (d) total PP2A-C in rosette leaves. The experiments were repeated three times. Columns marked are significantly different from WT according to student's *t* test; $p < .05$ two stars; $p < .1$ one star; ($p < .15$ one star in brackets)

were revealed, with many redundant groups. Response to stress/GO:0006950 contained 101 genes, and 65 genes were upregulated, whereas 36 genes were downregulated relative to WT (Table 1 and Table S2a). For the *lcmt1* mutant, this GO term was also significantly enriched, containing 104 genes; 45 were upregulated, and 59 were downregulated (Table 1 and Table S2b). Defence response/GO:0006952 was a significantly enriched gene set for both *pme1* and *lcmt1* relative to WT (Table 1), and many of these genes were also included in the stress responsive genes. For example, from the 65 stress-responsive genes upregulated in *pme1*, 37 were also classified as defence response genes. Constitutive expression of defence genes and autoimmunity reactions was previously detected in a PP2A mutant, *pp2a-b′γ* (Trotta et al., 2011). The *pp2a-b′γ* mutant developed brown spots, indicating a constitutive immune response in this mutant. Such spots were observed only for *pp2a-b′γ*, not for the *pme1* or *lcmt1* mutants growing alongside with *pp2a-b′γ* in our growth chambers. Furthermore, the defence genes found to be constitutively upregulated in the *pp2a-b′γ* mutant (Trotta et al., 2011) were generally not upregulated in *pme1* and *lcmt1* (data based on Table S1). Marker genes for immune response, *FRK1* (At2g19990) and *NHL10* (At2g35980), were previously tested in several *PP2A* mutants (*pp2a-c4*, *pp2a-a1*, *pp2a-b′η*, *pp2a-b′ζ*) without giving indications of constitutive immune response (Segonzac et al., 2014). Similarly, in *pme1* and *lcmt1*, *FRK1* expression was not different from WT, and *NHL10* expression was only slightly induced (1.6-fold). In conclusion, RNA-seq data for *pme1* and *lcmt1* did not give clear evidence for a constitutive immune response. The defence genes enriched in *PME1* and *LCMT1* need further investigations to obtain a coherent picture.

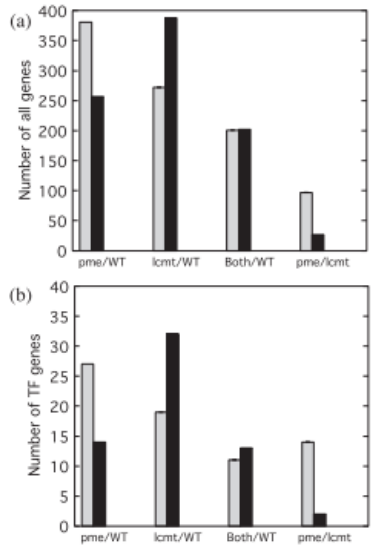

FIGURE 4 Number of genes twofold upregulated and downregulated in *pme1* and *lcmt1* mutant lines. (a) All genes. (b) Transcription factor (TF) genes. Upregulated genes are represented by grey columns; downregulated genes are represented by black columns

For the *pme1* mutant, a set of 14 genes involved in flavonoid biosynthesis was significantly enriched relative to WT. From these genes, 12 were upregulated and 2 were downregulated. Increased activity in the flavonoid pathway is a typical stress response, but this pathway was significantly enriched only for *pme1*, not *lcmt1*. When the 403 genes coexpressed in *pme1* and *lcmt1* were analysed, response to stress again appeared as a significantly enriched set of genes (68 genes; Table 1 and Table S2c). PANTHER's molecular function search revealed "oxidoreductase activity" as an enriched gene set for both *pme1* (61 genes) and *lcmt1* (64 genes) versus WT. Again, for *pme1*, more genes were upregulated (42) than downregulated (20), whereas, for *lcmt1*, fewer genes were upregulated (25) than downregulated (39; Table 1). Except for the significance of upregulated genes related to the flavonoid pathway, no striking differences between *pme1* and *lcmt1* were revealed using the enrichment analysis tools. The gene set with twofold differentially expressed genes in *pme1* versus *lcmt1* did not point to specific groups other than stress-related (response to chemicals) and oxygen-affected genes (Table S2h).

Transcription factors have an especially high impact on growth, development, and responses to the environment. Accordingly, TFs were inspected using the TAIR functional categorization tool. When comparing *pme1* versus WT, 27 TFs were upregulated and 14 TFs were downregulated. When comparing *lcmt1* versus WT, only 19 TFs were upregulated, whereas 32 were downregulated (Figure 4b). When *pme1* was compared directly with *lcmt1*, 16 TFs were differentially expressed in *pme1* and *lcmt1* by at least factor 2 (Figure 4b and Table 2). Strikingly, when *pme1* was compared directly with *lcmt1*, 14 TFs were higher expressed in *pme1*, and only two TFs were lower expressed in *pme1* in comparison with *lcmt1* (Figure 4b and Table 2). Among the TF genes was *FLC* (*Flowering locus C*), which was 5.8 times higher expressed in *pme1* than in *lcmt1*. FLC is an important inhibitor of flowering induction, and this fits with *pme1* flowering later than *lcmt1* (Figure 5). Some other TFs identified (Table 2) are also related to development and shape in plants: BEE1 (BR ENHANCED EXPRESSION) positively modulates shade avoidance (Cifuentes-Esquivel et al., 2013), and MYBL2, in addition to being involved in regulation of anthocyanin synthesis, binds to the brassinosteroid regulator BES1 and acts as a corepressor for down-regulating brassinosteroid repressed genes (Ye, Li, Guo, & Yin, 2012). Hence, two of the TFs are known to be involved in brassinosteroid signalling and further strengthen the findings that

TABLE 1 GO enrichment analysis for genes more than two times differentially expressed in *pme1* and/or *lcmt1* compared with WT using analysis tool described by Mi et al. (2013)

GO term	Gene sets compared	Genes (n) input/reference	Enrichment (fold)	*p* value	Genes differentially regulated (n) Up	Down
Biological process						
Response to stress (GO:0006950)	*pme1* versus WT	101/2699	1.80	1.29E-02	65	36
	lcmt1 versus WT	104/2699	1.74	5.18E-05	45	59
	pme1 and *lcmt1* versus WT	68/2699	1.85	1.15E-03	38	30
Defence response (GO:0006952)	*pme1* versus WT	52/1265	1.98	7.34E-03	37	15
	lcmt1 versus WT	52/1265	1.85	4.36E-02	26	26
Flavonoid biosynthetic process (GO:000981)	*pme1* versus WT	14/110	6.12	2.80E-04	12	2
Molecular function						
Oxidoreductase activity (GO:0016491)	*pme1* versus WT	61/1385	2.12	6.22E-05	42	20
	lcmt1 versus WT	64/1385	2.08	5.61E −05	25	39
	pme1 and *lcmt1* versus WT	43/1385	2.28	7.58E-04	24	19

Note. Only gene sets significantly enriched, with *p* value < .05 are listed.

TABLE 2 Transcription factors more than twofold differentially expressed in *pme1* versus *lcmt1*

Locus	Common name(s)	Gene description extracted from TAIR plus from reference given
Genes high in *pme1* and low in *lcmt1*:		
At1g10585		A basic helix–loop–helix (bHLH; IPR011598) DNA-binding superfamily protein.
At1g18400	BR Enhanced Expression 1, BEE1	Encodes the brassinosteroid signalling component BEE1, which modulates the shade avoidance syndrome in Arabidopsis seedlings. Has bHLH domain (IPR011598)
At1g71030	MYB-like 2, MYBL2	A proline-rich region potentially involved in transactivation is found in the C-terminal part of the protein. Acts as a corepressor of BES1 in the brassinosteroid signalling pathway (Ye et al., 2012) Has SANT/MYB domain (IPR001005)
At1g75490		A member of the DREB subfamily A-2 involved in response to drought. Has AP2/ERF domain (IPR00147)
At2g21650	Maternal effect embryo arrest 3, MEE3; RAD-like2, ATRL2 RADIALIS-like	Member of a small sub-family of single MYB transcription factors. Involved during early embryogenesis, early photomorphogenesis, and represses transition to flowering (Hamaguchi et al. 2008, li et al. 2015) Has Hsp40 domain (IPR15609). Has SANT/MYB domain (IPR001005)
At2g26150	Heat shock transcription factor A2, HSFA2	Member of heat stress transcription factor (Hsf) family. Involved in response to misfolded protein accumulation in the cytosol. Has HSF domain (IPR011991)
A2g28700	AGAMOUS-like 46, AGL46	Transcription factor like, with MADS box (IPR002100)
At4g36570	RAD-like 3, RL3	Member of a small sub-family of single MYB transcription factors. Has heat chock protein Hsp40 domain. Has SANT/MYB domain (IPR001005)
At4g39250	RAD-like 1, RL1; RADIALIS-like SANT/MYB 2, RSM2	Member of a small sub-family of single MYB transcription factors. Has heat shock protein Hsp40 domain. Has SANT/MYB domain (IPR001005)
At5g10140	Flowering locus C, FLC; AGAMOUS-like 25, AGL25	Repressor of transition to flowering. Has MADS-box domain (InterPro:IPR002100)
At5g14340	MYB domain protein 40, MYB40	Member of the R2R3 MYB factor gene family Has SANT/MYB domain (IPR001005)
At5g39519	Arabidopsis NAC domain containing protein 92, ANAC092,	Encodes a NAC-domain transcription factor. Positively regulates ageing-induced cell death and senescence in leaves. Has NAM domain (IPR003441)
At5g44260	Tandem CCCH zinc finger protein 5, TZF5	Zinc finger C-×8-C-×5-C-×3-H type family protein Zinc finger, CCCH-type (InterPro:IPR000571)
At5g47220	Ethylene response factor 2, ERF2	Encodes a member of the ERF (ethylene response factor) subfamily B-3 of ERF/AP2 transcription factor family. The protein contains one AP2 domain. Has AP2/ERF domain (IPR001471)
Genes high in *lcmt1* and low in *pme1*:		
At2g20880	ERF53	Belongs to AP2/ERF superfamily. Regulates drought induced genes.
At5g64060	NAC domain containing protein 103, NAC103	Takes part in unfolded protein response (UPR), activates UPR gene promoters. Induced by ER stress (Sun et al. 2013).

PP2A-C methylation is important in brassinosteroid signalling (Wu et al., 2011). Strikingly, five of the 14 TFs on the list of upregulated TFs in *pme1* versus *lcmt1* contain an SANT/MYB domain (IPR001005; Table 2). These include MYBL2 and three of the six members of the small RAD-LIKE gene family. This RAD LIKE family has not been much studied in Arabidopsis, but, from expression studies and comparison with tomato and antirrhinum, these genes are anticipated to participate in plant-specific developmental programs during embryo, leaf, and fruit formation (Barg et al., 2005; Baxter, Costa, & Coen, 2007). For example, *MEE3* (*RADIAL SANT LIKE 1*/*RSM1*) is homologous with *RADIALIS* in antirrhinum and is important for its flower asymmetry. Arabidopsis does not have such asymmetric flowers, but the apparent involvement of *LCMT1* knockout in reducing expression of the *RAD*-like genes may be of importance for altered morphological traits, such as long petioles (Figure 5e,f). This deserves future investigation.

3.6 | Phenotypes—Flowering time and visual appearance

Both the *lcmt1* and *pme1* knockout lines appeared healthy and completed their life cycle (Figure 5). For *lcmt1*, visual differences from WT were clear regarding rosette density as well as time of flowering (Figure 5). The *lcmt1* knockout line was early flowering in both short days (Figure 5a,b) and long days (Figure 5c,d). The *lcmt1* mutant was early flowering according to all criteria, for example, shorter time to shooting, lower number of leaves at shooting (Figure 5a–f), lower number of days to first flower, and number of leaves at flowering (data not shown). The *pme1* mutant had fewer leaves at shooting time than WT in long days (Figure 5d). The *lcmt1* seedlings grown on agar plates had a shorter main root and fewer lateral roots than WT, whereas *pme1* and $ptpa_{ox}$ were not distinguishable from WT (Figure 5g).

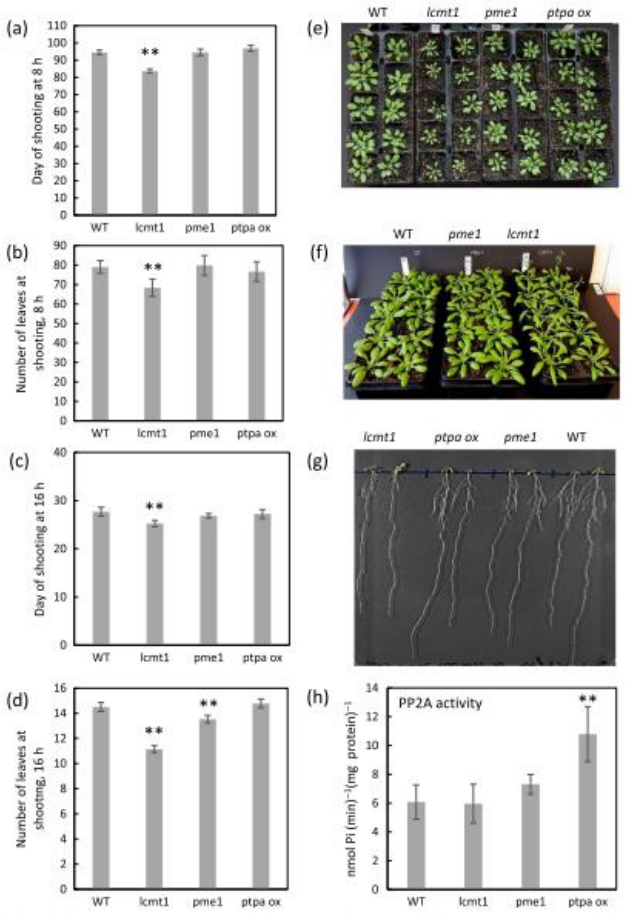

FIGURE 5 Flowering time, seedling phenotypes, and PP2A activity. (a) Average day of shooting for WT and *lcmt1*, *pme1*, and $ptpa_{ox}$ mutants growing in 8-hr light/16-hr dark cycles. (b) Average number of leaves on the day of shooting at 8-hr light/16-hr darkness. (c) Average day of shooting at 16-hr light/8-hr darkness. (d) Average number of leaves on the day of shooting at 16-hr light/8-hr darkness. (e) Plants grown for 6 weeks in 8-hr days, WT, *lcmt1*, *pme1*, and $ptpa_{ox}$, two rows of each. (f) Plants grown for 4 weeks in 16-hr days. (g) Representative plants showing roots of 10 days old seedlings growing on ½ MS salts (here N was reduced to 0.1 mM) with 1% sucrose. The results in (a) and (b) are from 35 WT, 19 *lcmt1*, 19 *pme1*, and 18 $ptpa_{ox}$ plants. The results in Figure 5c,d are from 20 WT, 29 *lcmt1* 30 *pme1*, and 27 $ptpa_{ox}$ plants. (h) PP2A activity in WT, *lcmt1*, *pme1*, and $ptpa_{ox}$ seedlings grown in ½ MS medium under standard conditions. Columns marked are significantly different from WT according to student's *t* test, $p < .05$ two stars; $p < .1$ one star

3.7 | PP2A activity

Protein phosphatase 2A activity tended to be slightly lower in *lcmt1* and slightly higher in *pme1* than in WT, but these differences were not statistically significant (Figure 5h). The *PTPA* overexpressor line clearly revealed higher PP2A activity, which is in line with effects observed previously for plants constitutively overexpressing PTPA-GFP (Chen, Zhu, Shen, & Zhang, 2015).

4 | DISCUSSION

Protein phosphatase 2A activity is crucial for plants to pass through the life cycle from seeds to mature flowering plants and new seeds. Knockout of either of the two subgroups of PP2A catalytic subunits (Ballesteros et al., 2013), or the two B/B55 subunits (Heidari et al., 2011) is detrimental to the plant. However, when either of the PP2A methylating/demethylating enzymes PME1 or LCMT1 were knocked out, Arabidopsis still looked healthy and completed its life cycle; hence, expression of these PP2A regulators is not a prerequisite for plant survival. It is intriguing that these genes are so strongly conserved in plants, which indicates that they have important functions, and searches in the TAIR database did not reveal any close paralogs for these genes (Altschul, Gish, Miller, Myers, & Lipman, 1990). Although not essential under our growth conditions, these genes may have been essential during evolution and may still be essential for survival under harsh or competitive conditions.

PME1 has, to our knowledge, not been studied in plants. In all our experiments, the level of unmethylated PP2A-C was lower in *pme1* than in WT, confirming that PME1 is involved in keeping the balance between methylated and unmethylated PP2A-C in Arabidopsis. Methylation/demethylation of PP2A-C is a posttranslational regulation mechanism expected to occur rapidly. Additionally, de novo synthesis and degradation of PP2A-C may also contribute to the balance between unmethylated and methylated PP2A-C. The fact that the level of unmethylated PP2A-C increased rather rapidly also in the *pme1* mutant, where efficient demethylation of PP2A-C is unlikely to take place because of impaired *PME1*, indicates that de novo synthesis was important for providing unmethylated PP2A-C under some conditions (Figure 2a).

Some regulatory effects of PP2A occur directly at the protein level, without inducing changes in the transcription of genes. On the other hand, the posttranslational regulation of specific proteins by PP2A will influence signal transduction chains and lead to changes in transcriptional activity. Protein phosphatases are involved in defence responses, both by directly regulating proteins' activity and regulation of protein kinase cascades and by altering transcript levels. PP2A is implicated in defence responses in Arabidopsis at the level of PAMP (pathogen-associated molecular patterns) perception (Segonzac et al., 2014) and is a target of bacterial effector proteins (Jin et al., 2016). It is tempting to expect plant PP2A to be involved also in further downstream defence signalling by acting opposite to protein kinases and inhibiting MAPK signalling cascades, as has been found for MAPKs in mammalian cells (Asai et al., 2002; Junttila, Li, & Westermarck, 2008; Lassowskat, Bottcher, Eschen-Lippold, Scheel, & Lee, 2014; Macho & Zipfel, 2014; Rodriguez, El Ghoul, Mundy, & Petersen, 2016). However, such targets of PP2A in plants still remain to be identified, and the basis for enrichment of defence genes in *pme1* and *lcmt1* needs further investigation.

An interesting difference in gene expression in *pme1* and *lcmt1* mutants was that a large set of genes was higher expressed in *pme1* than in *lcmt1* (Figure 4a,b), suggesting that PME1 acts more as an inhibitor of gene expression whereas LCMT1 more promotes gene expression. This indicates that the high methylation level of PP2A-C is necessary for promoting expression of several genes. In support of this, 14 TFs were higher expressed in *pme1*, which has a high level of methylated PP2A-C, compared with *lcmt1*, which has only unmethylated PP2A-C. Only two TFs were more highly expressed in *lcmt1* than in *pme1* (Figure 4b and Table 2).

In the *pme1* mutant, the level of unmethylated PP2A-C was on average 30% lower than in WT. In striking contrast, the *lcmt1* mutant had about five times higher levels of unmethylated PP2A-C than WT (Figure 1). This is reflected in the *lcmt1* mutant having a far more distinct phenotype than *pme1*. The *lcmt1* mutant had a clearly visible phenotype regarding rosette appearance, flowering time, and root growth (Figure 5). The RNA-seq analysis showed that flowering inhibitors *FLC* and *MEE3* were more downregulated in *lcmt1* than in *pme1*, indicating that PP2A-C methylation status influenced these genes and affected flowering time. Growth of roots was clearly impaired in the *lcmt1* mutant, with both shorter main roots and poor growth of lateral roots (Figure 5g). Enhanced effects of ABA and NaCl on root growth in a *lcmt1* knockout has been reported previously, substantiating impaired root growth in *lcmt1* under various conditions (Chen et al., 2014).

A tendency of lower PP2A activity extracted from *lcmt1* relative to WT would be expected according to previous experiments from Chen et al. (2014). Variable assay methods between research groups have probably contributed to a smaller difference between WT and *lcmt1* in our experiments. Overexpression of *PTPA* clearly led to increased PP2A activity (Figure 5h). This is in line with results from plants overexpressing PTPA–GFP fusion protein (Chen et al., 2015). These data imply that the different phenotype observed for *lcmt1* (Figure 5) cannot be accounted to the PP2A activity as measured in vitro and underpin that the effects are caused by the low degree of PP2A-C methylation. Changes in methylation degree are expected to result in changes in the affinity between B subunits and PP2A-C (Janssens et al., 2008), which again leads to changes in PP2A affinity towards different substrates.

Our results clearly showed that environmental stressors such as flooding, salt, and nutrient deprivation influence the methylation status of PP2A-C. RNA-seq analysis of mutants showed that *PME1* had more inhibitory effects on gene expression than *LCMT1* and indicated that *PME1* and *LCMT1* genes have important functions in various stress reactions, including defence to pathogens.

ACKNOWLEDGMENTS

This work was supported by a grant from the Norwegian Research Council (Grant 213853/F20 to CL) and cofinanced by the rector of the University of Agriculture in Krakow through a scholarship to AK.

ORCID

Cathrine Lillo http://orcid.org/0000-0002-8470-8983

REFERENCES

Alonso, J. M., Stepanova, A. N., Leisse, T. J., Kim, C. J., Chen, H., Shinn, P., ... Ecker, J. R. (2003). Genome-wide insertional mutagenesis of *Arabidopsis thaliana*. *Science*, *301*, 653–657.

Altschul, S. F., Gish, W., Miller, W., Myers, E. W., & Lipman, D. J. (1990). Basic local alignment search tool. *Journal of Molecular Biology*, *215*, 403–410.

Arnaud, N., Murgia, I., Boucherez, J., Briat, J. F., Cellier, F., & Gaymard, F. (2006). An iron-induced nitric oxide burst precedes ubiquitin-dependent protein degradation for *Arabidopsis AtFer1* ferritin gene expression. *The Journal of Biological Chemistry*, *281*, 23579–23588.

Asai, T., Tena, G., Plotnikova, J., Willmann, M. R., Chiu, W. L., Gomez-Gomez, L., ... Sheen, J. (2002). MAP kinase signalling cascade in *Arabidopsis* innate immunity. *Nature*, *415*, 977–983.

Ballesteros, I., Dominguez, T., Sauer, M., Paredes, P., Duprat, A., Rojo, E., ... Sanchez-Serrano, J. J. (2013). Specialized functions of the PP2A subfamily II catalytic subunits PP2A-C3 and PP2A-C4 in the distribution of auxin fluxes and development in *Arabidopsis*. *The Plant Journal*, *73*, 862–872.

Barg, R., Sobolev, I., Eilon, T., Gur, A., Chmelnitsky, I., Shabtai, S., ... Salts, Y. (2005). The tomato early fruit specific gene *Lefsm1* defines a novel class of plant-specific SANT/MYB domain proteins. *Planta*, *221*, 197–211.

Baxter, C. E., Costa, M. M., & Coen, E. S. (2007). Diversification and co-option of RAD-like genes in the evolution of floral asymmetry. *The Plant Journal*, *52*, 105–113.

Berardini, T. Z., Mundodi, S., Reiser, L., Huala, E., Garcia-Hernandez, M., Zhang, P., ... Rhee, S. Y. (2004). Functional annotation of the Arabidopsis genome using controlled vocabularies. *Plant Physiology*, *135*, 745–755.

Booker, M. A., & DeLong, A. (2016). Atypical PP2A protein phosphatase gene families do not expand via paleopolyploidization. *Plant Physiology*, *173*(2), 1283–1300.

Bradford, M. M. (1976). A rapid and sensitive method for the quantitation of microgram quantities of protein utilizing the principle of protein-dye binding. *Analytical Biochemistry*, *72*, 248–254.

Braun, P., & Gingras, A. C. (2012). History of protein-protein interactions: From egg-white to complex networks. *Proteomics*, *12*, 1478–1498.

Brautigan, D. L. (2013). Protein Ser/Thr phosphatases—The ugly ducklings of cell signalling. *The FEBS Journal*, *280*, 324–345.

Brewis, N. D., Street, A. J., Prescott, A. R., & Cohen, P. T. (1993). PPX, a novel protein serine/threonine phosphatase localized to centrosomes. *The EMBO Journal*, *12*, 987–996.

Castermans, D., Somers, I., Kriel, J., Louwet, W., Wera, S., Versele, M., ... Thevelein, J. M. (2012). Glucose-induced posttranslational activation of protein phosphatases PP2A and PP1 in yeast. *Cell Research*, *22*, 1058–1077.

Chen, J., Hu, R., Zhu, Y., Shen, G., & Zhang, H. (2014). Arabidopsis phosphotyrosyl phosphatase activator is essential for protein phosphatase 2a holoenzyme assembly and plays important roles in hormone signaling, salt stress response, and plant development. *Plant Physiology*, *166*, 1519–1534.

Chen, W. W., Yang, J. L., Qin, C., Jin, C. W., Mo, J. H., Ye, T., & Zheng, S. J. (2010). Nitric oxide acts downstream of auxin to trigger root ferric-chelate reductase activity in response to iron deficiency in Arabidopsis. *Plant Physiology*, *154*, 810–819.

Chen, J., Zhu, X., Shen, G., & Zhang, H. (2015). Overexpression of *At*PTPA in Arabidopsis increases protein phosphatase 2A activity by promoting holoenzyme formation and ABA negatively affects holoenzyme formation. *Plant Signaling & Behavior*, *10*. e1052926

Cifuentes-Esquivel, N., Bou-Torrent, J., Galstyan, A., Gallemi, M., Sessa, G., Salla, M. M., ... Martinez-Garcia, J. F. (2013). The bHLH proteins BEE and BIM positively modulate the shade avoidance syndrome in Arabidopsis seedlings. *The Plant Journal*, *75*, 989–1002.

Cohen, P., Alemany, S., Hemmings, B. A., Resink, T. J., Stralfors, P., & Tung, H. Y. (1988). Protein phosphatase-1 and protein phosphatase-2A from rabbit skeletal muscle. *Methods in Enzymology*, *159*, 390–408.

Cohen, P., Klumpp, S., & Schelling, D. L. (1989). An improved procedure for identifying and quantitating protein phosphatases in mammalian tissues. *FEBS Letters*, *250*, 596–600.

Douglas, P., Pigaglio, E., Ferrer, A., Halfords, N. G., & MacKintosh, C. (1997). Three spinach leaf nitrate reductase-3-hydroxy-3-methylglutaryl-CoA reductase kinases that are regulated by reversible phosphorylation and/or Ca2+ ions. *The Biochemical Journal*, *325*(Pt 1), 101–109.

Farkas, I., Dombradi, V., Miskei, M., Szabados, L., & Koncz, C. (2007). Arabidopsis PPP family of serine/threonine phosphatases. *Trends in Plant Science*, *12*, 169–176.

Garbers, C., DeLong, A., Deruere, J., Bernasconi, P., & Soll, D. (1996). A mutation in protein phosphatase 2A regulatory subunit A affects auxin transport in Arabidopsis. *European Molecular Biology Organization*, *15*, 2115–2124.

Gentry, M. S., Li, Y., Wei, H., Syed, F. F., Patel, S. H., Hallberg, R. L., & Pallas, D. C. (2005). A novel assay for protein phosphatase 2A (PP2A) complexes in vivo reveals differential effects of covalent modifications on different *Saccharomyces cerevisiae* PP2A heterotrimers. *Eukaryotic Cell*, *4*, 1029–1040.

Guo, F., Stanevich, V., Wlodarchak, N., Sengupta, R., Jiang, L., Satyshur, K. A., & Xing, Y. (2014). Structural basis of PP2A activation by PTPA, an ATP-dependent activation chaperone. *Cell Research*, *24*, 190–203.

Heidari, B., Matre, P., Nemie-Feyissa, D., Meyer, C., Rognli, O. A., Moller, S. G., & Lillo, C. (2011). Protein phosphatase 2A B55 and a regulatory subunits interact with nitrate reductase and are essential for nitrate reductase activation. *Plant Physiology*, *156*, 165–172.

Hill, K. (2015). Post-translational modifications of hormone-responsive transcription factors: The next level of regulation. *Journal of Experimental Botany*, *66*, 4933–4945.

Hoagland, D. R., & Arnon, D. I. (1950). The water-culture method for growing plants without soil. *Circular. California Agricultural Experiment Station*, *347*, 1–32.

Hu, R., Zhu, Y., Wei, J., Chen, J., Shi, H., Shen, G., & Zhang, H. (2016). Overexpression of *PP2A-C5* that encodes the catalytic subunit 5 of protein phosphatase 2A in *Arabidopsis* confers better root and shoot development under salt conditions. *Plant, Cell & Environment*, *40*, 150–164.

Huber, S. C., MacKintosh, C., & Kaiser, W. M. (2002). Metabolic enzymes as targets for 14-3-3 proteins. *Plant Molecular Biology*, *50*, 1053–1063.

Janssens, V., Longin, S., & Goris, J. (2008). PP2A holoenzyme assembly: *In cauda venenum* (the sting is in the tail). *Trends in Biochemical Sciences*, *33*, 113–121.

Jin, L., Ham, J. H., Hage, R., Zhao, W., Soto-Hernandez, J., Lee, S. Y., ... Mackey, D. (2016). Direct and indirect targeting of PP2A by conserved bacterial type-III effector proteins. *PLoS Pathogens*, *12*. e1005609

Junttila, M. R., Li, S. P., & Westermarck, J. (2008). Phosphatase-mediated crosstalk between MAPK signaling pathways in the regulation of cell survival. *FASEB Journal*, *22*, 954–965.

Kataya, A. R., Heidari, B., & Lillo, C. (2015). Protein phosphatase 2A regulatory subunits affecting plant innate immunity, energy metabolism, and flowering time—Joint functions among B′eta subfamily members. *Plant Signaling & Behavior*, *10*. e1026024

Kleinboelting, N., Huep, G., Kloetgen, A., Viehoever, P., & Weisshaar, B. (2012). GABI-Kat SimpleSearch: New features of the *Arabidopsis thaliana* T-DNA mutant database. *Nucleic Acids Research*, *40*, D1211–D1215.

Kwak, J. M., Moon, J. H., Murata, Y., Kuchitsu, K., Leonhardt, N., DeLong, A., & Schroeder, J. I. (2002). Disruption of a guard cell-expressed protein phosphatase 2A regulatory subunit, *RCN1*, confers abscisic acid insensitivity in Arabidopsis. *Plant Cell*, *14*, 2849–2861.

Lassowskat, I., Bottcher, C., Eschen-Lippold, L., Scheel, D., & Lee, J. (2014). Sustained mitogen-activated protein kinase activation reprograms defense metabolism and phosphoprotein profile in *Arabidopsis thaliana*. *Frontiers in Plant Science*, *5*, 554.

Lillo, C., Kataya, A. R., Heidari, B., Creighton, M. T., Nemie-Feyissa, D., Ginbot, Z., & Jonassen, E. M. (2014). Protein phosphatases PP2A, PP4 and PP6: Mediators and regulators in development and responses to environmental cues. *Plant, Cell & Environment*, *37*, 2631–2648.

Liu, D., Li, A., Mao, X., & Jing, R. (2014). Cloning and characterization of *"TaPP2AbB"-alpha*, a member of the PP2A regulatory subunit in wheat. *Public Library of Science one*, *9*. e94430

Longin, S., Jordens, J., Martens, E., Stevens, I., Janssens, V., Rondelez, E., … Van Hoof, C. (2004). An inactive protein phosphatase 2A population is associated with methylesterase and can be re-activated by the phosphotyrosyl phosphatase activator. *The Biochemical Journal*, *380*, 111–119.

Longin, S., Zwaenepoel, K., Louis, J. V., Dilworth, S., Goris, J., & Janssens, V. (2007). Selection of protein phosphatase 2A regulatory subunits is mediated by the C terminus of the catalytic subunit. *The Journal of Biological Chemistry*, *282*, 26971–26980.

Longman, M. R., Ranieri, A., Avkiran, M., & Snabaitis, A. K. (2014). Regulation of PP2AC carboxylmethylation and cellular localisation by inhibitory class G-protein coupled receptors in cardiomyocytes. *Public Library of Science one*, *9*. e86234

Macho, A. P., & Zipfel, C. (2014). Plant PRRs and the activation of innate immune signaling. *Molecular Cell*, *54*, 263–272.

McAvoy T. & Nairn A.C. (2010) Serine/Threonine Protein Phosphatase Assays. *Current Protocols in Molecular Biology*, 92:18.18:18.18.1—18.18.11. https://doi.org/10.1002/0471142727. mb1818s92.

Mi, H., Muruganujan, A., Casagrande, J. T., & Thomas, P. D. (2013). Large-scale gene function analysis with the PANTHER classification system. *Nature Protocols*, *8*, 1551–1566.

Michniewicz, M., Zago, M. K., Abas, L., Weijers, D., Schweighofer, A., Meskiene, I., … Friml, J. (2007). Antagonistic regulation of PIN phosphorylation by PP2A and PINOID directs auxin flux. *Cell*, *130*, 1044–1056.

Moorhead, G. B., De Wever, V., Templeton, G., & Kerk, D. (2009). Evolution of protein phosphatases in plants and animals. *The Biochemical Journal*, *417*, 401–409.

Muday, G. K., Brady, S. R., Argueso, C., Deruere, J., Kieber, J. J., & DeLong, A. (2006). RCN1-regulated phosphatase activity and EIN2 modulate hypocotyl gravitropism by a mechanism that does not require ethylene signaling. *Plant Physiology*, *141*, 1617–1629.

Murashige, T., & Skoog, F. (1962). A revised medium for rapid growth and bio assays with tobacco tissue cultures. *Physiologia Plantarum*, *15*, 473–497.

Pernas, M., Garcia-Casado, G., Rojo, E., Solano, R., & Sanchez-Serrano, J. J. (2007). A protein phosphatase 2A catalytic subunit is a negative regulator of abscisic acid signalling. *The Plant Journal*, *51*, 763–778.

Prickett, T. D., & Brautigan, D. L. (2006). The alpha4 regulatory subunit exerts opposing allosteric effects on protein phosphatases PP6 and PP2A. *The Journal of Biological Chemistry*, *281*, 30503–30511.

Rodriguez, E., El Ghoul, H., Mundy, J., & Petersen, M. (2016). Making sense of plant autoimmunity and 'negative regulators'. *The FEBS Journal*, *283*, 1385–1391.

Segonzac, C., Macho, A. P., Sanmartin, M., Ntoukakis, V., Sanchez-Serrano, J. J., & Zipfel, C. (2014). Negative control of BAK1 by protein phosphatase 2A during plant innate immunity. *The EMBO Journal*, *33*, 2069–2079.

Skottke, K. R., Yoon, G. M., Kieber, J. J., & DeLong, A. (2011). Protein phosphatase 2A controls ethylene biosynthesis by differentially regulating the turnover of ACC synthase isoforms. *Public Library of Science genetics*, *7*. e1001370

Sontag, J. M., Nunbhakdi-Craig, V., & Sontag, E. (2013). Leucine carboxyl methyltransferase 1 (LCMT1)-dependent methylation regulates the association of protein phosphatase 2A and Tau protein with plasma membrane microdomains in neuroblastoma cells. *The Journal of Biological Chemistry*, *288*, 27396–27405.

Tang, W., Yuan, M., Wang, R., Yang, Y., Wang, C., Oses-Prieto, J. A., … Wang, Z. Y. (2011). PP2A activates brassinosteroid-responsive gene expression and plant growth by dephosphorylating BZR1. *Nature Cell Biology*, *13*, 124–131.

Trotta, A., Wrzaczek, M., Scharte, J., Tikkanen, M., Konert, G., Rahikainen, M., … Kangasjarvi, S. (2011). Regulatory subunit B'gamma of protein phosphatase 2A prevents unnecessary defense reactions under low light in Arabidopsis. *Plant Physiology*, *156*, 1464–1480.

Uhrig, R. G., Labandera, A. M., & Moorhead, G. B. (2013). *Arabidopsis* PPP family of serine/threonine protein phosphatases: Many targets but few engines. *Trends in Plant Science*, *18*, 505–513.

Waadt, R., Manalansan, B., Rauniyar, N., Munemasa, S., Booker, M. A., Brandt, B., … Schroeder, J. I. (2015). Identification of open stomata1-interacting proteins reveals interactions with sucrose non-fermenting1-related protein kinases2 and with type 2A protein phosphatases that function in abscisic acid responses. *Plant Physiology*, *169*, 760–779.

Wang, R., Liu, M., Yuan, M., Oses-Prieto, J. A., Cai, X., Sun, Y., … Tang, W. (2016). The brassinosteroid-activated BRI1 receptor kinase is switched off by dephosphorylation mediated by cytoplasm-localized PP2A B' subunits. *Molecular Plant*, *9*, 148–157.

Wepf, A., Glatter, T., Schmidt, A., Aebersold, R., & Gstaiger, M. (2009). Quantitative interaction proteomics using mass spectrometry. *Nature Methods*, *6*, 203–205.

Wu, J., Tolstykh, T., Lee, J., Boyd, K., Stock, J. B., & Broach, J. R. (2000). Carboxyl methylation of the phosphoprotein phosphatase 2A catalytic subunit promotes its functional association with regulatory subunits in vivo. *European Molecular Biology Organization*, *19*, 5672–5681.

Wu, G., Wang, X., Li, X., Kamiya, Y., Otegui, M. S., & Chory, J. (2011). Methylation of a phosphatase specifies dephosphorylation and degradation of activated brassinosteroid receptors. *Science Signaling*, *4*, ra29.

Xing, Y., Li, Z., Chen, Y., Stock, J. B., Jeffrey, P. D., & Shi, Y. (2008). Structural mechanism of demethylation and inactivation of protein phosphatase 2A. *Cell*, *133*, 154–163.

Ye, H. X., Li, L., Guo, H. Q., & Yin, Y. H. (2012). MYBL2 is a substrate of GSK3-like kinase BIN2 and acts as a corepressor of BES1 in brassinosteroid signaling pathway in Arabidopsis. *Proceedings of the National Academy of Sciences of the United States of America*, *109*, 20142–20147.

SUPPORTING INFORMATION

Additional Supporting Information may be found online in the supporting information tab for this article.

How to cite this article: Creighton MT, Kolton A, Kataya ARA, et al. Methylation of protein phosphatase 2A—Influence of regulators and environmental stress factors. *Plant Cell Environ*. 2017;40:2347–2358. https://doi.org/10.1111/pce.13038

Paper IV:

Light regulation of nitrate reductase by catalytic subunits of protein phosphatase 2A

This paper is not included in Brage for copyright reasons.